

**LARGE SCALE SPATIO-TEMPORAL FORCING OF PELAGIC-
COASTAL COUPLING: DISENTANGLING THE EFFECTS OF
ENVIRONMENTAL CHANGE ON INTERTIDAL
INVERTEBRATE RECRUITMENT**

THESIS SUBMITTED IN FULFILLMENT OF THE REQUIREMENTS FOR THE
DEGREE OF
DOCTOR OF PHILOSOPHY
OF RHODES UNIVERSITY
(MARINE BIOLOGY)

BY

CARLOTA FERNÁNDEZ MUÑIZ

JUNE 2018

Abstract

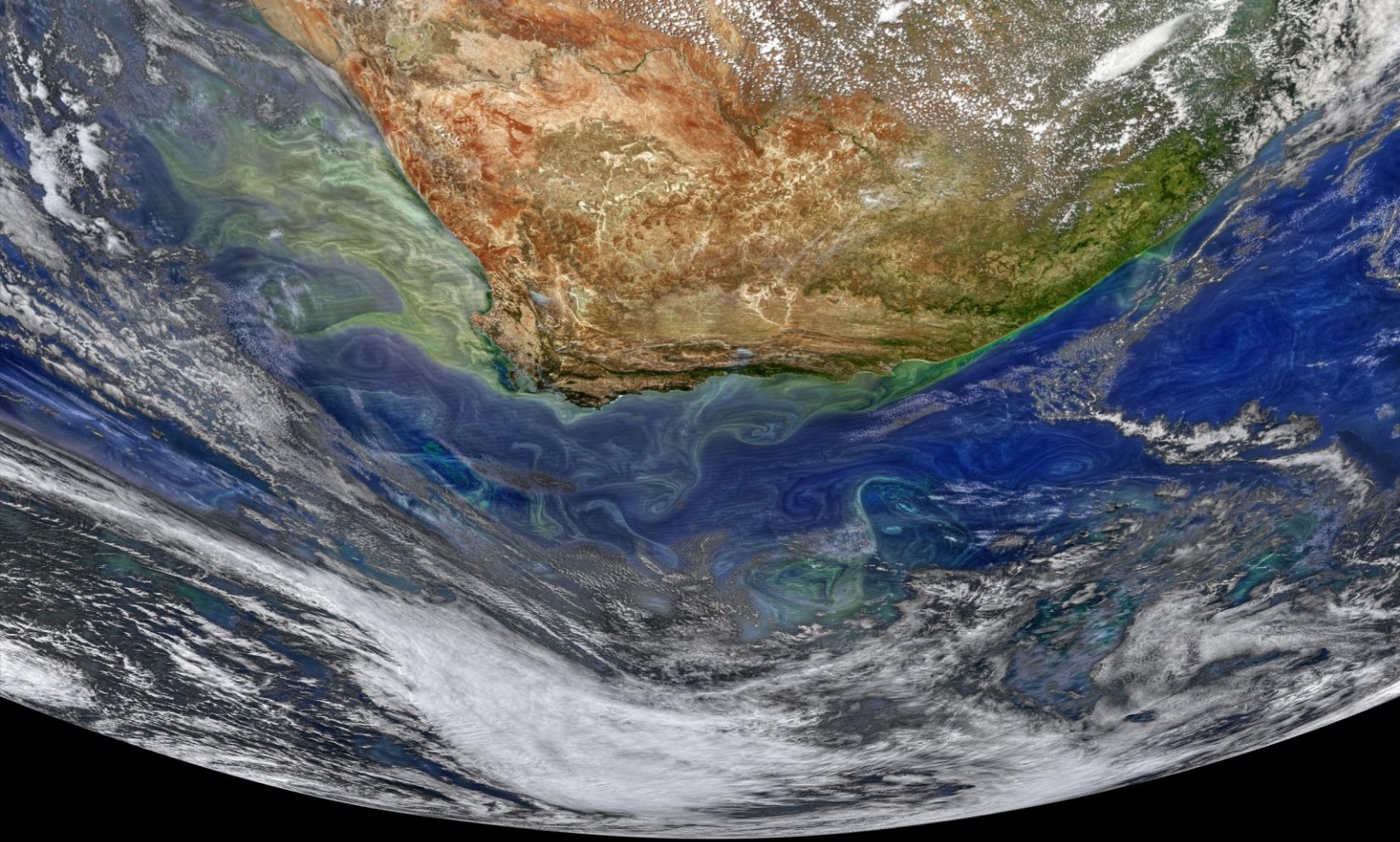
Marine systems are driven by the relationships among organisms and environmental conditions. Anthropogenic-induced changes during the past decades have started to alter climatic drivers which have the potential to alter the physical, chemical and biological environment. In coastal systems, biogeography is influenced by the temporal variability in the conditions of the water mass. In addition, many marine benthic organisms develop in the water mass and rely on the conditions that link the pelagic and benthic systems for population maintenance. Such pelagic-coastal coupling indicates that changes in the trophic system during development can be transferred to the adult populations through changes in propagule supply. Thus, changes in environmental conditions can influence benthic populations directly (e.g. through larval advection) or indirectly, through their influence on the phytoplankton community (e.g. through the development of HABs).

The South African coastline shows clear alongshore patterns of faunal biomass and species richness. On the south coast, strong longitudinal patterns of recruitment of intertidal organisms exist, with areas of particularly high recruitment. HABs of unprecedented spatio-temporal magnitude have recently developed along the south coast, including the areas where benthic recruitment is most intense. The present thesis used these blooms to study changes in intertidal recruitment directly or indirectly associated with their occurrence. Using a combination of remote sensing data to study the environmental conditions of the water mass in the innermost part of the Agulhas Bank, and estimates of mussel and barnacle recruitment rates to integrate the effects of conditions in the water mass during larval development, this thesis aimed to: (1) understand the conditions that triggered the development of an HAB of the dinoflagellate *Lingulodinium polyedrum* during summer of 2014, (2) determine the direct or indirect effects of that bloom on recruitment of intertidal organisms, and understand the factors that affect recruitment along the coast, (3) determine if the environmental factors during bloom development produced any carryover effects on recruit growth and mortality, and (4) determine the factors that drive changes in community biomass and composition along the south coast, the long-term trends in those factors, and possible changes experienced in recent years.

Water column stability during spring, before the development of the red tide, followed by alternating periods of upwelling and relaxation during summer and autumn, seemed to promote the development and persistence of *L. polyedrum*. Recruitment of mussels and barnacles was estimated during the reproductive season of mussels in 2014, coinciding with the red tide, and during the following year. Alongshore patterns in recruitment were found, with higher mussel recruitment in the absence of the red tide and the opposite pattern in barnacles. Alongshore patterns in SST and chlorophyll matching those of recruitment were also found, with higher SSTs and lower chlorophyll during the red tide than the following year. Growth and mortality rates in

barnacles did not differ between years during the first five months after settlement. This suggests that the factors which produced differences in recruitment between years did not produce carryover effects detectable at the temporal scales studied.

Further analysis of 15 years of satellite-derived environmental data showed significant cooling trends potentially driven by a long-term seasonal acceleration of the Agulhas Current in autumn around two upwelling centres on the south coast, coinciding temporally with the reproductive period of mussels and barnacles, and spatially with the areas of highest recruitment. In addition, the comparison of SST and chl-a conditions during the first and the second half of the period of study showed that seasonality of both variables has changed in large areas over the shelf, with increasing importance of shorter-term variability, which would in turn decrease environmental predictability. Thus, the conditions observed during the present study, particularly during 2015, when upwelling seemed to be more intense, may presage the potential effects of identified long-term cooling trends at the upwelling centres. Although the general trend shows cooling around those areas, conditions can vary greatly among years, favouring different taxa. Changes in the Agulhas Current System are affected by changes in distant areas in the Indian Ocean basin. Such tele-connection is unlikely to be unique to this system and indicates the importance of understanding trends in major large scale climatic drivers and their regional effects in order to make predictions about coastal systems.



(<https://oceancolor.gsfc.nasa.gov/>)

Table of contents

Abstract.....	ii
Table of contents	v
Acknowledgements.....	ix
Chapter 1	1
1. General introduction	2
1.1. Sources of environmental change.....	3
1.2. Intertidal communities	5
1.3. Study area	6
1.4. Study aims / overview	10
Chapter 2	12
Environmental drivers of a red tide of the dinoflagellate <i>Lingulodinium polyedrum</i> of unprecedented spatio-temporal magnitude along the south coast of South Africa.	13
2.1. Introduction.....	13
2.1.1. Red tide occurrence in the South African coast	15
2.2. Materials and methods.....	16
2.2.1. Spatio-temporal limits of the red tide.....	16
2.2.2. Environmental conditions co-occurring with high chl-a concentrations	18
2.2.3. Seasonal environmental conditions	20
2.3. Results	21
2.3.1. Spatio-temporal limits of the red tide.....	21
2.3.2. Environmental conditions co-occurring with high chl-a concentrations	25
2.3.3. Seasonal environmental conditions	29
2.4. Discussion	37
2.4.1. Winter pre-conditioning of the water mass.....	38
2.4.2. Red tide triggering and maintenance mechanisms	39

2.4.3. Red tide species and their environmental conditions	41
2.4.4. Future perspectives	43
Chapter 3	46
Interannual variability in recruitment patterns of intertidal invertebrates under contrasting environmental conditions.	47
3.1. Introduction	47
3.1.1. The influence of food during larval development; particle size and food quality	48
3.2. Material and methods.....	51
3.2.1. Biological sampling.....	51
3.2.1.1. Mussels	51
3.2.1.2. Barnacles.....	53
3.2.2. Environmental variables	56
3.2.2.1. Upwelling and turbulence indices	56
3.2.2.2. Wave height.....	56
3.2.2.3. Chlorophyll-a and sea surface temperature	57
3.2.3. Data analysis	57
3.2.3.1. Environmental predictors of recruitment	57
3.2.3.2. Variation in longitudinal patterns of recruitment	58
3.2.3.3. Differences between years in the environmental conditions	59
3.3. Results	60
3.3.1. Environmental predictors of recruitment.....	61
3.3.2. Variation in longitudinal patterns of recruitment.....	65
3.3.3. Differences between years in the environmental conditions	67
3.4. Discussion	70
3.4.1. Limitations of the study	70
3.4.2. Mussels	71

3.4.3. Barnacles	74
3.4.4. Comparing taxa	75
Chapter 4	78
Indirect effects of environmental conditions during larval development on growth and mortality rates of barnacle juveniles	79
4.1. Introduction	79
4.2. Material and methods.....	81
4.2.1. Barnacle recruitment in Infanta and Jongensfontein.....	83
4.2.2. Juvenile barnacle growth	83
4.2.3. Juvenile barnacle mortality.....	84
4.2.4. Environmental conditions during barnacle growth	85
4.2.5. Long-term conditions in SST and chl-a.....	86
4.3. Results	86
4.3.1. Barnacle recruitment in Infanta and Jongensfontein.....	86
4.3.2. Juvenile barnacle growth	87
4.3.3. Juvenile barnacle mortality.....	89
4.3.4. Environmental conditions during barnacle growth	89
4.3.5. Long-term conditions in SST and chl-a.....	92
4.4. Discussion	94
Chapter 5	98
Long-term trends in environmental drivers of coastal ecosystems	99
5. 1. Introduction	99
5.2. Materials and methods.....	102
5.2.1. Spatial patterns of temporal variability.....	102
5.2.2. Long-term environmental conditions.....	104
5.3. Results	105

5.3.1. Spatial patterns of temporal variability.....	105
5.3.1.1. SST.....	105
5.3.1.2. Chlorophyll-a	106
5.3.1.3. Changes in temporal variability of SST and chl-a	110
5.3.2. Long-term environmental conditions.....	114
5.4. Discussion	118
5.4.1. Spatial patterns of temporal variability.....	118
5.4.2. Long-term environmental conditions.....	122
Chapter 6	126
6. Synthesis.....	127
6.1. Environmental changes in water mass conditions.....	128
6.2. The future of benthic organisms	131
6.3. Conclusions	133
Appendix I	135
I.1. Introduction.....	135
I.2. Materials and methods.....	137
I.2.1. Sample collection and splitting procedure	137
I.2.2. Data analysis	138
I.3. Results.....	139
I.4. Discussion.....	141
Appendix II.....	145
Appendix II.1	145
Appendix II.2	146
Appendix II.3	147
References	148

Acknowledgements

First of all, I have to thank to my supervisors Prof. Christopher McQuaid and Dr. Nicolás Weidberg. To you, Christopher, I am especially grateful for trusting me to do what was supposed to be an MSc and finally developed into this PhD. You gave me a great opportunity to join your lab without knowing anything about me. Thank you for putting up with me throughout the years, for not complaining when I went to discuss problems with you while you were preparing your morning coffee, for not killing me because of my ability to always reply “yes, but...” in every discussion, and for your quick responses to every problem, question and writing piece that I have sent in these four years. BUT most of all, thank you for your constant support to do this, even when it took this long.

To you, Nico, I have to thank you both as a supervisor and as a friend, even before this thesis started. Thank you for teaching me a great deal of the science that I know to this day, for always making the time to help me with my data, and for listening to the many absurd ideas that I have had during the years. I cannot express with words how grateful I am that you took me when I was still an undergrad, and that you managed to convince Christopher to take me as a student afterwards. To you, I owe you showing me my first plankton sample and my first barnacle nauplii about eight years ago, which got me hooked into this. I know how much I complain, and that is why I appreciate even more that you put up with me.

This thesis would not have been possible without the help of many students from the Coastal Research Group, the Department of Zoology & Entomology, and the people that helped during the many, many sampling trips at any stage. There were too many people who willingly helped (probably misled by my lies, in which I always maintained that we were going on a beach trip). Thank you to those who, in addition to help, made sure I would not die in the rocky shore: Jaqui, Cristián, Morgana, Nico, Marilú, Justin, Diane, Pam, Dani, Claudia, Aldwin, Olwethu, and Christopher. Many more people helped with fieldwork even before I arrived, so thank you if I have missed your name here. To my office mates, Natanah (Molline, to me), Rosali, and Isabel, thank you for not murdering me because of all my chit-chat and for not judging me (not too much, at least), for my cookie addiction.

A lot of people have passed through Grahamstown during these four years, and I need to thank to all of those who shared this time with me and who left a lot of memories and friendships. Thank you to Nico, Marilú, Morgana and Rachel for adopting me when I arrived, for making the transition between continents so smooth, and for all the food and fun. I also need to thank for being fed (and overfed), and for all the fun involved, to the families Lemahieu-McDonald, Smith-Mónaco, and Porri-Stoloff. Also thanks to Tosca’s brownies which kept my energy levels high while writing.

Gracias a mis padres, M^a Josefa y Agustín, por mantenerme y apoyarme más allá de lo aceptable, y a mis hermanos María y Pablo. A Lorién y Claudia, gracias por todo el apoyo, por acogerme cada vez que vuelvo a casa y porque después de tantos años siga pareciendo que nunca me fui de España.

This PhD was supported by the South African Research Chairs Initiative of the Department of Science and Technology and the National Research Foundation. Special thanks go to Mrs. Ticia Swanepoel and Mrs. Gwen Johnson, who always made sure that I had whatever I needed for my research. Thank you Ticia, for all the extra work that you have had to do for me during these years, for always listening when I had a bad day, and for keeping funds for my lab material. I very much appreciate it.

Finally, I would like to thank to the South African Weather Service, for the wind data provided, and to the many other institutions that work to obtain and to make accessible remote data. Without it, this thesis would have not been possible.

1. General introduction

The study of complex biological systems, including marine ecosystems, requires integrating physical, chemical and biological information at the right spatial and temporal scales (Chang and Dickey 2001). Thus, the system will operate as a whole and, when any part is modified, the effects will be transferred through its different components. The human approach to deal with such levels of complexity is to divide the system of study into its components, following a reductionist approach (Inchausti 1994, Planque 2015). For decades, considerable effort has been made to understand the relationships among marine organisms, and between these organisms and their environment (Connell 1961b, Dayton 1971, Menge 1976, Paine et al. 1985). Nevertheless, the influence of climate change on the physical, chemical, and biological components of ecological systems, has made it essential to study how those components interact among themselves under changing conditions in order to forecast future ecosystem dynamics (Hallett et al. 2004, DeYoung et al. 2008, Beaugrand et al. 2008, Urban 2015, Urban et al. 2016). Thus, understanding how marine systems operate worldwide under changing conditions will require the ability to include interactions among trophic levels (Van der Putten et al. 2010) and their relationships with the water mass (Belanger et al. 2012).

In coastal marine systems, strong links exist between the benthic and the pelagic systems. Adults in benthic populations are influenced by biological interactions (such as competition or predation), and by environmental conditions. The predominance of different conditions will produce different responses in the community and alter the relative importance of top-down and bottom-up factors (Menge 1992, 2000). The majority of these benthic species undergo planktonic larval development and conditions in the water mass will influence the survival or growth of larvae (for example Olson and Olson 1989, O'Connor et al. 2007), as well as the transport mechanisms that allow delivery to suitable settlement sites (for example Pineda et al. 2007, Porri et al. 2008). Thus, changes in the marine environment can affect both established adult organisms and the supply of new propagules due to the coupling between the pelagic and the benthic coastal systems, extending from the coastline to depth. Compared to the open ocean, conditions in shelf systems support high primary productivity, particularly in coastal areas (Ryther 1969, Rowe et al. 1975), which in turn supports complex food webs and high species diversity. Due to the relatively small volumes of water that they contain, it is likely that environmental changes will have a larger or at least more immediate influence in shelf systems than in the open ocean, and that they will affect larger numbers of species and organisms. This combination of factors highlights the importance of identifying the sources of variability in abiotic factors, and of addressing how changes in environmental conditions will be transferred among different parts of the system.

Rocky shore systems in particular, are of great interest since they cover a great portion of the coastline worldwide and support high biomass and species diversity (Borthagaray and Carranza 2007, Hawkins et al. 2016). The critical influence of environmental conditions is observed, for example, in the way they drive biogeographic patterns and changes in community composition (Navarrete et al 2005, Blanchette et al. 2008, Wieters et al. 2009). In fact, variability in processes that operate at large scales, such as upwelling, have been described as shaping biogeography (Tapia et al. 2014, Fenberg et al. 2015). Changes in abiotic conditions thus have the potential to alter biological systems at large spatial and/or temporal scales. In the case of South Africa, marked biogeographic patterns occur along the coastline (Bustamante and Branch 1996a, Awad et al. 2002, Gibbons et al. 2010, Whitfield et al. 2016). Along the coast, differences in food sources for filter feeders between the west and south coasts reflect variability in upwelling regimes (Puccinelli et al. 2016). In fact, the currents that dominate nearshore hydrodynamics on the west coast and on the south and east coasts (the Benguela and Agulhas currents respectively) have very different hydrodynamic and physico-chemical properties, resulting in large-scale differences in environmental conditions which eventually affect the associated biological communities. Within the south coast itself, alongshore patterns in abundance of organisms also occur at smaller scales (Awad et al. 2002, von der Meden et al. 2008).

The south coast is under the influence of the Agulhas Current, one of the strongest Western Boundary Currents in the world (Lutjeharms 2006). A broad shelf extends along the south coast and, like other shallow coastal areas, it holds areas that are important for the larvae of fish and benthic invertebrates. Multiple changes in the Agulhas Current have been described recently, including warming of the current (Rouault et al. 2009), and changes in wind patterns within the ocean basin which influences the current (Backeberg et al. 2012, Wu et al. 2012). Thus, changes in the current, as well as in the areas where the current originates, have received considerable attention due to the importance of the current in global climate (Beal et al. 2011). Additionally, changes in the current may translate into major changes in coastal hydrodynamics with important consequences for the associated ecosystems. In particular, temporal variability in the water mass that reflects changes transmitted downstream by the major current system, may eventually alter the typical temporal scales of variability in pelagic-coastal coupling. The analysis of the relationship between early developmental stages of marine organisms and conditions during development may thus indirectly show the effects of environmental conditions on the stages that link the benthic-pelagic biological systems, and presage possible outcomes of changing conditions for benthic organisms.

1.1. Sources of environmental change

Climate change is expected to influence the conditions that drive coastal ecosystems in different direct and indirect ways (Harley et al. 2006, Hoegh-Guldberg and Bruno 2010). Direct changes are

expected in physico-chemical water properties such as temperature or pH (Orr et al. 2005, Feely et al. 2009, Roemmich et al. 2012). Changes are also expected in the climatic conditions which will change the environmental conditions for organisms, but affect them indirectly. An example of this is spatio-temporal variability in wind patterns. Bakun (1990) proposed that an increase in intensity and duration of trade winds, mainly driven by higher sea-land thermal contrasts due to global warming, can be expected to intensify coastal upwelling worldwide. Changes in stratification and mixing dynamics are also expected, due to increasing frequencies of winter storms (Bromirski et al. 2003), or warming of surface waters (Roemmich and McGowan 1995, Stocker et al. 2013). Nevertheless, warming will not be equal around the globe, and some areas will experience stronger warming than others (Roemmich et al. 2012, Stocker et al. 2013).

Such changes in water mass conditions are expected to alter phytoplankton communities in multiple ways (Behrenfeld et al. 2006, Falkowski and Olivier 2007, Paerl and Huisman 2009, Morán et al. 2010, Winder and Sommer 2012, Wells et al. 2015). For example, temperature affects the metabolism of phytoplankton, so warmer temperatures have been proposed to favour smaller size phytoplankton groups, which would affect species composition (Morán et al. 2010). Beyond the direct physiological effects of changing temperature, warming can be expected to increase stratification in certain areas such as the south coast of South Africa. The associated deepening of the thermocline and reduced mixing, will therefore reduce nutrient loading from bottom recirculation into the euphotic areas. In addition, the spring bloom of phytoplankton in temperate areas follows a succession of different groups of organisms, starting with diatom growth triggered by changes in photoperiod and physical structure of the water column (Sverdrup 1953, Eilertsen et al. 1995, Huisman et al. 1999), with subsequent increases in dinoflagellate abundances. Thus, changes in the natural transition between winter mixing and summer stratification, or the timing of each phase, may have major consequences for the ecosystem (Edwards and Richardson 2004, Winder and Schindler 2004). Changes in nutrient availability can have particularly important effects on phytoplankton competitive hierarchies, linked to their abilities to take up nutrients (Falkowski and Oliver 2007). In particular, dinoflagellate species can show multiple adaptations regarding nutrient uptake. For example, dinoflagellates are motile and can perform vertical migrations, allowing the uptake of nutrients at depth and their return to photic areas for photosynthesis, while diatoms cannot perform these vertical movements as they do not swim (Blasco 1978, Eppley et al. 1984, MacIntyre et al. 1997, Park et al. 2001). In addition, increasing numbers of dinoflagellate species have been reported to be mixotrophs (able to photosynthesise and to graze on other plankton), a condition that provides nutritional advantages under limited availability of inorganic nutrients (Jeong et al. 2005a, Stoecker et al. 2006). Many dinoflagellate species produce harmful algal blooms with detrimental effects for the ecosystem and even human health. Variation in environmental conditions associated with climate change, such as warming and

stratification, favour superior competitors which are often found to produce harmful algal blooms (Paerl and Huisman 2008, 2009, Glibert and Burkholder 2011, Glibert et al. 2014, Wells et al. 2015).

1.2. Intertidal communities

Changes in the timing or species composition in the phytoplankton, or in the environmental conditions in the water mass due to changing climate may affect the organisms that rely on the planktonic system at any stage of their life cycle. In the case of benthic communities, the vast majority of animals have planktonic larvae (Thorson 1950, Martin et al. 2014), hence, changes in the phytoplankton community may affect food sources during those stages. As a result, the maintenance of populations depends not only on adult survival and reproduction, but also on the successful replenishment of new individuals. Intertidal communities are strongly shaped by abiotic stresses (for example heat and desiccation) which form a gradient across different heights on the shore, largely reflecting the duration of emersion. Physiological tolerance of abiotic stress contributes to the determination of patterns of vertical zonation (Foster 1971, Connell 1972, Bertness et al. 2006). Biotic interactions (particularly competition and predation) operate on the template of potential species to determine actual community composition across the shore (Menge 1976). Because the vast majority of benthic species have planktotrophic larval development, this adds another layer of complexity to the determination of species presence and abundance. During larval development in the water column, both biotic and abiotic conditions influence survival (Strathmann 1985, Fenaux et al. 1994). The duration of planktonic development is strongly influenced by temperature and food availability/quality, affecting competition for resources and survival. Thus, the risk of natural mortality and predation will be affected by developmental times, with longer developmental times resulting in higher mortalities (O'Connor et al. 2007, Tapia and Pineda 2007). For example, the last larval stage of barnacles (the cyprid), does not have a digestive system and relies on larval reserves until a digestive system is developed in the metamorphosed juvenile. After reaching a stage competent to settle, organisms are influenced by flows in the water mass that allow delivery to the adult settlement areas (Farrell et al. 1991, Bertness et al. 1996, Dudas et al. 2008, Rilov et al. 2008, Shanks and Shearman 2009). After settlement, organisms are influenced by conditions in the adult areas, and thus, the environmental and biological stressors that regulate adult communities in intertidal areas are also applied to the newly settled organisms. The change from planktonic to benthic life modes involves a period of great stress for organisms, in which high, often extremely high, mortalities have been reported immediately following settlement (Gosselin and Qian 1996, Hunt and Scheibling 1997, López et al. 1998, Jarrett 2000, von der Meden et al. 2012).

Thus, large reproductive investment by the adults, large larval pools, or high settlement of organisms do not necessarily imply high numbers of recruits, with recruitment being defined as the number of organisms that survive to a given period of time after settlement (Pineda et al. 2010). The

combination of all the factors that affect the larval pool and survival after returning to the adult areas may greatly affect the number of individuals that will eventually survive to reproductive age. Consequently, the early stages of development and their interaction with the environment have important implications for population dynamics (Pineda et al. 2010). Recruitment reflects the results of the combined effects of biological and environmental determinants in a holistic way, but it does not provide information on how, or at which temporal scales, specific factors affect the study organisms. Nevertheless, studying recruitment allows us to consider the overall effects of benthic-pelagic coupling in a way that resembles real conditions, as opposed to compartmentalising information.

A large proportion of intertidal habitats worldwide are composed of rocky shores. In addition to the biotic and abiotic control of communities, some organisms also have the ability to modify abiotic conditions due to their presence or due to the structural changes that they produce (for example the building of dams by beavers). Examples of such organisms (referred to as ecosystem engineers) in marine benthic communities can be found in seaweeds and mussels (Thompson et al. 1996, Borthagaray and Carranza 2007). The presence of these organisms modifies habitat availability and the environmental conditions for other organisms (Harley 2011, Lathlean and McQuaid 2017). In addition, canopy forming algae, like kelps, can act as ecosystem engineers (Smale et al. 2013), and provide other ecosystem services such as food for benthic filter feeders in the form of particulate organic matter, allowing higher biomass than would be possible with only phytoplankton productivity (Bustamante and Branch 1996b, Tallis 2009). In the case of mussels, some species create mussel beds which modify temperature and create habitat for other organisms that live on or among their shells (Lathlean et al. 2016). Along the south coast of South Africa, as in many other areas worldwide, large mussel beds can be found dominating one of the shore levels in rocky shores.

1.3. Study area

Different oceanographic regimes dominate the South African coastline. The west coast is influenced by the cold Benguela Current which flows towards the equator. The Benguela system is one of the most productive Eastern Boundary Upwelling Systems (EBUSs; Thomas et al. 2001, Carr and Kearns 2003). South-easterly winds promote the upwelling of nutrient-rich deep water, resulting in high productivity in the region (Nelson 1992, Carr 2001). In contrast, the south and east coasts are influenced by the Agulhas Current, which carries warm, oligotrophic water from the tropical region (Lutjeharms 2006).

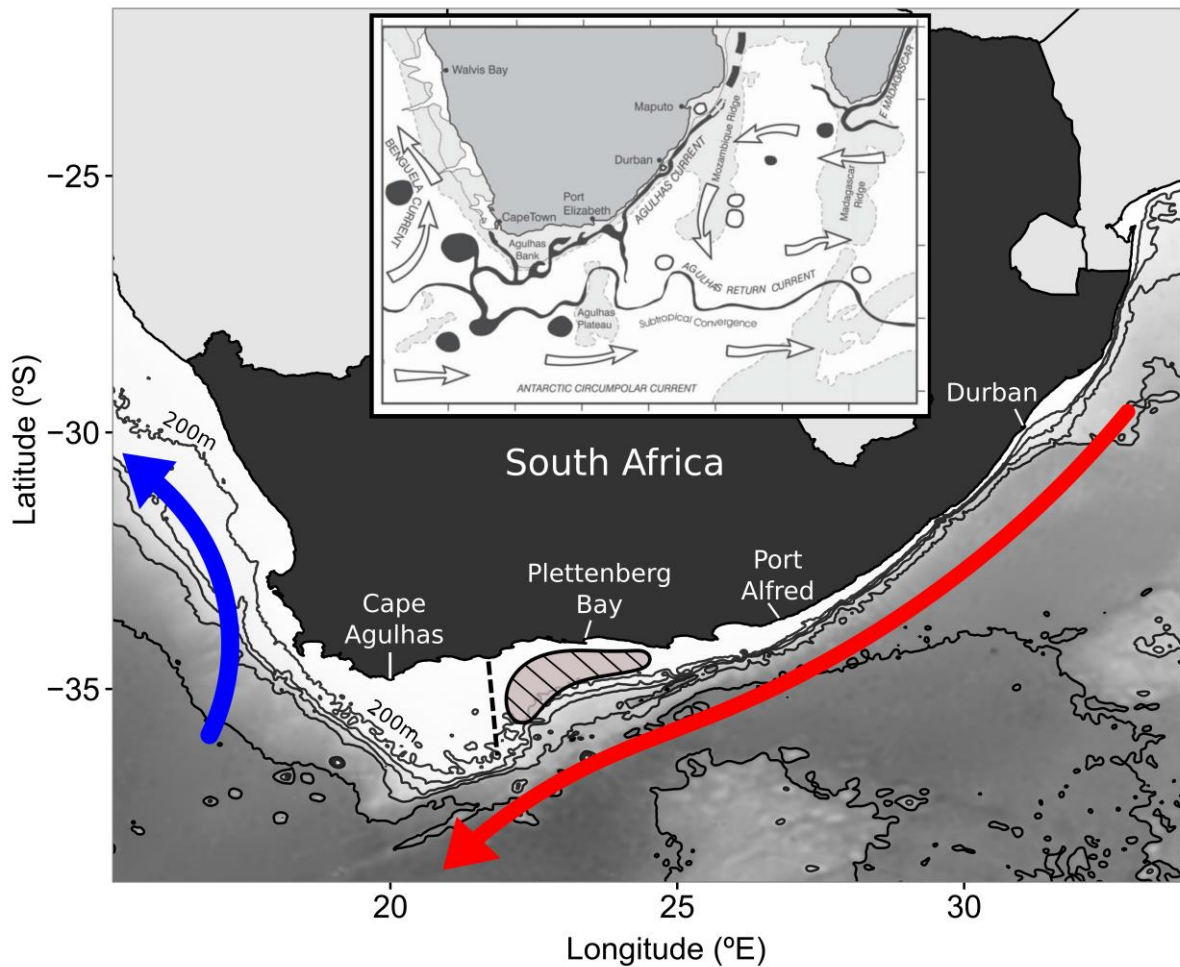


Fig. 1.1. Map of the South African coastline with bathymetric profile. Contour lines represent the 200, 500, 1000, 2000 and 4000m isobaths. Red and blue arrows point the direction of flow of the Agulhas Current and the Benguela Current, respectively. The shelf area from Cape Agulhas to Port Alfred, approximately, is referred to as the Agulhas Bank. Shaded, striped area represents the approximate position of the “cold ridge”. Dashed line ca. 22°E represents the division of the bank in its western and eastern parts for the present study. Upwelling cells occur off Plettenberg Bay and Port Alfred. Inset figure shows the general flow of the Agulhas Current (in black), with the retroflexion area between the Indian and Atlantic oceans (inset obtained from Lutjeharms 2006). Eddies and rings that spin off the current are indicated in black circles).

Water is fed to the Agulhas Current through the Mozambique Channel, the East Madagascar Current, and the Indian Ocean subtropical gyre (Stramma and Peterson 1990, Lutjeharms 2006). The vertical structure of the current is complex and it contains water masses from different sources (Beal et al. 2006). The current flows southwards following the shelf break and deflecting offshore as the shelf widens to form the Agulhas Bank (Fig. 1.1). The shape of the Agulhas Bank resembles an inverse triangle which covers the entire south coast and extends more than 200km offshore at its point of maximum width, ca. 21°E (Fig. 1.1). Along the east coast, south of Durban (ca. 31°E), the shelf is very narrow and widens ca. 27°E (around Port Alfred). In the central part of the south coast the shelf widens again (ca. 22°E). The bottom topography promotes dynamic and energetic flows

due to the friction of the current with the bottom, particularly in the areas where the shelf widens. Changes in the width of the shelf modify the direction of the current's flow and induce shear-edge stress, which promotes the upwelling of shelf bottom waters (Schumann et al. 1982, Lutjeharms et al. 2000). Thus, bottom friction contributes to the development of two semi-permanent upwelling centres around Plettenberg and Port Alfred (ca. 24°E and 27°E, respectively Fig. 1.1) (Schumann et al. 1982, Lutjeharms et al. 2000).

Although forcing by the Agulhas Current influences the two cells, different mechanisms drive upwelling in each area. Around Port Alfred, easterly winds displace surface waters offshore by Ekman transport, and promote the current-induced sub-surface upwelling to reach the surface (Lutjeharms et al. 2000). In contrast, the origins of the bottom water upwelled around Plettenberg are not clear. Different mechanisms have been proposed, including the westwards transport of water from Port Alfred to the Plettenberg area (Swart and Largier 1987, Lutjeharms et al. 1996), and shelf-edge upwelling at the shelf break, which would be transported northwards onto the Agulhas bank (Gill and Schumann 1979, Jackson et al. 2012). Winds along the south coast are predominately alongshore (Schumann 1989) and, although westerly winds are prevalent during the year (Goschen and Schumann 2011), periods of strong easterlies occur, especially during summer (Schumann 1987), promoting the upwelling of the sub-surface water mass. This is particularly evident in the lee of headlands, including Cape Seal, at the western limit of Plettenberg Bay (Schumann et al. 1982). In addition to the influence of the current on upwelling dynamics, friction between the Agulhas Current and shelf waters promotes other structures such as eddies, meanders, and plumes which affect hydrodynamics over the shelf (Rouault and Penven 2011, Jackson et al. 2012, Porri et al. 2014, Weidberg et al. 2015).

Based on the shape of the shelf and how it influences hydrodynamics in the area, this thesis will refer to the western (west of 22°E) or the eastern Agulhas Bank (east of 22°E). Highest primary and secondary productivity along the south coast are found over the eastern bank, around the two upwelling centres at Plettenberg and Port Alfred (Largier et al. 1992, Peterson et al. 1992, Hutchings 1994, Verheye et al. 1994, Roberts 2005, von der Meden 2009). In particular, due to the presence of upwelling, an area of cold water has been described off Plettenberg (Swart and Largier 1987). Swart and Largier (1987). Due to high abundances of organisms around that area relevant to the topic of this thesis, the feature will be referred to as the “cold-ridge” following Roberts (2005) (Fig. 1.1).

The Agulhas Current follows the shelf break and retroflects into the South Indian ocean (Lutjeharms and van Ballegooyen 1988). At this retroflexion, rings and eddies are shed from the Agulhas Current and travel northwards into the Atlantic, crossing the Equator and finally joining the Gulf Stream (Bjastoch et al. 2008, Beal et al. 2011). The leakage of water from the Agulhas Current into the Atlantic means that any change in the Agulhas Current may potentially be

transferred to other regions and have effects on global climate (Biaostoch et al. 2008, 2009, Beal et al. 2011). Strongest flows in the current occur around summer, coinciding with strongest wind curl in the ocean basin that influences its sources. Warming trends have been described in recent years in the Agulhas Current System (Rouault et al. 2009, 2010a). One mechanism that has been proposed as a trigger for that warming is increasing wind stress curl in the Indian Ocean, which is correlated with increased temperatures in the area where the current retroflects (Rouault et al. 2009, Backeberg et al. 2012). Coinciding with the warming trends in the Agulhas Current, year-round cooling was reported in the shelf downstream of the Port Alfred upwelling cell (Rouault et al. 2009, 2010b).

In recent years, red tides of large spatio-temporal magnitude have occurred along the south coast (Bornman et al. 2014, van der Lingen et al. 2016), including the areas where cooling has been reported. Such events may indicate changes in the water mass which promoted their development. Along the South African coastline, highest mussel biomass occurs on the west coast, but large mussel beds can also be found on the south coast (von der Meden et al. 2008). Thus, it becomes important to understand the mechanisms which may have contributed to the development of those red tides and the possible effects of changes in phytoplankton structure and environmental conditions for benthic organisms in the area through the connection of the pelagic and benthic systems. On the south coast of South Africa, rocky shores include four main zones: the littorinid zone, the upper balanoid, the lower balanoid, and the cochlear/mussel zone. Barnacle and mussel zones occupy a great portion of the intertidal, and both taxa exhibit larval development, although their larval stages differ markedly. Mussel larvae, like those of most bivalves, go through different stages from short-lived trocophores to D-stage veligers and eventually to plantigrades which are competent to settle. On the other hand, barnacles typically undergo six naupliar stages before turning to the non-feeding, fast swimming cyprid stage that is able to attach to the substratum and metamorphose into a juvenile (Young et al. 2002). The two taxa are filter feeders, but their mechanisms to capture food particles differ during the larval stages. Mussel larvae use the velum to capture particles which are directed to the oesophagus and eaten or rejected. Meanwhile, the larvae of barnacles use their antennae to capture food particles, resembling a sieving mechanism. The different mechanisms result in different particle size preferences and limitations among taxa, suggesting that changes in food structure in the water column may affect each taxon differently (Vargas et al. 2006). Thus, although the two taxa occupy much of the space on rocky shores along the south coast of South Africa, food conditions may operate differently on the two groups by affecting the period which connects the pelagic to the benthic stages. Understanding the direct or indirect effects of water mass conditions on the pelagic stages is essential to determining possible repercussions for adult communities.

The main mussel species on South African rocky shores are the indigenous *Perna perna* Linnaeus (the brown mussel) and the invasive *Mytilus galloprovincialis* Lamarck (the Mediterranean mussel), although the indigenous *Choromytilus meridionalis* Krauss (the black mussel) can also be found (Branch et al. 2007) and *Semimytilus algosus* has recently become invasive on the west coast (De Greef et al. 2013, Skein et al. 2018). Populations of *P. perna* and *M. galloprovincialis* show different geographical distributions that correspond with their tolerance of physiological stress (Tagliarolo et al. 2016). *M. galloprovincialis* currently extends from the south of Namibia to East London in South Africa (Zardi et al. 2007b). *P. perna* occurs along the south and east coasts of South Africa as two different genetic lineages (Zardi et al. 2007b). Population structure in this species is thought to be driven by differential larval delivery across the surf zone varying on scales of hundreds of meters (Porri et al. 2006). *M. galloprovincialis* and the two different lineages of *P. perna* have different physiological tolerances to physical stressors which affect their metabolism during emersion/immersion periods, and which may influence their competitive abilities (Rius and McQuaid 2006, 2009, Tagliarolo and McQuaid 2015). For example, gaping behaviour in *P. perna* results in lower tolerance to desiccation, which makes *M. galloprovincialis* a better competitor in higher shore areas (Nicastro et al. 2010b). On the other hand, the attachment strength of *P. perna* is superior to that of *M. galloprovincialis*, offering higher resistance to wave exposure in lower or more exposed areas (Zardi et al. 2006a, Nicastro et al. 2010a). Thus, in the areas where the two species overlap, a vertical pattern of distribution appears. *P. perna* dominates the lower mussel zone, *M. galloprovincialis* dominates the upper limit, and the two species form mixed populations in the middle (Bownes and McQuaid 2006).

The main species of barnacles in the intertidal along the south coast of South Africa are *Chthamalus dentatus*, *Tetraclita serrata* and *Octomeris angulosa* (Dye et al. 1992, Boland 1997, Branch et al. 2007). Little research on barnacle population dynamics of these species has been done on this coast compared to mussels. Comparisons between the West and South coasts, although with only one sampling site on the latter at Mossel Bay, point to differences in the pelagic environments between the two systems as the main cause of the higher abundances of barnacles along the South coast (Boland 1997).

1.4. Study aims / overview

The south coast of South Africa has recently experienced red tide events that covered almost the totality of the coast and implied a temporal change in phytoplankton composition (Bornman et al. 2014, van der Lingen et al. 2016). The presence in the water of any red tide forming organism may alter the quality/availability of food and possibly affect organisms which feed on phytoplankton during any stage of their life cycle. Directly, changes in food composition may affect larval development and have the potential to compromise the survival and supply of propagules.

Indirectly, the conditions in the water mass which promote the development of a red tide may affect the duration of larval development or the flows which allow delivery to settlement sites. Thus, conditions during larval stages may compromise propagule availability for adult populations in multiple ways. Due to the particular importance of mussel beds along the south coast, changes in their populations may also affect other organisms that benefit from the habitat created by mussel beds and affect the entire community if that habitat is compromised.

The present thesis used a red tide of unprecedented spatio-temporal scale as a means of examining its effects on the trophodynamics of the intertidal system. Given the large spatial scale of the study, it was logistically impossible to monitor larval settlement and instead recruitment patterns of mussels and barnacles were used to represent one outcome of benthic-pelagic coupling. Recruitment patterns of intertidal mussels and barnacles were used, as they integrate the effects of variability in pelagic conditions during previous larval phases as well as post-settlement processes. Environmental conditions, including food availability, were studied at relevant temporal scales in order to understand their effects on recruitment patterns and to provide insight on how future changes (resembling similar conditions) may influence adult communities. Thus, chapter 2 examines the environmental conditions in the water mass to understand what changes may have led to the development of the red tide. Chapter 3 indirectly studied the effects of changes in the trophodynamics of the system, and the co-occurring environmental conditions, by examining the associated changes in recruitment for the two predominant taxa of intertidal organisms. Chapter 4 studied carryover effects of larval condition for organisms that developed under altered food conditions by examining growth rates of barnacle recruits. Chapter 5 determined the frequencies of temporal variability of temperature and chlorophyll-a in the inner-shelf, and analysed trends in the main conditions which may have affected these coastal areas over the last 15 years in an attempt to infer future trends in physical drivers of the benthic-pelagic coupling. Chapter 6 synthesises the overall findings in the context of the existing literature. In addition, due to the large recruitment abundances encountered, a new sub-sampling methodology was developed to optimise laboratory processing of samples. Such methodology can be extended for future research studies and is presented in Appendix I.

Chapter 2

Environmental drivers of a red tide of the dinoflagellate *Lingulodinium polyedrum* of unprecedented spatio-temporal magnitude along the south coast of South Africa



Red tide observed in Algoa Bay (December 2014).

Environmental drivers of a red tide of the dinoflagellate *Lingulodinium polyedrum* of unprecedented spatio-temporal magnitude along the south coast of South Africa.

2.1. Introduction

Phytoplankton composition and abundance in continental waters of temperate systems vary seasonally. In coastal waters of temperate systems, two peaks of high phytoplankton biomass generally appear in spring and autumn (Brown 1992, Bode et al. 1996). Thus, phytoplankton blooms are usually described as a sudden increase in biomass, produced when the physical and nutritional requirements for growth are met (Cloern 1996). Temporal succession in the phytoplankton community has been described as starting with the bloom of diatoms at the beginning of spring, believed to be triggered by a change in photoperiod and water column physical structure (Sverdrup 1953, Eilertsen et al. 1995, Huisman et al. 1999, Siegel et al. 2002). Due to their physical characteristics, diatoms will bloom using the inorganic nutrients available in the photic zone via the physical processes that promote nutrient replenishment (e.g. upwelling and mixing from deeper waters), and thus, their maximum biomass will be limited by nutrient supply. Around summer, when nutrients in the photic zone become limiting due to higher stability of the water mass, autotrophic and mixotrophic flagellates with the ability to perform vertical migrations to take up nutrients from deeper waters are able to dominate the phytoplankton community (Hasle 1950, Blasco 1978, Cullen and Horrigan 1981). Thus, the advancement of the season could result in an increasingly diverse planktonic community and increased summer productivity.

Some phytoplankton species can reach very high abundances when they bloom in the water mass, and due to the pigments present in the cells, water colouration can change. Because of their characteristic colour, those phytoplankton blooms are commonly referred to as red tides. In the literature, the term Harmful Algal Blooms (HABs) is more frequently used (Anderson et al. 2012), due to the noxious effects that usually accompany high densities of these organism in the water mass. Thus, the terms red tide or HAB do not refer to any particular organism in the phytoplankton community, but to any species that can finally produce any sort of deleterious effect in the marine system (Hallegraeff 2003). Due to this lack of specificity in the general terminology, although the literature preferentially uses the term HAB, the present study will refer to any event of this sort by the term *red tide*, to avoid confusion when discussing blooms of other species in the phytoplankton which do not produce any deleterious effect. Red tide forming organisms have been described in virtually all types of aquatic systems, from freshwater and riverine systems, to brackish and marine systems (Glibert et al. 2005, Paerl and Huisman 2009, Hallegraeff 2010). A focus on marine systems has resulted in the description of organisms that can occupy either the benthic (Mangialajo et al.

2008), or the pelagic realms (Turner and Tester 1997). This widespread distribution is a consequence of considering multiple taxonomic groups in the term *red tide*, including cyanobacteria (Paerl and Fulton 2008), diatoms (Bates and Trainer 2006), and dinoflagellates (Burkholder et al. 2006).

The ecological, economic, or health-related consequences of red tides greatly depend on the species involved (Trainer et al. 2010). The highest concern usually regards species that can produce toxins that affect humans. Some toxins can be accumulated in filter feeders, like shellfish, which are human resources and have the potential to cause human illnesses (Grindley et al. 1969), while other toxins can cause mass faunal mortalities (Grindley et al. 1964). In some cases, the toxins produced can be sprayed into the air by wave action and result in respiratory problems for humans (Pierce et al. 2005, Grattan et al. 2016). Thus, in areas where marine resources are extracted, or aquaculture activities are developed, red tides can directly affect product availability and translate into economic losses (Álvarez-Salgado et al. 2008). Other forms of environmental damage can happen even without the production of toxins, and are related to anoxic conditions due to the accumulation of biomass of the bloom (Glibert et al. 2005), or from the clogging (Zingone and Enevoldsen 2000) or mechanical damage of fish gills (Mardones et al. 2015). Such effects of red tides only address the negative impacts that they can produce on human activities. Nevertheless, red tides can produce changes at the ecosystem level by interfering with nutrient availability for other species in the phytoplankton community, modifying the timing of the peak of phytoplankton biomass, or interfering with grazing pressure (Sunda et al. 2006).

An apparent increase in the frequency, duration, or timing of red tide events has raised concerns during the last few decades (Hallegraeff 1993, Anderson et al. 2002). Due to the threats that these organisms represent in terms of human health (Grattan et al. 2016), and potential economic losses, increasing effort has been applied to understanding the conditions that promote the appearance and persistence of red tides, and to implement methods that improve predictive capability for different types of organisms (Anderson et al. 2001, Glibert et al. 2010, Anderson et al. 2011, Berdalet et al. 2014, Wells et al. 2015). Regarding the environmental conditions that promote their proliferation, each taxonomic group has its own peculiarities and requirements. Among the organisms that can cause red tides in marine systems, dinoflagellates are particularly important (Smayda 1997). A key factor linked to the formation of red tides, is eutrophication (Cloern 2001, Heisler et al. 2008, O'Neil et al. 2012). Relatively isolated water bodies such as lakes or enclosed seas often experience increased concentrations of nutrients of anthropogenic origin. Nevertheless, red tides are not limited to spatially restricted water masses and are frequently observed in areas under the influence of strong seasonal upwelling, like Eastern Boundary Upwelling Systems (EBUSs; Kudela et al. 2005, Trainer et al. 2010, Pitcher et al. 2017). It has been suggested that the relaxation of upwelling could be one of the factors contributing to the development of red tides in areas influenced by upwelling (Fraga et al. 1988, Smayda 2002, Fawcett et al. 2007), as has been suggested

for blooms of different dinoflagellate species (Thomas and Gibson 1990, Smayda 1997, Estrada and Berdalet 1997). This relies on the idea that flagellates are more sensitive to turbulence than diatoms (Margalef 1978, Smayda 1997). Nevertheless, the ability of flagellates to proliferate more efficiently with increased stability in the water column could simply be the result of their ability to exploit different mechanisms to take up nutrients during periods of poor mixing in the euphotic zone, when nutrients have already been depleted, as experienced during the relaxation of upwelling. For example, dinoflagellates have been described as being able to perform vertical migrations, a mechanism which would allow them to take up nutrients in deep waters and return to shallower areas where the light regime is suitable for the photosynthesis (MacIntyre et al. 1997). In addition, many dinoflagellate species have been described as mixotrophs, i.e. depending on nutrient availability they can either photosynthesise or feed on other organisms in the water column (Stoecker et al. 2006). Thus, although the exact mechanisms that influence the development of red tides will be species-specific, the most basic requirement for the proliferation of any phytoplankton species is the availability of nutrients in combination with the appropriate levels of light, temperature, and water mixing.

2.1.1. Red tide occurrence in the South African coast

The coast of South Africa is a transitional region between the Atlantic and Indian Oceans. The differences in the physical properties of the two water masses translate into major biological differences between the West and East parts of the coast. The West Coast is under the influence of the Benguela Upwelling System and dominated by the influence of seasonal upwelling driven by trade winds (Schumann 1987). The south and east coasts are located on the southwest margin of the Indian Ocean and are strongly influenced by the Agulhas Current. The south coast is located in a temperate region, with seasonality in the environmental conditions which drives seasonality in the planktonic system. In general, the phytoplankton community along the south coast has been described to produce biomass peaks in spring and autumn (Brown 1992), as in other temperate systems (Bode et al. 1996, Rivas et al. 2006). Although the south coast experiences localised coastal upwelling in some areas (Schumann 1982), the frequency of events is lower than on the West Coast. Thus, the regular provision of nutrients in the Southern Benguela Upwelling System on the west coast drives the highest productivity along the South African coast (Bustamante et al. 1995). Nevertheless, upwelling centres on the south coast have also been associated with increased productivity (Boyd and Shillington 1994). Red tide events have appeared at high frequencies along the West Coast for decades (Pitcher and Calder 2000), and multiple studies have addressed the relationship between upwelling and red tides in the area (Pitcher and Nelson 2006). Red tide records along the south coast have rarely been reported and their spatial or temporal magnitudes are not particularly big or long lasting (Pitcher and Calder 2000). Nonetheless, a remarkable event

was reported in 2011 along the south coast (van der Lingen et al. 2016), where the dinoflagellate *Gonyaulax polygramma* Stein was present during summer.

In summer 2013, a new red tide caused by the dinoflagellate *Lingulodinium polyedrum* (Stein) Dodge (synonym *Gonyaulax polyedra* Stein), was detected in plankton samples by the South African Environmental Observation Network (SAEON). The dinoflagellate was initially reported inside Algoa Bay (c. 26°E, Fig. 2.1), and later extended along the south coast of South Africa, persisting for several months. *L. polyedrum* is a planktonic marine dinoflagellate distributed almost worldwide. Due to its good response to laboratory culturing, multiple aspects of the biology of the organism have been studied and covered in a very complete review by Lewis and Hallett (1997). The cell is surrounded by a cellulose theca and reaches sizes that range between 42 and 54 µm (see references in Lewis and Hallett 1997). Spherical cysts surrounded by spines can be produced through sexual reproduction, with a variable size between 31 and 54 µm (see references in Lewis and Hallett 1997). Cysts can rest in the sediments and enable the development of new blooms when environmental conditions are favourable. The presence of *L. polyedrum* has been reported in most EBUSs (Walsh et al. 1974, Blasco 1977, Trainer et al. 2010), but its growth has been described as inhibited under certain levels of turbulence in the water due to the detachment of the flagellum (Thomas and Gibson 1990).

The present chapter aims to (1) describe the spatial and temporal extension of the bloom of *Lingulodinium polyedrum*, (2) identify environmental conditions in the water previous to and during the bloom which could have contributed to its development, and (3) address the temporal variability in the water mass adjacent to the south coast and its potential role in altering the structure and/dynamics of the phytoplankton community.

2.2. Materials and methods

2.2.1. Spatio-temporal limits of the red tide

In summer 2013, a red tide caused by the dinoflagellate *Lingulodinium polyedrum* was detected in plankton samples by the South African Environmental Observation Network (SAEON). The dinoflagellate was initially reported inside Algoa Bay (c. 26°E, Fig. 2.1), and later extended both east and west along the south coast of South Africa, persisting for several months. To delimit the spatial and temporal extension of the red tide, satellite imagery of chl-a was examined. Level-3 daily data from the MODIS Aqua satellite were downloaded for chl-a and SST from the Ocean Biology Processing Group (OBPG) from NASA (<https://oceancolor.gsfc.nasa.gov/>), using 4 km resolution (referred to as *pixels*). MODIS Aqua products were selected due to the long-term availability of data (from June 2002 until March 2017 at the moment of the study), which allowed the examination of

conditions during the development of the red tide and during previous years, as opposed to other satellite products released later on (such as VIIRS, for example). Measurements for SST were selected from the 11 μ daytime dataset, and OCx algorithm processed data were selected for chl-a. Images of chl-a and SST were analysed for the period 1st June 2012 until the 31st May 2015. The entire south coast of South Africa was studied, from Cape Agulhas (c. 20°E) to East London (c. 28.5°E), a distance of c. 770km, extending approximately 120km offshore to cover most of the inner Agulhas Bank. Although species composition may have varied between peaks of abundance of *L. polyedrum* in the water (and during the peaks of abundance themselves), previous studies indicate a tendency of red tide blooms to be dominated by a single species (Smayda 1997, Smayda and Reynolds 2003). Thus, although phytoplankton composition during the period of study cannot be determined based solely on remote estimates of chl-a, the possibility of *L. polyedrum* (or other red tide forming organism) contributing significantly to the high chl-a values observed is a reasonable assumption. Values of chl-a over 30mg m⁻³ have been proposed to represent chl-a concentrations characteristic of red tide blooms (Dr. Stewart Bernard, pers. comm.) and this criterion was used to identify the presence of a red tide in this thesis. Thus, the presence of chl-a values over 30mg m⁻³ was analysed for three years: the year when the red tide caused by *L. polyedrum* was observed (from here on referred to as *year 2014* for simplicity), the previous year (referred to as *year 2013*) and the following year (referred to as *year 2015*). Data for each year were divided by season following the definitions used by Brown (1992), i.e. June – August (winter), September – November (spring), December – February (summer), and March – May (autumn). For each season of each year, and for each individual pixel, values of chl-a that indicated a red tide were recorded (i.e. the number of days per season where each pixel exceeded the 30mg m⁻³ threshold was calculated). However, temporal persistence of individual blooms within each season cannot be inferred from satellite data alone. For example, the intrinsic presence of gaps in satellite data (resulting from cloud coverage, for example), or the development of sub-surface blooms before conditions are observed at the surface, prevent satellite measurements being used to analyse the totality of days where conditions indicated a red tide. In fact, Probyn et al. (1994) described the presence of sub-surface chl-a maxima in nearshore waters along the Agulhas Bank (eastwards of Cape Agulhas), and in the area of the cold-ridge. Although surface chl-a estimates from satellite are limited and cannot describe the development of blooms when they are initiated at depth or during phases of low cell densities, the presence of chl-a values exceeding the established chl-a threshold offered a simple estimate of presence/absence of values indicative of red tides. Therefore, the temporal persistence of individual blooms within each season cannot be inferred at fine spatio-temporal scales due to these limitations and the results should be taken with caution, considering that higher spatial or temporal extension may have occurred without being detected. Nonetheless, values of chl-a over

the selected threshold indicated that chl-a reached levels beyond an average phytoplankton bloom and should be taken into consideration when examining possible effects for higher trophic levels.

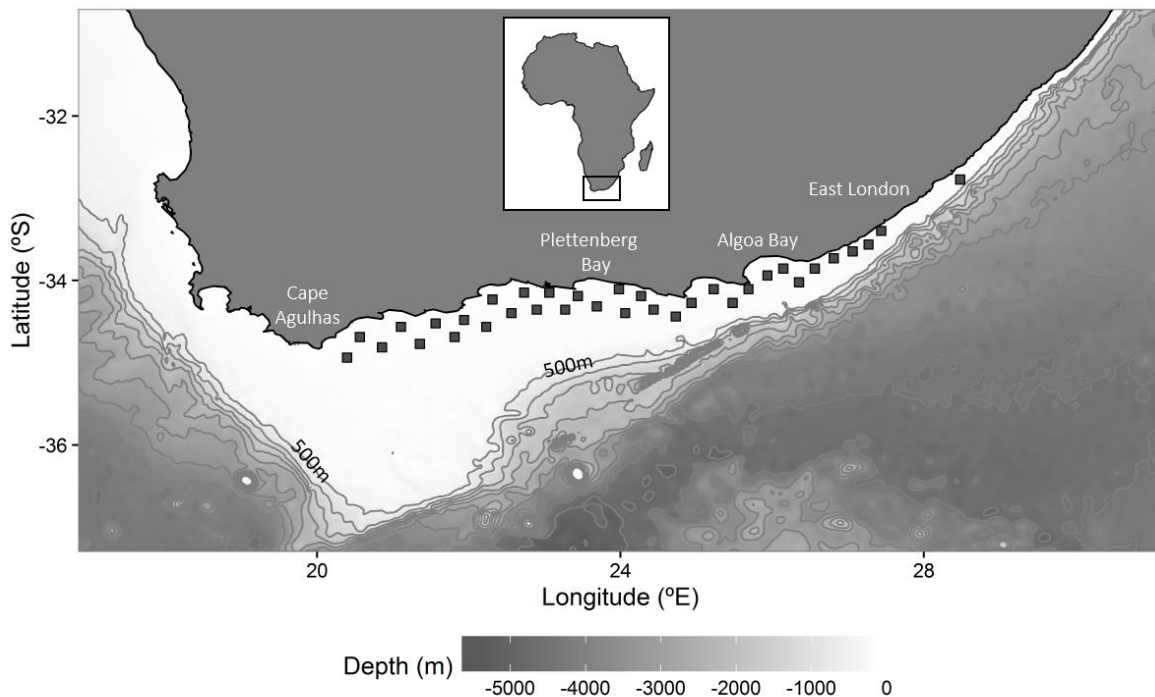


Fig. 2.1. Map of the South Coast of South Africa with bathymetric profile. Contour line around the white area delimits the 500m isobath. Grey squares represent the 35 sites along the coast where chl-a, SST, upwelling index and turbulence were estimated to examine the environmental conditions before the red tide of 9th February 2014.

2.2.2. Environmental conditions co-occurring with high chl-a concentrations

Daily values of chl-a along the coast were evaluated during summer and autumn to delimit the red tide. Four specific dates were selected when the spatial extension of the red tide seemed to be represented at a broad spatial scale along the coast: the 9th of February, the 13th of March, the 28th of April, and the 18th of May 2014. For each of these dates, chl-a values were extracted for the same areas along the coast as in the previous analysis, at 4km resolution. SST data were obtained from the OBPG from NASA (<https://oceancolor.gsfc.nasa.gov/>) and used to determine the temperature conditions before the development of the bloom on each day. Eight-day averages of SST (11 μ daytime) were obtained from level-3 MODIS Aqua images, also with 4km resolution and for the same area. Four images of eight-day averages were used to describe the conditions prior to each date selected for chl-a, thus covering approximately one month of temperature data (Table 2.1).

During autumn 2015, chl-a values over 30mg m⁻³ were again detected at high frequencies along the south coast of South Africa (Fig. 2.2.), indicating that the phytoplankton present in the water reached chl-a levels characteristic of a red tide. During that period, the dinoflagellate *Noctiluca*

scintillans was present in plankton samples collected by SAEON in Algoa Bay (26°E; Dr. Thomas G. Bornman, pers. comm.). Thus, following the same approach used for *L. polyedrum* in 2014, chl-a and SSTs conditions were examined for five of the best satellite images that depicted the event of 2015 along the coast: the 9th of March, the 31st of March, the 8th of April, the 19th of April, and the 12th of May 2015. In this case, chl-a was examined approximately every two weeks, and eight-day averages of SST were examined for the period between the 8th February 2015 and the 14th May 2015 because the chl-a measurements were not evenly spaced in time.

Table 2.1. Dates selected to study the *Lingulodinium polyedrum* red tide, and overall period of eight-day averages of SST used to examine approximately one month of temperature prior to the development of the bloom on each day (right hand column).

SST measurements		Selected dates for <i>L. polyedrum</i> red tide
Start date	End date	
07/01/2014	07/02/2014	09/02/2014
08/02/2014	11/03/2014	13/03/2014
28/03/2014	28/04/2014	28/04/2014
13/04/2014	14/05/2014	18/05/2014

Chlorophyll-a values on the 9th of February 2014 were used to examine the environmental conditions in the water mass that could have contributed to the development of the bloom at a short time scale, using upwelling index, turbulence, and SST as the variables most likely to have contributed to bloom development. This allowed the examination of the relationship between chl-a and environmental conditions at a specific time across a large spatial area through linear regression. Analysis was limited to a single date because the ranges in the environmental conditions during the entire period when the red tide occurred would have obscured any underlying pattern if several dates were to be used. For that date, 35 pixels were selected along the coast to cover a wide range of chl-a values, from low concentrations to values that would indicate the presence of the red tide (Fig. 2.1). For each of those 35 sites, daily satellite SSTs (level-3, 11 μ daytime SST, OBP, NASA; <http://oceancolor.gsfc.nasa.gov/>) were selected with 4km resolution. Zonal and meridional daily wind speed at 10m height were obtained from the European Centre for Medium-Range Weather Forecasts Reanalysis (ERA – Interim dataset downloaded from <http://apps.ecmwf.int/>), with 0.125° resolution for each of the 35 sites. An upwelling index was calculated as a component of the Ekman transport in the N-S direction, initially described by Bakun (1973), as follows,

$$UPW = \rho_a * C_D * v * v_x * f^{-1} * \rho_w^{-1} \quad (\text{Eq. 2.1})$$

where ρ_a represents air density (1.22 kg.m⁻³), C_D is drag coefficient (0.0014), v is the wind velocity, v_x is the alongshore vectorial component of wind speed (the west-east component of wind), f is the

Coriolis parameter (9.96×10^{-5} at middle latitudes) and ρ_w is water density (1025 kg.m^{-3}). Positive values of the upwelling index can be interpreted as offshore displacement of the surface water mass, indicative of upwelling, and negative values as downwelling. Turbulence was estimated following Pringle (2007) as,

$$\varepsilon = (v/1000)^3 * k^{-1} \quad (\text{Eq. 2.2})$$

where v is the wind velocity and k is the Von Karmen's constant (0.41). To determine the conditions and the period of time that would explain the patterns in chl-a best, one to seven-day moving averages were calculated from the 9th of February and going backwards up to one week for each variable. Simple linear regressions were performed for each variable for all the time lags using the function *lm* from the package *stats* in R version 3.2.0. (R Core Team 2015).

2.2.3. Seasonal environmental conditions

SST – Seasonal averages of SST were calculated from MODIS Aqua daily data with 4km resolution for each year between June 2013 and May 2015, inclusive. Seasons were defined as above. Seasonal anomalies in SST were calculated using eight-day averages of SST from MODIS Aqua, with 4km pixel resolution. For each pixel, seasonal anomalies were calculated as the difference between the average SST in each pixel for each season of each year and the general average on each pixel for the entire time series (from July 2002 until April 2017).

Chl-a – Seasonal averages of chl-a were calculated for the same temporal series as SST anomalies, also using eight-day averages with 4km resolution.

Winds – Zonal and meridional monthly wind speeds at 10m height from ERA – Interim, with 0.125° resolution, were used to calculate seasonal averages along the coast (from July 2002 until March 2017).

Currents – Water currents were obtained from the Hybrids Coordinate Ocean Model and Navy Coupled Ocean Data Assimilation (HYCOM + NCODA) Global Analysis GLBu0.08, experiments 90.9, 91.0 and 91.1, depending on the periods required (data downloaded from the ERDDAP server from [NOAA](https://erddap.noaa.gov/)). The area selected covered the south coast from 20 to 28.5°E and offshore to 36°S , with 0.08° resolution. Seasonal averages were calculated for the three years of interest between June 2012 and May 2015. All figures were plotted using the package *ggplot2* (Wickham 2009) in R version 3.2.0. (R Core Team 2015).

2.3. Results

2.3.1. Spatio-temporal limits of the red tide

Around December of 2013, at the beginning of austral summer, SAEON reported a red tide-forming dinoflagellate, *L. polyedrum*, in plankton samples from Algoa Bay (c. 26°E). The number of days per season when chl-a values exceeded 30mg m⁻³ was estimated for the three years of study (Fig. 2.2). For all the seasons of each year, some pixels exceeded the threshold, which could have been due to very productive blooms (produced by red tide-forming organisms, other organisms in the phytoplankton, or by high amounts of particulate organic matter). During spring 2014 (Fig. 2.2F), chl-a values over the threshold could be observed in Algoa Bay (c. 26°E), where the presence of *L. polyedrum* was originally confirmed from plankton samples. During summer and autumn 2014, higher frequencies were detected, and larger areas were affected (Fig. 2.2G-H). Thus, during summer of 2014, i.e. the *L. polyedrum* red tide, chl-a values over 30mg m⁻³ extended along the coastline between 22 and 28°E, extending approximately c. 30-40km offshore. In addition, high values of chl-a extended further offshore showing a tongue towards the west, in the centre of the Agulhas Bank (c. 21-22°E). During autumn (Fig. 2.2H), *L. polyedrum* extended along the entire south coast between the 20 and 28.5°E, with particularly high frequencies between Mossel Bay (c. 22°E) and Plettenberg Bay (c. 23°E). During autumn the following year (Fig. 2.2L), high frequencies of chl-a over the threshold considered were again detected, indicating the occurrence of a second red tide. Plankton samples collected by SAEON attributed this second red tide to *Noctiluca scintillans*, another red tide-forming dinoflagellate. The highest frequencies found during the bloom of *N. scintillans* in autumn were also found between Mossel Bay and Plettenberg Bay, but with high chl-a frequencies also around Tsitsikamma (c. 24°E).

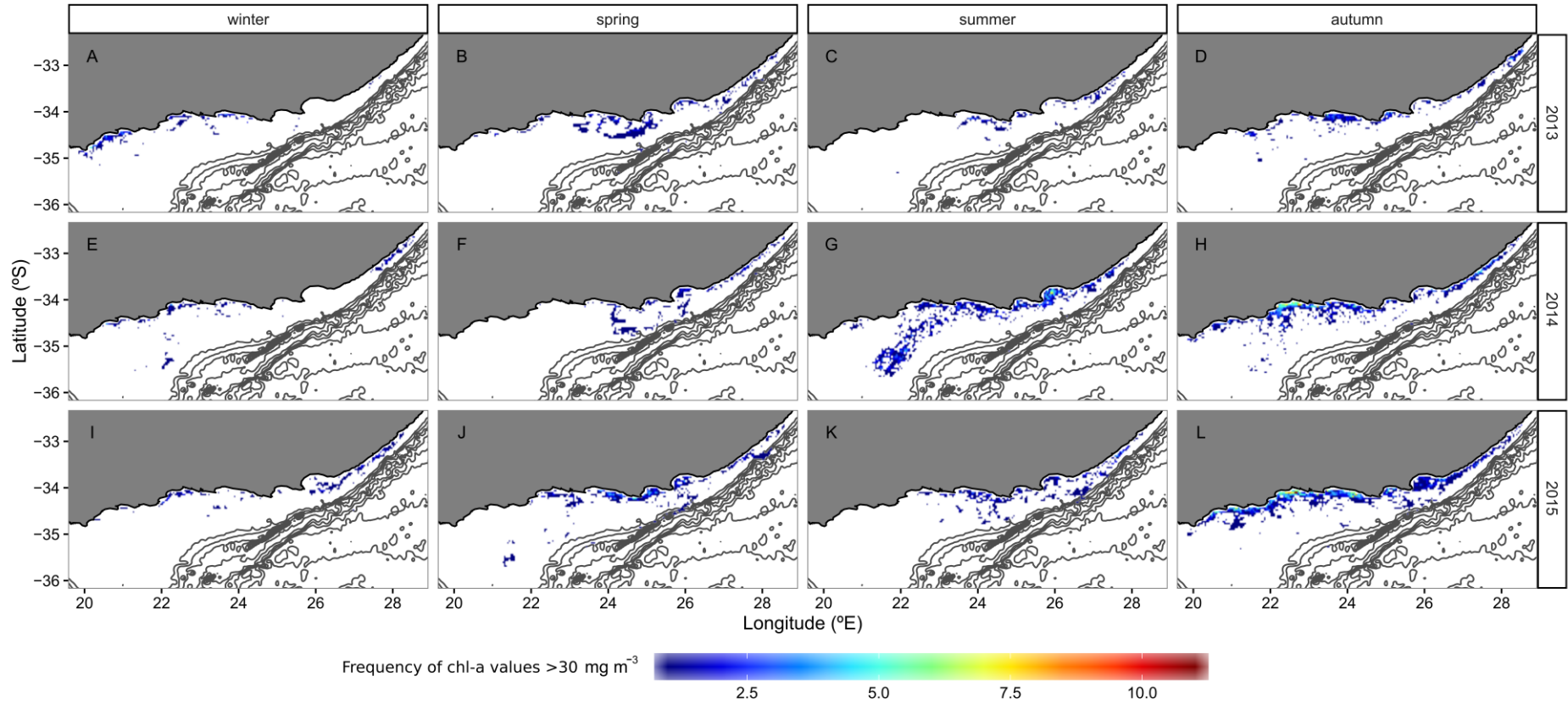


Fig. 2.2. Number of days per season and year where chl-a exceeded 30 mg m⁻³ along the South Coast of South Africa. Year 2013 corresponds to a year without a reported red tide, year 2014 to the *Lingulodinium polyedrum* red tide, and year 2015 to the *Noctiluca scintillans* red tide.

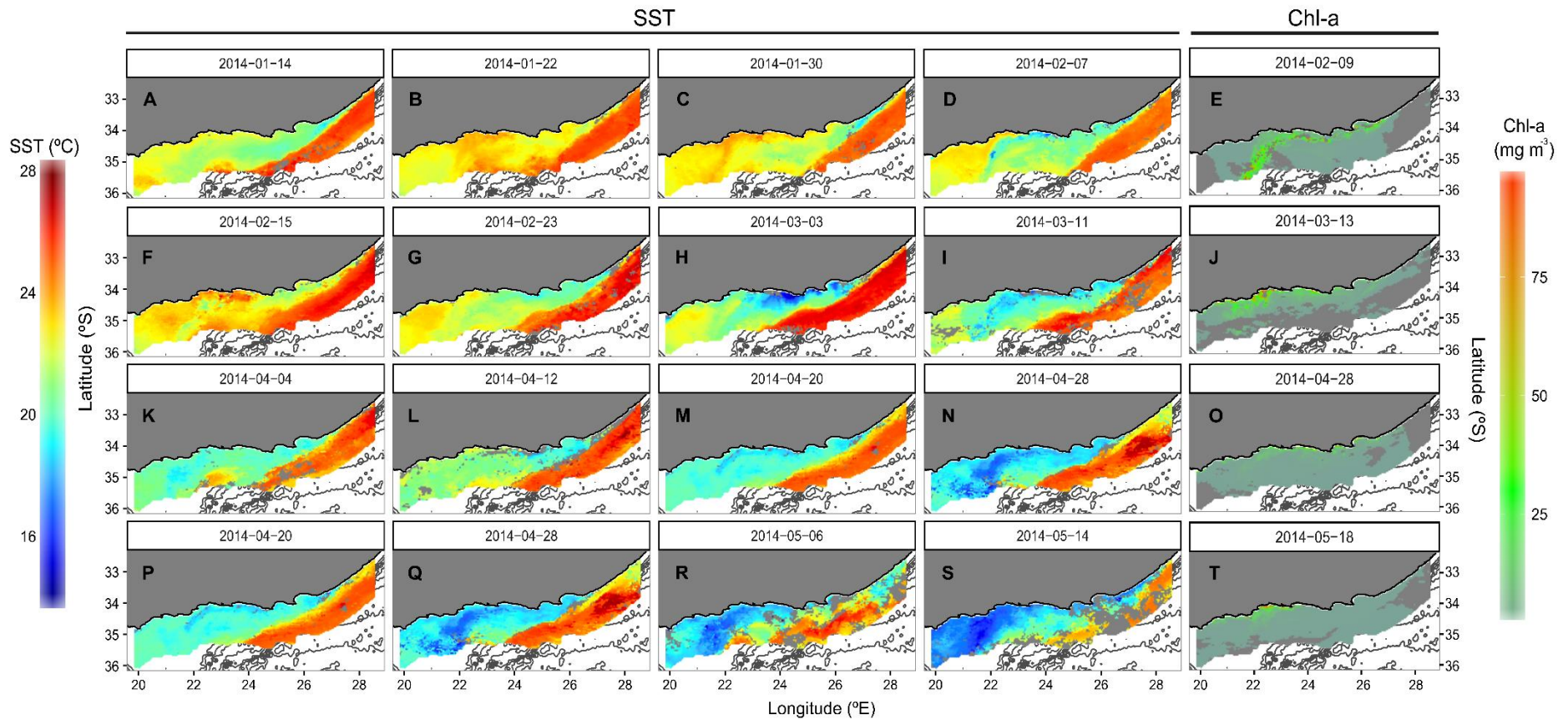


Fig. 2.3. Daily values of chl-a (mg m^{-3}) along the South Coast of South Africa on four selected dates to show the *Lingulodinium polyedrum* red tide (E, J, O, T). Bright green represents values of chl-a that exceeded the red tide threshold selected (30 mg m^{-3}). The four panels preceding each chl-a map show eight-day averages of SST ($^{\circ}\text{C}$) prior to each selected chl-a date (see Table 2.1). Grey areas represent missing data in all panels. Contour lines represent the bathymetry. Note that panels M-N are the same as P-Q and SST images are not continuous.

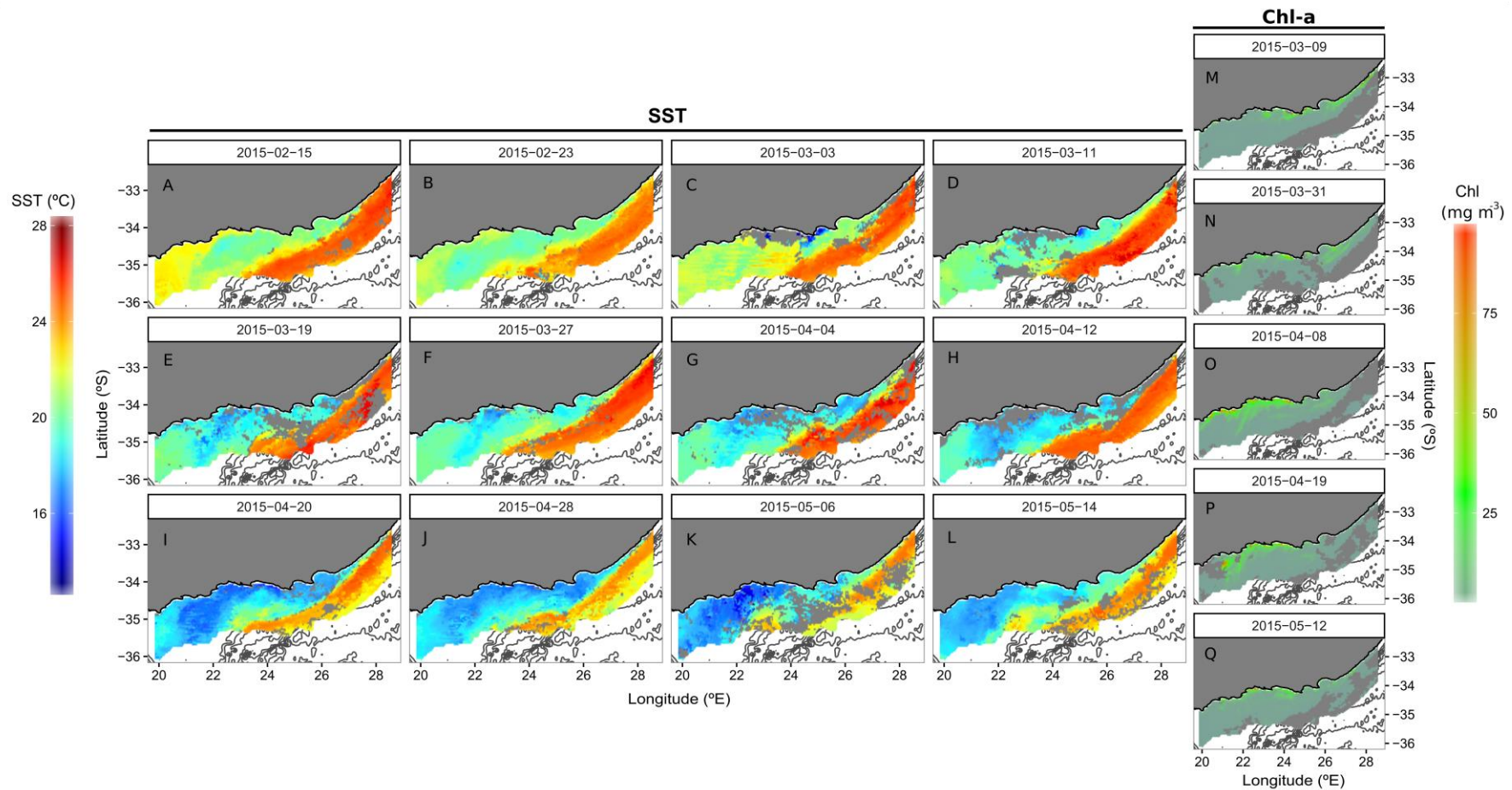


Fig. 2.4. Values of chl-a (mg m^{-3}) for five selected dates in austral autumn of 2015 along the South Coast of South Africa (M – Q). Chl-a values in panels M – Q represent the bloom caused predominantly by *Noctiluca scintillans*. Chl-a values were too close in time so eight-day averages of SST ($^{\circ}\text{C}$) were represented for the period from the 7th February 2015 to the 14th May 2015. Grey areas represent missing data in all panels. Contour lines represent the bathymetry profile.

2.3.2. Environmental conditions co-occurring with high chl-a concentrations

The best four satellite images when *L. polyedrum* seemed to be present in the water were selected, one for each month, between February and May 2014 (Table 2.1). In general, warm periods of SST, followed by cooling of the waters around the upwelling centres located around Plettenberg Bay (c. 24°E) and Port Alfred (c. 27°E), which can provide nutrient-rich cold waters from deeper layers, (see Chapter 1), seemed to result in *L. polyedrum* blooming within a period of a month (Fig. 2.3).

9th February 2014 – The spatial extension of the *L. polyedrum* red tide was highest in February (Fig. 2.3E), extending along the coast between the 22 and 27°E, and extending further offshore in the central area (c. 21-22°E). Eight-day composite images of SST (Fig. 2.3A-D) covering approximately one month before the date selected for chl-a, revealed warm surface waters which extended along the south coast, particularly over the central area (c. 21-24°E) during the last two weeks of January (Fig. 2.3B-C). Thus, the water mass experienced some warming in average SST compared to the previous eight-day period (Fig. 2.3A), except for the area around Port Alfred (c. 27°E), where a semi-permanent upwelling cell is located (Lutjeharms 2006). During the period between the 31st of January and the 7th of February (Fig. 2.3D), cold waters were observed in the central area of the south coast (c. 22-24°E), which suggests the upwelling of bottom waters around the upwelling cell located around the Plettenberg area, and in the area southwest of Port Alfred (c. 27°E).

13th March 2014 – Red tide levels of chl-a were found closer to the coast (Fig. 2.3J) than on the 9th of February, extending from Cape Agulhas (c. 20°E) to St. Francis (c. 25°E), and inside both St. Francis Bay (c. 25°E) and Algoa Bay (c. 26°E). Two weeks of warm SST during mid-February (between the 8th and the 23rd of February) followed the red tide of the 9th of February. Again, cold waters appeared in the central area of the south coast (c. 22 – 27° E) during approximately two weeks before the bloom of the red tide on the 13th of March.

28th April 2014 – The spatial extent of the red tide in April was greatly reduced (Fig. 2.3O) compared to the previous two months. Its presence was constrained to the first few km off the coast, between Mossel Bay (c. 22°E) and St. Francis (c. 25°E), and inside the bays of St. Francis and Algoa (c. 25 and 26°E, respectively). Red tide levels of chl-a were also found around Cape Agulhas (c. 20°E), and between Cape Infanta (c. 21°E) and Jongensfontein (c. 21.5°E). At the beginning of April, surface waters over the continental shelf were cooler than during the previous months, although coastal waters around Mossel Bay (c. 22°E) experienced some warming between the 5th and 12th of April, with subsequent cooling for another two weeks, before the appearance of high chl-a levels.

18th May 2014 – By May, the *L. polyedrum* red tide had reduced considerably in spatial extent and was mostly found around Mossel Bay (c. 21 – 23°E), with some traces around Cape Infanta (c. 21°E), (Fig. 2.3T). After the week of the 20th of April, surface waters continued to cool offshore over the Western

Agulhas Bank between the 21st of April and the 14th of May (Fig. 2.3Q-S). The red tide was constrained to around Mossel Bay, in areas where slightly warmer water seemed to have been retained close to the coast, when upwelling started to intensify between the 21st of April and the 7th of May (c. 22°E, Fig. 2.3Q-R).

During autumn 2015, a bloom of *N. scintillans* along the south coast was also examined. In general, visual inspection of SST conditions during that period did not show any evident change in the water mass conditions prior to the dates selected to depict the bloom of *N. scintillans* (Fig. 2.4F-Q). During March 2015, *N. scintillans* seemed to be close to the coast (Fig. 2.4A-B), extending mostly between c. 23 and 28°E. The maximum spatial extension was reached during April (Fig. 2.4C-D), when the bloom extended between c. 20 and 25°E along the coast, but also spread further offshore than during March. At the middle of May, the bloom was only found close to the coast (Fig. 2.4E).

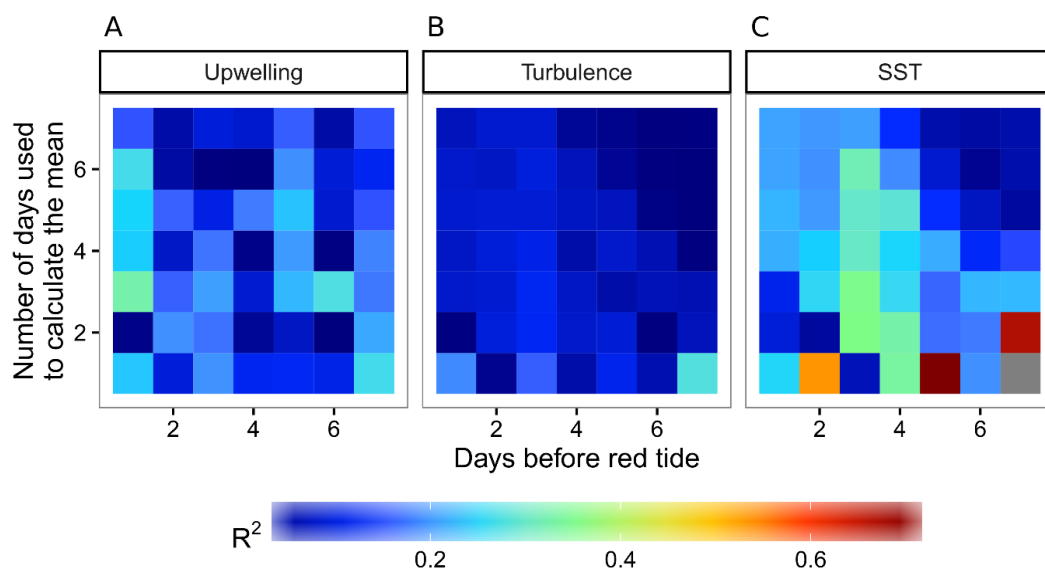


Fig. 2.5. R² values from lagged linear regression models for upwelling index (A), turbulence (B) and SST (C). The horizontal axis represents the number of days before the *L. polyedrum* bloom for the 9th of February 2014, with *one* being the red tide day. Vertical axis represents the number of days that were averaged for each linear regression.

Simple linear regressions using different temporal lags were used to try to ascertain the conditions that could have promoted the bloom of *L. polyedrum*, focusing specifically on the bloom observed on the 9th of February. As visual inspection of the environmental conditions for *N. scintillans* did not show evident patterns in SST conditions, the analysis was not performed for that species but only for *L. polyedrum*. Upwelling index, turbulence, and SST were selected, as these variables are likely to

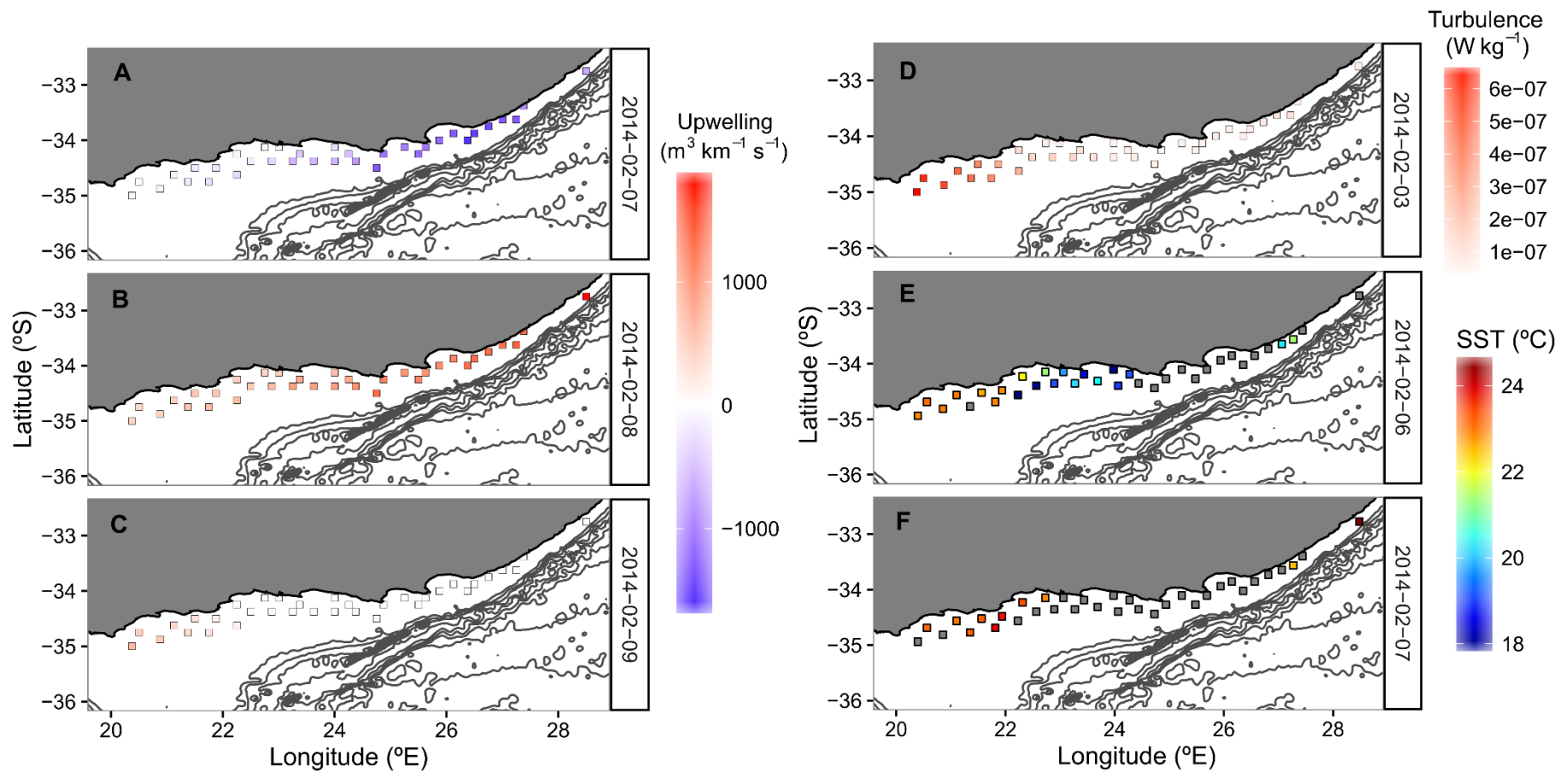


Fig. 2.6. Values of upwelling index (A – C), turbulence (D), and SST (E – F) for the time lags that best explained the chl-a values observed on the 9th of February 2014 along the South Coast of South Africa, selected from linear regression analysis. Note that each variable has its own scale. Negative values of upwelling index indicate downwelling and positive upwelling. Grey squares represent missing data.

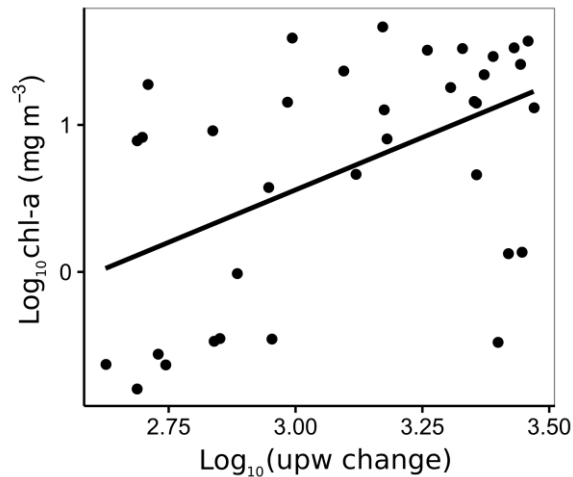


Fig. 2.7. Linear regression ($R^2=0.25$; $p<0.01$) between log-transformed chl-a (mg m^{-3}) and upwelling change (unitless, difference between upwelling index on the 8th and 7th of February).

modify the conditions in the water mass at short-time scales and to influence water column stability and nutrient availability. In the case of upwelling, the time period that best explained the appearance of the red tide bloom was an average of three days before the development of the bloom (Fig. 2.5A). Thus, the best temporal lag of upwelling explained 32.4% of the variance in chl-a on the day chl-a was estimated ($F_{1,33}=15.81$; $p<0.001$). Inspection of the upwelling index along the coast revealed that during the three-day lag before the appearance of the red tide, a reverse in upwelling conditions was observed, from downwelling to upwelling, with another change to neither upwelling or downwelling on the day when chl-a was measured (Fig. 2.6A-C). For turbulence, the conditions that best explained the bloom occurred seven days before the bloom (Fig. 2.5B). Turbulence seven days before the red tide explained 27.4% of the variance ($F_{1,33}=12.46$; $p<0.01$). In general, low turbulence was present in the area, except for the westernmost part of the Agulhas Bank (Fig. 2.6D). The area of low turbulence seems to correspond well with the area where the bloom appeared on the 9th of February (Fig. 2.3E). In the case of SST, the three models that explained the highest levels of variance (over 50%, Fig. 2.5C) had to be discarded due to the presence of high numbers of missing values of chl-a when the regression models were performed. A cluster of multiple time periods seemed to explain similar amounts of variability (around 35%). The best model for SST involved SST three days before the red tide, averaged over the two preceding days. This explained 35.7% of the variance ($F_{1,21}=11.66$; $p<0.01$). Inspection of SST values over the lag period of interest showed that a high proportion of the SST values used for the linear regressions were missing (missing data=71.4%, Fig. 2.6E-F). This suggests that the use of daily values for SST in this context could be unreliable. Although the negative relationship of chl-a with upwelling and SST can be contradictory, lagged linear regressions were used to select the time periods which explained the highest percentage of variance (Fig. 2.5), but both predictors do not necessarily need

to describe the same mechanism. Based on previous mechanisms that promote the appearance of red tides in surface waters (e.g. Ryan et al. 2017), SST conditions could depict the period of cell growth while upwelling would be related to the vertical transport of the dinoflagellate population to the surface. To determine the effect of upwelling on dinoflagellate vertical transport, change in upwelling conditions was examined. Upwelling rates from the best time lag were used to calculate the change in upwelling as the difference between the 8th February and the 7th February. A significant positive relationship was present between upwelling change and chl-a (both transformed to the logarithm of base 10 to better represent a linear relationship; Fig. 2.7; $R^2=0.25$; $p<0.01$). Because positive values of upwelling index denote upwelling and negative downwelling, a positive relationship between chl-a and upwelling change would indicate more chl-a with a more intense reverse from downwelling to upwelling. Finally, the conditions present for each of the best models were tested for multicollinearity between predictors. All variables were found to be correlated and thus, no multiple regression model could be performed to identify the combined effects of more than one variable.

2.3.3. Seasonal environmental conditions

Differences in seasonal averages of SSTs along the south coast of South Africa were observed among the years of study before, during and after the development of the *L. polyedrum* red tide. In general, winter temperatures did not vary greatly among years, but surface waters over the shelf were warmer during spring and especially during summer of 2014, the year when *L. polyedrum* bloomed. Thus, seasonal averages calculated for 2014, the previous, and the following years, revealed that during winter 2014, the only obvious difference among winters was a mass water located around Algoa Bay (c. 26°E) which was colder and could be detected further offshore than in the other two years (Fig. 2.8E). The Agulhas Current extended westwards resulting in higher surface water temperatures over the central area of the coast off the continental shelf (c. 22 – 24°E; Fig. 2.8E). During spring 2014, warmer SSTs were found over the continental shelf in comparison with the other two years (Fig. 2.8F). Warm temperatures over the shelf prevailed during summer 2014, and colder waters were found only around the upwelling cell of Port Alfred (c. 27°E; Fig. 2.8G). During 2015 (Fig. 2.8I-L), colder waters were found over the continental shelf from spring until autumn (Fig. 2.8J-L). Thus, SSTs in the Agulhas Bank during 2015 were colder than the two previous years, particularly during summer (Fig. 2.8K).

Seasonal SST anomalies calculated for MODIS Aqua revealed quite obvious periodicity throughout the series (Fig. 2.9), with cycles of three to four years when temperatures were above or below the general average for the series. Spring and summer of 2013-2014, i.e. the year of the *L. polyedrum* red tide, showed higher temperatures than the general averages for those two seasons (Fig. 2.9). SSTs slightly above the general average were also present over the shelf during spring and summer of

2011-2012 (Fig. 2.9), when a bloom of *Gonyaulax polygramma* (van der Lingen et al. 2016), occurred along the south coast of South Africa. Nevertheless, temperatures over the shelf from spring until autumn of 2014-2015 were below the average for each season (Fig. 2.9), particularly during autumn, when *N. scintillans* appeared at the highest frequencies (Fig. Fig. 2.2L).

During spring and summer of 2014, the warmer SSTs observed over shelf waters, and particularly over the Agulhas Bank, were thought to have come from surface waters of the Agulhas Current. Thus, surface currents during spring and summer 2014 were expected to have introduced warm waters from the Agulhas Current towards the west, either through stronger, more persistent westwards flow, or through a change in the direction of water flow onto the shelf. Seasonal averages of surface currents showed strong differences in water velocity in the core area of the Agulhas Current among years (Fig. 2.10), but no obvious differences were evident in directionality or current speed that intruded onto the Agulhas Bank between 22.5 and 25°E as would have been expected based on the warm SSTs observed. In spring 2014 (Fig. 2.10F), the inner border of the Agulhas Current flowed further from the shelf edge than during the two other years. This would suggest that the warm waters observed over the Agulhas Bank during spring and summer of the red tide year were not influenced by an anomalous delivery of water from the Agulhas Current, but by a different process.

During winter of 2012, 2013 and 2014, strong westerly winds were present along the entire south coast (Fig. 2.11). Wind strength during those three years was higher than for most of the other winters observed in the series. During spring 2013-2014, during the bloom of *L. polyedrum* (Fig. 2.12B), strong south-westerly winds, which promote downwelling conditions, were present over the continental shelf. Strong south-westerly winds were also present during spring of 2011-2012 (Fig. 2.12A), during the bloom of *G. polygramma* over the Agulhas Bank (van der Lingen et al. 2016). Due to the orientation of the south coast of South Africa, winds from the west produce downwelling. Downwelling conditions (or upwelling relaxation), as well as solar radiation, will promote stability and contribute to the warming of surface waters. This would agree with the warm surface temperatures observed over the shelf during spring and summer during the *L. polyedrum* red tide (Fig. 2.9).

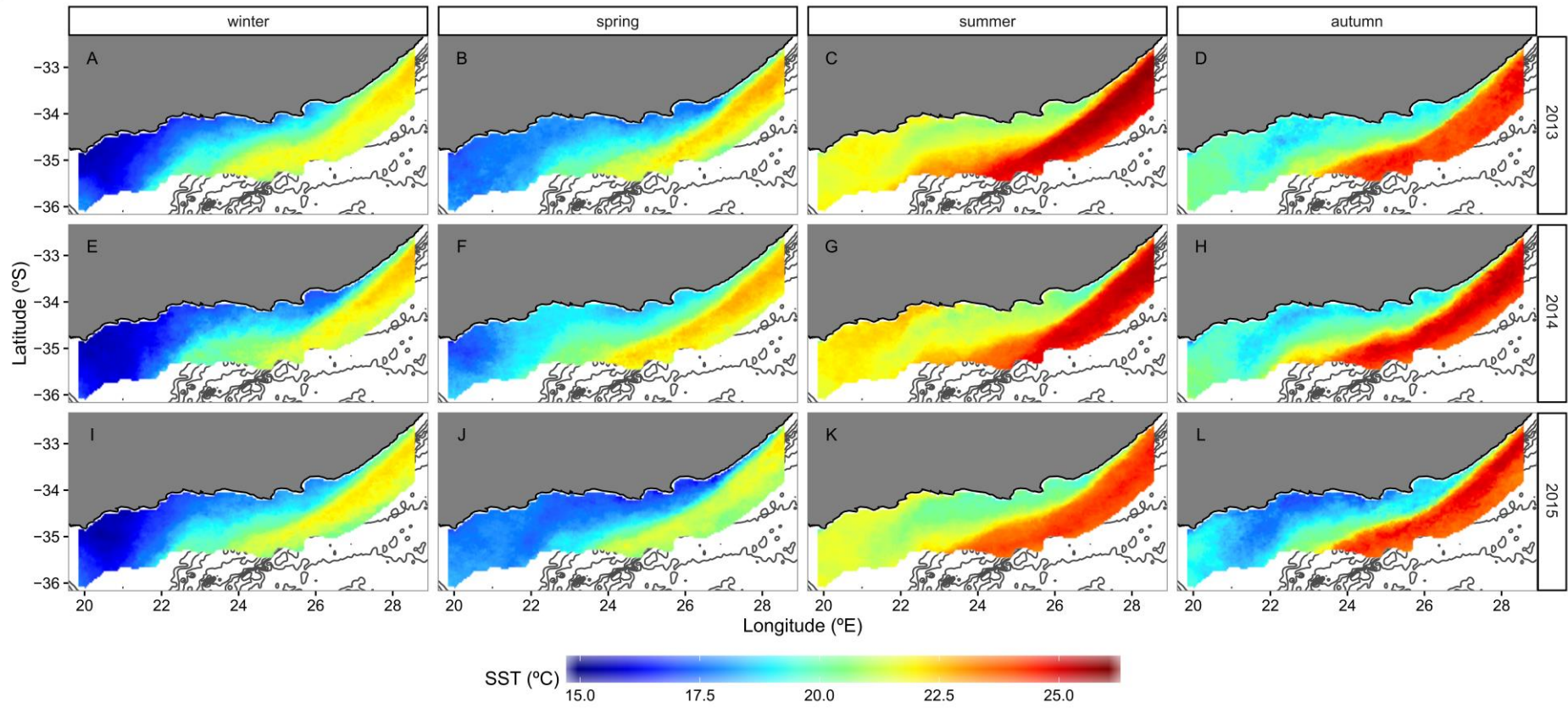


Fig. 2.8. Seasonal averages of SST (°C) for the year of the *L. polyedrum* red tide, the previous and the following years along the South Coast of South Africa.

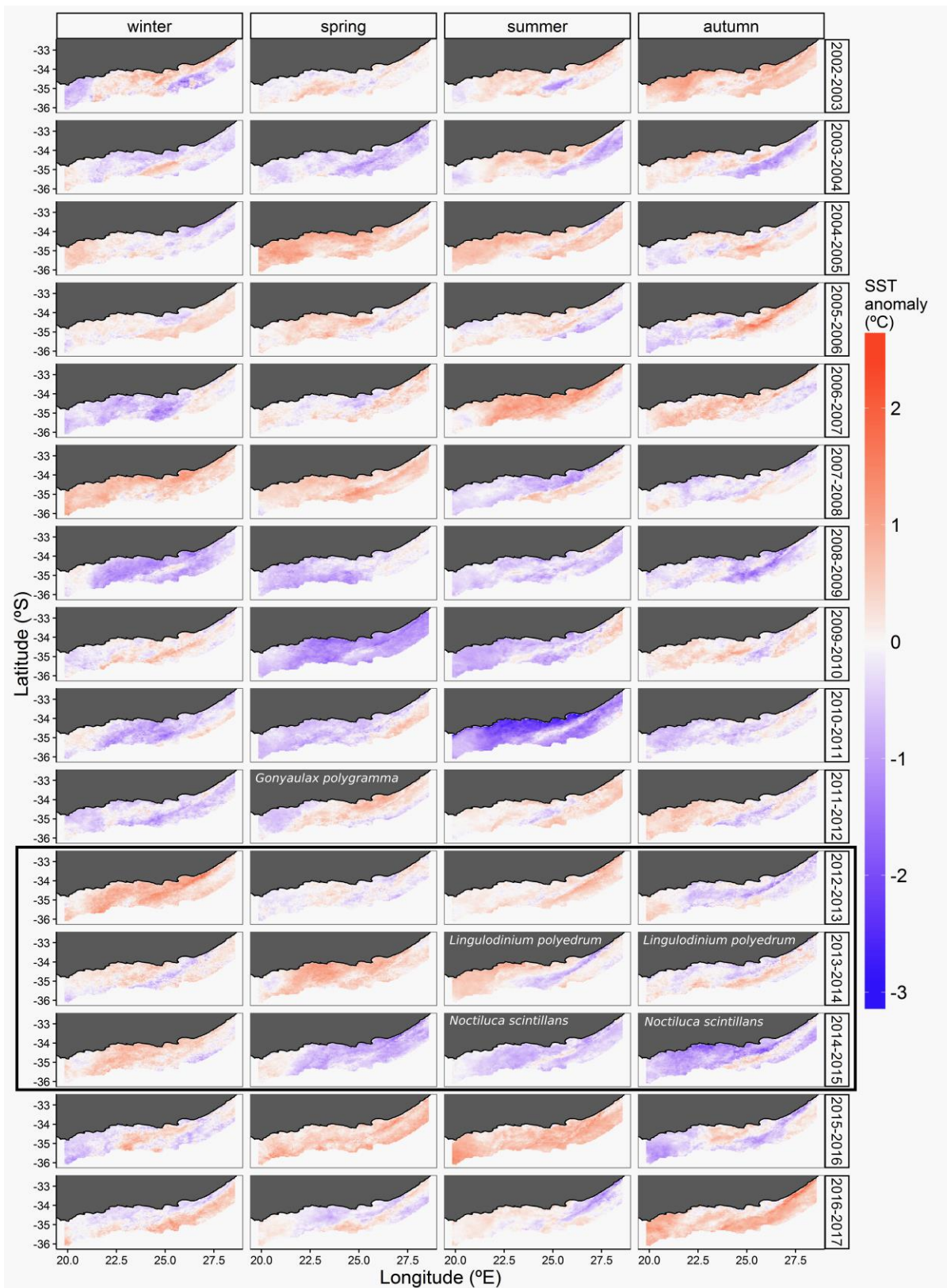


Fig. 2.9. Seasonal anomalies in SST ($^{\circ}\text{C}$) from July 2002 until 2017, calculated from eight-day averaged data at 4km resolution. Positive values (red) are interpreted as higher seasonal temperatures for the year than for the long-term seasonal average, and negative values (blue), as the opposite. The three years used for the rest of the analysis are delimited by the black box. Occurrence of red tides is indicated in the relevant panels.

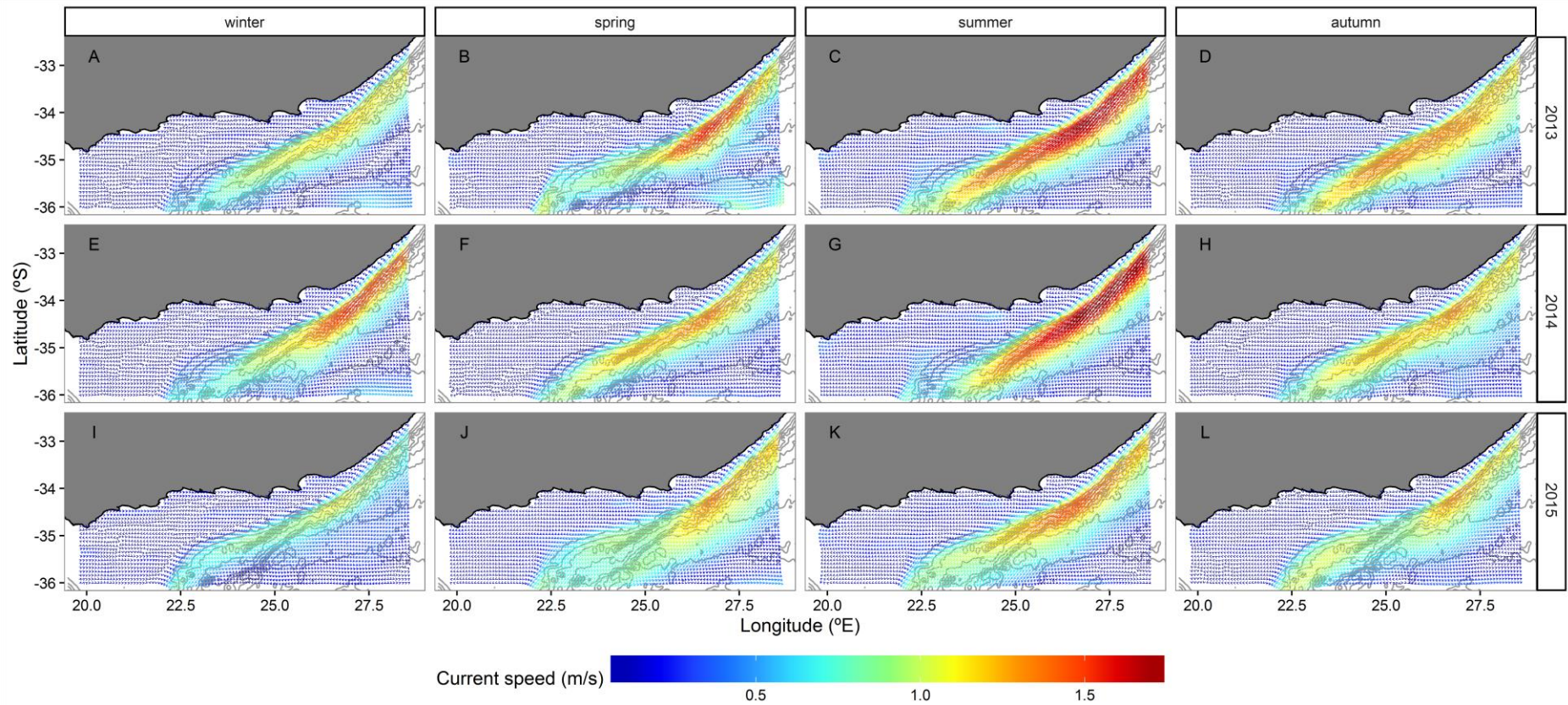


Fig. 2.10. Seasonal averages of surface water currents calculated from daily data produced in HYCOM+NCODA models along the South Coast of South Africa for 2013, 2014, and 2015. Both colour and length of the vector represent current speed (m s^{-1}).

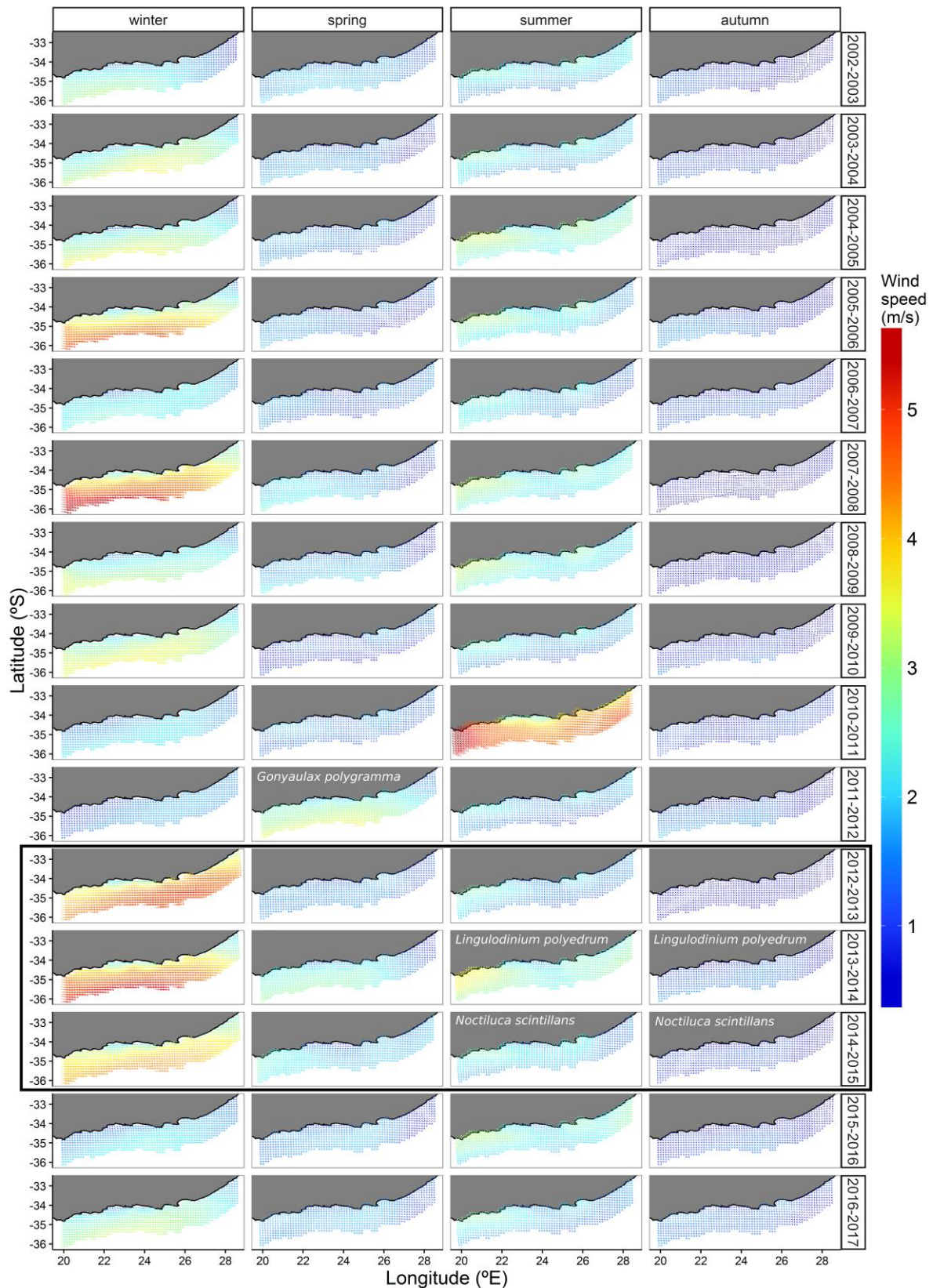


Fig. 2.11. Seasonal averages of wind speed (m s^{-1}) from July 2002 until March 2017, calculated from monthly averaged data. Both colour and length of the vector represent wind speed (m s^{-1}). The three years used for the rest of the analysis are delimited by the black box. Occurrence of red tides is indicated in the relevant panels.

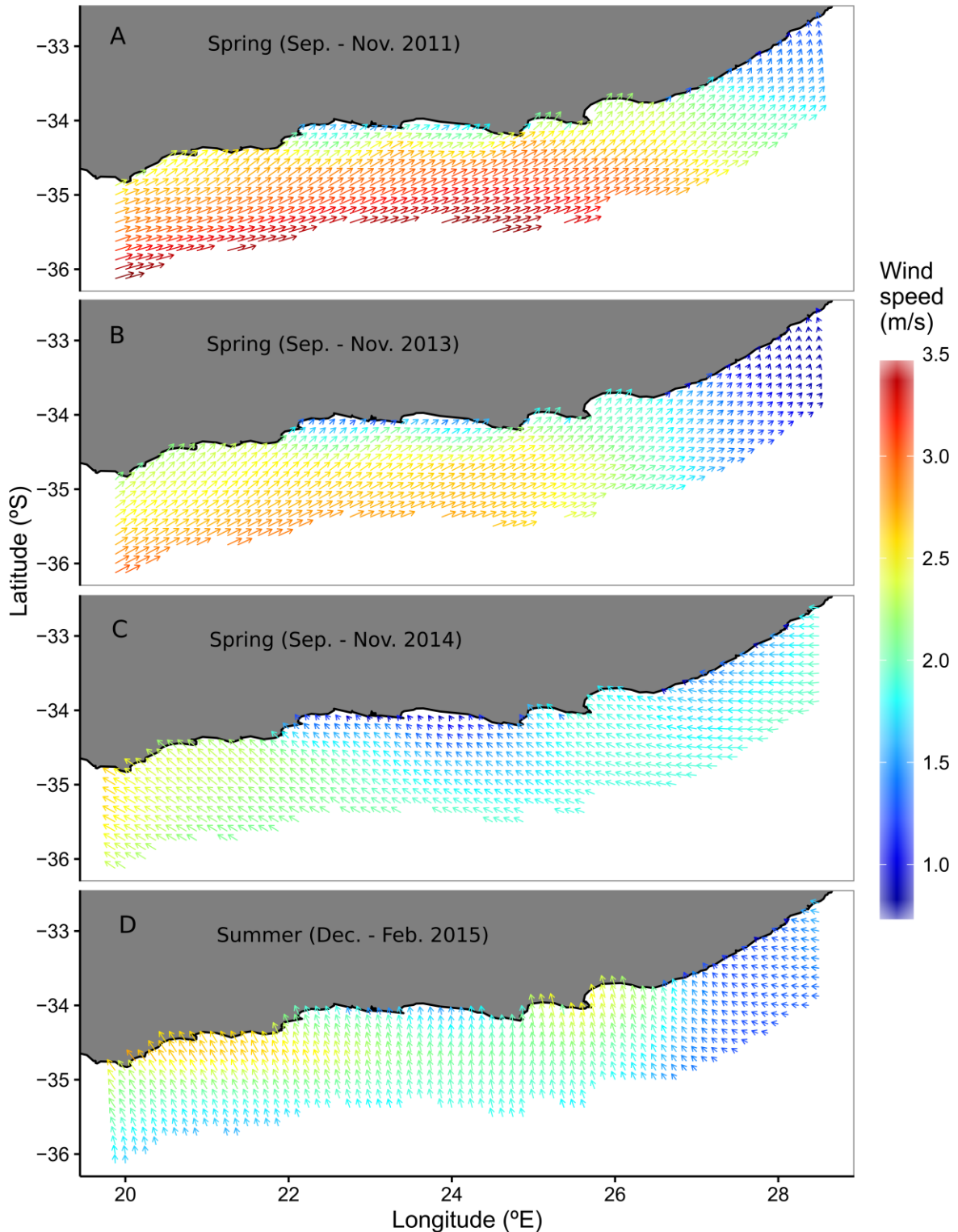


Fig. 2.12. Seasonal averages of wind speed (m s^{-1}) during spring preceding the bloom of *Gonyaulax polygramma* (A), the bloom of *Lingulodinium polyedrum* (B), and spring and summer preceding the bloom of *Noctiluca scintillans* (C and D). Colour and length of the vector represent wind speed (m s^{-1}). All panels are an enlarged version of those in Fig. 2.11 (note that the legend has been modified according to the ranges in the figures).

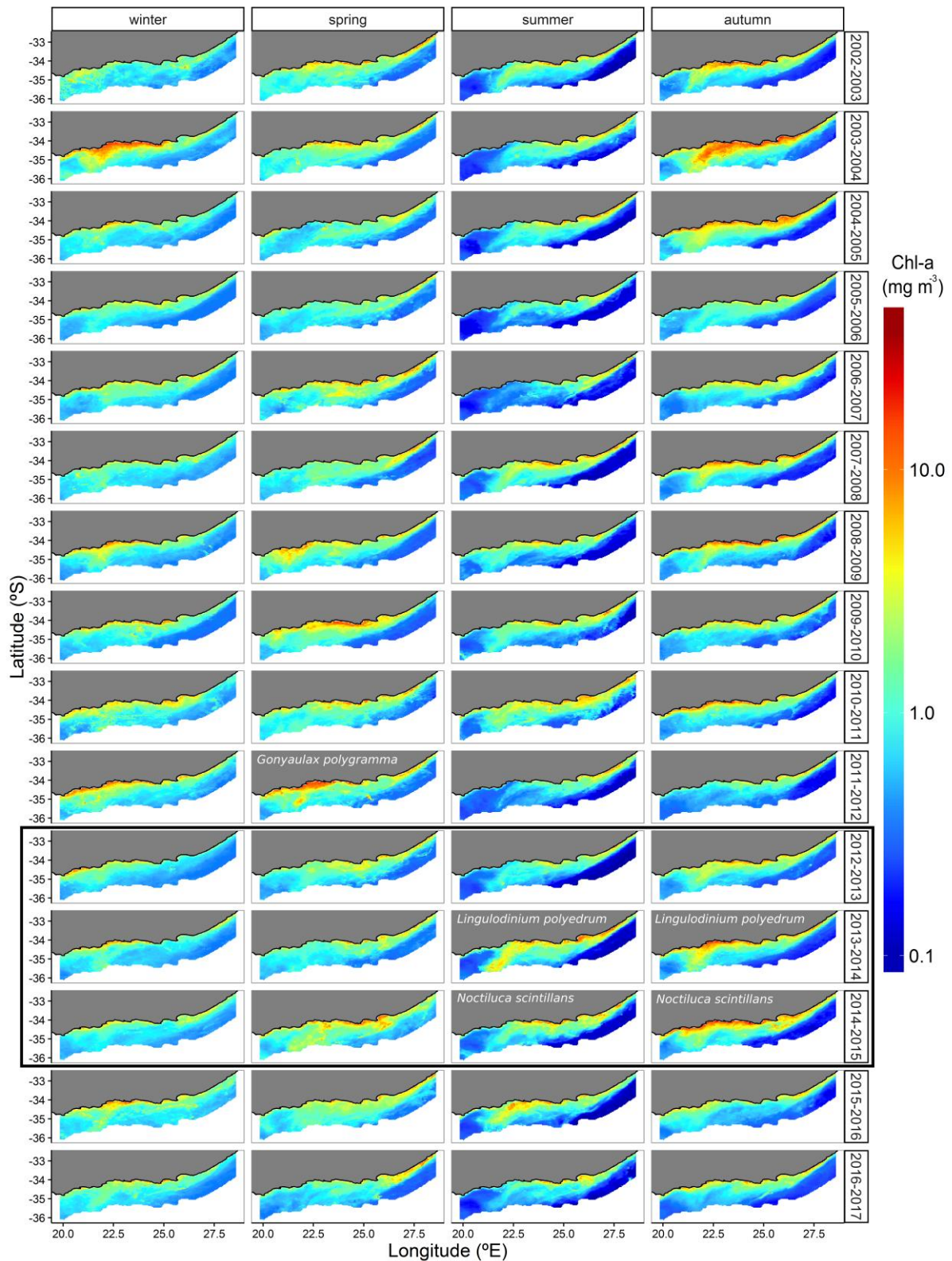


Fig. 2.13. Seasonal averages of chl-a (mg m^{-3}) from July 2002 until April 2017 calculated from eight-day averaged data, at 4km resolution. Note that colour scale bar is log-transformed. The three years used for the rest of the analysis are delimited by the black box. Occurrence of red tides is indicated in the relevant panels.

Seasonal averages of chl-a along the south coast showed very high chl-a averages (over 10mg m^{-3}), during summer and autumn of 2013-2014, and during autumn of 2014-2015, coinciding with the peak abundances of *L. polyedrum* and *N. scintillans*, respectively (Fig. 2.13). The presence of a *G. polygramma* bloom during spring and summer of 2011-2012, is reflected in very high seasonal averages of chl-a (Fig. 2.13, spring 2011-2012). Red tides caused by *L. polyedrum* have been reported by SAEON in subsequent years, but chl-a concentrations for the seasonal averages of later years did not reach the magnitudes observed during summer and autumn of 2013-2014 (Fig. 2.13). Very high concentrations along the coast previously appeared at the beginning of the data series, during the winter and autumn of 2003-2004 (Fig. 2.13), and during autumn 2004-2005 (Fig. 2.13), which could potentially reflect previous red tide events which were not reported.

In summary, based on the chl-a concentrations observed in satellite images, the red tide caused by *Lingulodinium polyedrum* peaked during summer and autumn of 2014, when it appeared to extend over the entire south coast of South Africa, from Cape Agulhas in the west (c. 20°E) to East London in the east (c. 28.5°E). At the beginning of summer, the *L. polyedrum* red tide spread offshore, covering both coastal waters and the Agulhas Bank, and during autumn, as the season advanced, and temperatures started cooling in offshore waters, the red tide blooms appeared to be restricted to coastal waters. Strong westerly winds, which produce downwelling, were present during winter and spring. Co-occurring with wind forcing, warmer SSTs were present over the continental shelf in spring and persisted during summer.

2.4. Discussion

At the end of 2013, and beginning of 2014, a red tide caused by the dinoflagellate *Lingulodinium polyedrum* was detected along the south coast of South Africa. Results suggest that strong mixing of the water mass during winter may have modified the conditions in the water mass preceding the red tide. Winter pre-conditioning, in combination with the predominance of downwelling favouring winds during spring, which promote conditions of stability in surface waters, may have resulted in conditions that favour the development of dinoflagellates over other species in the phytoplankton community, allowing *L. polyedrum* to bloom extensively along the coast and persist for several months.

Chl-a levels exceeding the threshold used to delimit the spatio-temporal presence of a red tide were found during all seasons of the three years of study (see Fig. 2.2). Thus, based on the chl-a threshold selected, levels that could be interpreted as a red tide would have been reached during periods when no red tides were reported in the water. The interpretation of these results as red tide-indicative values needs to be considered with caution, as satellite measurements have been found

to over or underestimate *in situ* values of chl-a (Kahru and Mitchell 1998, Hu et al. 2005). Different parameters which can be retrieved from satellite data have been proposed to detect the presence of specific red tide-forming organisms in the water. For example, Hu et al. (2011) proposed the combined use of enhanced red, green and blue (ERGB) images; chl-a; fluorescence line height (FLH); and a ratio of particulate backscattering coefficients obtained from two different algorithms, to distinguish areas affected by blooms of the toxic dinoflagellate *Karenia brevis* in coastal waters of the Gulf of Mexico. Kahru and Mitchell (1998) found that the ratio between two different wavelengths could differentiate blooms of *L. polyedrum* from other particles in the water which may produce an optical signature masked within the chl-a signal. The discerning mechanism proposed Kahru and Mitchell (1998) is probably due to the presence of specific chemical compounds produced by *L. polyedrum* which affect the absorption properties of the water mass. Nevertheless, although Kahru and Mitchell (1998) produced a methodology able to identify *L. polyedrum* using satellite data, the present study was limited by the wavelengths which are required by the method, not present in MODIS. Thus, although the information provided by satellite estimates of chl-a has constraints (e.g. misinterpretation of coloured dissolved organic matter as chl-a estimates, or inability to provide information on the species composition in the phytoplankton), it provides the opportunity to study events at larger spatial and temporal scales than is feasible for *in situ* sampling of the phytoplankton community. In addition, to characterise different species of red tide forming organisms, the analysis of different optical properties (likely to be species specific) would be required. Although satellites launched recently include spectral bands which could be of interest to identify *L. polyedrum*, the temporal resolution available would be shorter. Due to the general aims of the present thesis, determining any possible red tide event along the coast (not only *L. polyedrum*) was considered more appropriate than a focus on a highly specific identification mechanism. Thus, although the use of satellite estimates of chl-a has its caveats, a trade-off was required to study the possible effects of red tides on the marine system rather than the specific identification of *L. polyedrum* blooms.

2.4.1. Winter pre-conditioning of the water mass

Satellite data used to study the *L. polyedrum* red tide showed anomalously high values of chl-a, characteristic of a red tide, during summer and autumn of 2014. Although the spatial extent was variable in time, almost the whole of the south coast reached those chl-a levels at some point during those seasons. The south coast of South Africa experiences two annual peaks in phytoplankton biomass, during spring and autumn (Brown 1992). Wind patterns strongly determine water mass dynamics in the area, with predominance of alongshore winds (Schumann 1989). Westerly winds prevail along the south coast all year round (Goschen and Schumann 2011), and periods of strong easterly winds promote upwelling in certain areas along the south coast, particularly during summer (Schumann 1987). It is therefore expected that wind stress will strongly

modulate water mixing and nutrient availability. As in other temperate shelf areas, winter mixing contributes to the replenishment of inorganic nutrients to the photic zone (Lutjeharms et al. 1996) and in the case of the Agulhas Bank, deeper mixing occurs towards the west than towards the eastern part of the bank (Largier and Swart 1987). The present study showed that average wind forcing during winter was very similar during 2013, 2014, and 2015. During those three years, winter was characterised by very strong westerly winds and wind forcing appeared to be more intense than during other winters in the series (see Fig. 2.11). Although wind forcing was similar then, forcing from the Agulhas Current was much stronger during winter 2014, before the *L. polyedrum* red tide (Fig. 2.10). Stronger current flow may contribute to increase mixing over the shelf through the shedding of eddies and plumes that detach from the Agulhas Current (Lutjeharms et al. 1981, 1989, Swart and Largier 1987). Stronger mixing would contribute to deepen the mixed layer and to create a thicker layer with high nutrient availability. The importance of the mixed layer depth has been previously suggested to influence productivity in other shelf areas. For example, González-Gil et al. (2015) observed that, as opposed to the decrease in biomass predicted for warming scenarios, long-term trends in spring copepod biomass had increased and it was associated with long-term warming trends in the water mass. In addition, the mixed layer also experienced deepening during winter and was found to be strongly correlated to copepod biomass during the subsequent spring (González-Gil et al. 2015). In the present study, it is proposed that the combination of both stronger wind and current forcing during the winter 2014 may have resulted in deeper and stronger mixing, pre-conditioning the water mass and bringing nutrients into the surface layers before the spring phytoplankton bloom.

2.4.2. Red tide triggering and maintenance mechanisms

On the south coast of South Africa, the water mass becomes stratified during summer, as in other shelf areas in temperate systems (Lutjeharms 2006). Nevertheless, the prevalence of westerly winds during spring of 2014 seemed to increase stability in surface waters, which resulted in SSTs higher than the general average for the season in most parts of the Agulhas Bank (Fig. 2.9). Schlegel et al. (2017a) reported the occurrence of marine heatwaves (MHW) along the entire coastline of South Africa, with events affecting the water mass every year. The relationship of these events with abnormal conditions for the season was also reported (Schlegel et al. 2017b), with winds and currents as the main variables that determine the development of a MHW. Thus, the predominance of westerly winds during spring of 2014 may have modified the temporal evolution of temperature in surface waters during spring, resulting in the early stratification of the water mass which in turn affected the normal succession in the pelagic system. MHWs which caused strong high ecological (and economical) losses have been reported worldwide (Garrabou et al. 2009, Pearce and Feng 2013, Di Lorenzo and Mantua 2016). The largest impact in the pelagic system occurred in the East Pacific (McCabe et al. 2016), with abnormally high SSTs which affected the west coast of North America for

two and a half years (Bond et al. 2015, Gentemann et al. 2017). Associated to the Pacific warm anomaly of 2014/2015 (also referred to as “the Blob”), the diatom *Pseudo-nitzschia* sp. caused a highly toxic and extensive spatio-temporal bloom (McCabe et al. 2016, Zhu et al. 2017). Although blooms of *Pseudo-nitzschia* spp. are common in the area, the toxicity and spatial extension of that bloom was attributed to the particular conditions of temperature and nutrient availability associated with the evolution of the warm anomaly (McCabe et al. 2016, Zhu et al. 2017). McCabe et al. (2016) reported the presence of the toxic diatom in offshore waters (within the warm anomaly), before the bloom occurred in coastal waters. McCabe et al. (2016) therefore proposed that upwelling during spring resulted in the input of nutrients to the warm water mass, subsequently triggering the offshore bloom of *Pseudo-nitzschia* sp. which was later displaced onshore by spring storms.

Contrary to the mechanism of bloom development reported by McCabe et al. (2016), Ryan et al. (2017) detected the sub-surface development of *Pseudo-nitzschia* sp. in Monterey Bay during the period of the warm anomaly. Vertical samplings during upwelling relaxation allowed the detection of a sub-surface bloom in the thermocline/nutricline which was later advected to the surface by upwelling (Ryan et al. 2017). In the present study, the conditions in the water mass shared similar features to the Pacific warm anomaly. For example, the development of the *L. polyedrum* bloom was also unprecedented in its spatio-temporal extent. In addition, abnormal SSTs occurred along the south coast although they only occurred during spring and summer before the *L. polyedrum* red tide. Based on the thermal structure in the water mass, similar mechanisms of bloom formation could be expected during the bloom of *L. polyedrum*. Similarly to the nutrient limited pre-upwelling conditions during the Pacific warm anomaly, the abnormally warm shelf waters in the present study would have also been nutrient depleted during summer, when *L. polyedrum* abundances were highest. Although *L. polyedrum* seemed to be associated with periods of colder water (Fig. 2.3), likely showing upwelling (Fig. 2.6A-C), there was no evidence of *L. polyedrum* in offshore waters and it was originally detected in plankton samples from Algoa Bay (c. 26°E). This would suggest that the mechanism proposed by McCabe et al. (2016) does not apply for the present study. According to the present results (Fig. 2.3 and 2.6), cell growth of *L. polyedrum* was more likely to occur in the thermocline/nutricline during periods of upwelling relaxation/downwelling. Periods of active upwelling would advect the sub-surface bloom to the surface, where it would be detected in satellite estimates of chl-a (Fig. 2.3). This would agree with the stability conditions which have been previously associated with red tides caused by dinoflagellates (Pitcher et al. 1998, Smayda and Trainer 2010, León-Muñoz et al. 2018), including upwelling relaxation in upwelling systems (Pitcher et al. 1995, Pitcher and Boyd 1996, Probyn et al. 2000). Classically, diatoms are associated with conditions of higher turbulence than dinoflagellates (Margalef 1978, Smayda and Trainer 2010), although different species of dinoflagellates may have different ambient tolerances (Smayda 2000). This difference may be based on the markedly different swimming behaviours observed in the two

groups. While diatoms are not able to swim, dinoflagellates can be considered as quite strong swimmers relative to their body size. Thus, while increased stratification will result in the depletion of nutrients in the euphotic area and limit diatom growth, the swimming ability of dinoflagellates will allow them to migrate vertically to take up nutrients at depth and then return to the euphotic zone for photosynthesis (Walsh et al. 1974, Eppley et al. 1984). In particular, *L. polyedrum* has been previously reported to perform vertical migrations in both the laboratory and in the field (Walsh et al. 1974, Heaney and Eppley 1981), and to bloom after periods of stability of two to three weeks (Allen 1946, Margalef 1956). This mechanism can provide an advantage over other organisms in the plankton under nutrient limitation, but additional physiological features can contribute to the development and maintenance of dinoflagellate blooms. It has been reported that many species of dinoflagellates thought to be autotrophic also have phagotrophic mechanisms which allow them to feed on other particles in the plankton (Stoecker et al. 2006). Such species include *L. polyedrum* and other red tide-forming dinoflagellates (Jeong et al. 2005a). Therefore, under limitations of inorganic nutrients, e.g. during stratification of the water column, this mechanism would allow dinoflagellates to obtain nutrients from other organisms. This could also reduce populations of other organisms, offering an important competitive advantage over groups like diatoms, and allow dinoflagellates to persist for longer than if they were totally dependent on the availability of inorganic nutrients (Stoecker et al. 2006).

Thus, the behavioural and physiological adaptations of *L. polyedrum* as well as the results obtained, support the hypothesis that *L. polyedrum* would have proliferated in the sub-surface during stable conditions and reached the surface during upwelling. In the present study, the presence of anomalously warm water from spring through summer would promote the separation of water bodies with different physical characteristics, supporting strong stratification over the shelf during summer (Swart and Largier 1987), and complicating the transference of nutrients among different water masses, as opposed to the large-scale mechanism proposed by McCabe et al. (2016) in the Pacific.

2.4.3. Red tide species and their environmental conditions

Prior to the bloom of *L. polyedrum*, another red tide caused by the dinoflagellate *Gonyaulax polygramma* developed along the Agulhas Bank in spring of 2011 (van der Lingen et al. 2016). Van der Lingen et al. (2016) attributed the appearance of that red tide to downwelling favouring winds during summer which co-occurred with high chl-a satellite estimates (representative of a red tide). SST anomalies (spring and summer 2011-2012, Fig. 2.9) were above the general average of each respective season as was the case during the occurrence of the *L. polyedrum* bloom (spring and summer 2013-2014, Fig. 2.9). Nevertheless, the bloom of *G. polygramma* was reported only during spring (van der Lingen et al. 2016), as opposed to that of *L. polyedrum* which was first recorded in

December 2013 and lasted throughout summer and autumn 2014. Average wind conditions during spring of the *G. polygramma* and the *L. polyedrum* red tide years were quite similar, with south-westerly winds (Fig. 2.11) which would promote downwelling and stratification, conditions that would favour dinoflagellate growth over diatoms, as discussed in the previous section. Both *G. polygramma* and *L. polyedrum* belong to the order Gonyaulacales (Kim et al. 2006) and are very similar in morphology and behaviour. *G. polygramma* is also a phagotroph (Jeong et al. 2005b), therefore, environmental conditions similar to those observed during the bloom of *L. polyedrum* would also be expected to promote its growth.

During summer and autumn of 2015, a red tide caused by the dinoflagellate *Noctiluca scintillans* (Macartney) Kofoid (synonym *N. miliaris* Lamarck), was reported by the South African Environmental Observation Network (SAEON, see Figs. 2.2 and 2.4). The dinoflagellate seemed to appear in the water during summer and autumn, although the environmental conditions during those seasons were completely different to the previous year, with predominant colder than average SSTs along the south coast (Fig. 2.9). Nonetheless, major differences in morphology, behaviour, and physiology separate *N. scintillans* from *L. polyedrum* and *G. polygramma* (Elbrächter and Qi 1998). Two forms of *N. scintillans* have been described, both belonging to the same species (Elbrächter and Qi 1998). The form of green *N. scintillans* has an endosymbiotic relationship with a photosynthetic alga which allows it to feed as an autotroph or to prey on other organisms depending on the conditions (Elbrächter and Qi 1998). Red *N. scintillans* cells lack chloroplasts or an endosymbiont and therefore cannot photosynthesize (Balch and Haxo 1984), behaving exclusively as heterotrophs (Elbrächter and Qi 1998). Green and red *N. scintillans* have different temperature requirements and mostly occur in geographically separate areas (with some exceptions in tropical areas of the Indian Ocean; Harrison et al. 2011). The most widespread form is red *N. scintillans*, the organism that bloomed along the south coast of South Africa during summer and autumn of 2015 (from here on referred to as *N. scintillans* for simplicity throughout the present thesis).

Heyen et al. (1998) found that summer abundances of *N. scintillans* in the North Sea were linked to winter temperature conditions, with warmer winter SSTs resulting in higher abundances during summer, and vice-versa. In the present study, SSTs during winter preceding the *N. scintillans* bloom were warmer than the general average, similarly to the two previous years (Fig. 2.9). Nevertheless, SSTs were much colder from spring to autumn of the *N. scintillans* bloom, as opposed to the previous years (Fig. 2.9). Seasonal wind averages also showed predominant south-easterly winds during spring and summer of the *N. scintillans* bloom (Fig. 2.12C-D). Thus, wind and SST data suggest the occurrence of upwelling preceding and co-occurring with the bloom of *N. scintillans*. Meanwhile, south-westerly winds, which promote stratification and downwelling, dominated during spring of the previous years (Fig. 2.12A-B). Due to the heterotrophic condition of *N. scintillans*, the high chl-a values observed during summer and autumn would correspond to other organisms, suggesting

either a very productive phytoplankton community, or another red tide organism which was not reported by the South African Observation Network (SAEON). High phytoplankton availability would supply prey for *N. scintillans*, and the turbulence conditions associated with upwelling would complicate growth for other species like *L. polyedrum* or *G. polygramma*. In accordance with Heyen et al. (1998), here it is suggested that the shift from warm winter conditions to very productive, non-stable water conditions later in 2015 may have provided the hydrodynamic and biological conditions required for *N. scintillans* to bloom.

It is important to consider that since *N. scintillans* is not an autotroph, chl-a cannot be used directly to assess its presence (Balch and Haxo 1984). In addition, the distribution *N. scintillans* during its growth phase occurs in sub-surface waters, appearing in the surface during late stages when the bloom is about to collapse (Elbrächter and Qi 1998). In the present study, these limitations in the characterization of the bloom of *N. scintillans* may have resulted in its spatio-temporal under or over-representation, and therefore, the present results should therefore be taken with caution. Due to its heterotrophic requirements, *N. scintillans* appears to thrive under high abundances of diatoms, but it has a wide particle spectrum which includes eggs of fish (Hattori 1962) and copepods (Kimor 1979). This could potentially reduce predation pressure from copepods or fish larvae on other plankton species, but as eggs of other meroplanktonic species could also be included in the diet of *N. scintillans*, the effects of this dinoflagellate on the trophic web are not clear.

2.4.4. Future perspectives

Red tide records have increased over recent years along the south coast of South Africa, where they had previously rarely been reported (Pitcher and Calder 2000). Such increase is not exclusive to the south coast of South Africa (Anderson 1989, Hallegraeff 1993, Hallegraeff 2003). Although the species detected along the south coast of South Africa do not seem to pose a direct risk to human health, disruption of ecosystem dynamics at multiple levels could occur. For example, recent modelling of the environmental conditions related to red tides in the North Atlantic and the North Pacific has suggested that potential spatial ranges have expanded in those areas (Gobler et al. 2017). Changes in environmental conditions will affect the bloom of organisms in the phytoplankton directly by modifying their spatio-temporal ranges. Those changes can affect the trophodynamics in the pelagic and the intertidal environments through changes in phytoplankton composition and abundance. In the North Atlantic, Edwards and Richardson (2004) reported changes in the phenology of dinoflagellates and other planktonic groups of organisms in areas of the North Sea where long-term plankton records were available, with dinoflagellates reaching their peak of abundance earlier in the year. This change in the phenology of certain groups of organisms has the potential to alter the dynamics of the food web, uncoupling food production with higher trophic level consumers (Edwards and Richardson 2004). Do Rosário Gomes et al. (2014) also reported a shift

in phytoplankton composition during winter in the Arabian Sea, from diatom predominance to massive blooms of green *N. scintillans*. The shift in community composition occurred during winter, the upwelling season in the Arabian Sea, which would produce important changes in food web dynamics in the area.

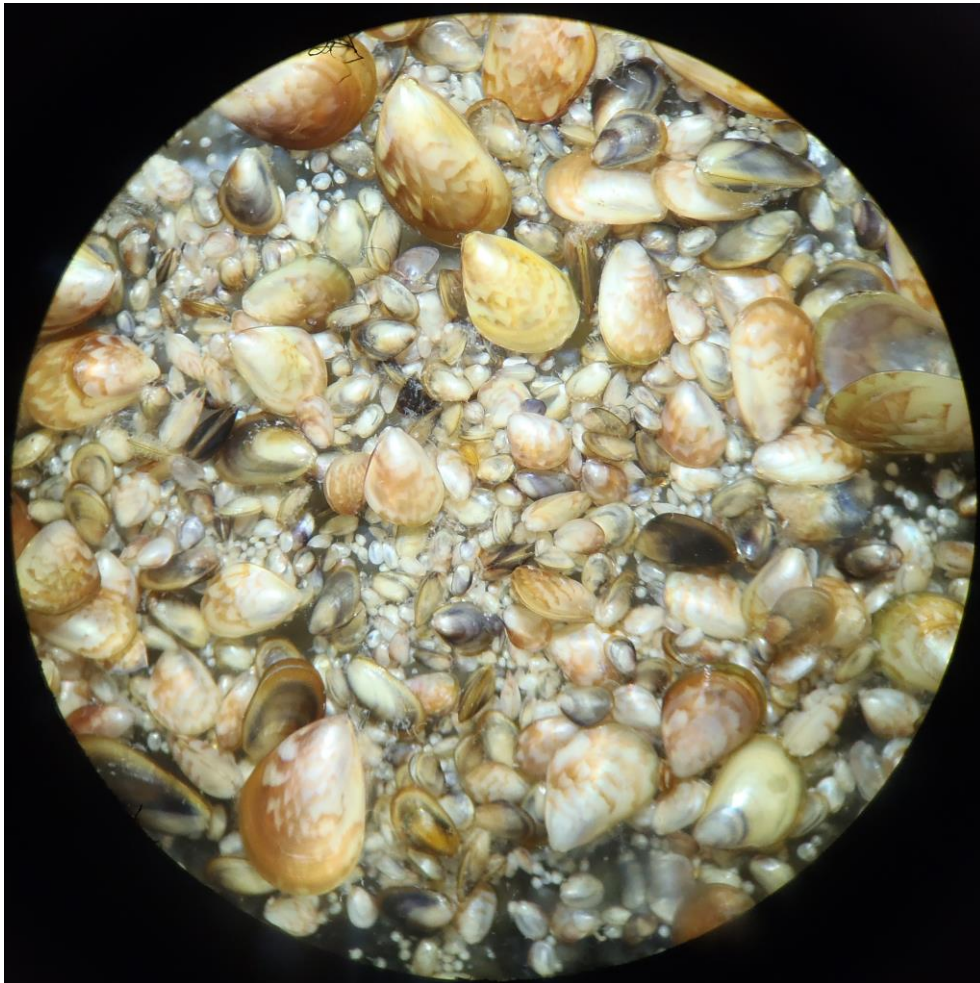
In the case of the south coast of South Africa, the area where the blooms of *G. polygramma*, *L. polyedrum*, and *N. scintillans* were observed, holds important biomasses of copepods (Boyd and Shillington 1994), and important commercial species like the chokka squid (Roberts 2005), sardines (Beckley and van der Lingen 1999), and mussels (von der Meden et al. 2008). In addition to changes in the phytoplankton community, the environmental conditions that promote the development of the red tide are also likely to affect physiological processes of higher trophic level organisms. Thus, changes in the patterns and seasonality of winds might affect the long-term dynamics and seasonality of upwelling in the south coast, and the temperature ranges at meso-scales. Mesocosm experiments by Sommer and Lengfellner (2008), showed changes in the phytoplankton community as a result of changes in temperature, which resulted in smaller cell sizes and lower biomasses. For instance, Sommer and Lengfellner (2008) discussed the implication of changes of this sort in larger scale patterns of carbon sequestration in the ocean. Thus, replacement of diatom biomass by dinoflagellates could reduce the carbon that is transformed into organic matter and sunk into the deep ocean, because of the differences in sinking patterns of the two groups. In addition, an increase in flagellate biomass could also contribute to increase respiration rates in surface layers with the subsequent reduction in net carbon sequestration. In fact, Do Rosário Gomes et al. (2014), reported that death cells of *N. scintillans* do not seem to sink directly but as faecal pellets from the organisms that prey on them (i.e. salps and gelatinous plankton), which would have implications to carbon sequestration rates to the deep ocean.

In summary, the changes in large-scale patterns of winds along the south coast of South Africa resulted in changes in upwelling and stratification, reflected on SST values, which translated into changes in the phytoplankton community. Changes in the phytoplankton composition or phenology over the continental shelf have the potential to affect the trophodynamics of the system, with negative effects being magnified for higher trophic levels. The recent increase in red tides observed in the area might reflect a trend of change in environmental conditions, stressing the importance of understanding the underlying mechanisms which are driving changes in the biological community, and to allow the prediction of potential future changes in the system. Here it is proposed that the environmental conditions that favoured the development of the *L. polyedrum* bloom started with the anomalous conditions experienced during winter, which pre-conditioned the water mass and may have increased nutrient levels. *L. polyedrum* is suggested to have reached unprecedented spatio-temporal ranges due to the specific nutrient conditions which may have originated during winter mixing, and not only to the conditions during the development of each

red tide. Winter preconditioning with different environmental conditions may also account for the bloom of *N. scintillans* the following year. Thus, deviations from the long-term seasonal environmental conditions should be incorporated in future prediction models, as they may hold the potential to influence later stages of the phytoplankton succession.

Chapter 3

Interannual variability in recruitment patterns of intertidal invertebrates under contrasting environmental conditions



Recruits of *Perna perna*, *Mytilus galloprovincialis* and *Choromytilus meridionalis*.

Interannual variability in recruitment patterns of intertidal invertebrates under contrasting environmental conditions.

3.1. Introduction

In recent decades, research in marine ecology has focused on the importance of successful recruitment of new individuals into the adult population as one of the key factors for population maintenance (Gaines and Roughgarden 1985, Menge and Sutherland 1987, Roughgarden et al. 1988, Underwood and Fairweather 1989, Menge 2000). For marine benthic organisms with planktonic stages of development, the return of young organisms to the adult habitat will depend on the success of all the developmental stages in the life cycle, from the production of gametes and fertilization, to the delivery of competent larvae to suitable settlement habitats and the transition from settlement to recruitment. These processes act on larval survival, delivery and post-settlement mortality in a sequential step-like fashion to determine recruitment success (Rilov et al. 2008, Pineda et al. 2010, Pfaff et al. 2015).

Along this sequence of processes, a set of biophysical environmental characteristics may affect larval performance with variable intensity and at different spatio-temporal scales. Some variables will be critical for development or survival of the larvae, and some will greatly influence delivery to settlement areas. For example, temperature (Hoegh-Guldberg and Pearse 1995, Gillooly et al. 2002, O'Connor et al. 2007) and to a lesser extent food (Allison 1994, Fenaux et al. 1994), influence larval physiology and determine the length of planktonic larval development (PLD). This is the time required for development before the organism reaches a competent stage, that is, when the organism has undergone all larval stages in its life cycle and is ready to settle in the adult habitat. In general, developmental times of marine invertebrates are shorter at warmer temperatures and in the presence of enough food (Pechenik et al. 1990), with increased developmental times potentially resulting in higher mortalities (Tapia and Pineda 2007).

Other variables like upwelling, turbulence or wave height, will affect flows in the water mass and influence the delivery of larvae and post-settlement transport, which determine recruitment distributions. In the case of upwelling, it has been described to influence cross-shelf transport of the water mass which affects delivery of larvae to the coast (Farrell et al. 1991, Dudas et al. 2009). Upwelling-downwelling dynamics will influence onshore-offshore transport depending on the position of larvae with respect to the opposing flows above and below the thermocline (Shanks and Brink 2005). Shanks and Brink (2005) proposed that if larvae behave like passive particles, when they are positioned above the thermocline they will be transported onshore by downwelling and offshore by upwelling, and the directions of transport will be the opposite if they are below the thermocline. If larvae swim across the vertical axis against the vertical flows forced by upwelling

and downwelling (Genin et al. 2005, Shanks and Shearman 2009), they can be able to maintain their position and avoid being carried offshore by cross-shelf currents. After delivery from the water mass into the shelf region, other mechanisms have been proposed to influence post-settlement transport after larvae reach the settlement substrata. Turbulence has been suggested as the main cue affecting larval vertical migrations to the bottom where they will be subjected to bed load transport (Young 1995, Pringle 2007). Sinking behaviours under turbulent flows which resemble surf zones have been reported in laboratory experiments, for example for larvae of mussels (Fuchs and DiBacco 2011) and gastropods (Fuchs et al. 2004). Within the inner shelf and close to the surf zone, the importance of waves for the recruitment of mussels has also been proposed via translocation of individuals (Navarrete et al. 2015, Pfaff et al. 2015, Shanks et al. 2017). Navarrete and co-workers (2015) found a positive correlation between wave height and recruitment of mussels, and proposed that competent larvae would settle in the subtidal and be transported to final sites by bed load transport across the surf zone.

Thus, different variables affect different stages of the larval cycle and can contribute simultaneously or during different steps to the final patterns observed. Therefore, while temperature and food are expected to operate at temporal scales that affect development of the larvae in the water column, the variables that affect larval delivery (e.g. upwelling, turbulence and wave height), are expected to influence settlement rates.

3.1.1. The influence of food during larval development: particle size and food quality

The presence of phytoplankton in the water is of major importance for higher trophic levels that use it as food (Townsend et al. 1994, Beaugrand and Reid 2003). For primary consumers that feed on phytoplankton cells at any stage of their life cycle (Vidal 1980, Turner et al. 2001), this establishes the base of the food web, and levels of phytoplankton will have effects that percolate to higher trophic levels (Cushing 1990, Platt et al. 2003, Sabatés et al. 2007). Food supply and quality influence the amount of energy that can be allocated for adult maintenance and reproduction (Toupoint et al. 2012), but in addition, the presence of phytoplankton in the water has been proposed to trigger spawning in multiple marine invertebrate taxa (Starr et al. 1990, 1991). This effect has been suggested for different benthic organisms including mussels, sea urchins and barnacles (Hawkins and Hartnoll 1982, Smith and Strehlow 1983, Starr et al. 1990). From an evolutionary point of view, the benefits that may have resulted from coupling reproduction with the bloom of phytoplankton in the water mass appear obvious. Cues for simultaneous spawning allow the synchronisation of intra-specific reproduction in species with external fertilization, provide food for the offspring, and the simultaneous reproduction of different species will reduce the risk of predation by reducing the rate of encounter of the offspring and predators.

Hence, when larvae co-occur in time with algal blooms (either HABs or normal multispecies phytoplankton communities), oceanographic features that promote the accumulation of particles with passive or limited swimming behaviour (e.g. fronts and internal bores) may promote their spatial co-occurrence (Holligan 1981, Franks 1992a, Lennert-Cody and Franks 1999, Smayda 2002, Helfrich and Pineda 2003, Höfer et al. 2017). Therefore, changes in the structure of the phytoplankton community will modify the food resources for early life stages of benthic organisms, and some fish larvae. The diet of the larvae of benthic organisms, such as barnacles and bivalves, is primarily based on diatoms and small dinoflagellates that measure only a few micrometres in size (Stone 1989, Raby et al. 1997, Vargas et al. 2006). The size of particles that larvae can handle is limited by the anatomical structures involved in capturing and processing those particles (Lora-Vilchis and Maeda-Martinez 1997). Nevertheless, particles larger than expected can be ingested by barnacle nauplii (Moyses 1963) and by some bivalve species like oysters and mussels (Baldwin and Newell 1991, Jeong et al. 2004). Previous studies on barnacles have found a correlation between intersacular spacing on the antennae and the sizes of algae that provide successful diets (Stone 1989). These spaces influence the maximum and minimum food particle sizes for each species, and different species can have different particle-size limitations (Moyses 1963). In addition, suitable particle sizes can change ontogenetically, with bigger particles being used as that space increases through subsequent developmental stages. In the case of bivalves, food particle sizes seem to be related to the diameter of the mouth and oesophagus, increasing in later veliger stages (Raby et al. 1997). Additionally, it appears that bivalve larvae are able to select preferred particle sizes for ingestion (Gallager 1988, Baldwin and Newell 1991).

Thus, the presence of HAB species which are non-toxic for larvae could result in contrasting effects for larval feeding. One of the positive effects of the presence of high density algal blooms could be increased food concentrations during the planktonic development of larvae. Nevertheless, negative effects could arise at multiple levels: (1) the high nutrient uptake of HABs, and the ability of mixotrophic species to consume other phytoplankton cells may reduce the diversity and biomass of preferred species; (2) not all species of phytoplankton have the same nutritional value and thus a diet based mainly on one species could affect growth or survival (Widdows 1991, Thompson and Harrison 1992, Galley et al. 2010); (3) large sized dinoflagellates can exceed the particle size that larvae are able to feed on, or have faster swimming speeds, making their capture difficult; (4) some mixotrophic flagellates can be both predators and prey for zooplankton, being able to feed on eggs and the naupliar stages of copepods, indicating their potential ability to feed on other small invertebrate eggs or larvae (Kimor 1979, Daan 1987, Jeong 1994); (5) HABs potentially enhance the abundance of predators of egg and larvae, resulting in increased predation pressure on other larvae when the bloom decays.

Along the Agulhas Bank, two peaks of chl-a have been described during spring and autumn (Brown 1992) as in other temperate shelf-systems. In addition, higher phytoplankton productivity occurs in nearshore waters along the coast, in the cold-ridge and closer to the shelf break where shelf-edge upwelling occurs (Probyn et al. 1994). All those areas have been reported to show sub-surface chl-a maxima during summer, with the maximum values reaching shallower waters towards the shelf break (Probyn et al. 1994). During autumn of 2014, phytoplankton composition was expected to be modified by the presence of *Lingulodinium polyedrum* in the water. The changes observed in the environmental conditions (see Chapter 2) had the potential to contribute to the persistence and domination of the phytoplankton community by *L. polyedrum*. This would be facilitated by the feeding advantages it has over diatoms, including mixotrophy and swimming behaviour (Jeong et al. 2005a). Thus, changes in food quality or availability, as well as changes in the environmental conditions (between the year 2014 with the red tide produced by *L. polyedrum* and the following with presence of *N. scintillans*), are likely to have affected the early development of marine benthic organisms and, in turn, recruitment rates. Although recruitment rates can be highly variable among years (Botsford 2001, Wing et al. 2003), inter-annual variability will ultimately be determined by the combination of physico-chemical and biological conditions, and transport mechanisms in the water mass (Shkedy and Roughgarden 1997, Dudas et al. 2009). Thus, although confounding effects can be present due to multiple processes operating simultaneously (affecting survival of larvae during their planktonic development, successful transport and delivery to the recruitment sites, and post-settlement mortality), changes in the environment are likely to co-vary or influence different processes simultaneously. Integration of the developmental period until recruitment in association with the environmental conditions present during the entire period, can produce the framework towards the overall direction of change in the system.

Although *L. polyedrum* is not toxic for mussels or barnacles, due to the large cell size of the dinoflagellate (42-54 µm, see references in Lewis and Hallett 1997), its ability to feed on other organisms (for example Jeong et al. 2005) and to persist in time, it was hypothesised that its presence in the water would disrupt the phytoplankton community and potentially alter the trophodynamics of the system. The present study focused on the potential effect of the interaction of *L. polyedrum* and the predominant species of mussels and barnacles in the study area. Mussels and barnacles along the South Coast of South Africa were selected due to their planktonic larval development and because these taxa are good proxies for changes that may affect any benthic organism with larval stages. In addition, high mussel coverage exists along the South Coast (von der Meden et al. 2008), therefore, changes that affect successful recruitment of new individuals have the potential to have an impact on an important ecological engineering species with consequences at the ecosystem level (Jones et al. 1994, Bruno et al. 2003). The species of mussels in the area comprise the brown mussel *Perna perna*, the mediterranean mussel *Mytilus galloprovincialis*, and the

black mussel *Choromytilus meridionalis*. These are low shore of subtidal species. Higher on the shore, the barnacles *Chthamalus dentatus*, *Tetraclita serrata*, and *Octomeris angulosa* can be found. Both mussels and barnacles have larval stages which will develop in the water column, during *ca.* four weeks for mussels (Satuito et al. 1994, Aarab et al. 2012) and two weeks for barnacles (e.g. Patel and Crisp 1960 and Kado and Kim 1996). The environmental conditions that promoted the appearance of the red tides during autumn 2014 and 2015, were expected to affect larvae during development and/or delivery. Thus, the present chapter aims to determine changes between years in recruitment of barnacles and mussels, and to determine possible interactions with the environment which can establish how changes in the system could affect future adult communities.

3.2. Material and methods

3.2.1. Biological sampling

Ten sites were selected along the south coast of South Africa to estimate mussel and barnacle recruitment (Fig. 3.1). Due to the timing of the *L. polyedrum* red tide, sampling was selected to take place in autumn, coinciding with one of the peaks of mussel recruitment for the South Coast of South Africa (Zardi et al. 2007).

3.2.1.1. Mussels

Ten plastic pot scourers (from here on referred to as *collectors*) were used as artificial substrata for mussel recruitment (Menge 1992, Porri et al. 2006, von der Meden et al. 2010). Collectors are made from a tubular mesh that is rolled into a disc shape. These were embedded within the mussel bed during low tide, attached to eye-bolts (Fig. 3.2). Recruitment was estimated for two entire months during each of two consecutive years. April and May of 2014 comprised the year of the *L. polyedrum* red tide. For comparison, recruitment during April and May of 2015 were selected to represent a normal year because, despite the occurrence of *N. scintillans*, the dinoflagellate *Lingulodinium polyedrum* was not reported to have produced another red tide. Due to the large spatial extent of the area sampled, collectors were replaced only once per month during the same spring tide period, with the exception of Plettenberg in May 2014, where sampling was delayed for two weeks due to weather conditions (Table 3.1). After one month of deployment, collectors were removed from the rock and preserved in 70% ethanol immediately after collection until samples were processed in the laboratory.

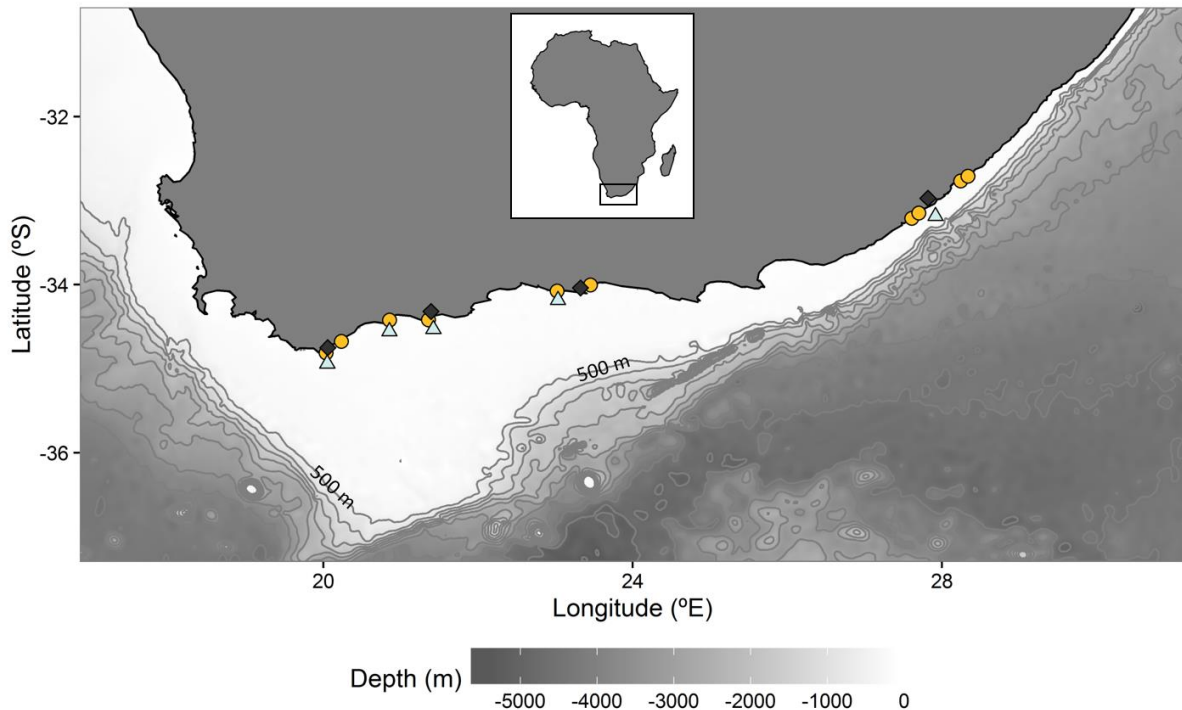


Fig. 3.1. Map of the South Coast of South Africa with the bathymetric profile. The first contour line delimits the 500m isobath. Yellow circles represent the 10 sites along the coast where recruitment was estimated (see Table 3.1). Black diamonds show the position of the four weather stations where wind data was collected. Blue triangles show the areas where wave height was estimated. The geographically closest weather station and wave record to each sampling site were used to estimate the upwelling and turbulence indices, and wave height respectively.

For each month and site, three replicates were analysed when possible. Some collectors were detached from the rock by rough sea conditions, which limited the number of replicates for some sites (total $n = 113$, Table 3.1). Mussel recruits were removed from the collectors by the addition of 10 ml of bleach in 250 ml of ethanol to dissolve the byssal threads (Connolly et al. 2001). Each collector was carefully unrolled and gently scrubbed in a bucket until all particles present were removed. Contents were filtered through a 75 μm sieve and stored in 70% ethanol. The contents were counted in a zooplankton counting chamber under a dissecting microscope (14x magnification). All individuals in each sample were counted except in the case of Brenton and Plettenberg in April and May of 2015. Due to the high abundances reached in these samples, only a 25% sub-sample was counted for those samples (see sub-sampling methodology developed in Appendix 1). To simplify the complex and time-consuming identification process, as well as to minimize the misidentification of younger individuals, only the predominant mussel species were counted and divided in two groups: (1) *Perna perna*, and (2) other mytilids (comprising mostly *Mytilus galloprovincialis* but including some *Choromytilus meridionalis*). Although the group *other mytilids* comprises more than one species, from here on it will be referred to as *species* for

convenience. Individuals were identified based on the morphological features described by Bownes et al. (2008). Due to the prolonged duration of exposure of the collectors on the rock, all the individuals that settled on the collectors were considered as *recruits* (minimum size=0.27mm, maximum=5.6mm). Counts were transformed into abundances per unit of surface area (m²) and per day for each mussel species. To estimate the area of each collector, a section of the mesh, here referred to as *fibre*, was removed from each of 10 different collectors. Fibres have a flattened shape and can be assumed to resemble a rectangular prism. Length and width at five different points of each face of the prism were measured and average values were used to estimate the surface area available in the prism. Fibres were weighed in a precision balance (up to four decimal places of a gram) and an area/weight factor was obtained. The area of each collector was calculated by multiplying the dry weight of the collector by this factor.

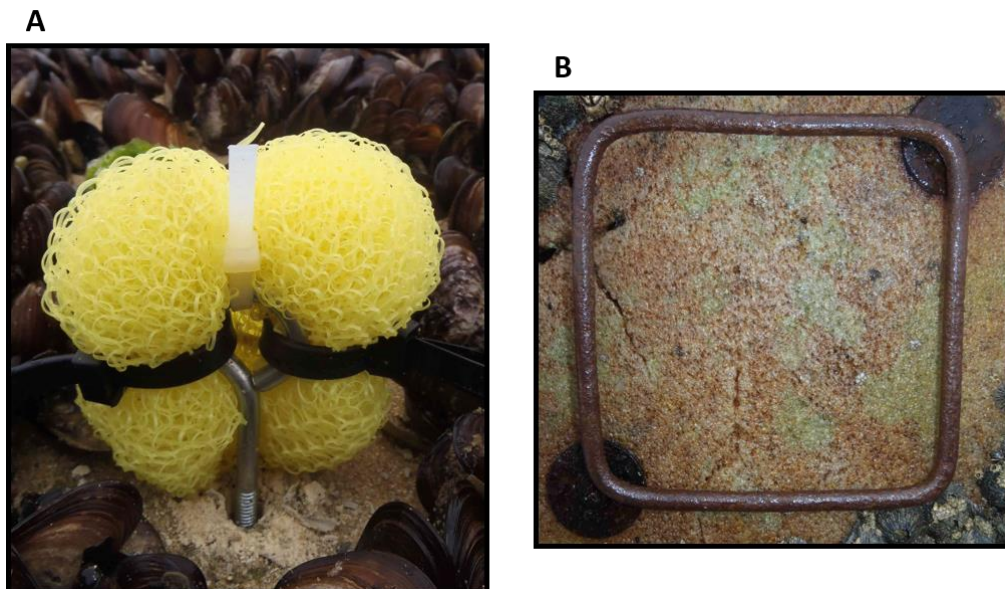


Fig. 3.2. Recruitment collectors used for mussels (A). Quadrats for barnacles (B).

3.2.1.2. Barnacles

At the beginning of the season in March 2014 (the year of the *L. polyedrum* red tide), 10 squares of natural rock substratum of 10x10 cm were cleared on the rock in the barnacle zone of each sampling site, each square from here on is referred to as a *quadrat* (Fig. 3.2). To avoid losing information on the individuals that recruited during autumn 2014 and to avoid repeated measurements in the data, 10 new quadrats were cleared the second year (in March 2015). Two screws were drilled into the rock to delimit diagonally opposite corners of the metal quadrat used to delimit the photographed areas. When the quadrats were placed on the rock, all adult barnacles and other organisms present within the quadrat were removed and the rock was scrubbed with a

metal brush, leaving it undisturbed thereafter. Photographs were taken after one month of clearing to determine recruitment rates and periodically after that (see Table 3.1). For each year and site, the five best quality photographs taken in April (approximately one month after the quadrats were cleared) were selected and all barnacle recruits in each quadrat were counted ($n = 100$). An exception was again made for Plettenberg Bay, where recruitment was so intense during the first month of the study that individual recruits were not recognizable. For that site, a small area where recognizable individuals could be counted was selected in each photograph. The software Coral Point Count with excel extensions (CPCe) (Kohler and Gill, 2006) was used to delimit areas covered by barnacle recruits to extrapolate the number of counts to the rest of the photograph. Although counts might have been underestimated for those photographs, this was considered preferable to overestimation. Due to different factors (e.g. irregularities of the substratum or presence of water on the rock) the quality of photographs and the percentage area where recruits could be counted was variable among replicates. To overcome those differences, a uniform grid of 49 points was superimposed inside the quadrat area on each photograph using the software CPCe. The number of points where the quality of the photograph allowed reliable counts was transformed to surface area in each quadrat and used to estimate total recruitment (mean quadrat area used was 87.81%; S.D. 13.87%; $n=100$). To standardize recruitment rates, all counts were converted into abundances of organisms per unit of surface area (m^2) and per day. Although the quadrats were usually placed in areas where *Chthamalus dentatus* was predominant, the small size of the individual recruits did not allow confident identification to species level. As a result, all barnacle species were grouped together. As done with mussels, barnacles will also be referred to simply as *species*.

Table 3.1. Site locations (from west to east), used for sampling mussel and barnacle recruitment during years 2014 and 2015. Start date refers to the date when collectors were first deployed for each sampling season. Subsequent sampling dates correspond to the removal of collectors used for mussel recruitment and the periods when photographs were taken for barnacles. The number of mussel collector replicates used is shown within parentheses for each month. For barnacles, recruitment was estimated only after one month (samples denoted in bold), and 5 replicates were used for each site.

Region	Site	Latitude	Longitude	Year 2014			Year 2015		
				Start date	1 st sampling	2 nd sampling	Start date	3 rd sampling	4 th sampling
1	Agulhas	-34.814336	20.035767	27/03/14	28/04/2014 (3)	28/05/2014 (1)	18/03/15	17/04/2015 (3)	17/05/2015 (3)
	Arniston	-34.67555	20.232514	27/03/14	28/04/2014 (3)	28/05/2014 (3)	17/03/15	17/04/2015 (3)	17/05/2015 (3)
2	Infanta	-34.42117	20.856461	28/03/14	29/04/2014 (3)	27/05/2014 (3)	19/03/15	18/04/2015 (3)	16/05/2015 (3)
	Jongensfontein	-34.419974	21.358295	01/04/14	30/04/2014 (3)	28/05/2014 (3)	20/03/15	16/04/2015 (3)	15/05/2015 (3)
3	Brenton	-34.075474	23.023671	02/04/14	01/05/2014 (3)	29/05/2014 (3)	21/03/15	19/04/2015 (3)	18/05/2015 (3)
	Plettenberg	-34.00509	23.455178	16/04/14	15/05/2014 (3)	17/06/2014 (3)	22/03/15	19/04/2015 (3)	18/05/2015 (3)
4	Kayser's Beach	-33.212176	27.611796	02/04/14	27/04/2014 (3)	29/05/2014 (3)	24/03/15	23/04/2015 (3)	21/05/2015 (3)
	Kidd's Beach	-33.147068	27.703277	02/04/14	27/04/2014 (1)	29/05/2014 (3)	24/03/15	23/04/2015 (3)	21/05/2015 (3)
5	Haga Haga	-32.766618	28.243178	02/04/14	28/04/2014 (3)	30/05/2014 (1)	26/03/15	22/04/2015 (3)	19/05/2015 (3)
	Morgans Bay	-32.711322	28.339829	02/04/14	28/04/2014 (3)	30/05/2014 (2)	25/03/15	22/04/2015 (3)	19/05/2015 (3)

3.2.2. Environmental variables

3.2.2.1. Upwelling and turbulence indices

Wind data were obtained from the South African Weather Service (SAWS). The closest weather station to each sampling site was selected to obtain hourly data of wind speed and wind direction (see Fig. 3.1). Each station was located at a different height (ranging between 4 – 149 m above sea level). Due to the variation in wind velocity as a function of height, each velocity was corrected to the height of the lowest weather station following Hsu et al. (1994),

$$v_{4m} = v_h * (4/h)^{0.11} \quad (\text{Eq. 3.1})$$

where v_{4m} is the velocity at the lowest height (in this case, the station in Struisbaai, located 4m above sea level), v_h is the wind velocity in each station and h is the height of each station. An upwelling index was calculated following the same equation as in chapter 2 (Bakun 1973), and using the corrected velocities from Eq. 3.1 in Eq. 3.2 as follows,

$$\text{UPW} = \rho_a * C_D * v_{4m} * v_{4m-x} * f^{-1} * \rho_w^{-1} \quad (\text{Eq. 3.2})$$

where ρ_a represents air density (1.22 kg m^{-3}), C_D is the drag coefficient (0.0014), v_{4m} is the wind velocity corrected to the height of the lowest station, v_{4m-x} is the alongshore vectorial component of wind speed, f is the Coriolis parameter (9.96×10^{-5} at middle latitudes) and ρ_w is water density (1025 kg m^{-3}). Positive values of the upwelling index can be interpreted as offshore displacement of the water mass, indicative of upwelling, and negative values as downwelling.

Turbulence was estimated following the same equation as in chapter 2 (Pringle 2007),

$$\mathcal{E} = (v_{4m}/1000)^3 * k^{-1} \quad (\text{Eq. 3.3})$$

where v_{4m} is the wind velocity corrected to the height of the lowest station and k is Von Karman's constant (0.41).

3.2.2.2. Wave height

Wave height data were downloaded from Windguru (<https://www.windguru.cz/>) at three-hour intervals, from the Global Forecast System model (GFS) for the closest location to each site (Fig. 3.1). This forecast system is based on the Wave Watch III (WW3) models developed by the National Oceanic and Atmospheric Administration (NOAA).

3.2.2.3. Chlorophyll-a and sea surface temperature

For each sampling site, chlorophyll-a (chl-a, OCx algorithm dataset) and sea surface temperature (SST, 11 μ daytime dataset) data were obtained from the Moderate Resolution Imaging Spectroradiometer (MODIS) Aqua. Level-3 files were downloaded the Ocean Colour website from NASA (<https://oceancolor.gsfc.nasa.gov/>) and processed with the software SeaWiFS Data Analysis System (SeaDAS) v7.3.1. (Fu et al. 1998) for pixel resolutions of approximately 4km. Daily values were extracted for both variables using the average for 3x3 pixel windows centred 15km offshore and orthogonal to each sampling site to avoid the error obtained in measurements close to land masses (Kahru et al. 2015).

3.2.3. Data analysis

Along the south coast of South Africa, longitudinal patterns in recruitment seem to be present (von der Meden 2009), with the highest abundances reached in the central area and a decreasing trend towards the west and the east. Due to those patterns, longitude was expected to influence recruitment rates along the coast strongly. Thus, *longitude* was selected as a continuous predictor of recruitment rates in the statistical analyses. It is also hypothesized that the presence of red tides along the coast during the two years of the study could influence the recruitment rates observed. Effects could arise from a direct influence of changes in food availability or quality, as a result of a shift from the normal phytoplankton community to a community dominated by the dinoflagellates present during the red tides. Indirectly, the environmental conditions that favoured the appearance of the red tides (for example changes in stratification) may also have influenced recruitment.

3.2.3.1. Environmental predictors of recruitment

In addition to the effect of food quality, chl-a, SST, upwelling index, turbulence and wave height were also considered to have a potential influence on recruitment. To include those variables in the analysis, a period at which they may affect recruitment must be selected. Due to the prolonged period of deployment of the collectors in the field, the exact time of recruitment of the organisms is unknown. To try to reduce that uncertainty, the environmental conditions during different time lags were examined to determine the time periods, if any, where each variable would have been more likely to have influenced recruitment. To do that, moving averages were computed for each variable going backwards from the date of removal of each collector from the rock. Based on the time scales that each variable is likely to operate at, different periods were selected to calculate the moving averages. Upwelling, turbulence and wave height were expected to operate at short time scales, affecting the delivery of larvae to the coast (Farrell et al. 1991, Young 1995, Navarrete et al. 2015). Therefore, two to 14-day moving averages were calculated from the day of removal of the collectors until 25 days before removal. Values of chl-a and SST were expected to have an effect on

a longer time scale, affecting the developmental time of larvae on the water column (Fenaux et al. 1994, Gillooly et al. 2002, O'Connor et al. 2007). For mussels, two to 45-day averages were calculated from the day of removal of the collector until 30 days before removal to account for the period of larval development of approximately one month under laboratory conditions (Satuito et al. 1994, Aarab et al. 2012). For barnacles, two to 21-day averages were calculated until 30 days before removal, considering they have a larval development of approximately two weeks (Patel and Crisp 1960, Qiu and Quian 1997). The average values obtained for each time lag were used in simple linear regressions as predictors of the observed recruitment rates. As recruitment estimates varied over several orders of magnitude, abundances were log-transformed for each taxon using the logarithm to the base 10 of the abundance plus 1, to allow for the relationship with the environmental variables to be linear. Simple linear regressions were calculated for each predictor at each time lag, treating each year separately to account for potential differences between years. Linear regressions were performed in R version 3.2.0. (R Core Team 2015). Due to the nature of the variables, particularly satellite data, missing data can be present. For each predictor and year, the results were ranked by highest variance explained using the R^2 coefficient. To avoid selecting time periods with missing values, data from the regression with the highest variance explained and without missing data were selected for each combination (Table 3.2). In the case of barnacles, chl-a and SST included high amounts of missing data for all the linear regression models during year 2015 and thus, no models were selected.

3.2.3.2. Variation in longitudinal patterns of recruitment

In the present study, Generalized Additive Models (GAMs, Hastie and Tibshirani 1986) were selected to determine if the patterns of recruitment along the coast differed between years. GAMs can cope with non-linear relationships and accommodate different responses to the different levels of the explanatory variables. The GAM smoothers (i.e. the curves that describe the relationship between response and predictor variables) are calculated according to the dataset used and therefore, they will not follow an equation with fixed parameters. To allow different curves to fit the longitudinal patterns of recruitment each year, the variable *year* was included as a factor in the GAM, allowing for its interaction with the continuous variable *longitude*.

Due to the potential effect that environmental conditions can have on recruitment along the coast, it is necessary to consider the effect of those variables in the model. Visual inspection of the relationship between longitude and the environmental predictors of recruitment selected through linear regression, revealed either linear or non-linear relationships. Since all predictors seemed to co-vary with longitude, the addition of environmental variables and longitude in the same GAM would result in multiple variables trying to account for the same portion of variability in the data, which would result in a reduction of the explanatory power of the model. Therefore, to avoid

collinearity problems, each predictor was used in a separate GAM, considering the different combinations between year and longitude, chl-a, SST, upwelling, turbulence or wave height. Due to the reduced sample size and the limited number of longitude values, restricted maximum likelihood (REML) was considered during GAM estimation. This method was selected to correct the degrees of freedom of the smoothing in order to avoid the degree of complexity of the smoothed curves overfitting the data. To meet the model assumptions for GAMs, the recruitment rates for each species were log-transformed prior to analysis to produce residuals that seemed to be normally distributed and without clear patterns of variance heterogeneity. Different GAMs were evaluated using the Akaike Information Criterion (AIC) to select the model that would result in the highest variance explained with the minimum number of parameters. Thus, three different model equations were fitted to predict the log transformed recruitment rates of each species as follows,

$$\log_{10}(1 + \text{Recruitment}_i) = \alpha + f_1(\text{Predictor}_i) \times \text{Year}_{\text{Red tide}, i} + f_2(\text{Predictor}_i) \times \text{Year}_{\text{Post red tide}, i} + \varepsilon_i \quad (\text{Eq. 3.4})$$

$$\log_{10}(1 + \text{Recruitment}_i) = \alpha + f(\text{Predictor}_i) + \text{factor}(\text{Year}_i) + \varepsilon_i \quad (\text{Eq. 3.5})$$

$$\log_{10}(1 + \text{Recruitment}_i) = \alpha + f(\text{Predictor}_i) + \varepsilon_i \quad (\text{Eq. 3.6})$$

where *Recruitment* signifies the recruitment rates observed for each species using one species at a time, α is the model intercept, f symbolises the curve fitted to each continuous variable, *Predictor* is the continuous variable used to predict recruitment (i.e. longitude, upwelling index, turbulence, wave height, chl-a or SST, one at a time), *Year* is the categorical variable for the years 2014 and 2015, and ε is the error of the model.

3.2.3.3. Differences between years in the environmental conditions

GAMs were also used to determine if the environmental conditions thought to influence recruitment differed between years along the coast. The conditions present during the time lags selected through linear regression were compared between years. Thus, the same model equations used in the recruitment analysis (Eq. 3.4 to 3.6). In this case, upwelling index, turbulence, wave height, chl-a and SST were the response variables (instead of recruitment), and longitude and year were the predictors used in the smoothing. This allows one to discriminate if the patterns in the environmental conditions that best explained the recruitment rates of each species were different between years. Due to the lack of appropriate results from the linear regressions for barnacles in the second year (Table 3.2), chl-a and SST were not compared for barnacles. REML was applied again and model selection was performed using the AIC. GAMs were performed using the *gam* function from the *mgcv* package (Wood 2006) in R version 3.2.0. (R Core Team, 2015).

3.3. Results

All the mussel species studied reached the highest recruitment rates (i.e. individuals per m² and day) at Brenton, regardless of month or year (Figs. 3.3 and 3.4) and recruitment decreased towards west and east. *Perna perna*, showed the highest recruitment rates in Brenton during 2015 (Fig. 3.3D, mean=872.81, S.D.=427.26). The peak of recruitment during 2014 was observed in April (also in Brenton), but it was lower than without its presence the following year (Fig. 3.3A, mean=237.11, S.D.=36.97). For other mytilids, recruitment peaked in Brenton on April of both years, but was higher during 2015 (Fig. 3.4A, mean=443.95, S.D.=73.02, and Fig. 3.4C, mean=4851.31, S.D.=1691.63).

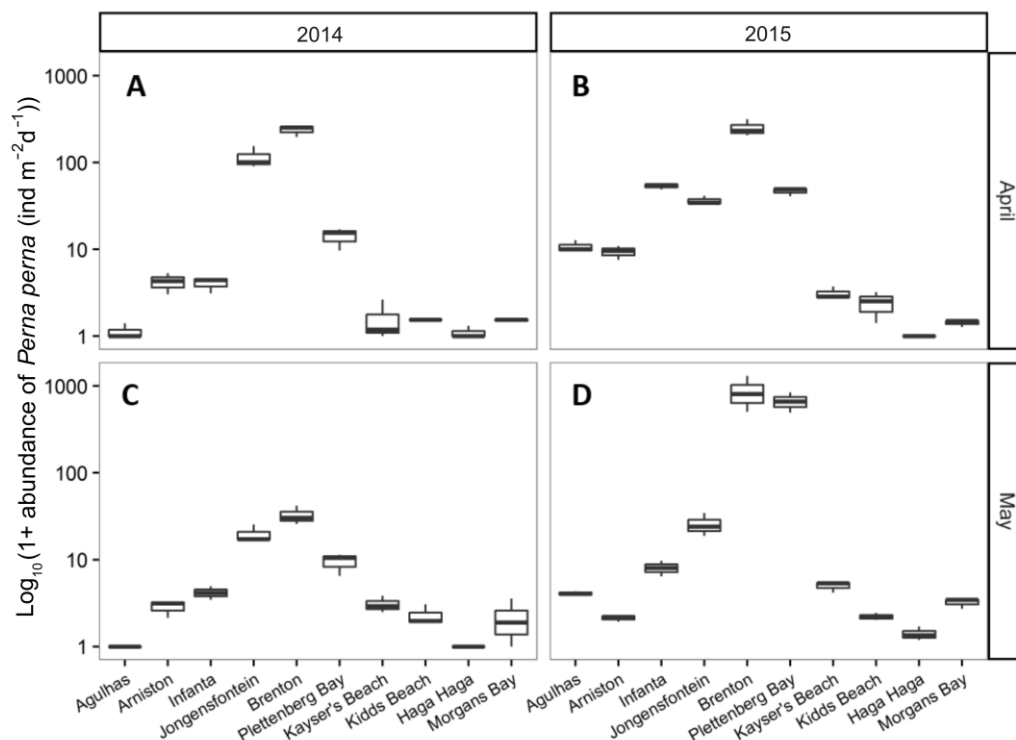


Fig. 3.3. Boxplots of the logarithm to the base 10 of the abundance plus 1 (individuals m⁻² d⁻¹) for *Perna perna* for the 10 sites sampled along the coast (from west to east). One month of recruitment is represented in each panel for year 2014 (panels A and C), and the following year (panels B and D).

Barnacle recruitment showed a longitudinal pattern similar to that for mussels during 2014 (Fig. 3.5A), with the highest recruitment rates occurred more towards the west, between Arniston and Plettenberg. The highest recruitment during 2014 occurred in Plettenberg (Fig. 3.5A, mean=1452.08, S.D.=991.12). Recruitment was lower on 2015, and the highest recruitment occurred in Arniston without any clear longitudinal pattern (Figure 3.6B, mean=184.77, S.D.=46.39). Thus, mussels and barnacles showed opposite recruitment patterns on both years, which could be a result of the selection of sampling months to include the mussel recruitment period but not necessarily adequately covering barnacle recruitment times due to insufficient information for the area.

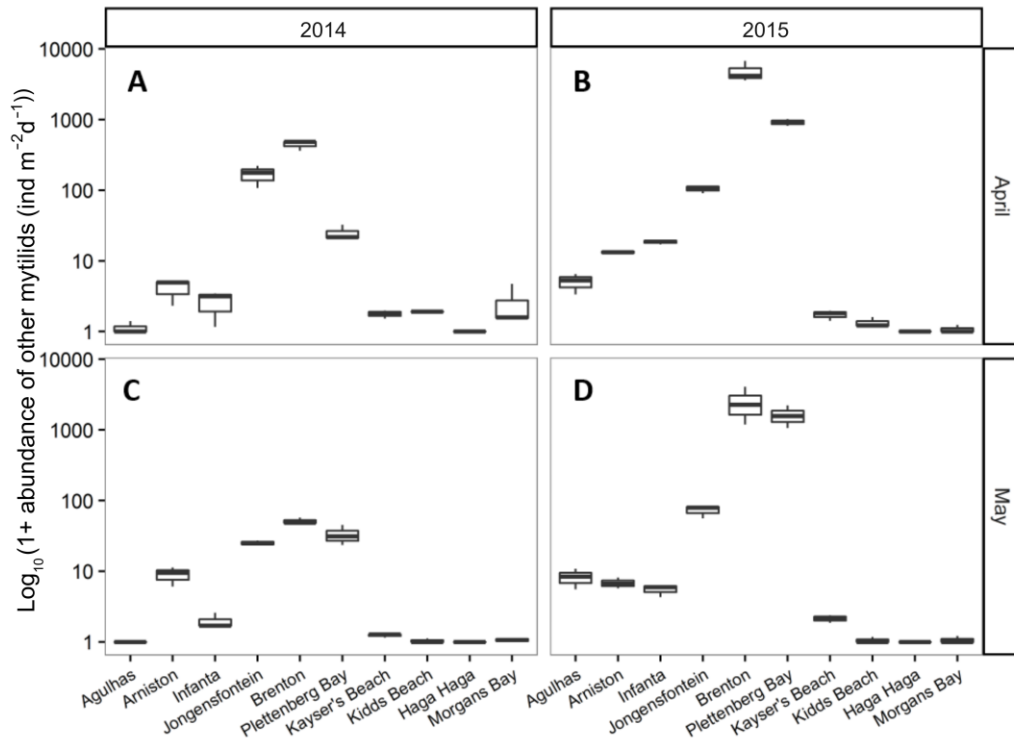


Fig. 3.4. Boxplots of the logarithm to the base 10 of the abundance plus 1 (individuals $m^{-2} d^{-1}$) for other mytilids (comprised by *Mytilus galloprovincialis* and *Choromytilus meridionalis*) for the 10 sites sampled along the coast (from west to east). One month of recruitment is represented in each panel for year 2014 (panels A and C), and the following year (panels B and D).

3.3.1. Environmental predictors of recruitment

Linear regressions were performed between the environmental conditions at different time lags and recruitment. To visualise the results from all the models produced, the explained variances from each individual regression (the R^2 values) were plotted in the form of a heatmap in Fig. 3.6. The x-axis of Fig. 3.6 shows the number of days before the collectors were removed from the rock, considering zero as the day that the collector was removed (which also coincides with the days when photographs were taken for barnacle quadrats), and the y-axis shows how many days were used to calculate the average values of the predictor. In general, environmental data will tend to be more related among periods which are close in time. In addition, conditions averaged over longer periods will share larger amounts of data for different lags, which will result in higher correlation of the data and results which are more similar. Based on that, visual inspection of the heatmaps should reveal the periods which were more likely to influence recruitment as a cluster of regressions with high R^2 values for similar time lags.

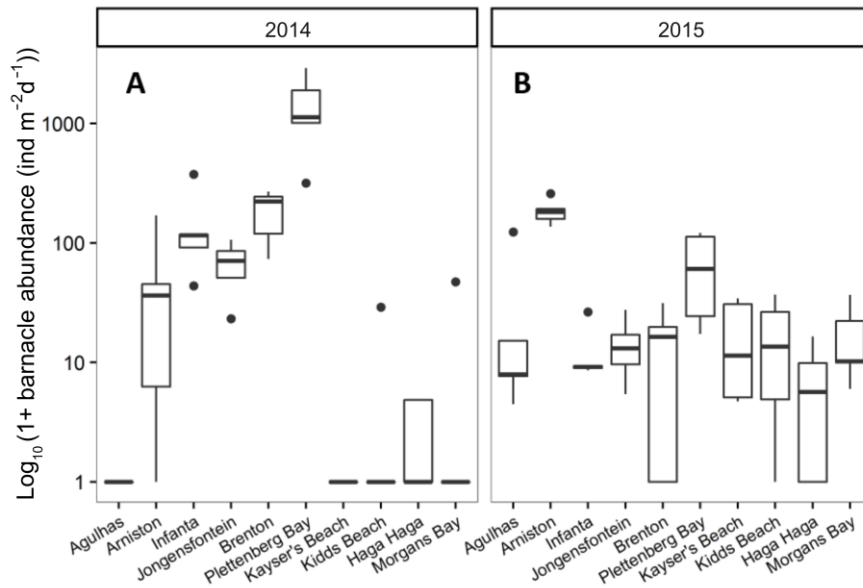


Fig. 3.5. Boxplots of the logarithm to the base 10 of the abundance plus 1 (individuals $m^{-2} d^{-1}$) for barnacles for the 10 sites sampled along the coast (from west to east). One single month of recruitment was estimated for 2014 (panel A), and 2015 (panel B).

The Pearson correlation coefficients, p-values, and degrees of freedom for each time lag selected (for each species and each environmental predictor, and which were selected based on the R^2 values), can be found in Table 3.2. A general overview of the results shows that the predictors that best explained the variance observed were not the same for the two species of mussels and barnacles. Thus, chl-a and SST explained the highest portion of variance for mussels. Conditions were averaged over shorter time periods during 2015 (averages 8 to 15 days shorter depending on the species and variable, see Table 3.2), and both predictors explained higher proportions of variance the same year. For barnacles, the regressions performed using chl-a and SST only showed a good relationship with the data over some periods of 2014 (Table 3.2). During 2014, the high R^2 values observed were spurious results due to the presence of missing data in the linear regressions (results not shown), and no time lag was found to explain the variance observed in recruitment the following year. Nevertheless, upwelling index, turbulence, and wave height, seemed to explain high portions of the variance in barnacle recruitment during 2014 (Table 3.2), although the correlation between recruitment and each of those variables showed opposite signs for each year.

Table 3.2. Results of the best linear regression models. *Lag* refers to the number of days before removal of the collector. Time average is the number of days used to calculate the average of the environmental conditions. R^2 coefficient is used as an estimate of the variance explained by each model and r is value of the Pearson correlation coefficient. The T-statistic, the degrees of freedom (d.f.) and the significance level from each the linear regression are also included. *** $p < 0.001$, ** $p < 0.01$, * $p < 0.05$, n.s.: not significant.

		Year	Lag	Average of days	R^2	r	T-statistic	d.f.	p-value	
<i>Perna perna</i>	Upwelling	2014	25	4	0.228	0.477	3.876	51	***	
		2015	5	2	0.291	-0.539	-4.874	58	***	
	Turbulence	2014	21	2	0.129	-0.359	-2.744	51	**	
		2015	24	2	0.054	-0.232	-1.815	58	n.s.	
	Wave height	2014	22	7	0.535	-0.731	-7.657	51	***	
		2015	7	2	0.349	-0.591	-5.576	58	***	
	Chl-a	2014	29	38	0.286	0.535	4.520	51	***	
		2015	9	25	0.704	0.839	11.747	58	***	
	SST	2014	30	28	0.413	-0.643	-5.989	51	***	
		2015	30	20	0.705	-0.840	-11.772	58	***	
	Other mytilids	Upwelling	2014	3	9	0.131	-0.362	-2.775	51	**
			2015	5	2	0.273	-0.523	-4.667	58	***
Turbulence		2014	21	2	0.046	-0.214	-1.567	51	n.s.	
		2015	4	2	0.017	0.130	0.999	58	n.s.	
Wave height		2014	22	7	0.324	-0.569	-4.944	51	***	
		2015	7	2	0.363	-0.603	-5.753	58	***	
Chl-a		2014	29	31	0.334	0.578	5.062	51	***	
		2015	9	22	0.675	0.821	10.972	58	***	
SST		2014	30	34	0.446	-0.668	-6.406	51	***	
		2015	30	19	0.740	-0.860	-12.846	58	***	
Barnacles		Upwelling	2014	15	8	0.746	-0.864	-11.863	48	***
			2015	8	8	0.203	0.451	3.502	48	**
	Turbulence	2014	20	2	0.582	-0.763	-8.172	48	***	
		2015	4	5	0.206	0.454	3.527	48	***	
	Wave height	2014	24	6	0.735	-0.857	-11.536	48	***	
		2015	10	14	0.210	0.458	3.569	48	***	
	Chl-a	2014	11	44	0.639	0.799	9.221	48	***	
		2015	NA	NA	NA	NA	NA	NA	NA	
	SST	2014	15	8	0.620	-0.787	-8.846	48	***	
		2015	NA	NA	NA	NA	NA	NA	NA	

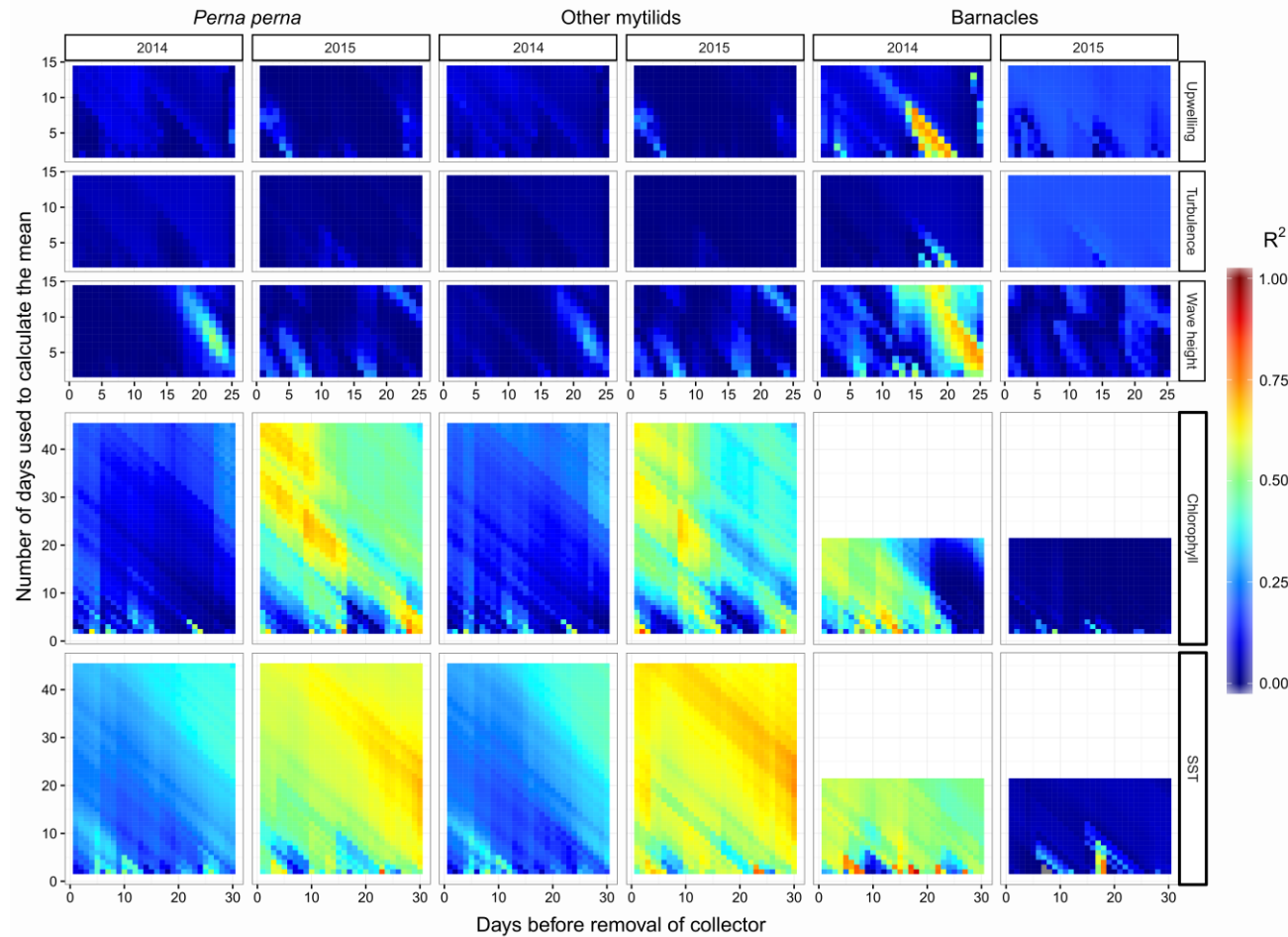


Fig. 3.6. Heatmap showing the R^2 values from each linear regression between the environmental conditions at different time lags and the log-transformed recruitment abundances for all the species of study. Each row of panels shows the results of the environmental predictors used. Each column of panels represents the results for 2014 and 2015 for *Perna perna*, other mytilids and barnacles, respectively. The combination between the horizontal and vertical axes show the time lag used for each regression, with the number of days before the removal of collectors on the x-axis and the number of days used to calculate the mean on the y-axis. Note that the length of the axes is variable, depending on the predictor used. Colour legend shows R^2 values between zero and one (0-100% variance explained). Each colour pixels represents the R^2 value of an individual linear regression model.

3.3.2. Variation in longitudinal patterns of recruitment

For the three species considered, the different GAM models used to select the variable that explains best the recruitment rates observed selected the model which allows the relationship of recruitment and longitude to vary for each year, i.e. the one in Eq. 3.4 (Table 3.3).

For *P. perna* the model with the lowest AIC (66.11) explained 85.8% of the variance. The model with one smooth function for each year was selected, with the curves that describe the relationship of recruitment with longitude were different for 2014 and 2015 ($p < 0.001$, Fig. 3.7A-B). The smooth function during 2014 showed a principal peak of recruitment around 22°E, and a secondary much lower peak to the east (Fig. 3.7A). The following year, recruitment was higher than during 2014, with a monotonic peak of recruitment around 23°E (Fig. 3.7B). The estimated degrees of freedom (edf) for each smooth function reflect the complexity of the curves as the approximate polynomial order of the function, (because the function itself is not described by a parametric equation). Thus, the edf for the year 2014 smoother was 6.25, while the following year it was 4.44, suggesting that the relationship of recruitment with longitude during 2015 was simpler than during 2014.

Table 3.3. Model selection results for Generalized Additive Models (GAMs) for recruitment ($\log_{10} 1+$ abundance (individuals $m^{-2} d^{-1}$)). The model selected by AIC for each species is highlighted in bold.

Model	<i>P. perna</i> AIC	Other mytilids AIC	Barnacles AIC
lon × year	66.11	1.75	171.91
lon + year	97.58	113.29	233.03
lon	126.37	153.17	231.19
upw × year	67.27	217.27	176.18
upw + year	237.94	235.82	187.19
upw	242.95	233.85	192.05
turb × year	266.30	162.98	175.84
turb + year	264.34	288.67	180.02
turb	266.53	287.42	197.17
wave × year	210.97	279.23	177.99
wave + year	222.69	286.47	191.78
wave	219.07	281.85	213.19
chl × year	146.61	230.21	NA
chl + year	162.03	219.96	NA
chl	161.86	220.24	NA
sst × year	148.26	167.00	NA
sst + year	150.36	183.09	NA
sst	148.50	182.15	NA

For other mytilids, the model with the lowest AIC (1.75) had the same structure as for *P. perna*, and explained 95.6% of the variance. Two smooth functions were required, one for each year ($p < 0.001$,

Fig. 3.7C-D). The function describing the relationship was again more complex for 2014 (edf=7.92) than for 2015 (edf=6.37). Three peaks of recruitment appeared during 2014 (Fig. 3.7C), a minor one to the west, a principal peak c. 22°E (the same as in *P. perna*), and a third very subtle peak to the east. The following year the structure of the smooth function was much simpler, with a single peak in the centre, again c. 22°E, and recruitment rates were higher than the previous year (Fig. 3.7D).

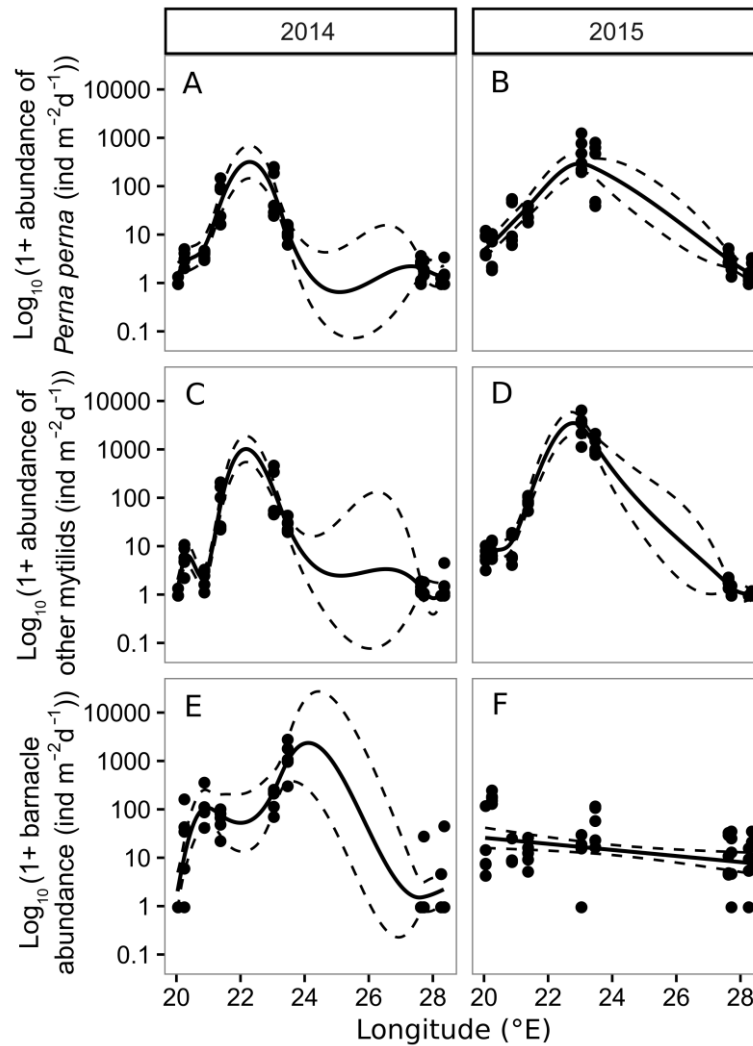


Fig. 3.7. Generalized Additive Models (GAMs) for the predictor selected through AIC (see description in text) for the log-transformed recruitment abundances of each species. Longitude was selected in all cases. Column panels show the model fitted for 2014 and 2015, respectively. Horizontal panels correspond to each species of study: *Perna perna* (A and B), other mytilids (C and D), and barnacles (E and F). Solid lines show the GAM smoothers from each model selected, and dashed lines show the 95% C.I.

Barnacles showed a very different relationship with longitude during both years. The model selected was also the one in Eq. 3.4. (AIC=171.91), which only explained 64.8% of the variance. The smooth function of year 2014 was highly significant ($p < 0.001$). Two peaks of recruitment were present, a smaller one to the west c. 21°E, and the most intense c. 24°E (Fig. 3.7E). Thus, during 2014

the structure of the smooth function was more complicated than the following year (5.59 and 1 edf, respectively). For 2015, the relationship with longitude was described by a linear regression (Fig. 3.7F, $p < 0.01$), reflecting that the longitudinal pattern in recruitment does not hold for barnacles during 2015 and shows a decreasing trend in recruitment rates from west to east.

3.3.3. Differences between years in the environmental conditions

In general, analysis of the environmental conditions selected from the best time lags (see Table 3.2) showed that the alongshore patterns varied between years (Fig. 3.8). The upwelling conditions were different for the two species of mussels and barnacles (Fig. 3.8A-C). For *P. perna*, the GAM selected for upwelling index (Eq. 3.4) included a function of longitude for each year (AIC=432.80), but none of the terms were significant. The model selected for other mytilids (AIC=419.08) included a non-significant effect of *year* ($p=0.09$) and a significant smoothing function for *longitude* ($p < 0.01$). In the case of barnacles, the best model (AIC=201.38) included significant differences between years ($p < 0.01$) and a significant longitudinal effect on upwelling during 2015 ($p < 0.001$ for the smoother on the second year).

Turbulence was highest in the west, with a sharp decrease towards the east (Fig. 3.8D to F). For *P. perna* and other mytilids (AIC=-1261.64 and -1265.63, respectively) turbulence values were a function of *longitude* ($p < 0.001$ in both cases) without differences between years. For barnacles, separate smoothing functions were selected for each year ($p < 0.001$ for each year).

The time lags selected for wave height for the two species of mussels were the same for both years and thus, the GAM results were the same. The best model (AIC=40.09) included different smoothers for each year ($p < 0.001$, Fig. 3.8G-H). The relationship of wave height with longitude was significant during 2015 ($p < 0.001$), although it was not significant during 2014 ($p=0.29$). For barnacles (Fig. 3.8I), wave height was significantly different on both years ($p < 0.001$), but the relationship with longitude was not ($p=0.11$).

Chl-a and SST during the lags selected showed significant differences between years for both species of mussels. The longitudinal pattern of chl-a showed higher values during 2015, with significantly different longitudinal patterns on both years ($p < 0.001$, Fig. 3.8J-K). For SST, the longitudinal pattern along the coast was the same, but temperatures during the lags selected were higher along the coast during 2014 ($p < 0.001$, Fig. 3.8M-N).

In summary, all the species studied showed different longitudinal patterns in recruitment each year, with the highest abundances reached in the central sites (except for barnacles during year 2015 which showed relatively low recruitment at all sites). In general, food availability and SST seemed to explain higher percentages of variability in mussel recruitment; and upwelling, turbulence, and wave height (which are more related with larval delivery) explained better the

variability observed in barnacle recruitment. In the case of mussels, chl-a and SST may have influenced recruitment over a shorter time lag during 2015 than on 2014. Mussel recruitment was highest during 2015, when chl-a was higher, and SST was lower along the coast than during 2014. In the case of barnacles, highest recruitment was present during 2014. Chl-a and SST did not show a good relationship with barnacle recruitment, but upwelling, turbulence, and wave height seemed to negatively correlate with recruitment during 2014.

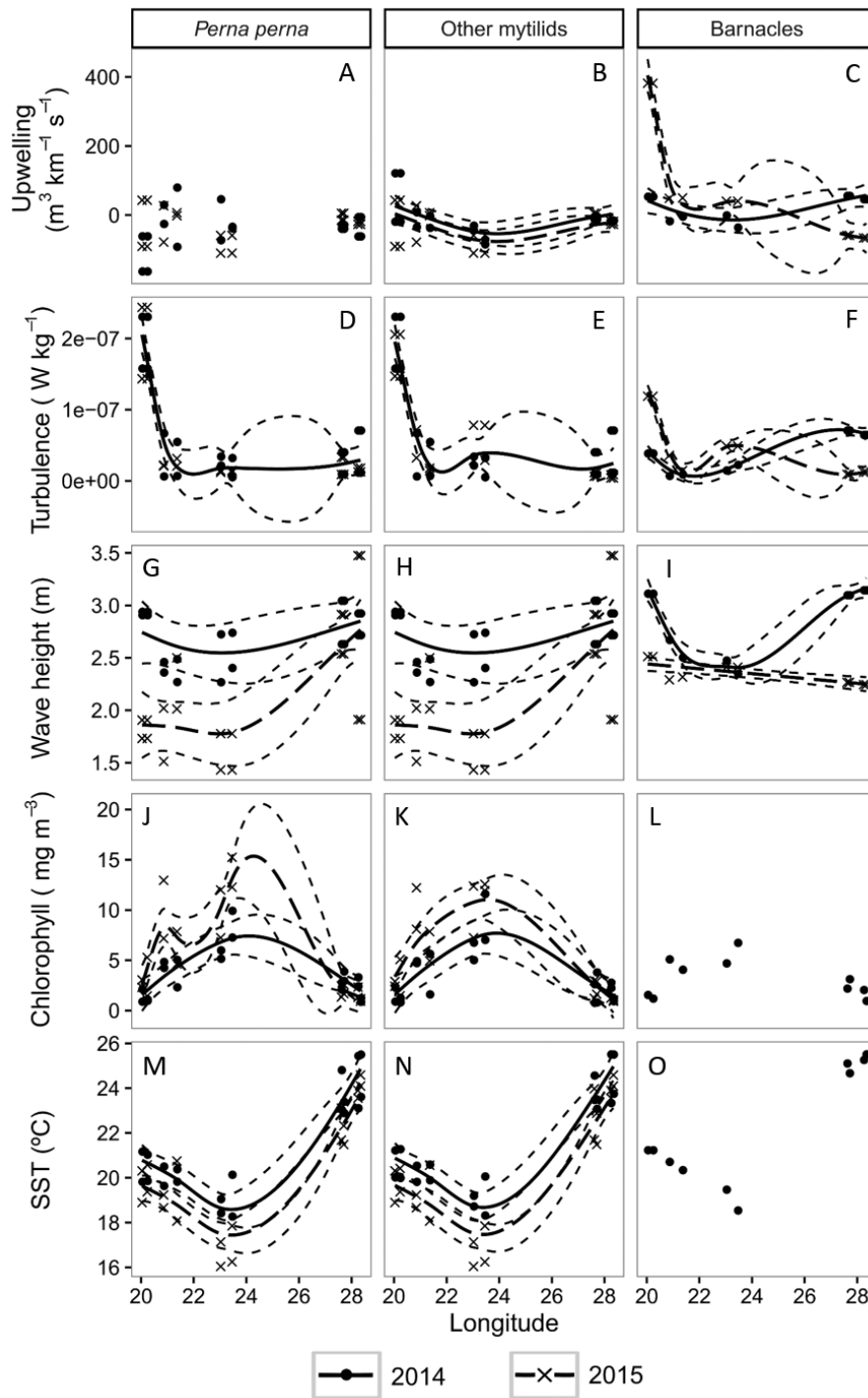


Fig. 3.8. Generalized Additive Models (GAMs) for each environmental predictor of recruitment during the time lags that best predicted recruitment for each species and year along the South Coast of South Africa (see description in text). Horizontal panels correspond to each predictor and vertical panels to each species of study. Dots and crosses represent years 2014 and 2015, respectively. Solid lines show the GAM smoothers for year 2014. Dashed lines show the smoothers for year 2015. Short-dashed lines show the 95% C.I. for each respective smoother.

3.4. Discussion

Strong differences in recruitment of mussels and barnacles were observed during the two years of study, with highest mussel recruitment during autumn 2015, when *Lingulodinium polyedrum* was not present, and the opposite pattern observed for barnacles. A possible caveat which could affect the recruitment estimates could arise from the sampling period selected for barnacles. While sampling was carried out to coincide with the peak of mussel recruitment in the region (Zardi et al. 2007), little information is available on the reproductive periods of barnacles for the same area. Therefore, it is possible that the peak of barnacle recruitment might not have overlapped with that of mussels and could have been missed during 2015. This could also have been affected by the use of a single month of recruitment data for barnacles, as opposed to the two months used for mussels. The high recruitment rates observed the first year suggest that even if variable, barnacle recruitment does occur during the study period. Nevertheless, the uncertainty on timing of barnacle recruitment prevents from linking recruitment patterns to inter-annual variability, and thus, the results presented here should be taken with caution.

3.4.1. Limitations of the study

The present study had several limitations that should be considering during the interpretation of the results. First, due to the nature of the study it was not possible to estimate the relative contributions of the various predictors of recruitment. Hence, the effects of variability in food supply (produced by changes in phytoplankton composition/abundance during a red tide event) cannot be separated from the effect of variability in the environmental conditions which may have led to the development of such event. Nevertheless, environmental conditions in a complex system are likely to influence each other or co-vary. Thus, even if confounding effects arise because multiple variables drive the system simultaneously, considering multiple components will provide the framework in which the system operates and expose the effects of co-dependent variables. Secondly, recruitment rates of marine organisms are variable between years (Smith 1985, López et al. 1998, Botsford 2001, Wing et al. 2003), including mussels and barnacles (Broitman et al. 2005, Porri et al. 2006, Menge et al. 2009, Tapia and Navarrete 2010). Although inter-annual variability in recruitment affects the interpretation of the results obtained between years in the present study, variability is associated with changes in the environmental conditions that affect the return of competent larvae to the coast, including mechanisms which influence upwelling dynamics (Connolly and Roughgarden 1999, Broitman et al. 2005). Again, although the comparison of recruitment rates between years cannot support conclusions about the effects of changes in the trophodynamic system caused by the presence of red tides, the environmental conditions existing during the periods of study, which influenced the appearance of each red tide, are also expected to influence recruitment. Therefore, changes in recruitment produced by changes in the environment

or by the presence of the dinoflagellate were considered an acceptable proxy of change in the system as a result of a red tide event.

The origin of the datasets used to study the relationship between environmental variables and recruitment also deserves additional consideration. Intertidal, nearshore, and offshore waters are affected differently by different factors such as coastal upwelling, river discharge, nearshore ocean currents, turbulence, or heat transfer with the atmosphere, resulting in different conditions on each level. In fact, differences of several degrees have been reported between intertidal and satellite temperature estimates (Smale and Wernberg 2009, Lathlean et al. 2011, Smit et al. 2013). In the present study, SST and chl-a data were estimated over 12x12km areas centred 15km offshore from the recruitment sites (i.e. between nine and 21km offshore). Such areas were selected to reduce the error that land masses may produce on satellite estimates, however, conditions offshore will not reflect nearshore or intertidal conditions. Although larval retention mechanisms may keep larvae closer to the coast than the areas selected to estimate SST and chl-a (see for example Tapia and Pineda 2007, Morgan et al. 2009), it was not possible to estimate temperature or chl-a in nearshore waters during the periods of study. Although satellite estimates will not accurately describe SST variability or extreme values, strong correlations have been reported between satellite and benthic temperatures measured in shallow waters (10-12m depth, Smale and Wernberg 2009). Thus, without more adequate mechanisms to measure nearshore conditions at relevant scales, satellite estimates have been considered an adequate alternative in previous similar studies (Broitman et al. 2008, Woodson et al. 2012, Filgueira et al. 2015, Mazzuco et al. 2015).

3.4.2. Mussels

Differences in SST and chl-a conditions were found between both years and mussel recruitment showed a strong relationship with both variables. A positive correlation appeared with chl-a, and negative with SST during the periods of study. During 2014, a simpler longitudinal pattern in recruitment appeared, which would agree with the spatial structure of mussel recruitment described for the South Coast of South Africa in previous studies (von der Meden 2009). The alongshore patterns during 2015 revealed consistently lower SSTs, and higher chl-a levels during the study period than during 2014. The patterns of chl-a and SST during mussel recruitment periods agree with the lower SSTs observed along the South Coast during autumn of 2015 (see Results section in Chapter 2). Temperature dependence of developmental times has been proposed for organisms with larval stages in marine (Gillooly et al. 2002, O'Connor et al. 2007), as well as in

terrestrial systems (Álvarez and Nicieza 2002, Bayoh and Lindsay 2003). Gillooly and co-workers (2002) modelled the influence of SST for developmental times, based on the effects of temperature on the kinetics of metabolic processes (Gillooly et al. 2001). Based on the metabolic theory of ecology (MTE), shorter developmental times would be expected at higher temperatures (Gillooly et al. 2002). In the context of this study, higher SSTs during autumn 2014 would be expected to reduce the period that larvae spend in the plankton. This could be expected to translate into positive effects on survival by reducing the time that larvae are exposed to planktonic predators or food limitation in the water. Models developed by O'Connor and co-workers (2007) predict increasing survival rates of organisms with higher temperatures during development. Based on this, SSTs observed during the 2014 would have been expected to have a positive effect on recruitment. Nevertheless, recruitment rates for mussels were higher on 2015, when SSTs were consistently lower than in 2014. Analysis over different lag periods between SST and mussel recruitment revealed that temperature best correlated with mussel recruitment over four-week and three-week periods for each year, respectively (Table 3.2). These periods approximately match the expected developmental periods of mussel larvae in the water (Aarab et al. 2012, Satuito et al. 1994). A possible explanation is that, although temperatures were higher during 2014, development could have been faster during the following year. Although SST was one of the predictors which best explained mussel recruitment, other factors are expected to have acted in combination with SST to influence mussel recruitment.

The central area around the Plettenberg upwelling cell (c. 24°E) experienced the lowest SSTs along the coast (see Fig. 3.8). Increased surface expression of periodic upwelling events during 2015 was suggested by the lower average SSTs observed during autumn 2015 (see Fig. 2.8), and the lower SSTs which occurred during the period in which recruitment was studied that year (Fig. 3.8). Periods of upwelling are expected to enhance primary productivity. Autotrophic phytoplankton, like diatoms, depend on the replenishment of nutrients in photic layers for their growth. When water column stratification increases, dinoflagellates, which have multiple nutrient acquisition mechanisms, can potentially outcompete diatoms and modify the structure of the trophic web. Proliferation of dinoflagellates can additionally result in competition with larvae for food, as both can potentially prey on diatoms. Thus, the higher temperatures observed along the coast during 2014, in addition to the results in Chapter 2 (Figs. 2.8 and 2.9), indicate warming of surface waters and increased water column stability during 2014. In addition to contributing to the development of *Lingulodinium polyedrum* blooms, this could have resulted in a decrease in diatoms, potentially resulting in higher competition for food between the larvae and *L. polyedrum*. During the following year, lower SSTs reflect increased mixing in surface waters. The upwelling of bottom water results in nutrient availability which favours diatom growth, and increased turbulence which has been proposed to impede dinoflagellate growth (Thomas and Gibson 1990). The relationship between SST and

recruitment could thus reflect an indirect effect of nutrient increase through upwelling and increasing food availability or quality for larvae during autumn 2015.

This interpretation would agree with the positive correlation observed between chl-a and mussel recruitment (see Table 3.2). The mismatch between the present results and the expected positive effects of temperature on development and subsequent recruitment suggests the influence of other factors such as food availability, in the form of chl-a, in combination to SST. Although the influence of temperature on metabolic rate is considered to be much greater than the effects of food (O'Connor et al. 2007), food availability can have profound effects on larval development and survival in both mussels (Phillips 2002, 2004) and barnacles (Moyses 1963, Qiu and Qian 1997). Co-occurring with lower SST, higher chl-a levels were observed along the South Coast in 2015 for the best correlations (see Fig. 3.8). As for SST, the best time-lag correlations between chl-a and mussel recruitment occurred during approximately four-week and three-week periods, respectively, for each year (Table 3.2). Thus, SST and chl-a may have had a combined effect, contributing to shorten mussel developmental times during 2015. This would agree with the results reported by Bayne (1965), who found that at higher food concentrations the developmental times for larvae of *Mytilus edulis* were shortened, almost reducing the time to reach the pediveliger stage by half. Pechenik and co-workers (1990) also showed that the combined effects of higher food concentration and higher temperature increased growth rates of *M. edulis*.

In general, the conditions that influence larvae during development seemed to explain more variability in recruitment patterns than the variables which are likely to influence delivery to the settlement sites (e.g. upwelling, turbulence or wave height). However, previous studies have reported a positive relationship between wave action and daily mussel recruitment on rocky shores of Eastern Boundary Upwelling Systems (EBUS; Pfaff et al. 2015, Navarrete et al. 2015). Navarrete and co-workers (2015) proposed that intertidal recruitment of two species of mussels found in the Chilean coast occurs sequentially, involving a relocation mechanism from the subtidal. Thus, Navarrete and co-workers (2015) proposed that competent larvae settle in the subtidal, beyond the surf zone, and are later transported to the intertidal by wave action, providing a positive correlation between recruitment and wave height. In contrast, a negative relationship was found between recruitment of both species of mussels and wave height in the present study. One explanation to these different findings could involve the study species. McQuaid and Phillips (2000), and McQuaid and Lawrie (2005) reported competent stages in the plankton of *M. galloprovincialis* and *P. perna*, respectively, the main species of focus in the present study, while Navarrete and co-workers (2015) did not find competent larvae in the plankton during their study. The effect of waves on recruitment could depend on behaviour post-metamorphosis, which could be species-specific, and depend on the ability of pediveliger stages to remain in the water column. The ability

of pediveligers to remain in the plankton could uncouple any dependence of recruitment on wave action. Another possible explanation could arise from the differences in temporal resolution between the present and previous studies. Navarrete and co-workers (2015), and Pfaff and co-workers (2015), collected samples daily to obtain a direct estimate between the conditions present in the water column and settlement. Along the coasts of Oregon and California, Shanks and co-workers (2017) found a positive relationship between wave height and recruitment using weekly estimates. In the present study, although recruitment and waves were examined using all time combinations that would produce biologically meaningful results, monthly recruitment rates could comprise multiple settlement events throughout the month (e.g. by recently metamorphosed larvae or by later pediveliger stages), or reflect differences in post-settlement mortality. As a result, even if there is an effect of waves on each settlement event, the short time scales at which they operate will be masked by the conditions between periods of successful settlement, preventing the model from identifying a general pattern in which wave height influences recruitment.

3.4.3. Barnacles

In contrast to mussels, barnacles reached higher abundances during 2014. Also in contrast to mussels, the environmental predictors that seemed to correlate with recruitment were different. SST and chl-a did not show any relationship with barnacle recruitment during 2015. Nevertheless, a relationship similar to that of mussels was found during 2014, with barnacle recruitment positively correlated with chl-a and negatively correlated with SST. Negative correlations of barnacle recruitment during 2014 occurred with upwelling (i.e. higher recruitment during downwelling conditions), turbulence and wave height. Periods of downwelling or upwelling relaxation have been previously correlated with barnacle recruitment (Farrell et al. 1991, Broitman et al. 2005). The negative relationships found with turbulence and wave height also support the interpretation that pulses of recruitment co-occurred with the relaxation of winds. A decrease in upwelling favourable winds would promote the approach of the water mass to the shore, and would also agree with low turbulence produced by wind. Farrell and co-workers (1991) observed that barnacle recruitment was associated with pulses of onshore transport of the water mass during periods of upwelling relaxation. Similarly, Broitman and co-workers (2005) found pulses of barnacle recruitment to be correlated with warmer conditions in the water mass, suggesting that the onshore transport of surface waters could have favoured recruitment. Recruitment estimates for mussels and barnacles in Broitman et al. (2005) showed the opposite relationship with SST to that in the present study. While they observed a strong relationship between barnacle recruitment and SST, estimates of barnacle recruitment in the present study did not show any relationship with temperature. In addition, the present results showed a strong relationship of mussel recruitment with SST and with chl-a, while Broitman and co-workers (2005) did not find a correlation between mussel recruitment

and temperature anomalies, with a possible explanation to this disagreement being the different pelagic duration of the study species.

3.4.4. Comparing taxa

Broitman and co-workers (2005) assumed longer developmental times for barnacles than for mussels (three to four weeks, and nine days, respectively). For *Mytilus galloprovincialis* (one of the predominant species in South Africa), Satuito and co-workers (1994) reported competent larvae after approximately 26 days (reared at 19°C). For *Perna perna*, Aarab and co-workers (2012) also found competent larvae after 26 days (reared at 21°C). In the case of barnacles, similar species to the ones in the present study have been reported to moult into cyprids after approximately 11-14 days (Patel and Crisp 1960, Brown and Roughgarden 1985, Kado and Kim 1996, Qiu and Quian 1997, Burrows et al. 1999, Chan 2003). In contrast to the situation for Broitman and co-workers (2005), the mussel species in the present study have considerably longer developmental periods than barnacles. Broitman and co-workers (2005) proposed that the relationship between recruitment and SST could reflect delivery during downwelling conditions. Similarly, the present study revealed a negative correlation between barnacle recruitment and upwelling index, (i.e. increased barnacle recruitment during downwelling). Here, it is proposed that the recruitment of organisms that spend longer periods in the plankton will exhibit a higher dependence on temperature and food conditions than organisms with shorter developmental times, which in turn are more influenced by the delivery of competent larvae to the settlement sites. Prior to a red tide-bloom, the concentration of cells in the water may be low and peak relatively rapidly. Considering that peaks in the concentration of cells will depend on the environmental conditions, blooms are likely to occur recurrently but not continuously in time. Thus, the chances of larvae co-occurring with a red tide bloom are lower for organisms with shorter developmental times, like barnacles, than for organisms which spend longer periods in the water, like mussels. Based on that difference, *L. polyedrum* may not have been present during the development of barnacles, but the frequency of surface blooms observed (at least one peak per month, see Chapter 2) indicates that it must have been present during parts of the development of mussels. Thus, one explanation for the differences in recruitment between mussel and barnacles could be based on the presence or absence of *L. polyedrum* during the development of the larvae.

Different temperature conditions or food supply between years may have also affected the timing of reproduction of adult mussels and barnacles, as well as other organisms. In fact, earlier warming of the water mass has been described to advance the timing of reproduction in bivalves (Philippart et al. 2003, Filgueira et al. 2015). Philippart et al. (2003) also reported reduced reproductive output for the bivalve *Macoma balthica* as a result of warmer winter conditions. The timing of larval release may also present a significant interannual variability as it is driven by multiple environmental

conditions that may affect mussels and barnacles in different ways. In barnacles, high phytoplankton concentrations and high frequency of storms have been identified as the main cues for synchronous larval release, probably as an evolutive response to larval starvation and predation (Starr et al. 1991, Gyory and Pineda 2011). Although phytoplankton availability was also linked to larval release in blue mussels (Starr et al. 1990), much higher concentrations were required to trigger release in the barnacle *Semibalanus balanoides* (Starr et al. 1991). However, the present study did not measure any reproductive parameter during the two years of study, and it remains unknown if conditions during gamete maturation and larval hatching may have resulted in reduced reproductive output, which would also negatively affect recruitment.

In addition to the environmental predictors used, other factors which cannot be assessed through this sort of study might provide alternative explanations to the opposite temporal trends observed for mussels and barnacles. Biological differences are present between both taxa, like larval size, developmental times, or swimming ability, which could influence the relationship between larvae and *L. polyedrum*. Bivalve veligers are generally smaller than barnacle nauplii, and the size of particles that larvae can handle is limited by the anatomical structures involved in capturing and processing those particles. In the case of mussels, Jeong and co-workers (2004) reported that *M. galloprovincialis* was able to prey on *L. polyedrum*, despite of the large particle size of the dinoflagellate. For barnacles, Moyses (1963) reported species of balanids to be able to develop at least to the cyprid stage when fed a large diatom ($75 \times 45 \mu\text{m}$), while a species of chthamalids was not able to develop when fed the same particles. Nonetheless, Griffiths (1979) observed barnacle nauplii of *Tetraclita serrata* to feed on eggs of *Choromytilus meridionalis* which measured $45\text{-}70 \mu\text{m}$, (slightly larger than *L. polyedrum*) after grabbing and piercing them. The ability of larvae to feed on large particle sizes might then be influenced by the hardness of the particle and the possibility of the larvae to pierce the cells. In the case of diatoms, nauplii might not be able to break the theca, but with thecate dinoflagellates like *L. polyedrum*, because the external cover is composed of multiple plates, the structure may be less resistant to mechanical stress when manipulated by the larvae. Thus, in the case of *L. polyedrum*, barnacle larvae might be able to manipulate the cells during periods like cell division, when the plates that compose the external cover are likely to be less resistant to damage or breakage. Thus, nauplius size, and particle size and hardness, might affect the ability of larvae to feed on the dinoflagellate. Overall, this would suggest the ability of larvae of mussels and barnacles to feed on *L. polyedrum*, which alone would not explain the differences in recruitment rates observed between both taxa in the presence of the dinoflagellate. Nevertheless, another important consideration of the differences in larval sizes are the differences in swimming velocities between mussels and barnacles. Swimming velocities of some balanids were around four times greater than in *Mytilus edulis* (0.43 and 0.11 cm s^{-1} , respectively, Chia et al. 1984). References in Lewis and Hallett (1997) give swimming velocities between 0.25 and 0.4 cm s^{-1} for *L. polyedrum*. This

could imply that when *L. polyedrum* is present in the water, barnacle nauplii might be able to capture the particle, but the greater swimming velocities of the dinoflagellate compared to the veligers will allow *L. polyedrum* to escape predation from mussels. Another possibility could imply that the ability to avoid the water masses affected by the red tide could be greater in barnacle nauplii than in mussel veligers. Greater swimming velocities in barnacle nauplii could allow them to avoid water masses affected by the *L. polyedrum* red tide and favour them to find other particles suitable for consumption. In fact, barnacle nauplii are known to perform diel vertical migrations (Tapia et al. 2010, Bonicelli et al. 2016) while veligers show less clear temporal patterns across the water column also influenced by wind turbulence (McQuaid and Phillips 2000, Weidberg et al. 2015). On the other hand, experimental work on *L. polyedrum* has revealed that this dinoflagellate swims upwards during the day, probably to enhance photosynthesis, and it is spread uniformly across the vertical axis during the night (Moorthi et al. 2006). Thus, faster nauplii would avoid the dinoflagellate by staying at the bottom during daytime, and such avoidance would be less clear for veligers. Such mechanisms may not be applied to barnacle cyprids as they tend to be located at fixed depths, usually close to the bottom (Tapia et al. 2010, Bonicelli et al. 2016), and they no longer feed. In addition to this, the presence of the dinoflagellate in the water could positively affect other organisms, like copepods which can also feed on larvae, increasing their abundances in the water (Fernández 1979, Huntley et al. 1986, Jeong 1994). Increases in predator abundances can also negatively affect larvae through increased mortality when the developmental times in the water are longer. The potential superior ability of barnacle larvae to feed on *L. polyedrum* could explain why the dependency of the environmental predictors that affect development is stronger in mussels than in barnacles. Thus, developmental times on barnacles might not have been negatively impacted by the red tide, resulting in a higher dependency of the water flows which allow larval delivery to the coast.

In summary, results in the present study suggest a stronger dependency of food and temperature for organisms with longer times of development. Environmental conditions which affect delivery would be associated to organisms with shorter periods of development. Although the data available is limited to two years of study, differences in SST and chl-a were evident between years. Mussel recruitment seemed to strongly resemble the longitudinal patterns observed on those variables. Thus, the presence of *Lingulodinium polyedrum* seemed to have negatively affected mussel recruitment, either through changes on the trophodynamics of the system, or through changes in the conditions also associated with the red tide, such as increased stability. Thus, variability in seasonal averages of SST and chl-a as observed during the past years (see Discussion in Chapter 2), could produce major changes in mussel recruitment. Due to the short life span of adult mussels, successive negative recruitment events could jeopardise population maintenance and pose a major threat for species which play a key role on benthic communities.

Chapter 4

Indirect effects of environmental conditions during larval development on growth and mortality rates of barnacle juveniles



Foam observed in Jongensfontein (16th April 2015).

Indirect effects of environmental conditions during larval development on growth and mortality rates of barnacle juveniles.

4.1. Introduction

Adult populations are affected by a complex combination of factors operating at multiple spatial and temporal scales. For organisms with complex life histories which include larval stages, the interaction between larvae and the environment will determine their fate and affect the population through larval supply (Thorson 1950, Alexander and Roughgarden 1996, Pineda 2000). Those larvae will be influenced by biotic (for example predation, competition or starvation) and abiotic factors (for example temperature, anoxia or water mass processes which determine larval delivery). Thus, temperature is inversely related to duration of developmental period in aquatic ectotherms (Gillooly et al. 2002). Although food availability also influences duration of larval development, its effect is less marked than that of temperature (Fenaux et al. 1994, Hoegh-Guldberg and Pearse 1995). In the case of crustaceans, both variables determine the period between moults, the energy accumulated, or size attained during each larval stage (Hartnoll 2001). In addition, changes in larval duration may affect biotic interactions. For example, longer duration of the planktonic life may increase the risk of predation and mortality in the water (O'Connor et al. 2007, Tapia and Pineda 2007), and the possibility that larvae will be exported by currents and lost (Pineda et al. 2007, Cowen and Sponaugle 2009).

Juvenile growth of marine organisms is strongly affected by water temperature and food concentration (Crisp 1960, Crisp and Bourget 1985). Nevertheless, larval condition is known to influence post-settlement development of juvenile marine invertebrates later in development (Pechenik et al. 1996, Pechenik et al. 1998, Pechenik 2006). Thus, temperature and food during larval development may play a key role in juvenile performance and, even if survival rates are not affected, the changes experienced by the larvae may be carried over and affect juvenile organisms. In the case of barnacles, differences in physiology and behaviour have been reported between the naupliar and cyprid stages. In general, barnacle development comprises six naupliar stages (with the last five stages being planktotrophic), and a cyprid stage which lacks a digestive system and relies on the reserves accumulated during the previous naupliar stages (West and Costlow 1988). Energy reserves accumulated during naupliar stages will be used both during the cyprid stage, and during the first days after settlement, until the feeding structures and digestive system of the juvenile are formed. Thus, food quantity and temperature during development have been reported to influence cyprid size and energy content, size at recruitment, initial growth rates, and survival of juvenile barnacles (Jarrett and Pechenik 1997, Qiu and Qian 1997, Pechenik et al. 1998, Hentschel and Emler 2000, Jarrett 2003, Thiyagarajan et al 2003a, Thiyagarajan et al. 2005). The lack of feeding

capability in the cyprid implies that the energy resources accumulated during naupliar stages must be allocated to return to the adult habitat and find a suitable substratum for settlement.

The amount of time that the larvae can delay metamorphosis in the search of suitable settlement substrata will be limited by the cyprid energy content (Pechenik et al. 1993, Jarrett and Pechenik 1997, Thiyagarajan et al. 2002). Delayed metamorphosis will deplete the energy available and reduce initial juvenile growth rates (Pechenik et al. 1993). In fact, Thiyagarajan et al. (2003b) analysed the effect of metamorphosis delay and food concentration on juvenile growth and survival, and concluded that delay of metamorphosis affects juvenile growth and survival more than food quantity during development (as energy reserves in the cyprid are depleted with time, which reduces the energy available until the juvenile is able to feed again). Food quality plays an important role in the energy reserves accumulated (Harder et al. 2001, Thiyagarajan et al. 2002). Different phytoplankton particles have different nutritional values, and therefore, diet composition may strongly affect energetic content, particularly regarding lipids (Leonardos and Lucas 2000a, 2000b, Marshall et al. 2010, Aranda-Burgos et al. 2014). Thiyagarajan et al. (2003a), reported that lipid reserves constituted the highest percentage of the energy reserves in cyprids of *Balanus amphitrite*, followed by proteins, with a small percentage of energy accumulated in the form of carbohydrates. Cyprid energy content, temperature, and food concentration during the first days after metamorphosis, also interacted and significantly affected growth rates up to five days after metamorphosis (Thiyagarajan et al. 2003a). Each individual variable had an effect on growth until 10 days after metamorphosis, but the interaction among them was no longer significant (Thiyagarajan et al. 2003a). Thus, although the effect of larval preconditioning was lost within the first two weeks after metamorphosis, smaller sizes at the time of settlement, or slower growth rates in the juveniles can strongly affect post-settlement processes, reducing the ability of juveniles to compete for space, and increasing the risk of predation (Jarrett 2000).

Thus, food quality and quantity have a critical longer-term influence through the nutrition acquired by larvae. Even if larvae are capable of feeding on a particular species of phytoplankton, it may provide inadequate nutrition. This could be of particular relevance during red tide blooms. Changes in the food realm produced by a mono-specific phytoplankton community may compromise later subsequent developmental stages which directly depend on the energy accumulated. For instance, Dam and Colin (2005) used the toxic dinoflagellate *Prorocentrum minimum* as food for the copepod *Acartia tonsa* and concluded that the negative effects observed were a consequence of the poor nutritional value of *P. minimum* rather than a matter of toxicity. Similarly, Prince et al. (2006) tested the effect of *Karenia brevis*, another toxic dinoflagellate, as food of *A. tonsa*, and suggested that the negative effects observed were also due to the poor nutritional value of the dinoflagellate.

Due to the importance of the supply of new organisms into intertidal populations for their replenishment, and the changes in recruitment rates observed between years, the present study aimed to test if survival and growth rates differed between the year affected by the *Lingulodinium polyedrum* bloom, and the following year with presence of *Noctiluca scintillans*, to detect potential medium-term temporal effects (on the scale of months) as a result of trophic shifts in the planktonic system or through changes in the environmental conditions.

4.2. Material and methods

Based on the strong differences in recruitment patterns of barnacles between 2014 and 2015 (see results in Chapter 3), growth, and mortality rates of juvenile barnacles, mainly *Chthamalus dentatus*, were examined to determine potential effects of the *L. polyedrum* red tide on the early stages of development. Because the sampling was part of the general coast-wide sampling for recruitment, and not initially planned to study early stages of development of barnacles, fundamental constraints were present for the study of growth and mortality rates. Thus, from the 10 sites used to estimate recruitment, only Infanta and Jongensfontein (Fig. 4.1A) provided sufficient photographs of adequate quality to follow growth for six months after initial recruitment during both 2014 and 2015. Site selection was constrained to these two sites due to the difficulty of finding enough identifiable solitary individuals throughout all photographs for both years. For example, although Plettenberg Bay had showed marked differences in recruitment between years, the excessive recruitment and subsequent overcrowding experienced during the autumn 2014 made it impossible to track individual organisms.

Table 4.1. Periods used to estimate recruitment, growth, and mortality rates during 2014 and 2015 delimited by start and end dates. Barnacle recruits were assigned to different age groups depending on presence/absence in the photographs. Start date refers to the first photograph where each barnacle recruit was observed, and end date refers to the last photograph where they were found. Note that each individual barnacle was assigned to a single age group for each site, and different barnacles were used each year (number of recruits in each group indicated as individuals).

Site	Age group	Red tide year			Post red tide year		
		Start date	End date	Individuals	Start date	End date	Individuals
Infanta	A	29/04/2014	27/05/2014	47	18/04/2015	16/05/2015	6
	B	27/05/2014	09/09/2014	14	16/05/2015	29/09/2015	16
	C	29/04/2014	09/09/2014	52	18/04/2015	29/09/2015	1
Jongensfontein	A	30/04/2014	28/05/2014	9	16/04/2015	15/05/2015	9
	B	28/05/2014	10/09/2014	37	15/05/2015	27/09/2015	20
	C	30/04/2014	10/09/2014	17	16/04/2015	27/09/2015	5

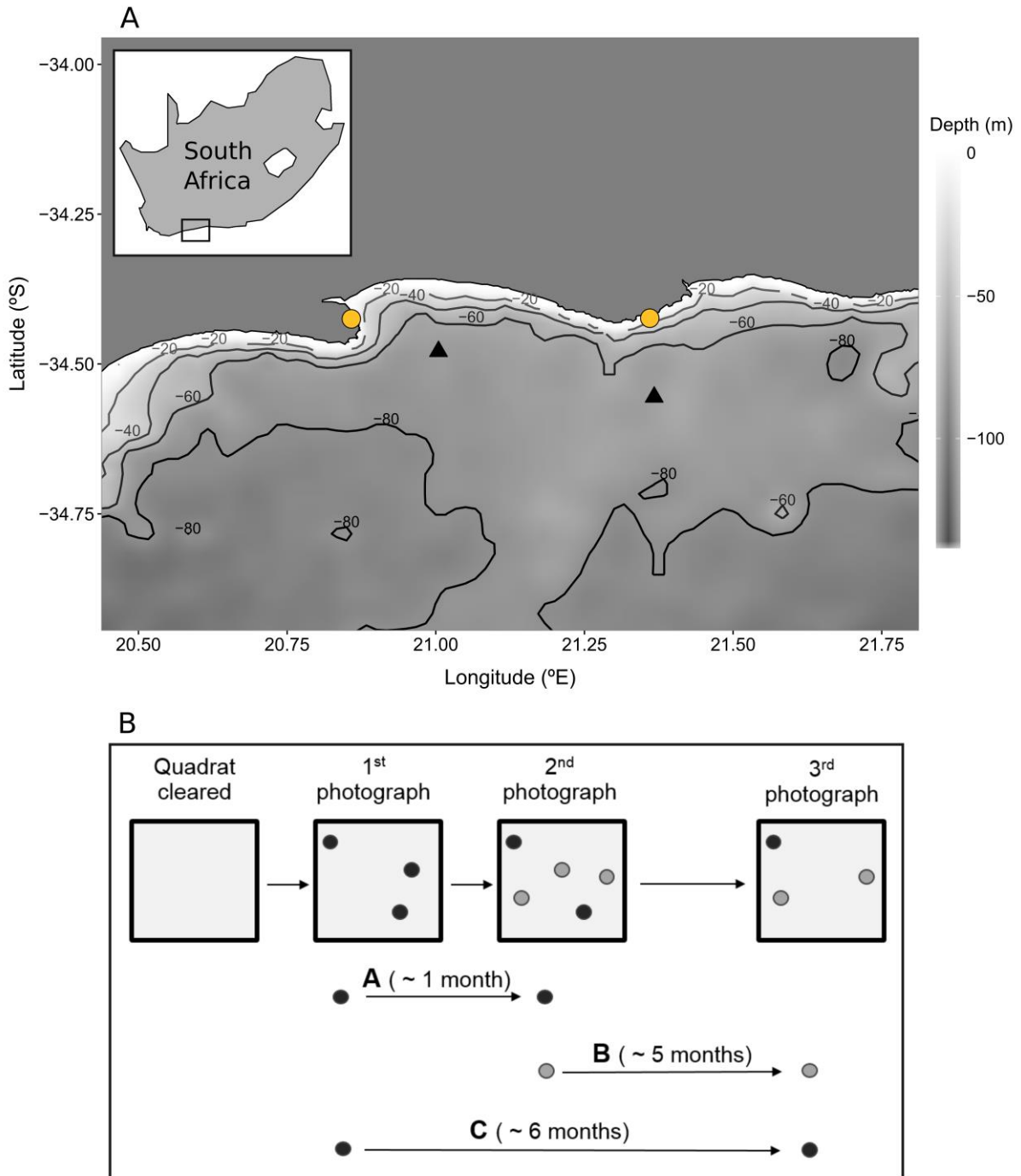


Fig. 4.1. (A) Study sites. Yellow circles show Infanta (left) and Jongensfontein (right). Black triangles show the position where selected satellite data were acquired, centred 15km offshore. Colour scale represents bottom depth, as well as contour lines. (B) Sampling design schematic. “Quadrat cleared” refers to the start date when quadrats were established and cleaned. 1st, 2nd, and 3rd photographs correspond to each date when quadrats were re-visited (see details in table 4.1). Note that barnacle recruits were included in a single age group (A, B, or C) and new quadrats were cleared during the second year of sampling.

4.2.1. Barnacle recruitment in Infanta and Jongensfontein

In addition to the recruitment estimates obtained during April each year (see material and methods in Chapter 3), recruitment was estimated again in May in Infanta and Jongensfontein for the same five quadrats used in April. To ensure that the same individuals counted in May had not been counted in April already, the corresponding photographs were compared to confirm that individuals settled only within the month prior to the photographs taken in May. All counts were converted to abundances per unit of surface area (m^2) per day, following the same procedure used in section 3.2.1 (see Chapter 3). In this case, the value for 'days' corresponded to the number of days elapsed between the photographs in April and May. Because the same quadrats were used to estimate recruitment in April and May, without clearing them between photographs, a Pearson correlation test was used to test for independence in the recruitment estimates obtained on both months. A highly significant positive correlation was found ($r=0.82$, $n=20$, $p<0.001$), indicating that recruitment in May was positively affected by previous recruitment in April.

Based on that, the assumption of independence for analysis of variance (ANOVA) was violated and thus, a repeated measures ANOVA was performed in Statistica version 13 (TIBCO Software Inc. 2017). The repeated measures ANOVA ($n=5$ per site and year, hence $n=20$ in total) included the factors *site* (random, 2 levels), and *year* (fixed, 2 levels). Recruitment rates were found to be not normally distributed, and variances were not homogeneous. The logarithm to the base 10 of the abundance plus 1 was applied to transform the data, which resulted in normally distributed data (Shapiro-Wilk's test, $p=0.23$ in April, $p=0.52$ in May), and homogeneous variances (Levene's test, $p=0.60$ in April, $p=0.81$ in May), with no clear patterns in the standardized residuals of the model. Analysis was performed on the log-transformed recruitment rates.

4.2.2. Juvenile barnacle growth

The same sites were used to compare growth rates of recently settled barnacles during 2014 and 2015. Due to the temporal and spatial extension of the general project, and because the analysis of growth rates was added to the project after recruitment results had been obtained, sampling resolution to estimate growth (and mortality rates in the following section), was restricted to three specific times. For each year, photographs were taken (Fig. 4.1B; Table 4.1): (1) approximately one month after the quadrats had been cleared (i.e. in April), (2) approximately two months after the initial clearing (i.e. in May) and (3) approximately six months after clearing (i.e. in September). Solitary recruits that were present in at least two of those photographs were selected, and their sizes were measured. ImageJ 1.50b Software (Schneider et al. 2012) was used to measure maximum basal diameter length. A section of known length in the metal square which delimited the quadrats was used to scale each photograph. Growth rates were calculated using only maximum basal

diameter, as it has been shown to correlate with basal area (Sanford and Menge, 2001). Standard growth rates were calculated as,

$$\text{Standard growth rate} = (\text{FD} - \text{ID}) / d \times \text{ID} \quad (\text{Eq. 4.1})$$

where FD (Final Diameter) indicates maximum basal diameter in the last photograph used (in mm), ID (Initial Diameter) is the maximum basal diameter in the first photograph where each individual appears (in mm), and d represents the number of days between photographs (in days). Due to the different times of recruitment, and survival of the individuals, growth rates can be grouped in three main periods of interest which from here on will be referred to as *age groups* for simplicity (Fig. 4.1B): (1) growth rates of individuals present in April and May which did not survive until September (age group A, $n = 71$), (2) growth of individuals first recorded in May that survived until September (age group B, $n = 87$), and (3) growth of individuals that appeared in April and survived for the entire period (age group C, $n = 75$). Each recruit was allocated to one age group, and only individuals that were solitary in all photographs were used to avoid growth limitation due to space. A factorial analysis of variance (ANOVA) was performed with *site* (random, 2 levels), *year* (fixed, 2 levels) and *age group* (fixed, 3 levels) as factors, in Statistica version 13 (TIBCO Software Inc. 2017). Type III sums of squares were selected to compute the factorial ANOVA as being more robust to unbalanced sample size among the groups. Data were not normally distributed (Shapiro-Wilk's test, $p < 0.001$). Log-transformation to the base 10 of the growth rates did not result in normally distributed data (Shapiro-Wilk's test, $p < 0.001$) and variances were not homogeneous (Levene's test, $p < 0.001$). Considering that the analysis of variance is robust to deviations from normality when sample sizes are large enough (Underwood 1997), data were not transformed for analysis.

4.2.3. Juvenile barnacle mortality

For each site, five photographs were selected for each year in April, May and September. The total number of recruits was counted for the same age groups used to estimate growth rates (Figure 4.1B). Quadrats were inspected to avoid counting the same individuals more than once. Individuals were compared among the three photographs to account for survivors. Standardised mortality rates were calculated for each age group as,

$$\text{Standardised mortality rate} = D / d \times R \quad (\text{Eq. 4.2})$$

where D indicates the number of individuals that died between the initial and the last photograph considered for each age group, d indicates the number of days between the initial and the last photograph, and R is the number of recruits present in the initial photograph.

A factorial ANOVA ($n=5$ per combination, hence $n=60$ in total) was performed with *site* (fixed, 2 levels), *year* (fixed, 2 levels) and *age group* (fixed, 3 levels) as factors, in Statistica version 13 (TIBCO

Software Inc. 2017). Data were not normally distributed (Shapiro-Wilk's test, $p < 0.001$), and variances were not homogeneous (Levene's test, $p < 0.001$). As transformation did not remove problems of non-normality or heteroscedasticity, untransformed data were analysed using the same design as for growth.

4.2.4. Environmental conditions during barnacle growth

In addition to the effect that food availability and temperature can have on larval survival and recruitment (Fenaux et al. 1994, O'Connor et al. 2007), these two variables are also important determinants of growth and survival of barnacle juveniles (Crisp and Bourget 1985, Pechenik et al. 1998, Thiyagarajan et al. 2003a). Thus, sea surface temperature (SST) and chlorophyll-a (chl-a) were examined during the periods when growth and mortality rates were estimated. Daily chl-a data were obtained from MODIS Aqua level-3 images, at 4km resolution (referred to as *pixels*), downloaded from the Ocean Biology Processing Group (OCBP) from NASA (OCx algorithm, <https://oceancolor.gsfc.nasa.gov/>). For SST, daily data from MODIS Aqua at 4km resolution were downloaded directly from the ERDDAP server from NOAA for the area of interest (11 μ daytime dataset, <https://coastwatch.pfeg.noaa.gov/erddap/griddap/erdMH1sst1day.html>). For both variables, daily averages of nine pixels were calculated (12x12km total area), centred 15km offshore of Infanta and Jongensfontein (Fig. 4.1A). Pearson correlation tests were applied in search of an overall influence of chl-a and SST on juvenile growth and mortality rates at the periods when these were estimated. Average values of chl-a and SST were calculated for each year, site and age group combination and Pearson correlation tests were performed against growth rates for each combination in R version 3.2.0. (R Core Team, 2015). Non-significant correlations were obtained between average growth and chl-a ($r = -0.48$, $t = -1.74$, $df = 10$, $p = 0.11$), and SST ($r = 0.49$, $t = 1.77$, $df = 10$, $p = 0.11$).

Based on the correlation results, values of daily SST, and chl-a, during the periods used for each age group were examined in more detail. Generalized Additive Models (GAMs, Hastie and Tibshirani, 1986) were used to study the non-linear structure of temperature for each period. The period in age group C was excluded from the analysis due to the limited number of individuals that were measured during the post red tide year (Table 4.1). Three different models were performed for the periods used in age groups A and B independently, and considering the conditions present in Infanta and Jongensfontein together,

$$\text{Predictor} = \alpha + f_1(\text{Day}_i) \times \text{Year}_{\text{Red tide}, i} + f_2(\text{Day}_i) \times \text{Year}_{\text{Post red tide}, i} + \varepsilon_i \quad (\text{Eq. 4.3})$$

$$\text{Predictor} = \alpha + f(\text{Day}_i) + \text{factor}(\text{Year}_i) + \varepsilon_i \quad (\text{Eq. 4.4})$$

$$\text{Predictor} = \alpha + f(\text{Day}_i) + \varepsilon_i \quad (\text{Eq. 4.5})$$

with *Predictor* being the environmental variable used (i.e. chl-a or SST), α being the intercept of the model, *Day* being the Julian day when satellite values of SST were measured, *Year* being the categorical factor 2014 or 2015, *f* being the smoothing function applied, and ϵ being the error term for the model. The presence of *L. polyedrum* or *N. scintillans* was included as the *Year* term in the models to accommodate differences in the non-linear structure of SST and chl-a during 2014 and 2015 in the same fashion as used in Chapter 3 (see material and methods therein). Restricted maximum likelihood (REML) was used during GAM model fitting, and model selection was performed using the Akaike Information Criterion (AIC). GAMs were performed using the function *gam* from the *mgcv* package (Wood 2006) in R version 3.2.0. (R Core Team, 2015).

4.2.5. Long-term conditions in SST and chl-a

The long-term temporal structure of chl-a and SST was analysed separately for Infanta and Jongensfontein. For each site, eight-day level-3 composite images from MODIS Aqua data, processed by the Ocean Biology Processing Group from NASA were downloaded from (<https://oceancolor.gsfc.nasa.gov/>). Eight-day averages of nine pixels at 4km resolution, centred 15km offshore, were calculated. Annual climatologies were constructed using data from the 1st of January 2003 until the 31st December 2012 as baseline conditions. The conditions during the years 2013, 2014, and 2015 were examined to determine differences in temperature and chl-a during those years that could potentially influence juvenile growth and survival. For each year used, conditions were smoothed with a 30-day running average. All figures were plotted using the package *ggplot2* (Wickham 2009) in R version 3.2.0. (R Core Team 2015).

4.3. Results

4.3.1. Barnacle recruitment in Infanta and Jongensfontein

As previously observed in the longitudinal structure of recruitment along the coast (Chapter 3, Fig. 3.5), the repeated measures ANOVA of the log-transformed recruitment rates in Infanta and Jongensfontein showed that recruitment was significantly higher during the year of the red tide caused by *L. polyedrum* than the following year (Table 4.2, $F_{1,16}=18.66$, $p<0.001$). Higher recruitment rates (almost one order of magnitude higher) were found during the year affected by *L. polyedrum*, and no significant differences were found between sites or between the two months sampled (Fig. 4.2).

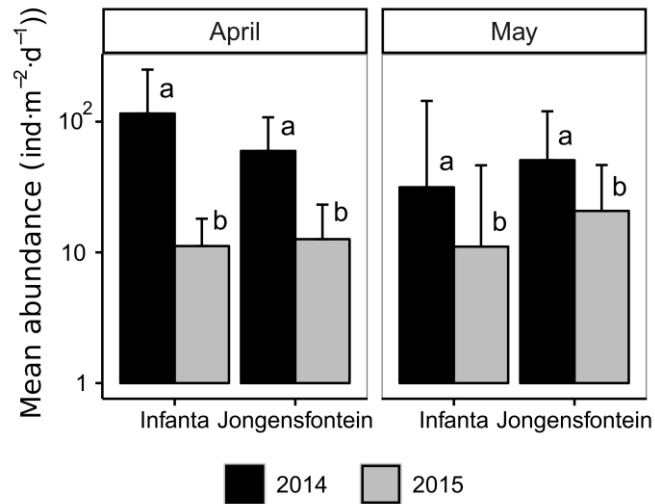


Fig. 4.2. Barnacle recruitment rates as logarithm to the base 10 of the abundance plus 1 (individuals $m^{-2} d^{-1}$) (Mean + S.D.; $n=5$ per site and year, hence $n=20$ in total) at Infanta and Jongensfontein during 2014 (black, with presence of *L. polyedrum*) and 2015 (grey, with presence of *N. scintilans*). Note that for the same year, the same quadrats were used to estimate recruitment in April and May, but different quadrats were used between years. Recruits were counted only in the first photograph where they appeared. Letters refer to the homogeneous groups from repeated measures ANOVA ($p < 0.05$).

Table 4.2. Repeated measures ANOVA of recruitment performed at two sites during 2014 and 2015. Recruitment was estimated during April and May of each year using the same quadrats (correlated abundances, Pearson correlation test, $r=0.82$, $n=20$, $p<0.001$). Si: site, Yr: year; *** $p < 0.001$, n.s.: not significant.

	df	MS	F	p
Si	1	0.04	0.18	0.68 (n.s.)
Yr	1	4.01	18.66	0.00 (***)
Yr × Si	1	0.10	0.48	0.50 (n.s.)
Error	16	0.21		
MONTH	1	0.11	0.86	0.37 (n.s.)
MONTH × Si	1	0.32	2.45	0.14 (n.s.)
MONTH × Yr	1	0.45	3.44	0.08 (n.s.)
MONTH × Yr × Si	1	0.05	0.36	0.56 (n.s.)
Error	16	0.13		

4.3.2. Juvenile barnacle growth

The factorial ANOVA of the standardized growth rates showed a significant interaction between year, site and age group (Table 4.3 complete data set, $F_{2,221}=7.88$, $p<0.001$, Fig. 4.3A). Due to the low number of recruits allocated into age group C (Table 4.1), a reduced version of the data set which excluded growth rates of group C was used. The same factorial ANOVA was used and the interaction between year, site and age group was still significant when age group C was not considered (Table

4.3, reduced data set, $F_{1,150}=12.93$, $p<0.001$). Bonferroni test revealed that individuals in age group A from Jongensfontein grew faster than individuals in any other group during the red tide (Fig. 4.3B).

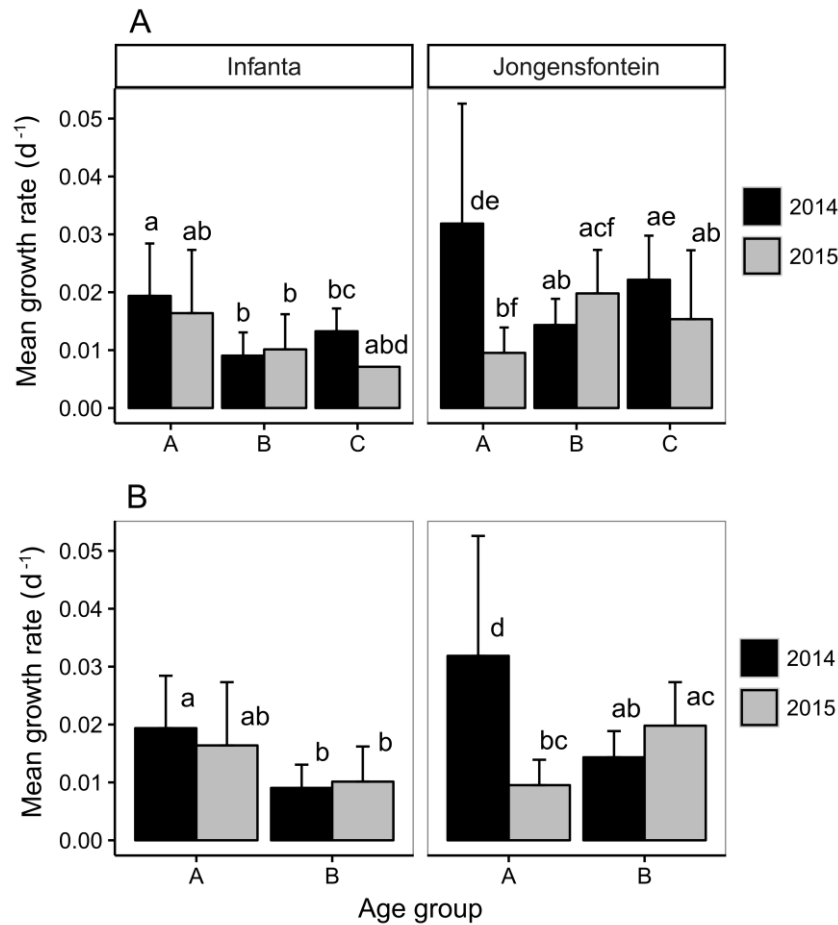


Fig. 4.3. Mean standardised growth rates (d^{-1}) (Mean + S.D.; $n=233$) for two sites during 2014 (black) and 2015 (grey), for the entire data set (A), and for the analysis with age group C excluded (B). Lower case letters show the homogeneous groups from factorial ANOVA ($p < 0.05$). For details on age groups, see Fig. 4.1 and Table 4.1.

Table 4.3. ANOVA results of standardised growth rates in two sites during 2014 and 2015 ($n=233$). Si: site (random), Yr: year (fixed), Gr: age group (fixed); *** $p < 0.001$, n.s.: not significant.

	Complete data set				Reduced data set			
	df	MS	F	p	df	MS	F	p
Yr	1	<0.001	4.10	0.29 (n.s.)	1	<0.001	1.57	0.43 (n.s.)
Si	1	<0.001	5.76	0.15 (n.s.)	1	<0.001	3.17	0.24 (n.s.)
Gr	2	<0.001	5.76	0.14 (n.s.)	1	<0.001	6.53	0.24 (n.s.)
Yr × Si	1	<0.001	0.37	0.60 (n.s.)	1	<0.001	0.40	0.64 (n.s.)
Yr × Gr	2	<0.001	1.85	0.35 (n.s.)	1	<0.001	1.80	0.41 (n.s.)
Si × Gr	2	<0.001	0.18	0.85 (n.s.)	1	<0.001	0.15	0.76 (n.s.)
Yr × Si × Gr	2	<0.001	7.88	<0.001 (***)	1	<0.001	12.93	<0.001 (***)
Error	221	<0.001			150	<0.001		

4.3.3. Juvenile barnacle mortality

Results of the factorial ANOVA to compare mortality rates did not show any significant interaction between site, year and age group. Significant differences in standardised mortality rates were only found between age groups (Table 4.4, $F_{2,47}=56.09$, $p<0.05$). No significant differences in mortality rates were found between years or between sites. Bonferroni *post hoc* test revealed that the standardised mortality rates in group A were significantly higher than in groups B and C, but mortality in groups B and C was not significantly different (Fig. 4.4).

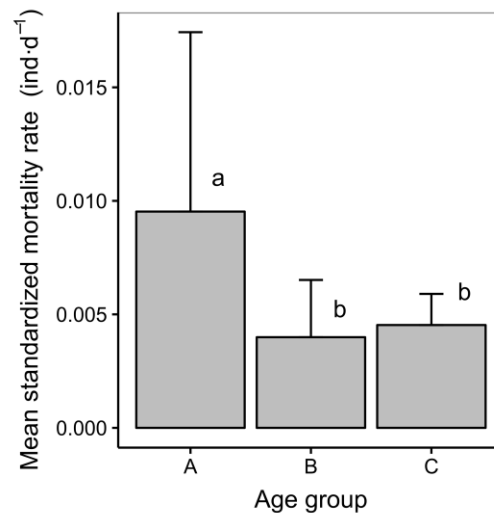


Fig. 4.4. Mean standardised mortality rates (individuals d⁻¹) (Mean + S.D.; n=5 per year, site and age group, hence n=60 in total). Lower case letters show the homogeneous groups from factorial ANOVA ($p < 0.05$). For details on age groups, see Fig. 4.1 and Table 4.1.

Table 4.4. ANOVA results of standardised mortality rates at two sites during the red tide and the following year (n=5 per site, year and age group, hence n=60 in total). Si: site (random), Yr: year (fixed), Gr: age group (fixed); * $p < 0.05$, n.s.: not significant.

	df	MS	F	p
Yr	1	<0.001	3.19	0.33 (n.s.)
Si	1	<0.001	1.25	0.53 (n.s.)
Gr	2	<0.001	56.09	0.02 (*)
Yr × Si	1	<0.001	0.73	0.48 (n.s.)
Yr × Gr	2	<0.001	0.31	0.76 (n.s.)
Si × Gr	2	<0.001	0.10	0.91 (n.s.)
Yr × Si × Gr	2	<0.001	1.35	0.27 (n.s.)
Error	47	<0.001		

4.3.4. Environmental conditions during barnacle growth

GAMs were used to examine the non-linear temporal structure of the environmental conditions that could have affected juvenile barnacles during the periods of study. In general, SST and chl-a

conditions differed between years during both periods considered for growth, thus different model structures were required to accommodate differences in the temporal structure present. Model selection through AIC indicated that the model specified in Eq. 4.3, i.e. the one with one smoother for each year, was the most suitable to describe temporal variability in SST. For the period considered for age group A, the model with the lowest AIC (151.68) explained 61% of the variance. One smoother was required for each year (Fig. 4.5A, smoother for year 2014 $p < 0.001$, smoother for year 2015 $p < 0.05$). Temperatures were higher during the first few days of the year with presence of the *L. polyedrum* red tide and decreased around Julian day 125 (beginning of May), during austral autumn (Fig. 4.5A). During the following year, temperatures were in general lower than the previous year, but two temperature peaks were obtained around Julian days 115 and 130, respectively (Fig. 4.5A). During the period considered for age group B, two smoothers were also required to fit the temporal structure of SST (Fig. 4.5B). The model in Eq. 4.3 was selected (AIC=471.30), explaining 62.1% of the total variance. The two smoothers required in the model were highly significant ($p < 0.001$). During year 2014, SST was lower during the first days of the period than during the following year (Fig. 4.5B). SST started increasing in the middle of winter, approximately after day 200 on 2014 (ca. mid-July; Fig. 4.5B), and around Julian day 220, several weeks later, the following year (ca. mid-August; Fig. 4.5B).

For chl-a, the model in Eq. 4.4 was selected during the period of age group A (AIC=105.60). General chl-a structure was similar during both years, but chl-a values were higher during 2015 (Fig. 4.5C, $p < 0.001$ for the smoothers on each year). The model explained 31.5% of the variance in chl-a during the period studied for age group A. For age group B, Eq. 4.3 was selected (AIC=101.03), explaining only 28% of the variance. During growth of juveniles in age group B, the two smoothers were highly significant ($p < 0.001$). Although both periods presented similar temporal structure with chl-a peaks during winter, slightly higher values of chl-a seemed to persist during year 2015, also showing a small peak in the middle of winter (ca. Julian day 190).

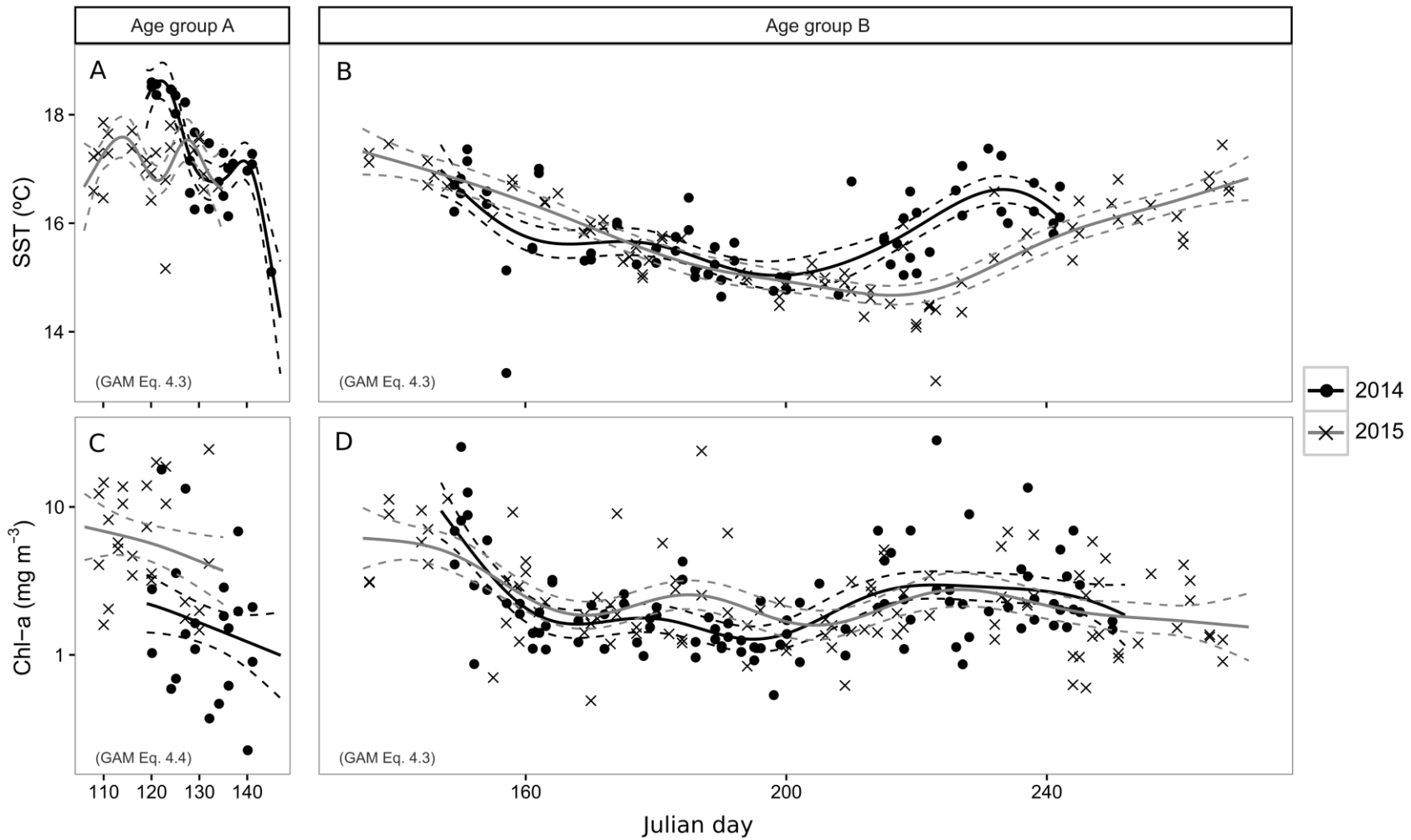


Fig. 4.5. Generalized Additive Models (GAMs) selected for SST (A – B) and chl-a (C – D) for each age group (see Fig. 4.1B). Solid lines represent the GAM equations selected and dashed lines the 95% C.I. in black and grey for years 2014 and 2015, respectively (see equations in text). SST and chl-a measurements in each panel are represented by black dots during year 2014, and by crosses during the following year.

4.3.5. Long-term conditions in SST and chl-a

Based on the different environmental conditions observed during the year 2014 and the following year in the GAM models, the annual cycles of SST and chl-a at Infanta and Jongensfontein were examined to determine if the conditions during those two years differed from usual site-specific seasonal conditions. In general, chl-a during the periods when barnacle growth was estimated during 2014 exceeded the values observed in previous years, and water temperatures were lower than the reference values during year 2015.

SST showed a marked annual cycle with temperatures ranging approximately between 15 and 22°C in winter and summer, respectively (Fig. 4.6A-B). In general, temperature ranges were more variable between Julian days 300 and 50 (approximately corresponding to austral summer), than during austral winter (Julian day 200, approximately mid-July; Fig. 4.6A-B). SST values during the year previous to the *L. polyedrum* red tide (i.e. 2013), were within the temperature ranges delimited by the period of reference (Fig. 4.6A-B). During the year of the *L. polyedrum* red tide (i.e. 2014), SSTs at the end of summer and beginning of autumn (Julian days 20-50, approximately end of summer) were higher than during the period of reference (Fig. 4.6A-B), and during the rest of the year, temperatures were within the ranges of previous years. During the following year, with presence of the red tide caused by *N. scintillans* (i.e. 2015), SSTs during the middle of austral autumn were below the ranges of the period of reference (ca. Julian days 60-120, Fig. 4.6A-B).

For both sites, the annual cycle of chl-a was also very marked, with minimum values in the middle of summer (approximately after day 350 and before day 50; Fig. 4.6C-D). The maximum values of chl-a extended from austral autumn (ca. Julian day 100) until spring (Julian day 300) for both sites. The maximum variability in chl-a (the maximum ranges during the period of reference), occurred in the middle of spring (after Julian day 300) and less markedly during autumn (before Julian day 100; Fig. 4.6C-D). During 2014, chl-a values higher than during the period of reference were present in Jongensfontein at the beginning of autumn (Julian day 75, Fig. 4.6D), representing the peak period of dinoflagellate abundance in the water. In the case of Infanta, chl-a values did not seem to greatly exceed the reference values during the same period of 2014 (Julian day 75, Fig. 4.6C). During the following year, very high values of chl-a were found at both sites in the middle of autumn (around Julian day 100, Fig. 4.6C-D). Chl-a values during that period were well over the reference values considered, particularly at Jongensfontein.

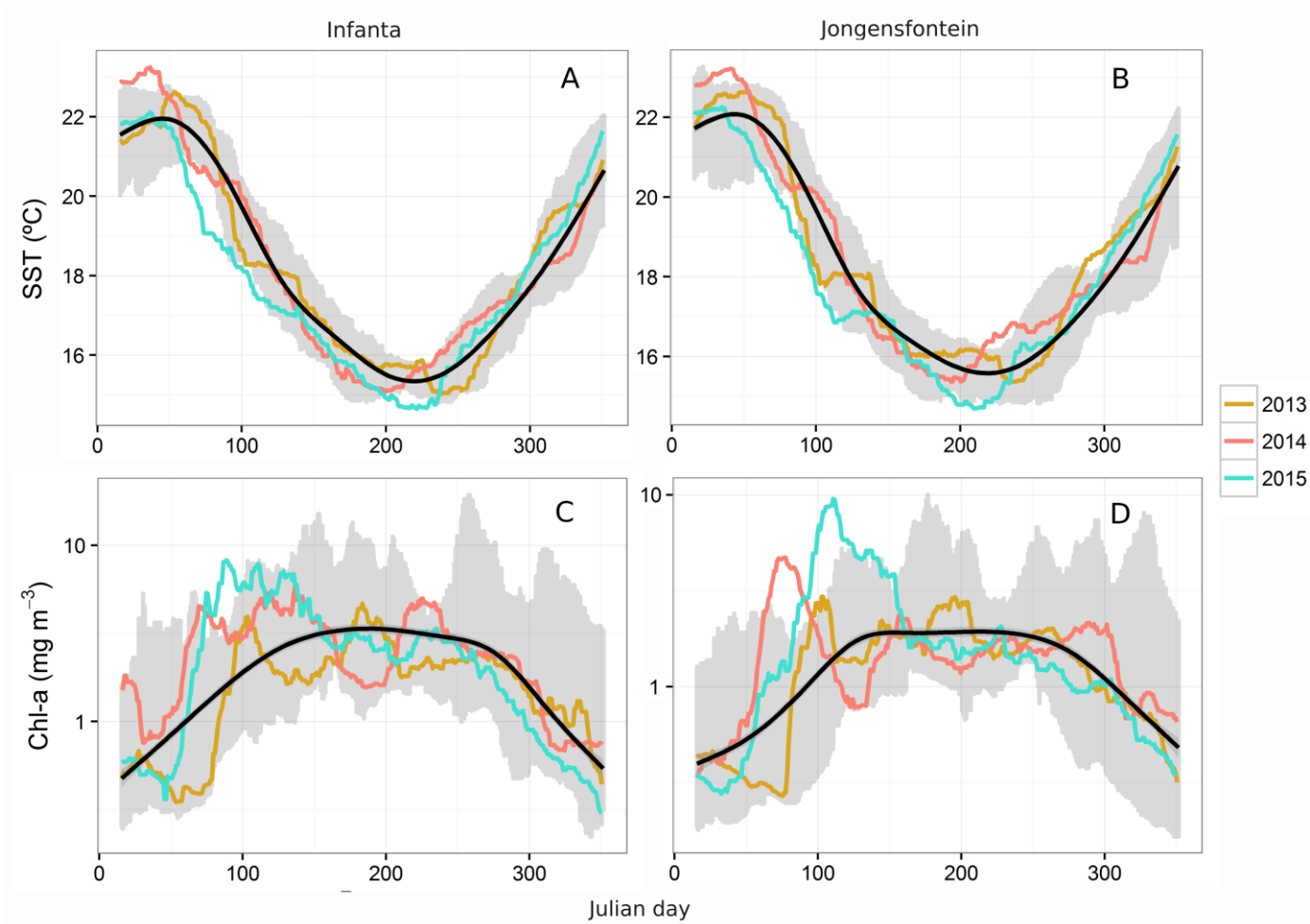


Fig. 4.6. Annual climatologies of SST (A – B) and chl-a (C – D) in Infanta and Jongensfontein. Grey shading in each panel represents the range (maximum to minimum) of values obtained for the reference period (1st January 2003 – 31st December 2012). Black lines represent a smooth function of the average conditions over the entire reference period shaded in grey. Conditions for year 2013 (yellow line), the *L. polyedrum* red tide year (pink line), and the *N. scintillans* (blue line) years are represented individually. Note that a 30-day running average was fitted to the data. Note that chl-a axis differs between sites.

4.4. Discussion

In general, barnacle recruitment was much higher during the *L. polyedrum* red tide year (i.e. 2014), but no differences in growth were found between years. The only exception was that one-month old barnacles from Jongensfontein grew faster during the *L. polyedrum* red tide year than any other class/year/site combination considered. Rates of mortality also seemed to be unaffected, with no significant differences between years. Study of the environmental conditions in the water during the periods of study revealed warmer temperatures and lower chl-a levels during 2014. Analysis of long-term records showed that higher temperatures occurred during 2014, approximately during summer, and later on returned to values within the long-term range of reference. SSTs during 2015 were below the minimum long-term ranges, lasting through autumn and winter. In the case of chl-a, values above the long-term ranges occurred during autumn of both years, but higher levels were recorded during 2015. Differences between years evident only in recruitment suggest that between-year differences in the water mass strongly affected the larval phases, but after successful settlement, intertidal processes and environmental conditions overrode any possible historic signature of conditions in the water mass.

The limited recruitment experienced during the second year negatively affected the number of individuals available to estimate growth rates or to compare between years. This resulted in a highly unbalanced design which compromised the power of the analysis. Therefore, although no consistent differences were observed in growth rates, even when age group C (the group with lowest sample sizes) was excluded from analysis, the present results should be taken with caution. Highly significant differences in recruitment were observed between 2014 and 2015, with no significant differences between sites, and without an effect of month. As previously discussed in Chapter 3, the interannual variability in recruitment rates could have been a result of: (1) the environmental conditions which promoted the development of *L. polyedrum*, (2) a change in the trophodynamics of the planktonic system during larval development, or (3) a combination of both (see Discussion in Chapter 3).

Although there was a strong difference in recruitment between years 2014 and 2015, there was no significant difference in mortality and the only difference in growth rates occurred in one-month old individuals from Jongensfontein during 2014, which grew faster than any other group (Fig. 4.3 and 4.4). During larval development, temperature and chl-a conditions are expected to affect energy reserves in the cyprid. Due to the lower SSTs, in comparison to year 2014, slower larval development was expected in the following year. Longer times of development, induced by lower temperatures and high food availability, should allow the accumulation of more energy reserves and result in larger organisms at the time of settlement. In general, in crustaceans the period between moults and the increase in size between moults depend on temperature and food

availability, with lower temperatures increasing the time between moults and producing larger individuals (Hartnoll 2001). Emlet and Sadro (2006) described a significant effect of temperature and of food concentration on cyprid size for the barnacle *Balanus glandula*, although the interaction of the two variables was not significant. For instance, the authors showed that under the same food concentrations, larvae would reach the cyprid stage in a shorter period of time when reared at high temperatures. At the same food concentrations, larger cyprids were obtained when reared at low than at high temperatures (Emlet and Sadro 2006). In the present study, temperature and chl-a conditions were different between years, but juvenile growth rates did not show different patterns between years. A possible explanation for this is that the ability to detect the effect of larval condition through changes in growth rates is limited to very early stages of juvenile growth. For example, Thiagarajan et al. (2003a) reported that cyprids with higher energy contents experienced significantly faster growth only during the first five days after settlement, and although growth rates were still higher after 10 days, the difference from cyprids with lower energy reserves was no longer significant. In the present study, the shortest period used to estimate growth rates was ca. one month, much longer than the periods previously proposed to show differences in growth attributable to larval condition (Thiagarajan et al. 2003a, Emlet and Sadro 2006).

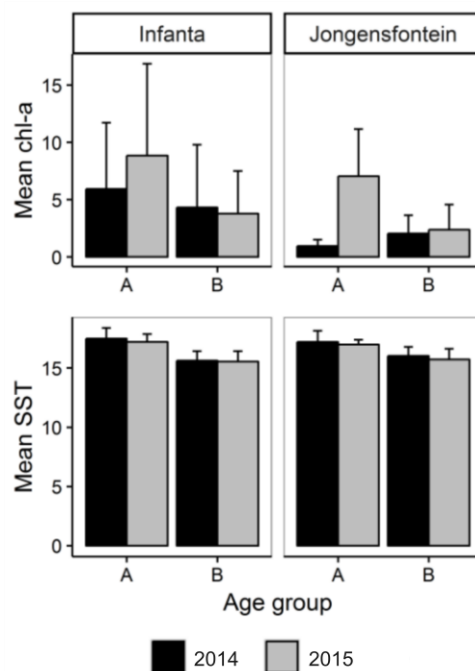


Fig. 4.7. Mean (+S.D.) chl-a (mg m^{-3}) and SST ($^{\circ}\text{C}$) conditions (top and bottom panels, respectively) in Infanta and Jongensfontein during 2014 (black) and 2015 (grey), during the periods considered for each age group.

Beyond the carryover effects of larval condition on early juvenile growth, temperature and food quantity are still major determinants of juvenile growth (Crisp 1960, Crisp and Bourget 1985).

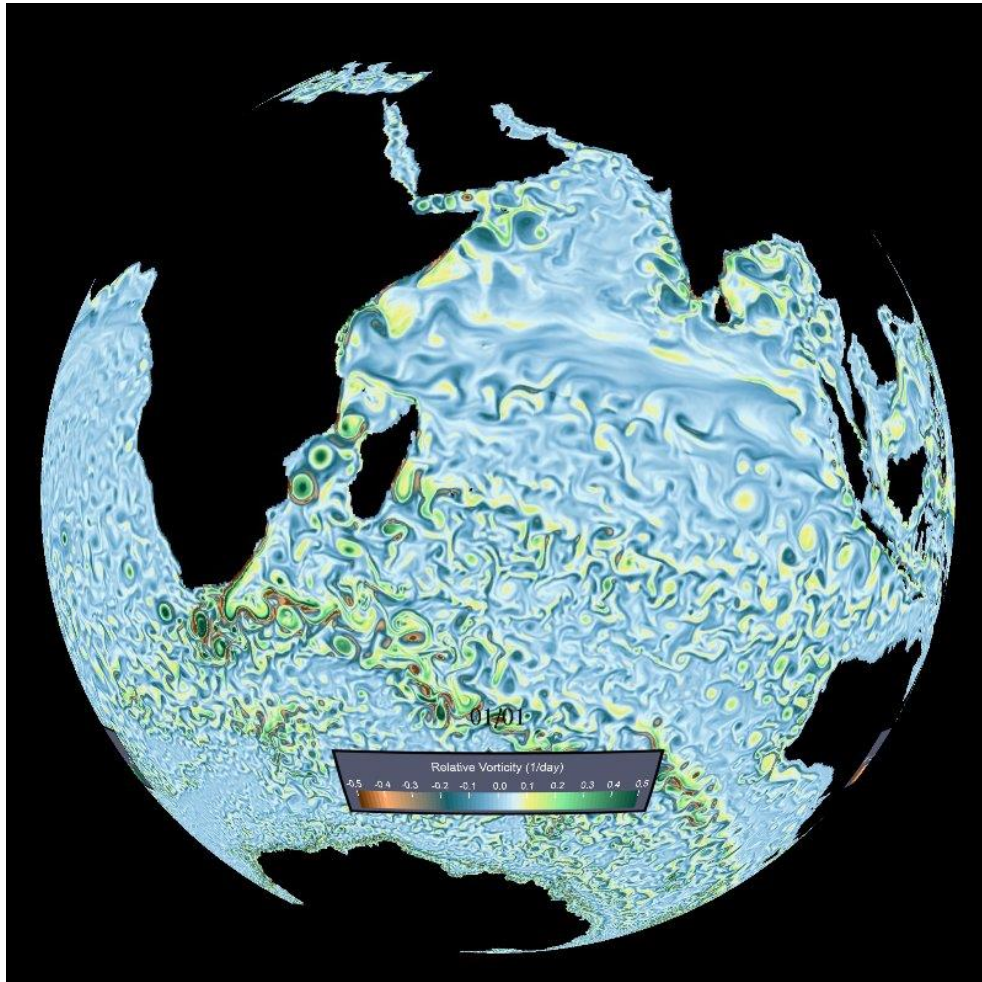
Temperature limits the velocity at which the cirri (the structures involved in capturing food particles) will move, and therefore, both temperature and food quantity/quality will affect growth rates (Qiu and Qian 1997, Thiyagarajan et al. 2002). During the period considered for each age group, average SST values were similar between years for each site (Fig. 4.7). Nevertheless, average chl-a in Jongensfontein during the period of growth considered for age group A during 2014 was much lower than the following year, and lower than in Infanta during the same period. This result strongly disagrees with the general relationship between growth and food availability. A possible explanation is that, although phytoplankton may be the major component of the diet during larval development, recruitment into the intertidal habitat may result in a shift in the particulate matter available for consumption. The presence of macroalgal detritus in the intertidal is excluded from the chl-a satellite measurements due to the distance from the coast used as chl-a estimates were centred 15km offshore to avoid measurement errors. Nonetheless, macroalgal detritus has been reported of key importance to support enhanced filter-feeder biomass in exposed shores as opposed to their sheltered counterparts (McQuaid and Branch 1985, Bustamante and Branch 1996b). Similarly, recent diet studies using stable isotopes have revealed the strong dependence of filter-feeders on suspended particulate matter (SPM) from an origin different from phytoplankton (Hill et al. 2008, Tallis 2009, Puccinelli et al. 2016). Puccinelli et al. (2016) studied the stable isotope (SI) and fatty acid (FA) signatures of adult mussels and barnacles along the South African coast. They found that the barnacle *Chthamalus dentatus* showed characteristic dinoflagellate and diatom trophic markers on the west coast, but no characteristic markers were obtained in the south and east coast. The absence of markers characteristic of phytoplankton led Puccinelli et al. (2016) to suggest that the diet of intertidal filter-feeders is strongly influenced by the hydrodynamic conditions which promote phytoplankton growth. For instance, the limited frequency of upwelling in the south coast was suggested to drive a stronger dependence on suspended particulate matter (SPM) of macroalgal origin in comparison to the west coast, where communities showed evidence of the importance of phytoplankton in their diets (Puccinelli et al. 2016). Hill et al. (2006) studied the isotopic composition of water samples along and across the South African coast, from the intertidal to 10km offshore, and reported a decrease in ^{13}C with increasing distance from the coast. This gradient in the carbon signatures of SPM would reflect a change from a phytoplankton dominated community offshore, to a higher contribution of macroalgae in the nearshore and intertidal (Hill et al. 2006). Such difference between offshore and nearshore waters would strongly influence meroplanktonic organisms, which would experience different food sources during the planktonic and the juvenile/adult parts of their life cycle. In the case of mussels, Hill et al. (2006) reported that more than 50% of the isotopic signal obtained from tissue samples of adult mussels corresponded to SPM from nearshore origin. Thus, adult tissue composition suggests that, although changes in the trophodynamic system may appear in the plankton, the effect of such forcing may not be applicable

at scales relevant to intertidal food sources. Thus, although the chl-a estimates from satellite used for analysis may not reflect variability in nearshore or intertidal waters, it was not possible to measure intertidal chl-a and offshore estimates were considered a consistent estimate which allowed interannual comparisons. In general, the interannual shift in recruitment observed did not impact population dynamics in the intertidal. The between-year differences in recruitment suggest that the major effects linked to the environmental conditions in the water mass may be restricted to the larval phases, which points to a marked pelagic-nearshore decoupling. Thus, the role of larval settlement as a key determinant of adult population structure (Gaines and Roughgarden 1985) may not hold in our study region, although substantial variability in the strength of such coupling has been found. Spatiotemporal mismatches have been observed between recruitment and adult densities for *Semibalanus balanoides* along the Atlantic coasts of Canada (Cole et al. 2011). On the other hand, high recruitment rates for the same species along the shores of Wales enhanced juvenile mortality and decreased individual growth (Jenkins et al. 2008). These density dependent mortality and growth rates typically occur at very high densities when free space becomes limiting, thus producing characteristic patterns in shape not observed in our study sites (Bertness et al. 1998).

Overall, this study suggests that, although larval condition may have differed between years, in turn influencing recruitment on the shore, the parameters estimated for the intertidal populations (growth and mortality) did not reflect this shift, and therefore, no evidence of a carryover effect was found. Quite on the contrary, once settlement occurred, nearshore conditions seemed to have overridden any previous differences in larval condition and removed any pelagic effect on growth and mortality on the shore.

Chapter 5

Long-term trends in environmental drivers of coastal ecosystems



Ocean surface vorticity from the Parallel Ocean Program (source: <https://sos.noaa.gov/>)

Long-term trends in environmental drivers of coastal ecosystems

5. 1. Introduction

In classical ecological theory, the distributions and abundances of marine benthic organisms were long assumed to be controlled by the interactions among organisms in the adult habitats. Thus, competition for resources (including the availability of space as a resource), predation, or disturbance in the environment were considered to drive the structure of adult communities (Connell 1961a, Dayton 1971, Menge 1976, Paine et al. 1985). Later, strong evidence of the importance of the supply of new organisms for population maintenance was provided (Connell 1985, Gaines and Roughgarden 1985, Underwood and Keough 2001). This resulted in a shift in the way that community ecology was understood, adding the influence of supply-side regulation and contributing to the improvement of the models available. Thus, successful supply of propagules plays a major role in structuring and maintaining the adult populations. The current understanding of community structure considers the structure of adult populations to be the result of a complex system of interactions among organisms and the environment, affected by multiple factors that operate at different spatio-temporal scales and which finally influence the availability of new propagules, their return to the benthic community, and their survival (Menge 2000, Pineda 2000). Nevertheless, the influence of the environmental conditions that affect organisms is usually addressed with limited spatial or temporal resolution due to the difficulties associated with data collection. In addition, there is also inherent variability in recruitment rates which may affect the results obtained depending on the spatio-temporal scales considered (Hawkins and Hartnoll 1982).

Along the coast of South Africa, strong changes exist in species distribution, diversity and biomass. Details on species richness in the west, south and east coasts can be found for algae (Bolton and Stegenga 2002), and benthic invertebrates (Awad et al. 2002) and are reflected in the recognition of different biogeographic regions (e.g. Emanuel et al. 1992). Nevertheless, information on biomass along the coast is scarcer, especially for studies that comprise multiple taxa at the same time, usually being restricted to the study of functional groups and not individual species (Bustamante et al. 1995, Bustamante and Branch 1996a). Marked patterns along the coastline can be found in both the species richness and biomass of benthic invertebrates. Species richness has been reported to reach its highest values on either the south or the east coast, depending on the taxonomic group of interest (Awad et al. 2002). In contrast, the highest biomass values for invertebrate taxa occur on the west coast, decreasing towards the east (Bustamante et al. 1995). Bustamante and Branch (1996a), found that biomass values were greatest on the west and decreased towards the east for the different functional groups examined, which included from primary producers to secondary consumers. Bustamante et al. (1995) reported the same west to east decreasing trend and, in

addition, found that the trend in nutrient availability followed the same pattern, with highest values in the west. Other studies that focused on single taxonomic groups, like mussels, revealed contrasting results. For example, Reaugh-Flower et al. (2010) estimated recruitment of the four principal species of mussels along the coasts of South Africa and Namibia and found recruitment rates were highest on the west coast and lowest on the south coast of South Africa. Nonetheless, a study with higher spatial resolution produced by von der Meden (2009), focusing on the South Coast, showed that mussel recruitment (including the two major species) followed a longitudinal pattern with highest abundances in the centre of the coast. Thus, superimposed to large scale contrasting patterns among coasts, there is a substantial mesoscale regional variability in recruitment which results in a complex spatial structure.

The general pattern of intertidal biomass around South Africa can be attributed to the contrasting oceanographic regimes that affect the different coasts. Thus, the Benguela Current on the West Coast, and the Agulhas Current on the south and east have very different physico-chemical characteristics. The presence of upwelling on the West Coast, which is one of the most important Eastern Boundary Upwelling Systems (EBUS) in terms of primary productivity (Thomas et al. 2001, Carr and Kearns 2003), results in the highest productivity in the region (Nelson 1992, Carr 2001). High abundances of benthic organisms, and high recruitment rates of intertidal invertebrates are also found on that area (Harris et al. 1998, Pfaff et al. 2011). Meanwhile, the South Coast includes the area where the continental shelf starts to widen to form the Agulhas Bank (Fig. 1.1). Along the South Coast, seasonal upwelling occurs in localised areas around capes, due to the reversal in wind direction to upwelling-favouring conditions during austral summer (Schumann 1987). Additionally, a semi-permanent upwelling cell is also located around Port Alfred (c. 27°E), caused by the shelf break deflection of the Agulhas Current (Lutjeharms et al. 2000, Goschen et al. 2012). Although sub-surface upwelling is current-induced, it is detected in surface during upwelling-favourable wind conditions (Rouault et al. 1995). Thus, on the South Coast, two phytoplankton blooms occur per year during spring and autumn (Brown 1992), similarly to other shelf regions located in temperate areas (Bode et al. 1996, Rivas et al. 2006). Although upwelling is also found on the East Coast, it is spatially restricted and occurs in the northernmost part of the country, c. 28.5°S, 32°E (Schumann 1982). Overall, this results in lower primary production on the east coast than the other coasts.

General patterns of biomass along the three coasts seem to correspond with the circulation of nutrients in the adjacent water masses. Nevertheless, the contrast between the Benguela and Agulhas Currents does not explain the community patterns that occur within each coast, including the longitudinal gradient of mussel recruitment along the South Coast reported by von der Meden (2009). Similar results were observed in the present study (see details in chapter 3), with mussel and barnacle recruitment following a unimodal function with its peak located in the centre of the South Coast. Thus, other factors operating on a regional scale along the South Coast may be driving the

large-scale distributions observed. Spatial patterns in community composition have been reported in EBUSs elsewhere (e.g. Navarrete et al. 2005, Broitman and Kinlan 2006). In those areas, variability in the environmental conditions that affect the early development of benthic organisms over scales of 100-1000s km were suggested to control the structure of the communities on the coast (Navarrete et al. 2005, Tapia et al. 2014). Along the coasts of Chile, changes in temporal variability of the upwelling forcing were proposed to influence the interaction of organisms with the environment and to determine shifts in community composition (Tapia et al. 2014). Variability in biomass of different functional groups has also been reported for the upwelling system on the West Coast of South Africa and associated with water temperature variability (Wieters et al. 2009).

Along the South Coast, the shelf area sustains high productivity, due to the combination of recirculation of nutrients from the shallow bottom and light availability, as observed in other parts of the world (Rowe et al. 1975, Han et al. 2012). In addition, the South Coast supports the highest number of endemic species along the coast (Awad et al. 2002), and the spawning grounds of important commercial species including sardines (Crawford 1981, Beckley and van der Lingen 1999), anchovies (Hampton 1987), and chokka squid (Augustyn 1990). Although upwelling at Port Alfred is semi-permanent, it appears that highest productivity is located around the more sporadic upwelling cell near Plettenberg Bay (Peterson et al. 1992, Hutchings 1994). Such a difference in productivity between both upwelling centres may be the consequence of contrasting temporal variability in the environmental conditions that drive productivity within each cell. Thus, it is likely that temporal variability may be strongly related to the spatial patterns observed in the intertidal communities along the coast.

In recent years, changes in the flow patterns of the Agulhas Current have been reported (Rouault et al. 2009, 2010b). A general cooling trend has occurred in the upwelling cells of the South Coast (Rouault et al. 2010a), and an increase in flow has been suggested by regional ocean models (ROM, Rouault et al. 2010a). Although the Agulhas Current influences large-scale climate patterns due to its importance in Atlantic Ocean circulation (Bjastoch et al. 2008, Beal et al. 2011), changes in temperature and/or flux in the Agulhas Current also have major consequences at a relatively local scale in southern Africa. Thus, the Agulhas Current strongly influences climate and rainfall patterns in South Africa (Walker 1990, Jury et al. 1993, Reason 2001), and is likely to influence local upwelling on the South Coast. Due to its influence on shelf waters, long-term changes in the Agulhas Current are likely to affect seasonality in shelf waters by altering the coastal dynamics of SST and chl-a. Because of the importance of SST and chl-a in the general development of benthic organisms (Phillips 2004, O'Connor et al. 2007), and particularly in the area of interest in the South Coast (see results Chapter 3), long-term variability in the coastal area may have profound effects, leading to potential changes in regional coastal ecosystems.

As suggested for EBUSs, it is likely that temporal variability in the environmental conditions that drive upwelling on the South Coast may be strongly related to the spatial patterns in recruitment and abundance of benthic organisms, including the productivity hot spot at the Plettenberg upwelling area. Thus, the present chapter aims to: (1) determine spatio-temporal patterns in the environmental conditions along the South Coast which may be driving biological production in focal areas, and (2) ascertain changes in the environmental conditions during recent years which may have consequences for temporal variability in the system and which may uncouple the biological cycles from the physico-chemical environment.

5.2. Materials and methods

5.2.1. Spatial patterns of temporal variability

The study area extended along the south coast of South Africa, from its southernmost point (i.e. Cape Agulhas, 19.94°E) to 28.48°E. This area was selected to include previous data on recruitment of intertidal populations (see Chapter 3, and von der Meden et al. 2008). To cover the water mass likely to interact with or affect coastal communities, data were collected for the area from the coastline to approximately 120km offshore, thus covering most of the inner Agulhas Bank. Sea surface temperature (SST, 11 μ daytime measures) and chlorophyll-a (chl-a, OCx algorithm processing) data were obtained from the Moderate Resolution Imaging Spectroradiometer (MODIS Aqua; downloaded from <https://oceancolor.gsfc.nasa.gov/>), with a resolution of 4km (4km blocks are referred to as *pixels*). Level-3 composite images of eight-day averages were obtained from the 9th July 2002 until the 27th September 2017 (Table 5.1, 701 eight-day composites in total) for each variable. The 4x4km pixels were used to calculate 12x20km areas (across and alongshore), from here on referred to as *megapixels*. Megapixels were used to simplify the analysis of such a large spatial and temporal dataset, and to reduce the high frequency of missing values that are usually present in satellite derived measurements.

Table 5.1. Spatial and temporal resolution of the environmental variables used to calculate long-term trends.

Variable	Start period	End period	Spatial resolution	Temporal resolution	Data source
SST	09/07/2002	27/09/2017	4km	8-day averages	MODIS Aqua
Chl-a	09/07/2002	27/09/2017	4km	8-day averages	MODIS Aqua
Currents	02/07/2002	16/01/2017	0.33°	5-day averages	OSCAR
Winds	01/07/2002	31/03/2017	0.125°	Monthly averages	ERA - Interim

A Principal Component Analysis (PCA) was performed on the time series of SST and chl-a values for each megapixel. PCAs allow the compression of the variability of a spatial array of time series. The variance in the dataset will then be split into the different components of the PCA, which describe the temporal variability in the spatial array (Tapia et al. 2014). This approach is suggested for oceanographic data where variables are measured in space and time (Thomson and Emery 2014), in order to cope with the complexity of the dataset and to obtain components of the variability that are not correlated to each other. Thus, a PCA was performed on the 8-day composites of SST, and chl-a, for the average of each megapixel. To remove the gaps in the dataset (see Table 5.2), linear interpolation was used, averaging the previous and the following value in the time series where gaps were present. With low percentages of missing data and short gaps (between one and four measurements), linear interpolation is considered a good method to build continuous time series (Kandasamy et al. 2015). Datasets without gaps were then used for PCA analysis of SST and chl-a. PCAs were performed using the function *prcomp* from the package *stats* in R version 3.2.0 (R Core Team 2015). The first and second components of the PCA were extracted for each megapixel to estimate the temporal frequency of variability for each megapixel.

Table 5.2. Description of missing data in the SST and chlorophyll-a data sets before linear interpolation was applied. Eight-day averaged data was used for both variables (701 eight-day periods in total, 5608 days).

Variable	Maximum megapixel data missing (%)	Mean megapixel data missing (\pm S.D.) (%)	Maximum gap size (days)
SST	5.7	1.19 \pm 0.75	16
Chl-a	14.83	4.79 \pm 4.11	40

Spectral analysis was performed on each megapixel of the eight-day time series to determine the temporal frequencies which explained most of the variability in SST and chl-a. Total variance was partitioned into five periods of interest following Tapia et al. (2014), calculating the sum of the spectral densities within each period (see Table 5.3): (1) frequencies greater than one year and shorter than three years (referred to as *inter-annual*), (2) frequencies close to an annual cycle (referred to as *seasonal*), (3) frequencies of variability shorter than the annual cycle (i.e. *intra-seasonal*), (4) short-term frequencies of variability (or *synoptic*) and, (5) *residual* variability for periods longer than three years, approximately. Spectral densities were estimated for each megapixel using the function *spectrum*, from the package *stats* in R version 3.2.0 (R Core Team, 2015).

Most of the temporal variability in SST and chl-a corresponded to seasonal and intra-seasonal frequencies, and consequently, those two periods were used to determine the relationship of seasonal and intra-seasonal frequencies of variability to the spatial patterns of recruitment of

mussels and barnacles. Simple linear regressions were performed on the logarithm to the base 10 of one plus the abundance of recruitment (for *Perna perna*, other mytilids, and barnacles), as a function of seasonal and intra-seasonal cumulative spectral densities, estimated for the megapixel closest to each recruitment site (see Figs. 5.4 and 5.5 for details). Recruitment rates were estimated for ten sites spanning the south coast for two months of each of two years (see Chapter 3, section 3.2 for details).

Table 5.3. Periods used to calculate the cumulative spectral densities for spectral analysis.

Frequency of variability	Period covered
Inter-annual	384 - 1152 days
Seasonal	101 - 383 days
Intra-seasonal	20 - 100 days
Synoptic	16 - 19 days
Residual	> 1152 days

In addition, the dataset used to examine the frequencies of variability of SST and chl-a was divided in two halves to determine if SST or chl-a had shown a change of periodicity during the 15 years of data, indicating changes in the seasonality of either variable. Data were divided into two blocks: 27th July 2002 until 15th February 2010, and 15th February 2010 until 11th September 2017. The same analysis used for the complete datasets was applied to each of the two data blocks, and cumulative spectral densities were calculated for the same periods, partitioning the variance in SST and chl-a into their inter-annual, seasonal, intra-seasonal, synoptic, and residual components.

5.2.2. Long-term environmental conditions

Seasonal trends on the south coast were calculated for SST, chl-a, water currents, and winds, for the same spatial area as in the previous section. The time span for the complete series was selected to start at the same time for all four variables, and covered approximately 15 years (from July 2002 until the beginning of 2017, see Table 5.1 for details on each variable). Given the need to have contemporaneous data, the period of analysis was limited by the availability of SST and chl-a. Although satellite measurements of SST and chl-a are available from the late 1970s, only MODIS Aqua was used to avoid inconsistencies in the series resulting from the different performances of multiple measuring instruments.

MODIS Aqua level-3 images of eight-day averages, at 4km resolution, were downloaded from the Ocean Biology Processing Group (OCBP) from NASA (<https://oceancolor.gsfc.nasa.gov/>) for SST (11 μ daytime measurements) and chl-a (OCx algorithm processing). Water currents along the coast were obtained from the model Ocean Surface Current Analyses Real-time (OSCAR), for zonal and

meridional current speeds predicted at 15m depth, using five-day averages with 0.33° resolution (https://coastwatch.pfeg.noaa.gov/erddap/griddap/jplOscar_LonPM180.html, ERDDAP server from NOAA). Monthly averages of wind data were obtained from the European Centre for Medium-Range Weather Forecasts Reanalysis for zonal and meridional direction (ERA – Interim), as well as wind speed, measured at 10m height, with a 0.125° resolution (data downloaded from <http://apps.ecmwf.int/>).

The periods used to calculate the seasonal averages for the austral hemisphere followed the same time periods that appear in Brown (1992), i.e. June – August (winter), September – November (spring), December – February (summer), and March – May (autumn). For each variable, seasonal averages were calculated for each year and area, using the highest spatial resolution possible. Although resolution was different for each variable (see Table 5.1 for details), for simplicity, the smallest area used for each variable will be referred to as a *pixel*. In the case of water currents and winds, the alongshore component (i.e. the west-east component), and the vector (calculated as the square root of the sum of squares of the zonal and meridional speed), were used in the regression analysis. To remove trends in the variability among years, seasonal anomalies were calculated for each variable as the difference between the seasonal average for the year and the seasonal average for the entire series. A simple linear regression was fitted to the seasonal anomalies calculated for each pixel and year and the magnitude and significance of the obtained slope was considered as a measurement of the long-term trend for each time series. The function *lm* from the package *stats* in R version 3.2.0 (R Core Team, 2015) was used. All figures were plotted using the package *ggplot2* (Wickham 2009).

5.3. Results

5.3.1. Spatial patterns of temporal variability

5.3.1.1. SST

Most of the variability in SST for the 15 years of satellite data along the south coast was explained by the first and second principal components of the PCA (74 and 5% of total variance, respectively). A marked annual cycle was present in the first and second principal components (Fig. 5.1A). Variability in the annual cycles was constant for all the 12x20km areas (referred to as *megapixels*) studied along the south coast (Fig. 5.2A). A sharp change in variability was shown in the second principal component (Fig. 5.2B), with the edge of the continental platform roughly delimiting areas of different frequency of temporal variability in SST cycles. In addition, highest PC2 scores were reached off Plettenberg Bay at 23°E and tended to decrease westwards to Cape Agulhas (c. 20°E, Fig

5.2B). Partitioning of spectral densities showed that most of the temporal variability in SST along the south coast corresponded to seasonal cycles between approximately three months and one year (Fig. 5.3A, see complete results in Appendix II.1). Shorter frequencies of variability gained importance along the shelf break, corresponding spatially with the upwelling cell of Port Alfred (c. 27°E, Fig. 5.3B).

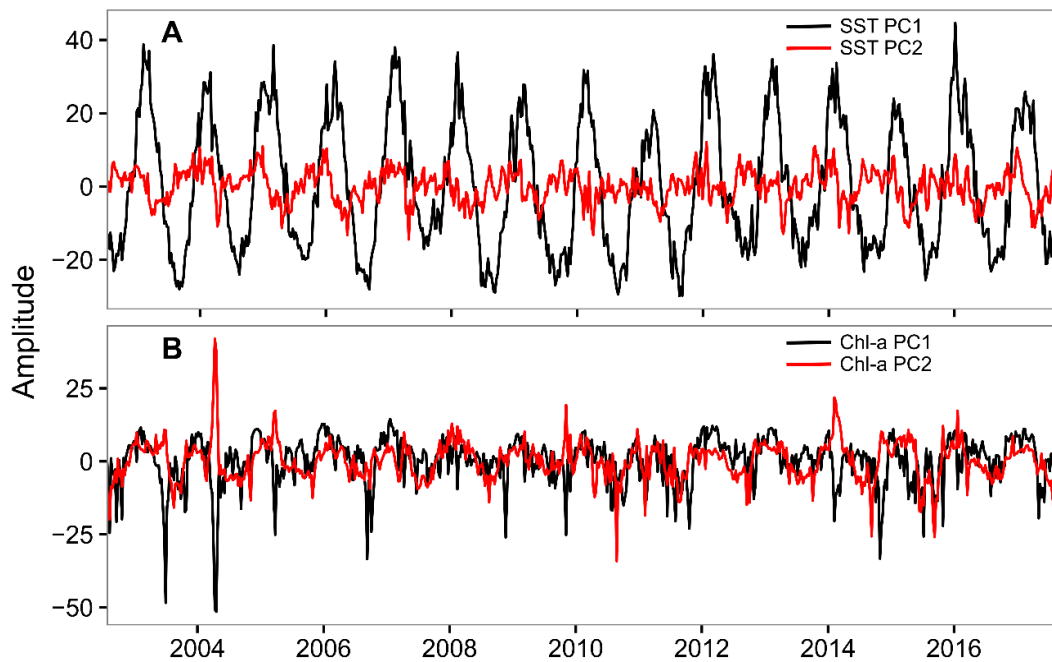


Fig. 5.1. Eight-day time series of the first (black lines) and second (red lines) principal components of SST (A), and chl-a (B). Time series comprises the period between July 2002 until September 2017. Note that the y-axis varies between panels.

Average annual SSTs (see Appendix II.2) showed a clear change in temperature conditions in the water mass over the shelf area and beyond the shelf break that resembled the change shown for PC2 scores. However, average annual SST conditions along the coast were a poor predictor of the spatial patterns of mussel and barnacle recruitment, with simple linear regression models explaining 31, 35, and 22% of the variability in recruitment of *Perna perna*, other mytilids, and barnacles, respectively ($p < 0.001$ for all regression models, Appendix II.3). Similarly, linear regression analysis showed that temporal variability in SST was a poor predictor of recruitment, with the seasonal and intra-seasonal components explaining less than 17% of the variability in recruitment for any of the study taxa ($p < 0.001$ for all regression analyses, Fig. 5.6).

5.3.1.2. Chlorophyll-a

In the case of chl-a, the first and second components of the PCA only explained 16 and 11% of the total variance, respectively. The first component showed a much less prominent annual cycle than for SST (Fig. 5.1B). As with SST, spatial variability in the first principal component was relatively

constant for all the megapixels along the coast, although this pattern was less clear than that shown by the PC1 loadings of SST (Fig. 5.4A). The second principal component showed a marked change in the frequency of temporal variability of chl-a along the coast (Fig. 5.4B). A clear change is observed at the shelf break, and between the central and the western areas of the Agulhas Bank.

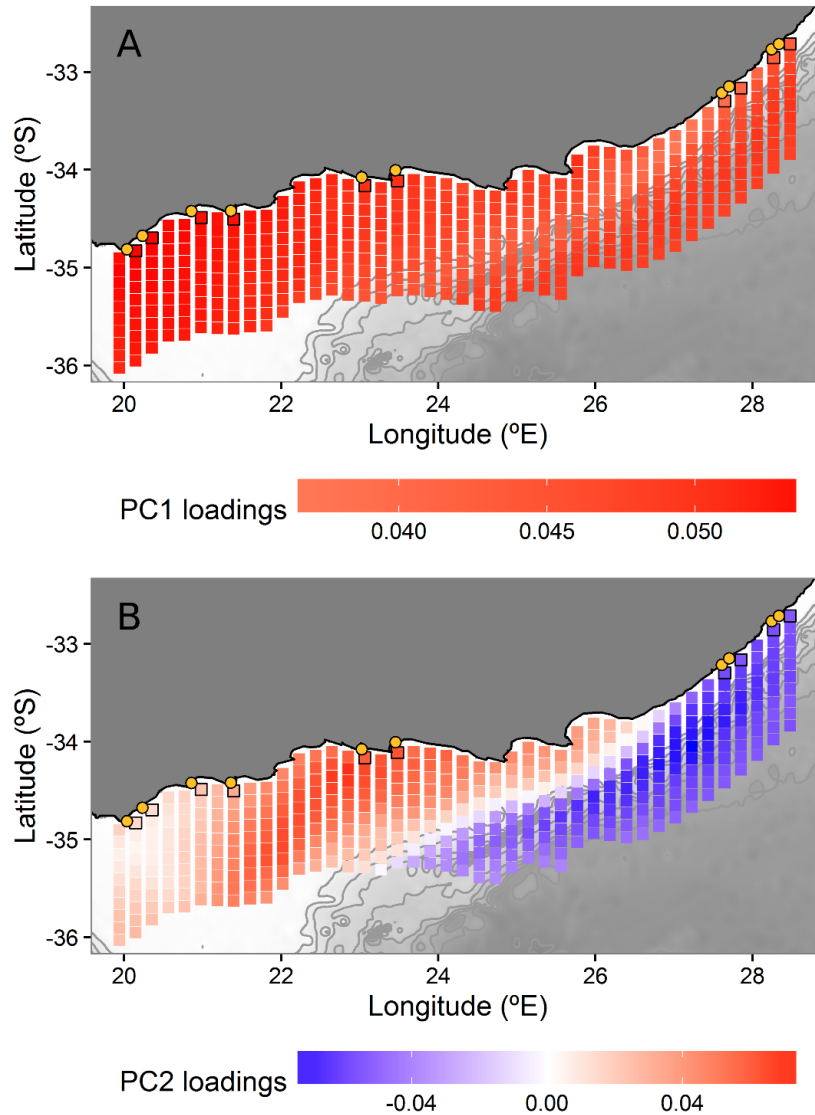


Fig. 5.2. SST first (A) and second (B) principal components for each megapixel in the study area. Positive values are represented in red and negative in blue. PCAs were calculated for eight-day averages of each variable and megapixel (see description in text). Sampling sites along the coast are represented by yellow circles. The megapixels closest to each sampling site and selected for analysis appear delimited by a square. Shaded areas and contour lines delimit the bottom profile, with the first contour line representing the 500m isobath. Note that scale-bars differ between panels.

Spectral analysis was performed on the time series of chl-a for each megapixel. In contrast to SST, seasonal frequencies did not dominate throughout the whole region (Fig. 5.5). Intra-seasonal variability (i.e. between three weeks and three months, approximately), dominated most of the

variability in chl-a, particularly along the shelf break, while seasonal and intra-seasonal frequencies of variability were important over the Western Agulhas Bank (Fig. 5.5, see complete results in Appendix II.1).

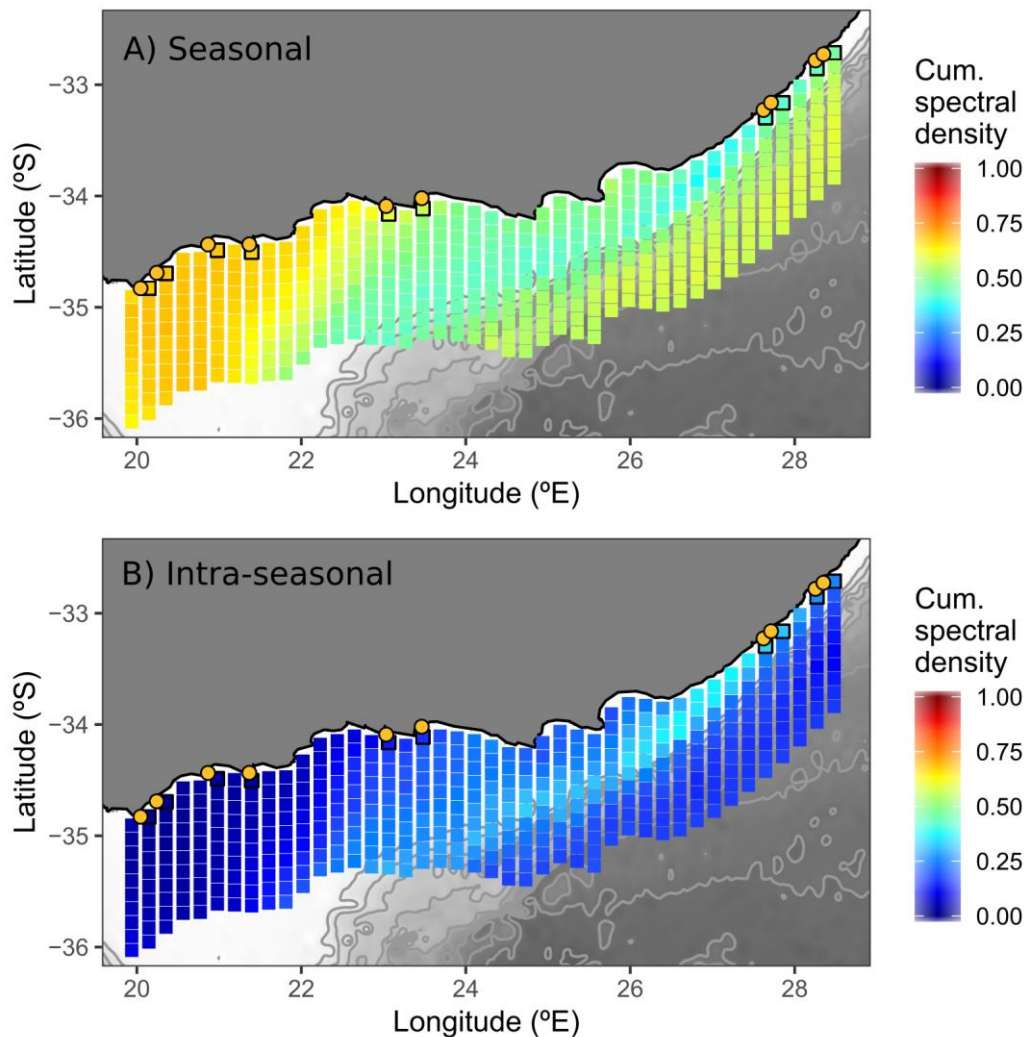


Fig. 5.3. Seasonal (A) and intra-seasonal (B) frequencies of variability in SST for each megapixel in the study area. Cumulative spectral densities were calculated for eight-day averages for each megapixel (see description in text). Sampling sites along the coast are represented by yellow circles. The 10 megapixels selected for linear regression against recruitment rates appear delimited by squares. Shaded areas and contour lines delimit the bottom profile, with the first contour line representing the 500m isobath. Note that scale-bars differ between panels. See full variance partitioning results in Appendix II.1

Unlike SST, average annual values of chl-a did not reflect the break observed in PC2 scores (see Appendix II.2). Simple linear regression analysis showed that average chl-a along the coast only explained around 30% of the variability in recruitment for the two mussel taxa, and only 13% of that of barnacles ($p < 0.001$ in all regression models, Appendix II.3). In contrast, temporal variability of chl-a was a very good predictor of spatial variability in mussel recruitment, with seasonal and

intra-seasonal frequencies of variability explaining almost double the variance explained by average annual chl-a alone, with 67 and 73% of variance explained by seasonal frequencies and, 55, and 58% by intra-seasonal for *P. perna* and other mytilids, respectively ($p < 0.001$ in all cases, Fig. 5.6). Recruitment for these taxa markedly increased with seasonal frequencies while the opposite trend was clear with the intra-seasonal band. Nonetheless, temporal variability in chl-a did not seem to be a good predictor of barnacle recruitment, explaining only 29% of the variability in recruitment for both seasonal and intra-seasonal frequencies of variability (Fig. 5.6).

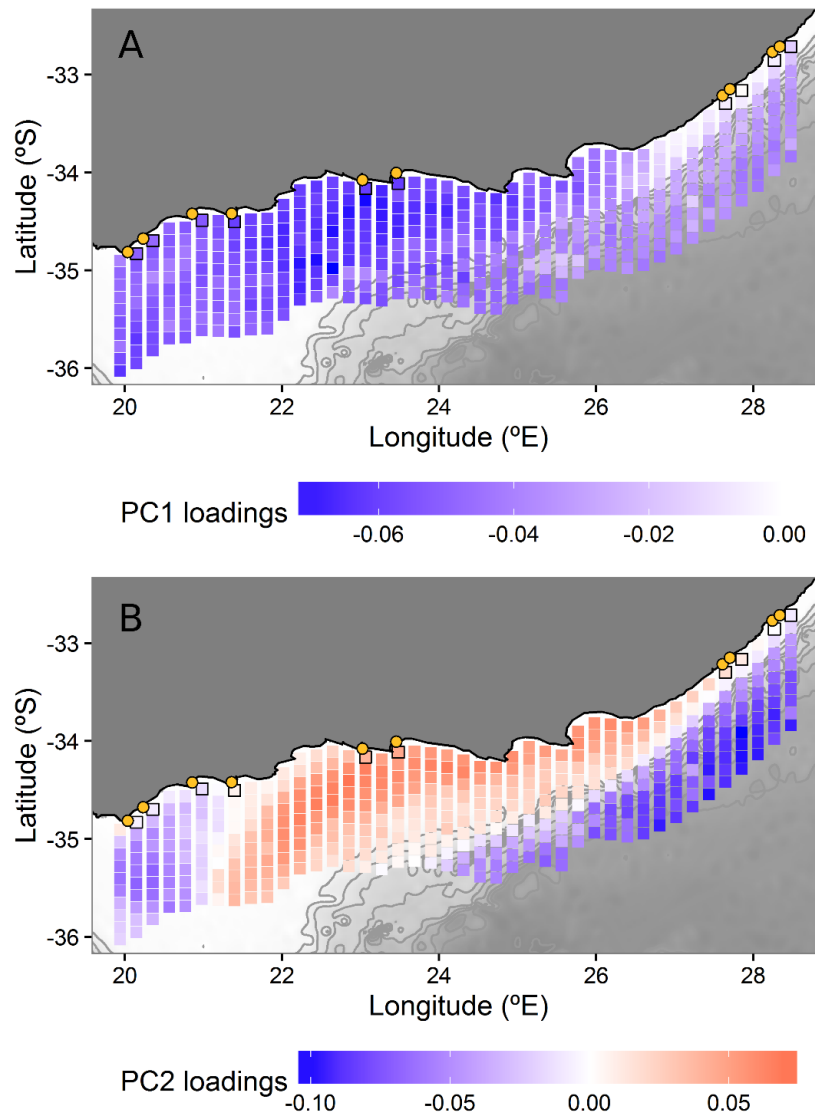


Fig. 5.4. Chl-a first (A) and second (B) principal components for each megapixel in the study area. Positive values are represented in red and negative in blue. PCAs were calculated for eight-day averages of each variable and megapixel (see description in text). Sampling sites along the coast are represented by yellow circles. The megapixels closest to each sampling site and selected for analysis appear delimited by a square. Shaded areas and contour lines delimit the bottom profile, with the first contour line representing the 500m isobath. Note that scale-bars differ between panels.

5.3.1.3. Changes in temporal variability of SST and chl-a

The analysis of change in periodicity between the first and second blocks of the SST and chl-a datasets showed that the importance of shorter frequencies of oscillation increased during the second half of the period of study, although such change only affected specific areas on the south coast (Figs. 5.7 and 5.8). During the period between July 2002 and February 2010, SST periodicity was predominantly seasonal along the entire area of study, except for the shelf break area, where variability in SST conditions showed the influence of shorter time scales (i.e. intra-seasonal). During the second half of the study period the importance of intra-seasonal frequencies of variability increased along the shelf break, reducing the importance of seasonal periodicity along that area i.e. the area around the Port Alfred upwelling cell (c. 27°E, Fig. 5.7).

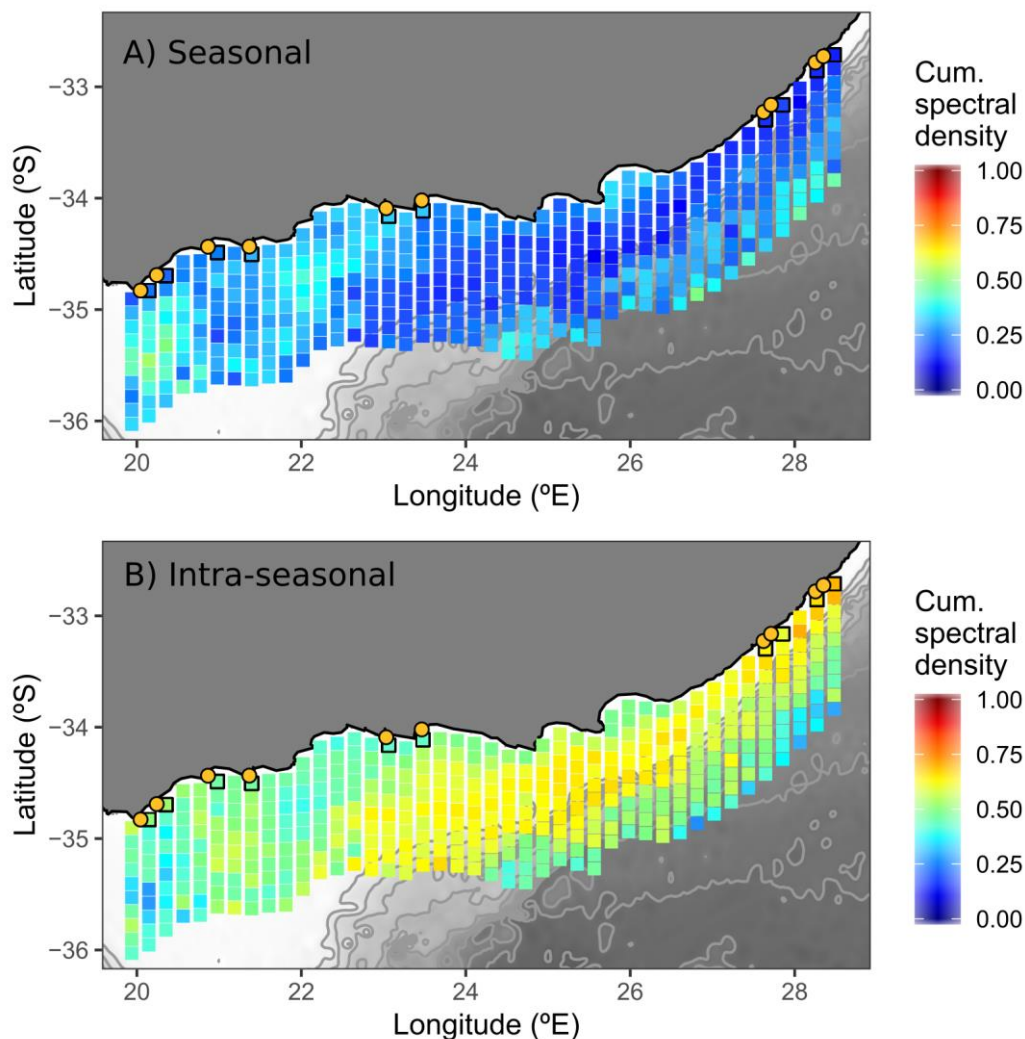


Fig. 5.5. Seasonal (A) and intra-seasonal (B) frequencies of variability in chl-a for each megapixel in the study area. Cumulative spectral densities were calculated for eight-day averages for each megapixel (see description in text). Sampling sites along the coast are represented by yellow circles. The 10 megapixels selected for linear regression against recruitment rates appear delimited by a square. Shaded areas and contour lines delimit the bottom profile, with the first contour line representing the 500m isobath. Note that scale-bars differ between panels. See full variance partitioning results in Appendix II.1.

In the case of chl-a, variability at scales of 21 to 100 days dominated most of the central and east parts of the study area (from c. 22°E eastwards, Fig. 5.8), and seasonal cycles dominated on the West Agulhas Bank (c. 20–22°E) and in areas very close to the coast until c. 26°E, markedly influencing the area of the Plettenberg upwelling cell (c. 23°E, Fig. 5.8). During the second half of the period of study (i.e. February 2010 until September 2017) seasonal periodicity around the Plettenberg upwelling cell was replaced by variability at intra-seasonal scales.

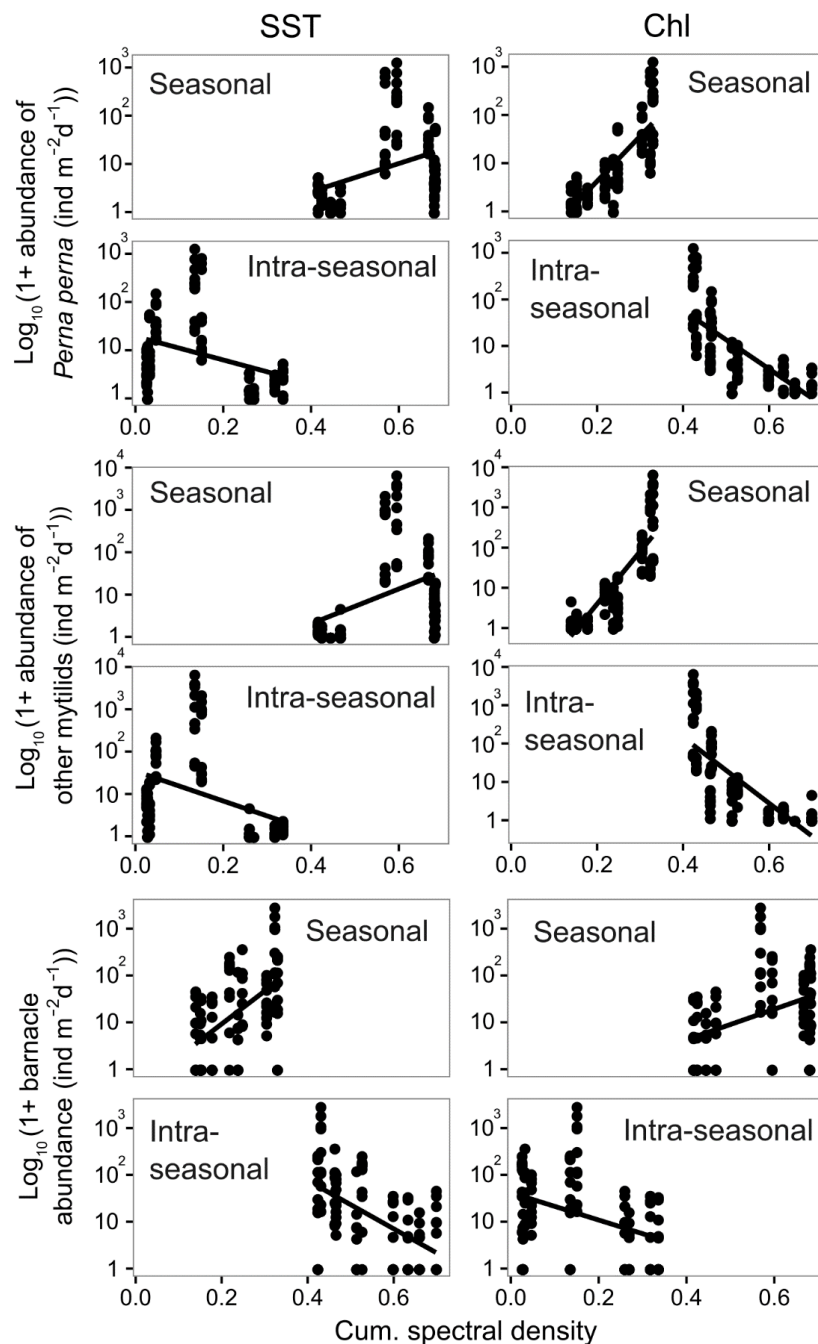


Fig. 5.6. Linear regressions of the log-scaled recruitment rates ($\text{ind m}^{-2} \text{d}^{-1}$) for *Perna perna* (first two rows), other mytilids (third and fourth rows), and barnacles (last two rows), and the cumulative spectral densities of SST and chl-a on the closest megapixel to each recruitment site (see Figs. 5.4 and 5.5 for megapixel positions).

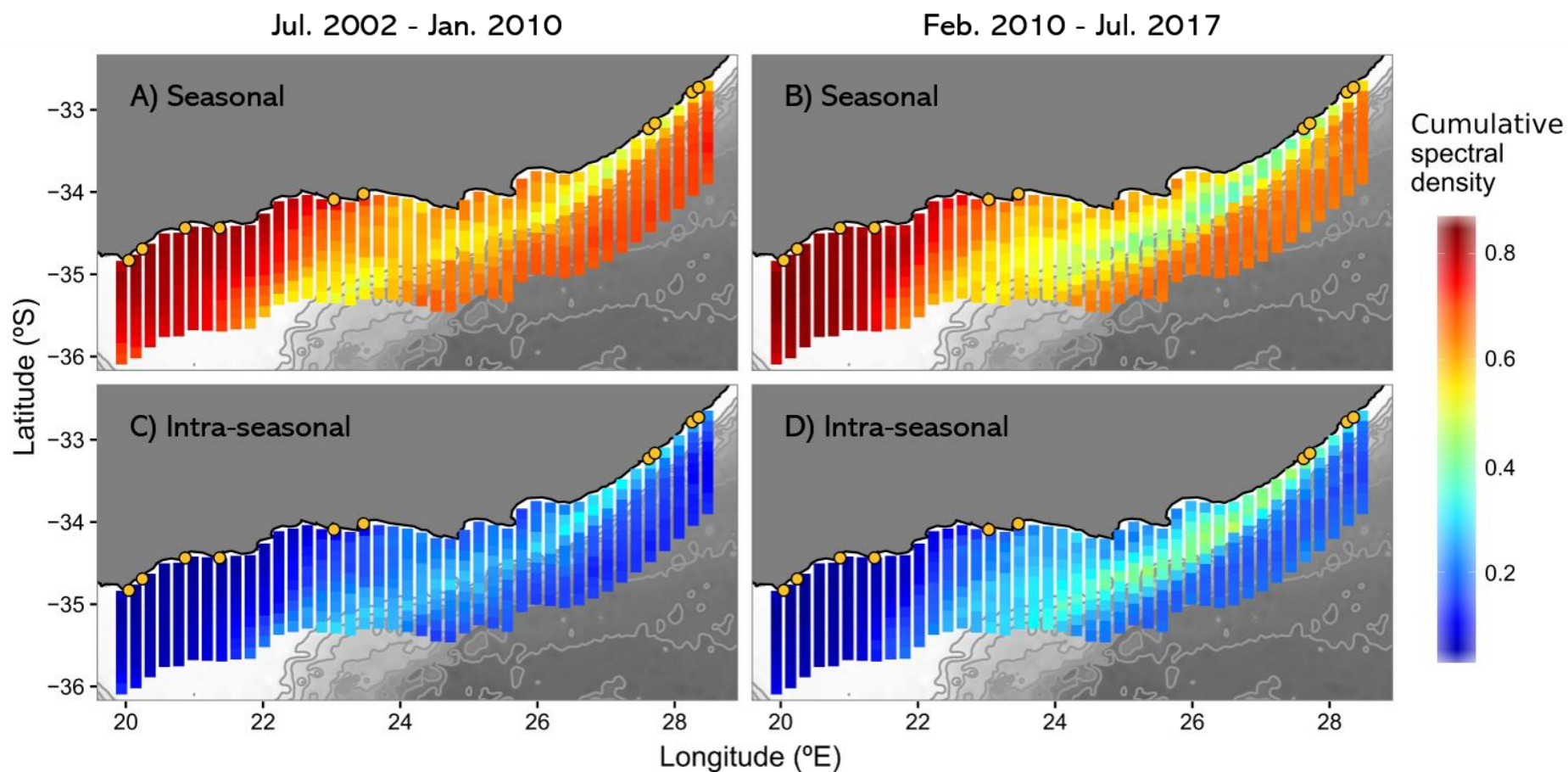


Fig. 5.7. Change in SST periodicity for each megapixel in the study area for the first half of the period of study (July 2002 to January 2010, panels A and C), and the second half (February 2010 to July 2017, panels B and D). Cumulative spectral densities were calculated for eight-day averages for each megapixel. Sampling sites along the coast are represented by yellow circles. Shaded areas and contour lines delimit the bottom profile, with the first contour line representing the 500m isobath.

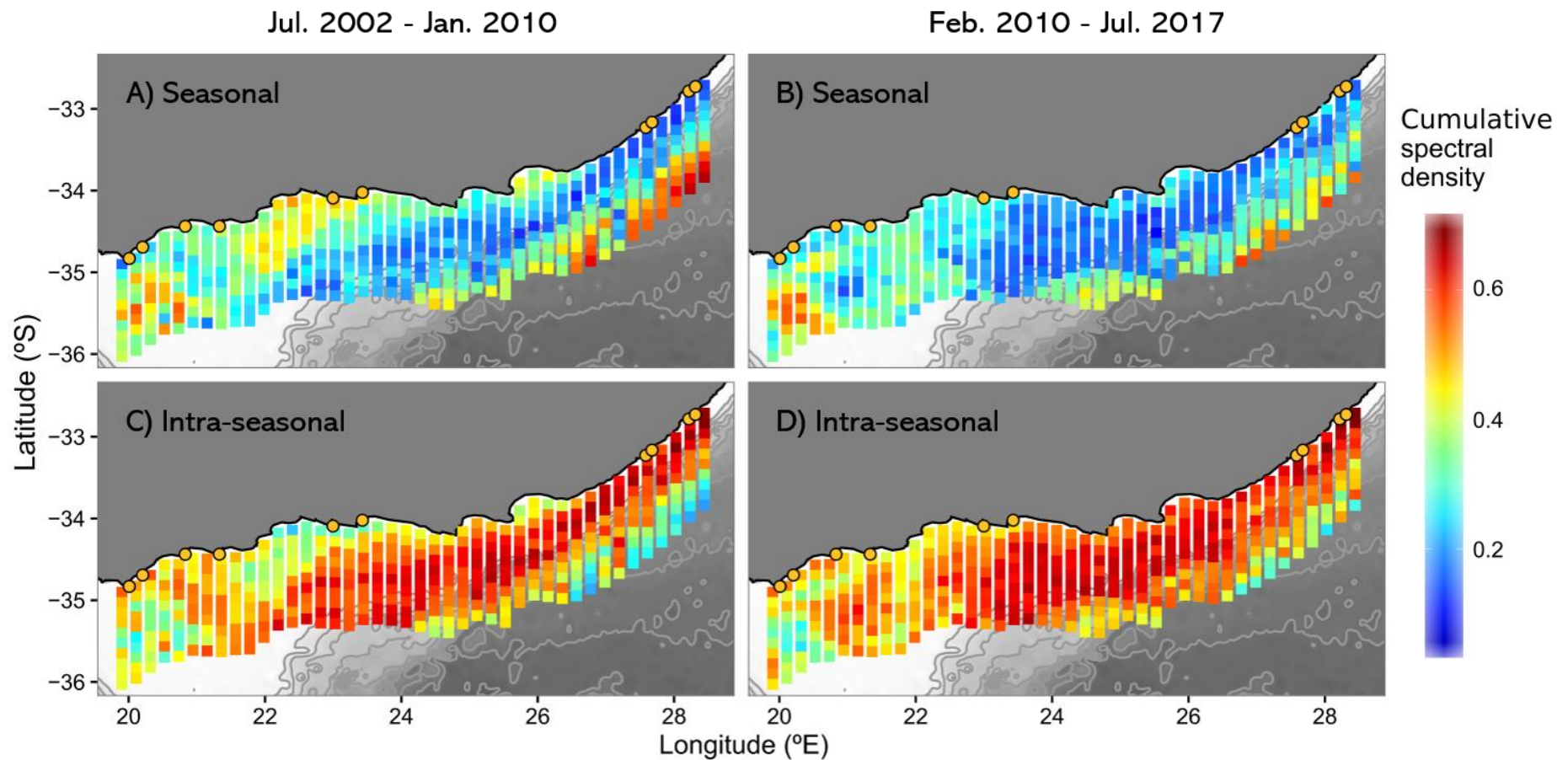


Fig. 5.8. Change in chl-a periodicity for each megapixel in the study area for the first half of the period of study (July 2002 to January 2010, panels A and C), and the second half (February 2010 to July 2017, panels B and D). Cumulative spectral densities were calculated for eight-day averages for each megapixel. Sampling sites along the coast are represented by yellow circles. Shaded areas and contour lines delimit the bottom profile, with the first contour line representing the 500m isobath.

5.3.2. Long-term environmental conditions

Most of the slopes of the linear regression models of seasonal SST anomalies, during the 15-year time series, were not significant (with some exceptions, Fig. 5.9A-D). Some of those significant models were isolated or did not seem to be biologically meaningful, therefore, a magnified picture is provided for autumn SST (Fig. 5.10), as it was the only season which provided significant models that clustered and seemed to be relevant to discuss. A non-significant warming tendency was present along most part of the south coast during winter, except for the westernmost part of the Agulhas Bank, where there was a cooling tendency. During spring and summer, opposite trends (again non-significant) were observed in the waters over the continental platform, where SST showed decreasing values over time, and the Agulhas Current, where temperatures seem to have increased. During autumn (Fig. 5.10), negative linear trends in SST were focused around two main areas: the upwelling cell of Port Alfred (c. 27°E), and the Plettenberg area (c. 23°E), where a second upwelling cell has been described. Linear regression trends were significant during autumn in these two upwelling centres. The slopes of the linear regressions indicate that, on average, temperature in the two upwelling centres during autumn has decreased by up to 0.1°C per year during the 15-year time series.

For the most part of the south coast, no significant trends were observed in the patterns of chl-a over the 15-year period, with the exception of the most coastal areas (Fig. 5.9E-H). In general, only a few pixels scattered along the coast showed a significant increase or decrease in chl-a values during the 15-years of data, with no particular areas where a clear pattern of change could be observed. Although some models were significant, no enlarged image is provided as they did not seem to provide relevant information. During winter, a decrease in the levels of chl-a occurred in coastal waters of the central area (c. 22 to 25°E). Trends of increased chl-a appeared in Algoa Bay during spring, with some pixels showing significant linear regressions. An increase in chl-a was also observed along the centre of the coast and onto the Agulhas Bank during summer, with some pixels around Plettenberg Bay (c. 23°E) producing models that were significant. A marked trend of decreasing chl-a was clear in autumn along the most central part of the south coast, although the models were not significant (Fig. 5.9H).

On the south coast of South Africa and within the mid/inner shelf, flow towards the west for currents or winds would contribute, through Ekman transport, to the displacement of surface waters away from the coast, promoting the upwelling of the bottom water mass. Therefore, the negative part in the x-axis of a vector (in this case, movement towards the west) would indicate upwelling-favouring flows, and the positive part downwelling-favouring flows. As a result, positive slopes from a linear regression (here calculated on this west-east component of the vector), would indicate either an increase in flow towards the east, or a change in flow movement from westwards

to eastwards. Thus, positive slopes would translate into downwelling-favouring conditions, and the opposite interpretation would stand for negative slopes. Off the shelf break, negative slopes would also point to an increase in the Agulhas Current westward flows over time. Seasonal averages of direction and magnitude of the west-east component of water currents during the 15-year period (Fig. 5.9I-L), showed an increase in the magnitude of water flow, and an increase in movement towards the east (i.e. positive values) over the Western Agulhas Bank in all seasons. Thus, positive slopes in the linear regression trends indicate an increase in the flow of water that favours downwelling and stabilization of surface waters. Most of the regression models for the west-east component of water flow were significant over the Agulhas Bank area. Over the shelf break and in deep waters of the south coast, in the area where the Agulhas Current trajectory starts to move offshore following the shelf break, the tendency was an increase in magnitude and direction of flow towards the west during all seasons, a pattern which was found to be significant except for summer. Within the northern part of the study area (i.e. 27.5-28.5°E), the magnitude of flow increased throughout the time series, but there were no changes in the direction of flow.

Trends in the seasonal averages of wind direction and magnitude were not significant for any of the linear regression models (Fig. 5.9M-P). The sign of the linear regression slopes can be interpreted in the same way as the slopes for water currents. In general, trends in winds did not match trends in water currents over the study region. A tendency towards downwelling-favouring conditions (i.e. a positive trend) was observed in the time series between autumn and spring in the east part of the coast. Although the models were not significant, an increase in the direction of wind flow that results in the displacement of surface waters from the Agulhas Current towards the coast would agree with the warming tendency observed in SST over the Agulhas Current during those seasons (Fig. 5.9A-D). A non-significant increase in upwelling-favourable wind flows (negative trend) was observed over the Western Agulhas Bank during spring and summer (Fig. 5.9N-O).

In general, long-term changes in the seasonal averages of SST, chl-a, currents, and winds seemed to behave in opposite ways in the area over the continental platform, and offshore waters. This break also coincides with the area where changes in the frequency of temporal patterns in SST and chl-a were observed for the second component of the PCA. Recruitment rates of mussels and barnacles seemed to be strongly correlated to the conditions of temperature and chl-a, with different periodicity patterns in those variables resulting in differences in the abundances of organisms. During autumn, coastal areas seem to have cooled around the two wind-induced upwelling centres on the south coast. Along the central area, chl-a seemed to have increased in summer and decreased in autumn during the period of study, although most of the models were not statistically significant.

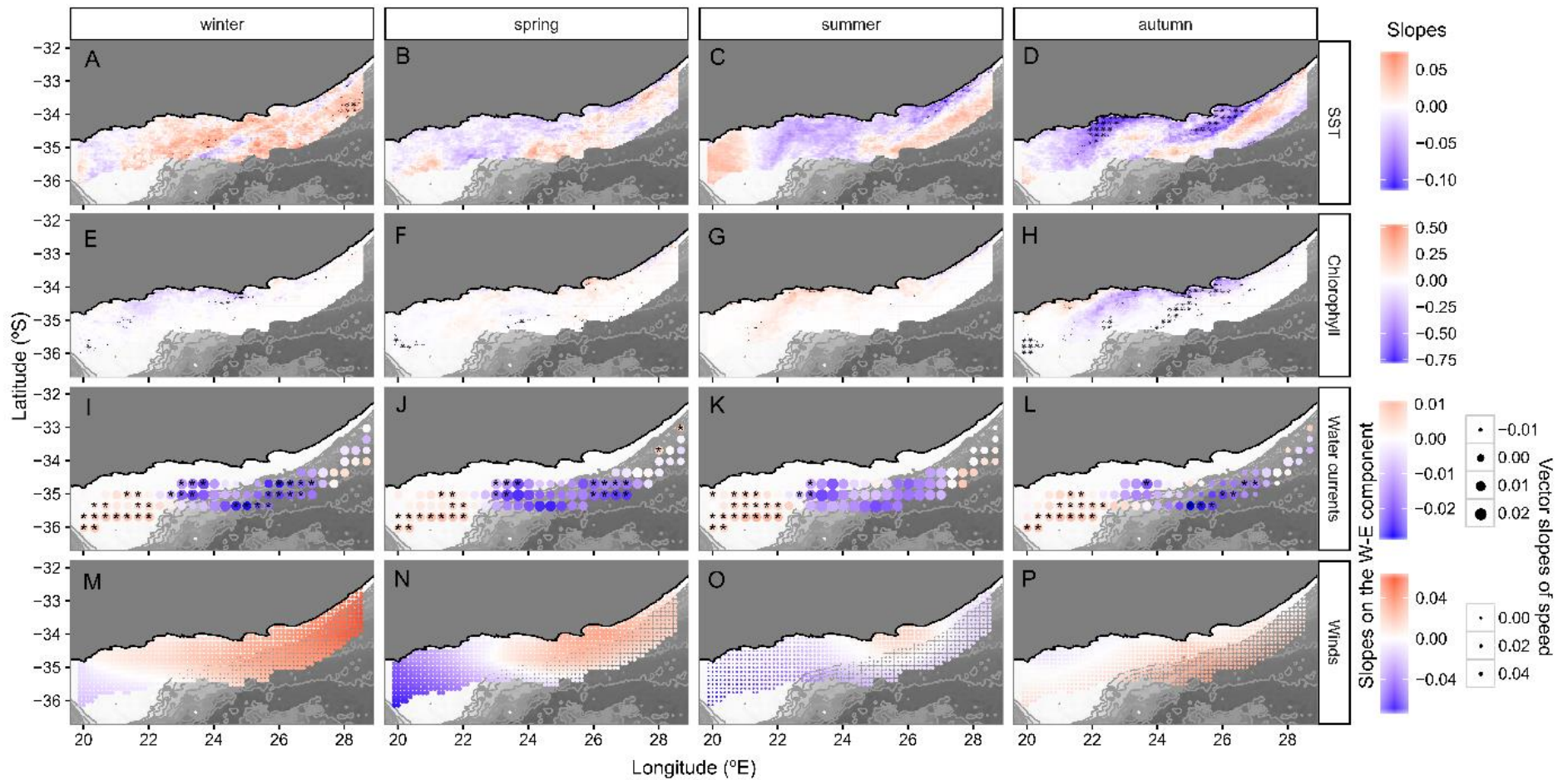


Fig. 5.9. Long-term trends for the anomaly values of SST (panels A-D), chlorophyll-a (panels E-H), water currents in the alongshore component (i.e. west-east, panels I-L), and winds also in the alongshore component (panels M-P). Colour scales represent the value of the slope after a linear regression was fit for each pixel. Size of the point for currents and winds represents the slope of the speed of the vector. Each significant model ($p < 0.05$) is indicated with a star. Note that the sizes of each pixel vary depending on the variable used (see Table 5.1). Negative slopes of water currents and winds correspond to upwelling-favouring conditions.

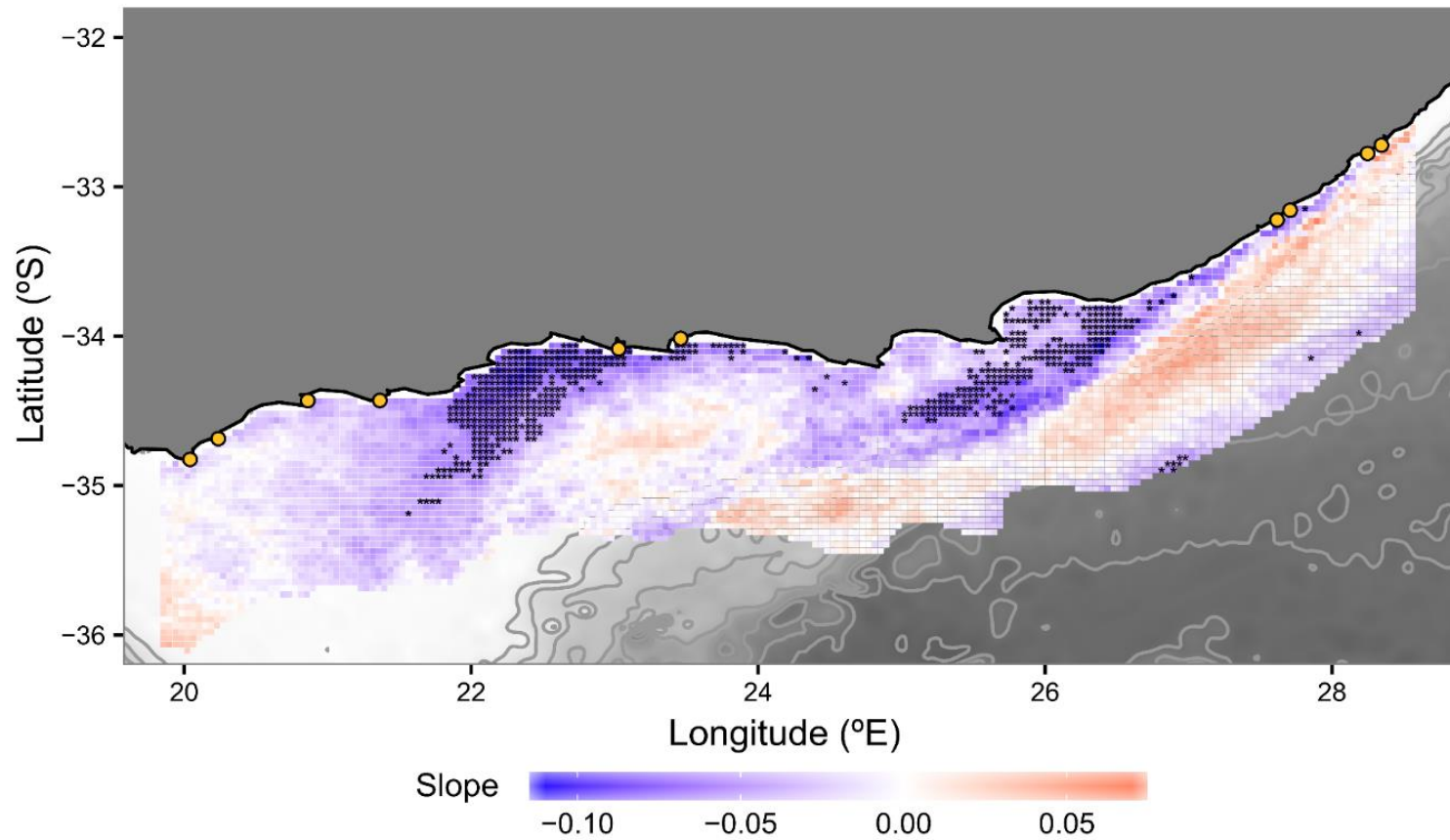


Fig. 5.10. Zoom in of long-term trends for the anomaly values of SST in autumn. Colour scales represent the value of the slope after a linear regression was fit for each pixel. Each significant model ($p < 0.05$) is indicated with a star. Sampling sites along the coast are represented by yellow circles.

5.4. Discussion

5.4.1. Spatial patterns of temporal variability

A marked spatial structure in the frequencies of temporal variability of SST and chl-a was observed along the South Coast of South Africa. The area of change coincided with the margins of the continental shelf, where the waters of the Agulhas Current are separated from the shallow areas over the continental shelf. Analysis of average annual SST and chl-a conditions, and mussel and barnacle recruitment, showed a poor relationship which did not successfully account for the spatial patterns observed in recruitment rates. In contrast, temporal variability of chl-a was found to be a strong predictor of mussel recruitment, although the relationship was weak for barnacles. These results suggest that large scale patterns of variation in the conditions that affect early stages of recruitment may play a major role in the structuring of the adult populations of benthic organisms. Similar changes in large-scale patterns of recruitment of new individuals and community composition have been described on the coast of central Chile (Broitman et al. 2001, Navarrete et al. 2005), along the West Coast of the United States of America (Broitman et al. 2008), and on the West Coast of South Africa (Wieters et al. 2009). In all those studies, it has been suggested that the topography of the coastline influences large-scale patterns of circulation (100-1000s km). Such topographically-driven changes in general flow patterns would modify the physico-chemical environment and influence benthic communities, shaping latitudinal distributions and abundances of organisms. For the coast of Central Chile in particular, major alongshore differences have been reported in recruitment rates and adult cover of benthic organisms (Navarrete et al. 2005), and algal biomass (Tapia et al. 2014). Tapia et al. (2014) attributed the changes observed to a change in the temporal regime of upwelling around a topographical discontinuity, which affects main current flow. On the West Coast of the U.S.A., Broitman et al. (2008) also found latitudinal changes in patterns of recruitment of benthic organisms and suggested a relationship between those patterns and the water temperatures, which depend on the frequencies of upwelling, also associated to topographical features. Thus, differences in upwelling frequency and/or intensity have the potential to translate into different productivity regimes which will be reflected in higher trophic levels. The areas where such variability in upwelling regimes has been proposed are all Eastern Boundary Upwelling Systems (EBUS), and therefore, strong interactions may occur between the wind patterns and the coastline topography. In those areas, upwelling occurs due to the combined forcing of major oceanic currents on the western limit of a land mass and the seasonality of trade winds.

Although this is also the case of the West Coast of South Africa (Shannon 1985), the East and South Coasts can experience seasonal local upwelling, promoted by wind forcing and the Agulhas Current around Plettenberg Bay (c. 24°E, Schumann et al. 1982, Probyn et al. 1994), and Port Alfred (c. 27°E,

Lutjeharms et al. 2000). Although the mechanisms that produce upwelling on the South Coast are different to those in EBUS, and both the frequency and intensity of upwelling are reduced, the present results suggest that the large-scale changes in temporal variability that appear to influence communities in EBUS, show similar effects on the distribution and abundances of benthic organisms in the South Coast of South Africa. An example of this is given by mussels, which are found at their highest abundances on the West Coast, both in terms of adult organisms and recruitment of new individuals (von der Meden 2009, Reaugh-Flower et al. 2010, 2011). Reaugh-Flower et al. (2010) studied mussel recruitment in the west, east and south coasts and found the highest recruitment on the West Coast and lowest on the South Coast. Nevertheless, von der Meden (2009) reported highest recruitment rates for mussels in the central area of the South Coast and a decreasing trend towards the east. The results reported by von der Meden (2009) agree with the longitudinal patterns in recruitment obtained in the present study (see Chapter 3), suggesting that the low recruitment rates presented by Reaugh-Flower et al. (2010) might be due to the selection of sites on the South Coast. In fact, the study sites in Reaugh-Flower et al. (2010) correspond with the easternmost area of the South Coast considered by von der Meden (2009), and in the present study (Chapter 3).

In the present study, the area shown to have a different temporal variability in SST and chl-a (Figs. 5.2 and 5.4) extends from the Eastern Agulhas Bank to north of the Port Alfred upwelling cell (c. 27°E), including the two upwelling cells. Very high recruitment rates were found in the central area around the Plettenberg upwelling cell (c. 23°E), however, according to the results in Reaugh-Flower et al. (2010) and von der Meden (2009), lower recruitment rates were found in the area downstream of the Port Alfred upwelling cell, in contrast to what would be expected for an area of productivity driven by upwelling. This difference in recruitment abundances between the upwelling cells at Plettenberg and Port Alfred, suggests that different mechanisms operate in the two cells. In fact, although temporal variability in SST did not prove to be a good predictor of recruitment along the coast, SST periodicity was markedly different in the area downstream of the Port Alfred upwelling cell, showing greater importance of short-term variability than any other area along the coast (see Fig. 5.3). Thus, variability at intra-seasonal frequencies translates into shorter changes in water conditions and lower predictability of conditions in the water mass. Similarly, temporal variability in chl-a was also found to be different in the two upwelling cells. Chl-a in the area around Port Alfred predominantly showed cycles between 21 and 100 days, shorter than in the area around Plettenberg, where seasonal and intra-seasonal variability were similarly important to chl-a periodicity. Here, it is proposed that the differences in the relative influence of the mechanisms that drive upwelling in each cell (i.e. wind and current forcing), are responsible for the alongshore patterns in recruitment, in a similar fashion as previously described for EBUS. Thus, upwelling produced by different mechanisms will influence the periodicity and magnitude of change in the

environmental conditions that affect recruitment of meroplanktonic organisms in different ways (in this case chl-a as a proxy of food supply) and therefore, different community structure may originate as a result of each mechanism of upwelling.

Cold waters are found in the area around Plettenberg (c. 24°E) during summer, extending to the southwest from the coast towards the Agulhas Bank, an area referred to as the “cold ridge” (Roberts 2005). Seasonal upwelling in the area has been proposed to enhance both primary (Largier et al. 1992) and secondary productivity (Peterson et al. 1992) during summer, from November to March (or even June in some years, Hutchings 1994). Upwelling enhances primary productivity by bringing nutrients from deep bottom waters to the photic zone where they can be used. Therefore, the area of seasonal upwelling will locally enhance productivity, and positively affect the organisms that rely on the planktonic environment during any part of their life cycle. The importance of the central part of the South Coast, in terms of productivity of high trophic levels, has previously been recognized for multiple groups of organisms (Hutchings 1994), from copepods (Boyd and Shillington 1994), to some economically important species like squid (Roberts 2005), which have their spawning areas between Plettenberg Bay and Port Alfred (Augustyn 1990). High chl-a values have also been reported in the surroundings of the Port Alfred upwelling cell and Algoa Bay, extending westwards along the coast and onto the Eastern Agulhas Bank (Probyn et al. 1994). Similarly, high fish abundances are also found along the coast, with emphasis on the upwelling areas along the South Coast (Booth 2000), with Port Alfred being a highly productive fishing area (Hecht and Tilney 1989). Nevertheless, copepod biomasses have been described as higher around the Plettenberg upwelling cell, decreasing towards the Port Alfred upwelling cell (Verheye et al. 1994, Hugett and Richardson 2000). Biomass of species that prey on copepods, like the chokka squid, are proposed to be associated to copepod availability, resulting in higher biomasses of squid around the cold-ridge than in Port Alfred (Roberts 2005). Thus, although both Plettenberg and Port Alfred are upwelling centres, the mechanisms that drive the upwelling of water in the two areas are not the same and levels of productivity differ between them. In the case of the Port Alfred upwelling cell, semi-permanent upwelling has been reported in the area (Lutjeharms et al. 2000), driven by the combined forcing of the Agulhas Current and the widening of the shelf around that area. In the case of the Plettenberg upwelling cell, the origin of the cold deep waters that are upwelled in the area is not clear. One of the proposed mechanisms is that the same water mass that is upwelled in the semi-permanent upwelling cell of Port Alfred could be transported towards the west and upwelled in the Plettenberg area (Swart and Largier 1987, Lutjeharms et al. 1996). Another possibility that has been suggested is that intensified flow of the Agulhas Current could produce shelf-edge upwelling (Gill and Schumann 1979), and that could force the water mass into the more coastal area. Recent sampling covering the entire Agulhas Bank (Jackson et al. 2012), suggested that the water mass that was observed in the area could have originated by shelf-edge upwelling and

moved northwards towards the coast. Thus, the water masses around the area could have different origins and be transported at depth by different mechanisms (Schumann and van Heerden 1988). Although the source of the water found in the Plettenberg upwelling centre is not clear, the annual reversal in the predominant wind direction experienced during summer on the South Coast (i.e. from winter westerly to summer easterly winds, Schumann 1987), has been proposed to produce the upwelling of the sub-surface cold water mass in the lee of headlands (Schumann et al. 1982). Likely, wind and Agulhas Current forcing contribute to the development of upwelling in both cells but probably with different intensity of each driver and at different time scales, resulting in the different periodicities observed (Figs. 5.3 and 5.5). Seasonality of upwelling in the two cells will result in marked changes in temperature and chl-a patterns throughout the year, in contrast to the areas outside of the influence of upwelling. This will affect the temporal patterns of variability in both SST and chl-a, and differentiate those areas from their surroundings. In addition, differences in the drivers of upwelling between the two upwelling centres will produce different temporal patterns in variability for each area, and differences in the magnitude of change of SST and chl-a. Thus, in the case of Port Alfred, persistent sub-surface expression of upwelling and the spatial location of the cell (in a transitional area of warmer and less productive surface waters), could result in less marked seasonality in temperature and phytoplankton cycles (i.e. more constant values throughout the year than the values experienced around Plettenberg), with short time scale variability exhibited in both temperature and chlorophyll. In the case of Plettenberg, seasonal upwelling during summer will produce longer cycles of variability, likely resulting in stronger seasonal peaks of primary production, when the conditions are favourable. In fact, longer periods were found to characterise temperature and chlorophyll cycles around Plettenberg (Figs. 5.3 and 5.5). These differences in frequency and intensity of change in temperature and chl-a could produce synchronous reproductive cycles for benthic organisms, and explain the high levels of recruitment observed around Plettenberg compared to Port Alfred. Thus, the combination of high food availability (in the form of high phytoplankton densities) and clear seasonality may enhance recruitment rates in this area when compared to other regions where high productivity is known to occur, as at Port Alfred. In fact, the presence of phytoplankton in the water has been described as one of the mechanisms that can trigger synchronous spawning in benthic and pelagic organisms (Starr et al. 1990, 1991), as well as one of the main factors that affect survival of larval stages of benthic organisms (Pechenik et al. 1990). Thus, marked seasonality in phytoplankton cycles could be one of the factors that determine high, synchronised recruitment and positively influence the maintenance of adult populations. This could be linked to the duration of availability of food resources for the reproductive season of adult organisms, and during the development of larval stages. Thus, increased magnitude of the phytoplankton bloom due to strong SST seasonality could play a major role on the reproduction and physiological requirements of organisms during early

stages of development and favour a shorter window of recruitment in Plettenberg, which could explain the higher recruitment around that area.

5.4.2. Long-term environmental conditions

Long-term changes in seasonal averages of SST, chl-a, currents, and winds, seemed to follow opposite trends in the area of the continental shelf and the offshore area, coinciding with the areas where the patterns of temporal variability were different in the previous section of the current discussion. Significant models showed a tendency of SST to decrease during autumn, centred at the upwelling cells of Port Alfred (c. 25-27°E) and Plettenberg Bay (c. 22-24°E), and extending towards the southwest from both areas. Although wind direction and magnitude did not show an increase in upwelling-favouring conditions around those two areas, water current flows over the Agulhas Current seemed to increase in magnitude in an upwelling-favouring direction. Thus, the decrease in SST around the two upwelling centres could be the result of increased upwelling through water mass forcing because of an acceleration of the flow of the Agulhas Current, as suggested by the westward displacement of currents outside of the shelf area (see Fig. 5.9). Changes in SST and chl-a periodicity also appeared in the two upwelling areas, with the cooling trend showed around Port Alfred coinciding with increase in importance of shorter scales of variability in SST.

Bakun (1990) hypothesised that the winds that promote upwelling in EBUS will intensify under global change conditions due to higher thermal sea-land contrasts. Increased warming over land masses during summer months will increase the differences in air temperatures between land and the water mass. That could promote an increase in alongshore winds during summer and result in an increase in upwelling. Although this hypothesis was proposed for EBUS (Bakun 1990), it could also hold for areas where seasonal wind-induced upwelling is observed, like the South Coast of South Africa, where alongshore winds predominate (Schumann 1989, Schumann and Martin 1991). Although upwelling is expected to increase in intensity and to last longer in EBUS under future climate scenarios, its behaviour will not be the same for all systems (Wang et al. 2015). In fact, the results point to a mismatch between trends in winds and currents over the region and may not support a direct link between local upwelling dynamics and thermal conditions (Fig 5.5). It is also unclear how enhanced coastal wind, typically restrained to the inner and mid shelves, may cause stronger currents further offshore.

Another possible explanation for the patterns observed could be the intensification of water mass forcing due to the acceleration, or increase in water flow, of the Agulhas Current. As previously discussed, forcing by the Agulhas Current drives upwelling in the Port Alfred area (Lutjeharms et al. 2000). Upwelling in Plettenberg could be driven by westward flow from Port Alfred (Swart and Largier 1987), or from the shelf-edge during intensification of the Agulhas Current (Gill and Schumann 1979). Examine of long-term data or re-analysis products have shown warming of the

main Western Boundary Currents (Wu et al. 2012, Shears and Bowen 2017). Since the 1980s, a warming trend has been reported in the Agulhas Current system (Rouault et al. 2009). Rouault et al. (2010b) proposed that an increase in water transport has occurred in the system based on simulations obtained through regional ocean models (ROMs) developed for that area. Similarly, Backeberg et al. (2012) also reported an increase in eddy instability in the area adjacent to the east coast of South Africa, which is likely to influence the area of the South Coast considered in the present study. Western boundary currents, like the Agulhas Current, are forced by the wind conditions in their ocean basin, and they strongly influence meteorological conditions in the adjacent areas (Lutjeharms 2006). Rouault et al. (2009) reported a cooling trend around the upwelling cell of Port Alfred and suggested that it could be related to an increase in flow from the Agulhas Current. In addition, they also proposed that increases in flow of the Current could result from increases in wind forcing over the ocean basin (Rouault et al. 2009). The present results for the South Coast of South Africa do not show significant changes in wind stress for the period examined (Fig. 5.9). Nevertheless, increased wind stress along the South Coast would only affect wind-driven upwelling dynamics, but not Agulhas Current forcing. Wind-induced acceleration of flow in the Agulhas Current is expected to originate upstream of the region considered in the present study. SST and wind conditions in the Western Indian Ocean have been described as varying between years depending on the mode of variability of the Indian Ocean Dipole (Saji et al. 1999, Saji and Yamagata 2003). Thus, a possible explanation is that, although significant trends and cycles in long-term wind variability were not observed in the region, these could be occurring at the Western Indian Ocean, thus influencing the structure of the Agulhas Current further downstream and driving its acceleration over the shelf break (Fig. 5.9). Wu et al. (2012) reported an intensification of the anticyclonic wind stress curl in the Indian Ocean gyre, and suggest that this could account for intensification in flow in the Agulhas Current. Thus, although in the present study decreasing trends in surface temperature in the upwelling cells of the South Coast are not supported by wind directionality or stress, increased upwelling in the South Coast may provide evidence of increased flows in the Agulhas Current resulting in stronger forcing of the water mass, as suggested by Rouault et al. (2009) and in the present results (Fig 5.9). Large-scale spatial studies usually examine data at resolutions which are too coarse to describe local processes, for example Rouault et al. (2010b). The present study considered seasonality before calculating the trends in the environmental conditions. The inclusion of seasonality in the analysis revealed that the cooling trend experienced in the upwelling centres was only significant during autumn, not during the rest of the year. Here, it is proposed that the seasonal variability in the trends observed could dramatically influence the biological community during one of the peaks of spawning of benthic species, i.e. autumn. In addition, the fine-scale spatial resolution used in the analysis indicates that the areas where change has been maximum are centred on the two upwelling cells and the areas

downstream of them specifically, and not simply around the Port Alfred upwelling cell as reported by Rouault et al. (2009). The opposing trends observed in the Agulhas Current (warming, Wu et al. 2012) and the shelf area (cooling, Rouault et al. 2009, and present results) highlight the importance of understanding contrasting hydrographical patterns forced by a common physical mechanism and how these interact with complex scale-dependent biological processes which may in turn alter spatio-temporal patterns of biomass/recruitment.

Thus, although upwelling seems to have intensified in autumn during the period of study, chl-a seems to have decreased in autumn and increased in summer in the central area. These results should be taken with caution because most of the linear regression models were not significant. For the South Coast, two phytoplankton blooms would be expected, during spring and autumn (Brown 1992). The increase in chl-a during summer and decrease in autumn could be the result of a change in the phenology of the autumn bloom, which could be developing earlier in the year. For example, changes in the timing of the peak of abundance for different functional groups have been observed in the North Sea (Edwards and Richardson 2004, Beaugrand and Kirby 2010). Changes in phenology have been attributed to changes in the environmental conditions in the water mass, which would alter the basis of the food web and influence the trophodynamics of the system (Kirby et al. 2008, Kirby and Beaugrand 2009). For example, it has been suggested that an increase in SST early in the year may be responsible for a shift in peak meroplankton abundance to earlier in the year (Edwards and Richardson 2004). However, the response of diatoms seems to be regulated by conditions in the photoperiod (Eilertsen et al. 1995), and diatoms did not appear to peak earlier in the year (Edwards and Richardson 2004). Thus, changes in the environmental factors that regulate the system could lead to the decoupling of the different components of the trophic system, and negatively influence food availability for consumers (Edwards and Richardson 2004). Nevertheless, dinoflagellates have been observed to peak earlier in the year in the North Sea (Edwards and Richardson 2004). The warming of the water mass in the North Sea also has been suggested to favour the spatial and temporal ranges of distribution of toxic algal species (Gobler et al. 2017). Along the Agulhas Bank, an increasing number of Harmful Algal Blooms (HABs), caused by different dinoflagellate species, has been detected in recent years (van der Lingen et al. 2016, and Chapter 2). Although the present results from SST models during spring and summer showed a decreasing trend in temperature, those models were not significant. That could have been the result of inter-annual fluctuations in temperature conditions. Oscillation in the seasonal averages of SST can be observed in the SST seasonal anomalies (Chapter 2, Fig. 2.8), showing periods of several years with SST above the long-term average for summer temperatures in the Agulhas Bank. The increase in stability in surface waters that resulted in higher SST during summer (see results in Chapter 2), could be related to the occurrence of those HABs as has been suggested for other systems (McCabe et al. 2016, Ryan et al. 2017).

In conclusion, analysis of the temporal variability of SST and chl-a has delimited for the first time the area of environmental variability which corresponds with the area of highest biological production described for the South Coast of South Africa. Thus, the importance of temporal variation around the two upwelling centres was identified, as well as the significant relationship with recruitment abundances of mussels and barnacles (Fig. 5.6). Decreasing trends observed in SST during autumn suggest an increase in intensity of upwelling around the two upwelling cells at Plettenberg and Port Alfred. Such a pattern matches both the observed acceleration of the Agulhas Current over the shelf break and the reduction of seasonal fluctuation in SST and chl-a in favour of shorter frequencies of variability. This correspondence suggests a sequence of causal relationships by which basin-scale climatic forcing drives Agulhas Current acceleration in the study region, which in turn increases shelf break-Agulhas mediated upwelling on intra-seasonal time scales with effects on the temporal variability of SST and chl-a. Eventually, this mechanism would affect recruitment rates through changes in the temporal availability of potential food resources in the phytoplankton community. In fact, variability in chl-a cycles at shorter time scales increased in importance for the Plettenberg upwelling cell over the last seven and a half years of the study. Such change could result in the occurrence of red tides outside the period of normal spring/autumn phytoplankton maxima for the region (cf Brown 1992) and resulting in increased unpredictability of chl-a conditions for the area. Thus, although chl-a conditions are becoming more unpredictable around the area with highest mussel recruitment, the effects on their populations may depend on the ability of the early stages of mussels to utilise the new resources that become available. The insight provided in temporal variability and its relationship with biological productivity should contribute to improved management of new and existing marine protected areas (MPAs) in the region. In addition, the seasonal differences reported in long-term variability suggest that the changes in SST and chl-a during the autumn spawning period of marine organisms may result in the un-coupling of the physico-chemical and biological systems as has been reported in the North Sea (Edwards and Richardson 2004). The spatial patterns of temporal variability found here may be applicable to understanding productivity in other shelf areas. Due to the limited volume of water over the continental shelves, ocean-atmosphere interaction puts these areas under higher risk of experiencing the effects of anthropogenically induced environmental change. The present results, therefore emphasise the importance of understanding the mechanisms that drive production, and presage a possible change in the future of the shelf system in South Africa, and in similarly environmentally-driven systems, under the current scenario of change.

Chapter 6

Synthesis

“... We look back at alchemists and laugh at what they were trying to do, but future generations will laugh at us the same way. We’ve tried the impossible – and spent a lot of money doing it. Because in fact there are great categories of phenomena that are inherently unpredictable.”

Michael Crichton (*Jurassic Park*)

6. Synthesis

In general, temporal variability of chl-a and SST along the south coast of South Africa was found to be different in the central area around the two upwelling centres, where higher primary productivity occurs, compared to the surrounding areas. In fact, temporal variability of chl-a and SST was found to be correlated to recruitment rates of mussels and barnacles. Within that area of high productivity, and along the entire south coast, red tides lasting for months have been reported in recent years. Blooms of two red tide-forming dinoflagellates, promoted by different oceanographic regimes, developed during the two years of the study: a bloom of *Lingulodinium polyedrum* during the first year, and one of *Noctiluca scintillans* during the second. The conditions that favoured the development and persistence of these events, and the changes that they produced in phytoplankton composition, did not affect mussel and barnacle taxa equally. Environmental conditions were markedly different between the two years, with unusually high SSTs during year 2014, but lower chl-a levels than the following year, for example. Analyses of winds and currents suggested that increased stratification may have occurred during the first year, while more intense or frequent upwelling may have occurred the following year. Recruitment rates of mussels and barnacles during two consecutive autumn periods, showed opposite patterns, with higher mussel recruitment during the second year and higher barnacle recruitment during the first. Thus, barnacles were favoured during the stable conditions of the first year and the presence of *L. polyedrum*, and mussels reached much higher abundances during conditions that seemed to indicate persistent upwelling, co-occurring with *N. scintillans*. Although differences of one order of magnitude were observed in barnacle recruitment between years, growth and mortality rates during the first five months after settlement did not differ. Such differences between recruitment and post-settlement growth/mortality patterns between years may reflect different environmental conditions between the offshore areas where larvae develop and those at their settlement sites. Thus, the order of magnitude difference in recruitment between the two years shows that, although the effects of conditions experienced during pelagic larval development may be compensated for in later stages of development, persistence of conditions such as those which led to lower larval supply during the first year would produce a bottleneck in the supply of new organisms to the adult populations.

The analysis of 15-year time series data showed significant cooling trends during autumn around the two upwelling centres on the south coast. Those cooling trends proved to be season specific and to coincide with the autumn reproductive period of the study organisms, and with the area where recruitment is generally highest along the coast. Thus, the conditions observed during the present study, particularly during the second year when upwelling seemed to be more intense, may presage the potential effects of the long-term cooling trends at the upwelling centres. Nevertheless, the

results show that, although the general trend shows cooling around those areas, conditions can vary greatly among years, favouring different taxa.

6.1. Environmental changes in water mass conditions

The inter-annual variability observed in early stages of development of mussels and barnacles, and their relationship with water mass conditions, highlight the importance of understanding the mechanisms that affect the nearshore water mass and how they will evolve in the future. The cooling of surface waters during autumn, as presented in Chapter 5, suggests that physical mechanisms have increased the frequency or intensity of upwelling around the upwelling cells of the south coast. The upwelling of nutrient-rich bottom waters into the photic zone favours primary producers, as well as higher trophic levels. Nevertheless, successive upwelling and stability conditions can also produce negative effects. In particular, such dynamics may promote the growth of species able to outcompete other organisms and dominate the phytoplankton biomass, many of them considered Harmful Algal Blooms (HABs, or red tides, as referred to in previous chapters). For example, along the west coast, red tides have been associated with the relaxation conditions following upwelling (Pitcher and Boyd 1996, Probyn et al. 2000). Thus, species which are autotrophic or mixotrophic are directly favoured by nutrient availability, but heterotrophic species can also be favoured by the increase in their prey. For example, although the red form of the dinoflagellate *Noctiluca scintillans* is a heterotroph, the supply of nutrients by upwelling increases the availability of prey in the phytoplankton and indirectly favours the dinoflagellate (Padmakumar et al. 2010).

In addition to the negative impacts of red tide forming organisms on human health and ecosystems (Sunda et al. 2006, Grattan et al. 2016), highly productive phytoplankton blooms can also affect the chemistry of the water mass. A tendency of increasing upwelling will supply nutrients and contribute to the support of higher biomass of phytoplankton. When these organisms die, they will sink and decompose, depleting oxygen in bottom waters. In the case of the Agulhas Bank, the shape of the shelf limits water exchange, particularly towards the west where the shelf is widest. Low-oxygen waters can appear in the Agulhas Bank (Eagle and Orren 1985). Chapman and Shannon (1987) reported lower oxygen concentrations at 50m depth than in surface waters, with maximum differences occurring during autumn, and suggested that such differences may be due to the decomposition of organic matter. On the Agulhas Bank, that period coincides with the autumn phytoplankton bloom. Red tide events during summer and autumn, such as those described in Chapter 2, would likely contribute to decrease oxygen levels in bottom waters along the Agulhas Bank. In fact, during a previous red tide caused by the dinoflagellate *Gonyaulax polygramma*, van der Lingen et al. (2016) reported low oxygen bottom waters and suggested their link with biomass decay from the bloom.

In addition to low oxygen conditions generated in situ, some deep-water masses also carry low oxygen concentrations. For example, upwelling of hypoxic bottom waters has been reported in Eastern Boundary Upwelling Systems (EBUS; Grantham et al. 2004, Monteiro et al. 2006). Monteiro et al. (2006) reported that two different water masses are upwelled in the Benguela Upwelling System, one of them being oxygen-depleted and the other being aerated. On the coast of Oregon (U.S.A.), Grantham et al. (2004) also reported the upwelling of a hypoxic water mass onto the shelf which resulted in mass mortalities of marine organisms. Although the Agulhas Current is a Western Boundary Current (WBC), and its physico-chemical properties differ from currents in EBUS, friction between the current and the bottom promotes the intrusion of intermediate-deep water masses onto the shelf and coastal upwelling, as discussed in previous chapters. Chapman and Largier (1989) detected the presence of Indian Ocean Central Water in bottom waters of the Agulhas Bank. Thus, these coastal communities will be influenced by the physico-chemical characteristics of a water mass that comes from the adjacent ocean basin. Nevertheless, the lower oxygen concentrations in bottom compared to surface waters, led Chapman and Shannon (1987) to suggest that oxygen depletion was likely to result from the decay of organic matter produced in the shelf, instead of coming from the water mass that is advected onto the shelf. Despite that, the complicated structure and the multiple sources of the Agulhas Current (Beal et al. 2006), in combination with the intensification reported in the current (Rouault et al. 2009), may require further investigation of the flows intruding onto the shelf and their characteristics to determine possible consequences of upwelling intensification for coastal organisms.

Low oxygen concentrations, either produced in the water column or advected from a hypoxic water mass, can produce mass mortalities of marine organisms (for example Pitcher and Probyn 2011). Nevertheless, hypoxia may also favour organisms that are better adapted to tolerate low oxygen environments. For example, the green form of *N. scintillans*, which occurs in the northern part of the Indian Ocean, is able to thrive under hypoxic conditions due to its symbiotic relationship with a chlorophyte (Do Rosário Gomes et al. 2014). In recent years, the appearance of hypoxic conditions in the Arabian Sea has favoured a shift from diatoms to *N. scintillans*, which may compromise trophic dynamics during the period when the main phytoplankton bloom occurs (Do Rosário Gomes et al. 2014). Thus, some phytoplankton species can produce large blooms which will reduce oxygen availability, and also outcompete other organisms in the altered environment, further affecting the system. When oxygen is depleted after biomass decays, winter mixing contributes to aeration of the water mass, particularly in shallow areas (Pitcher et al. 2014). Along the Agulhas Bank, the water column is stratified from spring to autumn, with mixing during winter. In Chapter 5, positive trends in SST were observed along the coast during winter, although they were not statistically significant. Warmer SSTs were found during the winters preceding the development of red tides in the present study. As previously suggested in Chapter 2, warm surface waters during winter may occur due to

the intrusion of eddies and filaments from the Agulhas Current onto the Bank. Warming of surface waters during winter could limit vertical mixing and complicate the replenishment of oxygen. Although no significant warming trends were observed during winter, 15 years of data represent a short period in the study of long-term trends in environmental conditions (Zheng et al. 2016). In fact, the south west Indian Ocean is affected by modes of variability such as the Southern Annular Mode (SAM), *El Niño* Southern Oscillation (ENSO), or the Indian Ocean Dipole (IOD), which fluctuate over periods of several years. Rouault et al. (2010a), using a period close to 30 years, reported that ENSO phases were related to upwelling/downwelling favourable winds, with cooling in the upwelling cells promoted by *La Niña* conditions. Such variability complicates the ability of linear regression models to find any significant trends. Although in Chapter 5 significant trends were detected in autumn for the same period, the intensification of the Agulhas Current (Rouault et al. 2009), and its strong influence as a driver of upwelling, may dominate over the interannual variability produced by climate modes such as ENSO. Hence, during winter, when the current is weaker, the effect of winds may not be strong or persistent enough to overcome interannual variability and show clear, significant trends.

Changes in the water chemistry over the shelf are not restricted to oxygen. Arnone et al. (2017), measured fluxes and fugacity of CO₂ of the water mass, from Cape Town (ca. 18°E) to Durban (ca. 31°E), and reported high variability near the upwelling centres of Cape Town, Port Alfred and Durban. The authors reported that the water mass in those areas had higher CO₂ concentrations than the air mass, and therefore, it was releasing CO₂ instead of absorbing it. These high CO₂ concentrations were attributed to the upwelled water masses, as they were related to colder waters (Arnone et al. 2017). Such results suggest that bottom waters in the Agulhas Bank, presumably from Indian Ocean Central Water (Chapman and Largier 1989), are CO₂ enriched compared to the water mass along the rest of the area. Several decades of increased atmospheric levels of CO₂ have resulted in the capture and export of CO₂ to depth. Nevertheless, CO₂ sequestration/release by the water mass depends on saturation levels which vary globally (Feely et al. 2004). In fact, areas in the Southern Ocean have been reported to be releasing CO₂ in the same manner as the upwelling areas along the south and east coasts of South Africa (Lovenduski 2012, Xue et al. 2015). Increased entrainment of enriched CO₂ waters onto the shelf produced by enhanced Agulhas-driven upwelling at the Port Alfred and cold ridge area, as described in Chapter 5, may reduce CO₂ sequestration rates even further. On the other hand, the addition of CO₂ to the water reduces the pH and makes the water more acidic. Reductions of seawater pH have major implications for calcifying organisms because of the affinity of low pH water for carbonate, which can make it unavailable for organisms such as mussels and barnacles (see review in Doney et al. 2009). In fact, increased CO₂ has been reported to decrease growth and calcification rates in molluscs (Kurihara and Shirayama 2004, Gazeau et al. 2007) and to contribute to the dissolution of calcareous structures in planktonic

organisms (Engel et al. 2005, Fabry et al. 2008). Thus, the positive effects on phytoplankton production of increased upwelling of nutrients during autumn may be counteracted by the negative effects of high CO₂ levels in the same water mass (Arnone et al. 2017) which is upwelled along the south coast. In addition, upwelling during autumn will also overlap with the reproductive period of mussels and barnacles, as observed in Chapter 3, and larvae will develop under more acidic conditions. The stress of development under low pH has been reported to reduce larval growth and shell thickness in the mussel *Mytilus edulis* (Gazeau et al. 2010), which could affect later recruitment.

6.2. The future of benthic organisms

The long-term changes around the upwelling centres of the south coast presage increased upwelling of deep, nutrient-rich water which may increase primary productivity during summer and autumn, the periods of seasonal upwelling along the south coast (Schumann et al. 1982). The presence of upwelling, leading to increased phytoplankton availability, may have positive effects for filter feeders during stages of development that rely on phytoplankton. For example, Chapter 3 showed that recruitment of mussel taxa was higher during the second year of study, under stronger upwelling conditions. Barnacle recruitment in contrast, was lower during the same period, indicating that environmental variability may not affect all taxa equally. As previously discussed in Chapters 3 and 4, temperature and food availability during larval stages play a major role in determining survival and developmental times, but favourable flows are essential for larval delivery to the settlement sites (for example Farrell et al. 1991). Increased upwelling could result in the offshore transport of larvae and consequent loss of individuals. For benthic organisms, it could also retain competent larvae in the water for longer periods before they can reach the settlement sites, which would increase the risk of predation and use of the energy reserves of certain organisms (for example barnacles) which do not feed during certain larval stages. Therefore, although the results in Chapter 3 showed that mussel recruitment was favoured under suspected upwelling conditions, timing between larval development and return to suitable settlement sites could also be critical.

Changes in stratification may also alter flows and compromise the ability of larvae to return to settlement sites. In fluid dynamics, vertical density differences, during stratification periods generate interfaces between different water layers, like thermo and haloclines, along which internal motions are transmitted shorewards. These internal motions occur more frequently and with higher intensity during seasons with stronger stratification (Cairns 1968, Cairns and Nelson 1970). In turn, internal motions have been associated with the settlement patterns of different intertidal taxa, indicating that they produce effective net onshore larval transport (Pineda 1991, 1999). Thus, changes in water column stratification during the periods of highest stratification in temperate areas (i.e. from spring to autumn), will affect the energy transferred by internal motions and cross-shore currents. Pineda et al. 2018, reported that warming associated with the “Blob”

heatwave and the 2015/16 El Niño in California negatively impacted barnacle settlement during those years, an effect associated with the deepening of the thermocline and the reduction in energetic transfer of cross-shore currents, this is similar to the results obtained by Hagerty et al. (2018). In the present study, higher barnacle recruitment occurred in autumn 2014, coinciding with warmer SSTs than the following year. The colder SSTs observed during autumn 2015 (see Fig. 2.9) suggest that stronger and/or more persistent upwelling may have occurred during that season. This might have contributed to vertical mixing and the reduction of stratification, possibly affecting internal motions. The decrease observed in recruitment could be associated with such changes in internal wave activity, but contrary to Hagerty et al. (2018) and Pineda et al. (2018), changes in cross-shore currents would be mediated by the changes in stratification produced by upwelling, instead of being driven by deepening of the thermocline during warm anomalies. Thus, the cooling trends described in Chapter 5, which I propose are a response to changes in the upwelling patterns along the coast, may negatively impact cross-shore flows and longer term studies should be carried out on the possible consequences for larval transport.

Recruitment rates observed in Chapter 3 for the two mussel taxa studied, the native *Perna perna* and other mytilids, which comprised mostly the invasive species *Mytilus galloprovincialis*, plus very small numbers of *Choromytilus meridionalis* (personal observation, from here on other mytilids will be considered as *M. galloprovincialis*), showed very similar recruitment rates between the two taxa during the first year. Nevertheless, during the second year, when upwelling was assumed to be more intense, and there were higher concentrations of phytoplankton in the water, the taxon including the invasive species reached recruitment rates an order of magnitude higher than those of the native species. Such results may suggest that the conditions during the second year favoured both species, but particularly *M. galloprovincialis*. Higher recruitment success of the invasive species may have major implications for *P. perna* along the south coast. Adult populations of *M. galloprovincialis* and *P. perna* along the south coast show vertical separation partly based on their tolerances of physical stresses. *P. perna* has stronger attachment and lower tolerance of desiccation, dominating in areas lower on the shore, while *M. galloprovincialis* shows higher tolerance of desiccation and lower resistance to wave action, and dominates in higher areas. Based on the importance of tolerance to physical stress for spatial segregation of adults, models that study the distribution of organisms are largely focused on the relationship between the adults and their environment, with insufficient focus on the influence of successful supply of new individuals into those models (for example Tagliarolo et al. 2015). Nonetheless, the south coast of South Africa experiences frequent sand translocation which covers the intertidal areas, with maximum rates in autumn (Bally et al. 1984, Zardi et al. 2008). Zardi et al. (2008) showed that *P. perna* experienced higher mortalities than *M. galloprovincialis* when buried by sand. In addition, *P. perna* occupies lower intertidal areas, which increases exposure to sand (Zardi et al. 2006b). The present results suggest

that after mortality of adult individuals, when new space is available for recruitment, recolonization rates of the invasive species will be higher than that of the native species (for example Erlandsson et al. 2006). Although stress due to physical conditions in the intertidal area after recruitment will increase mortality of the invader, which is less resistant to wave stress (Zardi et al. 2007a), if the higher recruitment rates of the invader are maintained, this differential propagule supply may compromise the maintenance of adult populations of *P. perna* and should be included in future modelling efforts.

Post-recruitment growth and mortality were not estimated for mussels, so that information on indirect effects produced by the presence or absence of red tides in the water is lacking. Nevertheless, the study of barnacle growth and mortality rates during the first five months after recruitment did not reveal any carryover effects due to sub-lethal effects on larvae. Barnacles are more dependent on energy reserves than mussels due to their non-feeding larval stages and their inability to relocate after settlement (Pechenik 2006). In the case of mussels, after larvae reach a competent stage and settle, translocation to more favourable habitats can still occur (Bayne 1964, Le Corre et al. 2013, Navarrete et al. 2015), while the selection of suboptimal habitats for barnacles will be permanent. The absence of between-year differences in growth and mortality of barnacles, suggests that trophic variability in intertidal areas did not vary between years, maybe due to different food sources from those in the plankton (Hill et al. 2008). The possible differences in larval nutrition experienced between years did not have any carryover effect detectable in the study of barnacle recruitment rates. Thus, no evidence suggests that the changes between years would have produced any change in growth or mortality of mussels.

6.3. Conclusions

Currently, the study of changes in the Agulhas Current System focuses on understanding its relationship with global (Beal et al. 2011) and local climate (Jury et al. 1993). Consequently, the spatial resolution of available models is inadequate to study biological processes in coastal systems, which are important areas in terms of productivity. Temporal cooling trends reported along the south coast of South Africa disagree between the present study (seasonal cooling during autumn) and previous studies (year-round cooling, Rouault et al. 2009). The different chemical properties of the water mass which intrudes into the area of highest productivity along the south coast, and the effects of nutrient availability for productivity in harmful and non-harmful phytoplankton species, makes it essential to understand temporal variability and future trends at the relevant spatio-temporal scales. The present thesis indirectly addressed the importance of environmental conditions in the water mass during the planktonic development of mussels and barnacles to understand how variability in the water column ultimately affected early juvenile abundances.

Obvious changes in phytoplankton composition appeared during the two years of study, with the presence of different red tide organisms along the coast, and mussels and barnacles showing opposite recruitment patterns between the two years. Conditions in the water mass along the south coast are largely driven by the forcing of the Agulhas Current, which influences coastal upwelling cells and helps to shape biogeographical patterns along the coast. Thus, coastal areas are indirectly tele-connected to distant areas through the Agulhas Current by mechanisms such as winds in the Indian Ocean basin (Rouault et al. 2009, Wu et al. 2012). That link with climate in remote areas highlights the importance of including temporal changes in climate when addressing future effects of environmental variability in coastal areas. In addition, the positive or negative effects of different environmental conditions are taxon, and even species-specific. In the case of the south coast of South Africa, the higher recruitment rates of an invasive mussel species, compared to a native one, under favourable conditions, indicates the potential to displace the native species and to modify community structure. Differential supply of new individuals will affect competition dynamics between the two species in intertidal areas, and alter the mechanisms that regulate the community, from competition and tolerance to stress, to processes that affect early stages of development and supply of new individuals. The tele-connection observed between local and distant areas is unlikely to be unique to the Agulhas Current System (Chen and Van den Dool 2003). Therefore, understanding the temporal variability in major climatic drivers and future trends may help to manage coastal resources.

Appendix I

I.1. Introduction

Studies that attempt to capture the spatial and temporal structure of zooplankton deal with very large numbers of samples which may contain very high abundances of organisms. Sorting and counting entire samples may not always be practical in terms of time and effort. To address this problem, multiple solutions using digital imaging systems have been developed (Grosjean et al. 2004, Benfield et al. 2007, Gorsky et al. 2010). Such systems process mesozooplankton in a more time efficient manner than human processing (Bell and Hopcroft 2008), and developments in image capture and computer capabilities have allowed the achievement of good levels of accuracy (Bi et al. 2015, Kydd et al. 2017). The advantages of using automated or semi-automated systems are evident for long-term and/or large-scale plankton studies, nonetheless, their applicability may be limited in other situations. For example, Bell and Hopcroft (2008) reported that identification of barnacle nauplii using ZooImage software was not accurate. Thus, automated systems may not be suitable in the case of studies which require the identification of organisms to the species level or even to stages of development as may be the case for some ecological studies (Benfield et al. 2007). Here, a modified sub-sampling methodology using laboratory micropipettes to process sample aliquots is proposed together with a simple calibration of the error in the procedure to allow its adaptation to study-specific requirements.

The traditional approach of counting planktonic organisms under the microscope can be extremely time consuming and it needs to be carefully planned to be efficient and produce reliable results. The most obvious way to cope with high abundances in samples is to count a fraction of the total sample by sub-sampling (Venrick 1978a). This approach is used in the study of many organisms from fish larvae (Morgan 2010), or mesozooplankton (Viitasalo 1995, Möllmann 2000, Gray and Kingsford 2003), to the larval stages of benthic organisms (Shanks and Brink 2005, Porri et al. 2014, Weidberg et al. 2015, Höfer et al. 2017). In all such cases, there are problems with deciding the splitting mechanism used to sub-sample and what fraction of the sample it is necessary to count (Venrick 1971, Alden et al. 1982). Within the planktonic realm organisms are not distributed homogeneously (Haury et al. 1978, Omori and Hamner 1982). They usually present clumped distributions as a result of their interaction with the physical environment present in the water mass (Folt and Burns 1999, Genin et al. 2005). Those patterns strongly influence the collection of animals during field sampling, and thus the conclusions derived from those studies. The use of sub-samples to estimate the abundance of organisms adds another component of variability in addition to field heterogeneity (Venrick 1971). Despite that, the variation resulting from sub-sampling has been reported to be of lower magnitude than environmental variation (Lee and McAlice 1979). It is

virtually impossible to determine the abundances of organisms in a sample from a fraction of it with perfect accuracy, but it is better to add variability due to sub-sampling if this allows greater replication through the inclusion of more samples (Venrick 1978b). To achieve the highest degree of resolution possible it is necessary to determine the minimum amount of information that it is necessary to extract from a sample in order to allow maximizing replication. Maximising replication by subsampling requires determining the minimum amount of information that it is necessary to extract from a subsample in order to allow confidence that it is a reasonable reflection of reality. In other words, how small can a subsample be while still being reliable?. Many techniques have been developed for sub-sampling, including the Folsom splitter (McEwen et al. 1954, Sell and Evans 1982), the Motoda splitter (Motoda 1959), the Stempel pipette (Frolander 1968), the whirling apparatus (Wiborg 1951, Kott 1953), or the Huntsman Marine Laboratory beaker technique (Van Guelpen et al. 1982), among others (McCallum 1979, Van Guelpen et al. 1982). The importance of producing reliable data has received considerable attention for decades (McEwen et al. 1954, Frolander 1968, Venrick 1971, Sell and Evans 1982). Plankton splitters and pipettes have acquired popularity with different types of samples and their use is widespread. The error introduced by sub-sampling is a great concern and most of the theoretical effort behind these studies was focused on determining the variability produced by the methodology applied (McCallum 1979, Alden et al. 1982, Van Guelpen et al. 1982). Nevertheless, little research has dealt with determining a minimum number of organisms to count (Alden et al. 1982).

Although many studies work with sub-samples obtained from these techniques, they apply different criteria in terms of the volume to process, or the minimum number of organisms that it is necessary to count. It still remains unclear how to address these questions, and multiple examples in the literature illustrate the problem. Some studies have identified a minimum size of the sub-sample that should be processed based on a minimum number of organisms present, but they have derived very different criteria: 30 individuals (Peterson 1979), 100 individuals (Shanks 2000, Shanks 2009), 200 – 500 individuals (Peterson 1995), over 500 (Hansson 1990), 500 – 1000 (Viitasalo 1995), to 700 – 1000 (Brinton 1962, Booth 1977). Similarly, different studies have identified a minimum volume that should be processed, or the fraction of the sample that should be sorted: one eighth (Ohman 2002), one tenth (Pulfrich 1997), 5 sub-samples of 5 ml (Helson and Gardner 2004), or two sub-samples of unknown size depending on the abundances of organisms (Möllmann 2000, 2002). In some studies, details about the sub-sampling methodology are unclear and the technique used is not specified (Möllmann 2000, 2002, Gray and Kingsford 2003, Helson and Gardner 2004). Usually only a brief description of the criteria used for sub-sampling is given without providing any reference, and in all cases (with the exception of Shanks 2000 and 2009), omitting the volume of the complete sample. The omission of this information assumes that the methodologies used are

sufficiently accurate, but in this way the lack of a common criterion for acceptability of the estimates is simply not addressed.

Thus, it is important to address explicitly the issue of the minimum fraction of a sample that it is necessary to process in order to represent the totality of the sample reliably. Here, it is proposed: (1) a time efficient sub-sampling technique which does not require specialised equipment, (2) a simple model that addresses this issue by explicitly identifying the amount of error that one is willing to accept. The model provides a way to: establish a minimum threshold of organisms to count per aliquot, decide the percentage of the sample that should be sorted, (which can be extended to any sub-sampling technique of interest for the study), take into account differences in variability when sub-sampling different species or particle sizes, and create personalized calibrations for the set of samples of interest, establishing their reliability.

I.2. Materials and methods

I.2.1. Sample collection and splitting procedure

Samples collected to estimate recruitment of intertidal invertebrate larvae were used. The samples were obtained from collectors that consisted of plastic scouring pads, shaped as a tubular mesh, rolled and attached to eye-bolts embedded in intertidal rocks. Collectors were deployed at different sites along the coast of South Africa for approximately one month. After that period, collectors were removed and stored in 70% ethanol. Six collectors were selected based on the variability of the organisms of interest they presented, ranging from low to very high abundances (from 1 to 4431 organisms in a sample). Bleach was added at a concentration of 10 ml for every 250 ml of ethanol to detach recently settled mussels from the plastic mesh. Each collector was carefully unrolled and gently scrubbed into a bucket until all particles were removed. The contents were filtered through a 75 μm sieve and preserved in 70% ethanol.

The samples were made up to 200 ml of ethanol in a 250 ml glass beaker and sub-sampled using a micropipette (5 ml maximum volume). To allow large particles to be sub-sampled, the end of the pipette tip was cut to create an aperture size of 5 - 6 mm. The contents were stirred thoroughly with the micropipette until all particles were re-suspended homogeneously. Special attention was paid to disentangle possible aggregates of phytoplankton with a pair of tweezers before splitting. 4 ml of sample were then pipetted, moving the pipette from the bottom to the top of the beaker, taking volume constantly but quickly to avoid sedimentation of the largest particles. The same mechanism of stirring and pipetting was repeated until a volume of 50 ml (a 25% aliquot of the sample) was extracted into a measuring cylinder. Although no test was used to estimate this, it was

considered that the repeated extraction of small, well mixed volumes and the conservative approach of removing a quarter of the sample would reduce the probability of uneven sub-sampling.

I.2.2. Data analysis

An inverse relationship has been previously described between the abundance of organisms in a sample and the percentage of error inherent in the sub-sampling methodology (McEwen et al. 1954, Alden et al. 1982). Higher abundances will lead to lower deviations in the sub-sample count than those obtained from samples with low abundances (Frolander 1968). With low abundances, the possibility of over or under representing the abundance in a fraction of the sample by chance increases. Thus, it is proposed that the higher the real abundances of organisms in the samples, the lower the error it would be produced by sub-sampling. To test this, six samples were chosen to cover a wide range of abundances of different organisms.

Longhurst and Seibert (1967) reported a greater reduction in the coefficient of variation of crustaceans than in chaetognaths using techniques that increase mixture during sub-sampling, and attributed that improvement to a higher tendency of crustaceans to produce clumps. Considering those results, it was hypothesized that differences in sedimentation rates of different taxa may influence the percentage of error resulting from the sub-sampling technique. To include this consideration in the analysis, organisms were counted for different taxa and assigned into 4 major groups which may have different sedimentation rates: mussel recruits, gastropods, barnacle recruits and barnacle cyprids (Table I). This factor is termed *size* in the analyses.

Table I. Minimum and maximum sizes (mm) encountered in the samples included for analysis for each taxon class.

Taxon class	Minimum size	Maximum size
Mussel recruits	0.27	5.60
Barnacle recruits	0.45	3.40
Gastropods	1.10	3.50
Barnacle cyprids	0.45	0.70

Abundances in the 25% aliquot were converted to a theoretical total by multiplying each count by four, from here on referred to as the *theoretical estimate* (TE), and compared with the abundances obtained from counting the entire sample, referred to as the *real total* (RT). The number of organisms counted in the whole samples were compared with the theoretical using a Student's t-test for paired samples to ensure the aliquot counts produced reliable results. Variances were not homogeneous, and the data were not normal. Transformation of the data did not improve the

conditions for the analysis, but the sample size was large enough to be robust to heterogeneous variances (Underwood 1997), and therefore, data were not transformed for this analysis. The difference in abundances in the theoretical estimate with respect to the real total was considered as a proxy of the error associated with sub-sampling and calculated as follows:

$$\text{Error} = ((RT - TE) / RT) \times 100$$

where RT represents the counts in the complete sample and TE are the counts calculated from the aliquot multiplied by four. The percentage of error of each count was calculated from the error estimated from the equation; note that this value can exceed 100%.

The relationship between the error and the abundance of the four different sizes of organisms present in the aliquot was studied using linear models. Variables were transformed prior to analysis using the natural logarithm of the value after adding 1 to eliminate zeros and to obtain a linear relationship. Different models were fitted to the data (Table II) to test the hypothesis that differences in the size of organisms may interfere with the error produced during sub-sampling. Models included the interaction of size and abundance in the aliquot (which considers different slopes and intercepts), as well as the effect of each variable independently (different slopes only). The most parsimonious model of all was selected using the Akaike Information Criterion (AIC), which determines which model best explains the relationship between the variables included. Linear models were performed using the *lm* function from the *stats* package in R version 3.2.0 (R Core Team, 2015). Figure I was plotted using the package *ggplot2* for R (Wickham 2009).

I.3. Results

The analyses performed to compare the real total and the theoretical estimates produced from the aliquots showed no statistical differences (Student's t-test for paired samples, $t = 1.22$; $df = 46$, $p > 0.05$), thus, the counts obtained with the micropipette sub-sampling technique for a 25% fraction of the sample were considered to represent the total samples adequately. The most complex model, i.e. abundance of organisms in the 25% aliquot and different slopes and intercepts for the four different levels of the factor size, to explain the percentages of error obtained was not significant ($F_{3, 39} = 0.14$; $p > 0.05$). Thus, there is insufficient support for the use of four different linear fits, one for each level of the factor size. The only variable in the linear model with a significant effect on the percentage of error was abundance in the 25% aliquot ($F_{1, 39} = 27$; $p < 0.001$). Model selection was ranked by value of AIC (Table II), starting with the most complex model (i.e. four different slopes and intercepts based on the levels of the factor size), and models including the effect of size were discarded.

Table II. Results of model selection based on the Akaike Information Criterion (AIC). Percentages of error produced during sub-sampling predicted using abundance of organisms in a 25% sub-sample ($\ln 1 + \text{individuals m}^{-2}$) and size classes (Table I). Best model highlighted in bold.

MODEL	AIC	R ² adjusted
Abundance × Size	17.49	0.36
Abundance + Size	12.01	0.40
Abundance	6.53	0.43

Based on the results from the AIC, percentages of error were correlated with abundances in the 25% aliquot (Fig. I). On its own, the number of organisms in a 25% aliquot explained 43% of the total variability in the error of the abundance estimate. The resulting equation of that linear regression model allowed a test of whether the error produced by sub-sampling for each individual count of interest lay within an acceptable range. The natural logarithm of the percentage error plus one (E) decreased linearly with the natural logarithm of the number of organisms plus one reached in a 25% aliquot (C), following the equation, $\ln(E) = -0.5253(\ln C) + 4.4931$ ($p < 0.001$, $R^2 = 0.44$, $n = 47$, Fig. I). Mathematical rearrangement of the equation allows an estimation of the minimum number of each organism of interest that must be encountered in the aliquot for a set value of percentage of error.

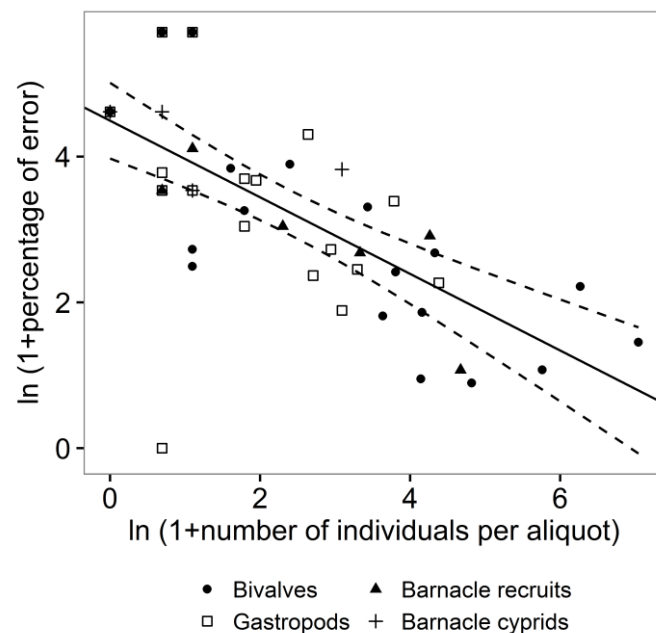


Figure I. Relationship between error ($\ln 1 + \text{percentage of error}$) and abundance ($\ln 1 + \text{individuals m}^{-2}$) in 25% sub-samples ($p < 0.001$, $R^2 = 0.44$, $n = 47$). Solid line represents the linear model selected by AIC. Dashed lines represent the 95% confidence intervals.

I.4. Discussion

Human effort is one of the main limiting resources for the study of large amounts of samples. Due to the importance of sampling to better capture the marine planktonic communities, a lot of effort has been dedicated for many decades to improving laboratory processing techniques. From the mid-19th century, the solutions for increasing laboratory efficiency focused on dividing the samples of interest and using only a fraction. Recognizing the uncertainties that the process of sub-sampling would produce, the effect on the variability resulting from fractioning was studied for practically every methodology available (for example van Guelpen et al. 1982). With the development of imaging and computer processing capabilities, the focus shifted from the optimization of effort using sub-samples to the use of automatic or semi-automatic imaging techniques (Benfield et al. 2007). Despite recent advances and the improvement of taxonomic identification of plankton by imaging systems, with their consequent increase in popularity, different constraints still prevent their completely automated and standardized use. The number of categories or taxa that imaging systems can recognize is restricted by the morphological similitude of the organisms, involving different rates of error or misidentification for different categories (Bell and Hopcroft 2008). The good results offered when dealing with mesozooplankton (for example Irigoien et al. 2008) offer a promising future to drive the understanding of community structure forward. Despite that, taxonomic problems may limit the use of imaging systems with larval stages, or in studies that deal with species of high morphological resemblance (for example Porri et al. 2006, Weidberg et al. 2014). Even if these limitations can be overcome, the constraint of identifying the error due to sub-sampling still exists. Marine samples usually present high biomasses and/or abundances that force the user to study only a fraction of the samples, whether using human or on imaging systems for their processing. Grosjean et al. (2004) outlined the necessity of sub-sampling before using the ZooScan, recognizing that the results obtained from a sub-sample had been previously reported to be variable depending on the skill of the operator (Longhurst and Seibert 1967) or apparatus used (Van Guelpen et al 1982). Sub-sampling variability will add a new uncertainty to the error already produced by the imaging technique. Different approaches will then perform differently depending on the focus of individual studies. To improve the general efficiency of sample processing it is thus necessary to recognize the strengths of the different resources available and to continue developing those procedures.

The present results provide a simple approach to calibrating any sub-sampling technique used for subsampling zooplankton samples. Using a micropipette to extract a 25% aliquot for taxa similar in size and morphological structure to the ones tested, should provide an estimate of the error for each count using the equation obtained from the model. Thus, the equation, $\ln(E) = -0.5253(\ln C) + 4.4931$ provides a method of deciding whether it is reasonable to use the data obtained from one sub-sample in future analyses, based on a maximum percentage of error that one is willing to

accept, or whether further sub-sampling is required. For example, with a count of 4 organisms in the sub-sample, the model would predict 37.38% error, while a count of 25 organisms would be associated with 15.14% of error. Therefore, it is possible to know the ranges of error that are produced *a priori*, allowing one to determine a minimum number of counts that will reach satisfactory levels of reliability and improve the investment of effort. In cases when low counts with large percentages of error are encountered, consecutive aliquots can be added to reduce the error up to the point of sorting the complete sample if necessary. The inclusion of additional sub-samples will approach the abundances of the real counts, resulting in a variable level of error among the samples studied. Despite that undesired effect, reaching an acceptable *and identified* level of error will allow the inclusion of information on rare taxa that otherwise would be omitted, as well as the ability to deal with taxa that vary in abundance among samples. Plankton studies that use sub-samples systematically and deal with variable abundances of organisms usually focus on the most abundant taxa, an approach that limits the information produced for rare species. If logistically restricted to the use of results from single sub-samples with the model proposed, it would be advisable to exclude from the analysis groups that have acceptably high levels of error as considered by Weidberg et al. (2014). Conversely, the minimum number of organisms required in the 25% aliquot to reach an acceptable level of error is obtained by rearrangement of the equation. For example, assuming 20 or 10% error is the maximum acceptable, for each taxon, a minimum of 15 and 53 individuals respectively, is required in the aliquot.

Nevertheless, there are several unavoidable limitations to our approach. Sub-sampling with a micropipette may not be adequate for some organisms, because of their larger body size, or because other techniques are appropriate. More critical was the low variability explained by the model (43%). This was most likely a consequence of the high dispersion produced by the variability within size classes as these showed a degree of overlap (Table I). This may have strongly influenced the selection of our model, which discarded differences in error among sizes (Table II). The natural samples used to test the model might also increase the error produced during sub-sampling. Despite that, subsampling captured the variability present in samples that were collected in the field in a more realistic way than the artificial plankton samples used in some studies (Longhurst and Seibert 1967, Van Guelpen et al. 1982). In other studies, the use of a single model for organisms of markedly different sizes or sedimentation rates may not be appropriate (e.g. euphausiids, Brinton (1962)), or copepods and chaetognaths (Longhurst and Seibert (1967)). Such differences might influence the response of the error to the number of organisms in the aliquot, requiring independent equations for each class, while it is expected that calibrations performed for a single species, or taxa that are more homogeneous in size, will explain a higher percentage of the variance.

The present model is constrained by the origin of the dataset and the technique used for sub-sampling, but the approach introduced in the data analysis remains applicable to other data sets or ways of sub-sampling. The main advantage of the procedure is that the reliability of the method can be tested for both sub-sampling technique and aliquot volume by calibrating the general response of the error to the abundances in the sub-sample. Thus, the procedure allows great plasticity in the conditions of choice for the calibration. Both factors, technique and volume, can be settled at the beginning of any study and the approach modified simply by counting one aliquot and the complete sample for a sub-set of collections. For some organisms, like meroplanktonic larvae, that can be present in thousands in samples, a 25% aliquot may contain excessively large numbers of organisms. In that case, aliquot size can be reduced, again to the point where the numbers involved produce an acceptable level of error. Based on the studies of Wiebe et al. (1973), Sameoto (1975) and Lee and McAlice (1979), the mean variance between any two sub-samples produced has been reported to be approximately 6% for the first two studies and 8% for the last one. Considering those results, when dealing with samples that do not allow the counting of the entire sample to create the model, several sub-samples could be used to produce the theoretical error. The results obtained will determine the model equation to choose the minimum number of organisms to count in processing the entire set of samples in further studies. For a single taxon, a linear regression will provide the equation parameters. In the case of a range of taxa, the linear model used here, which works in the same fashion as an analysis of covariance (ANCOVA), will determine if separate equations are necessary for the different classes. In addition, this approach can be used to test the variability involved in having samples processed by technicians with different levels of taxonomic expertise or skill, allowing one to ensure that the error produced is homogeneous among them. To achieve this, technician would be introduced as a factor in the model, with the null hypothesis of no differences among technicians, producing a single model to fit the data. If different models are required depending on the technician, the analysis is reporting evidence of differences among them that need to be resolved to avoid compromising the quality of the results. This could take the form of different aliquot criteria for each individual. A limitation to consider when applying the calibration is that the volume selected for the aliquot will be fixed. This implies that the calibration should be performed with a volume adequate to deal with high abundances. In cases of low abundances of a target organism in the aliquot, consecutive sub-samples can be sorted to reduce the high error rates associated with low numbers. If this is a recurrent pattern for many of the samples to be analysed, one should consider repeating the calibration with a higher percentage of the sample as the reference aliquot.

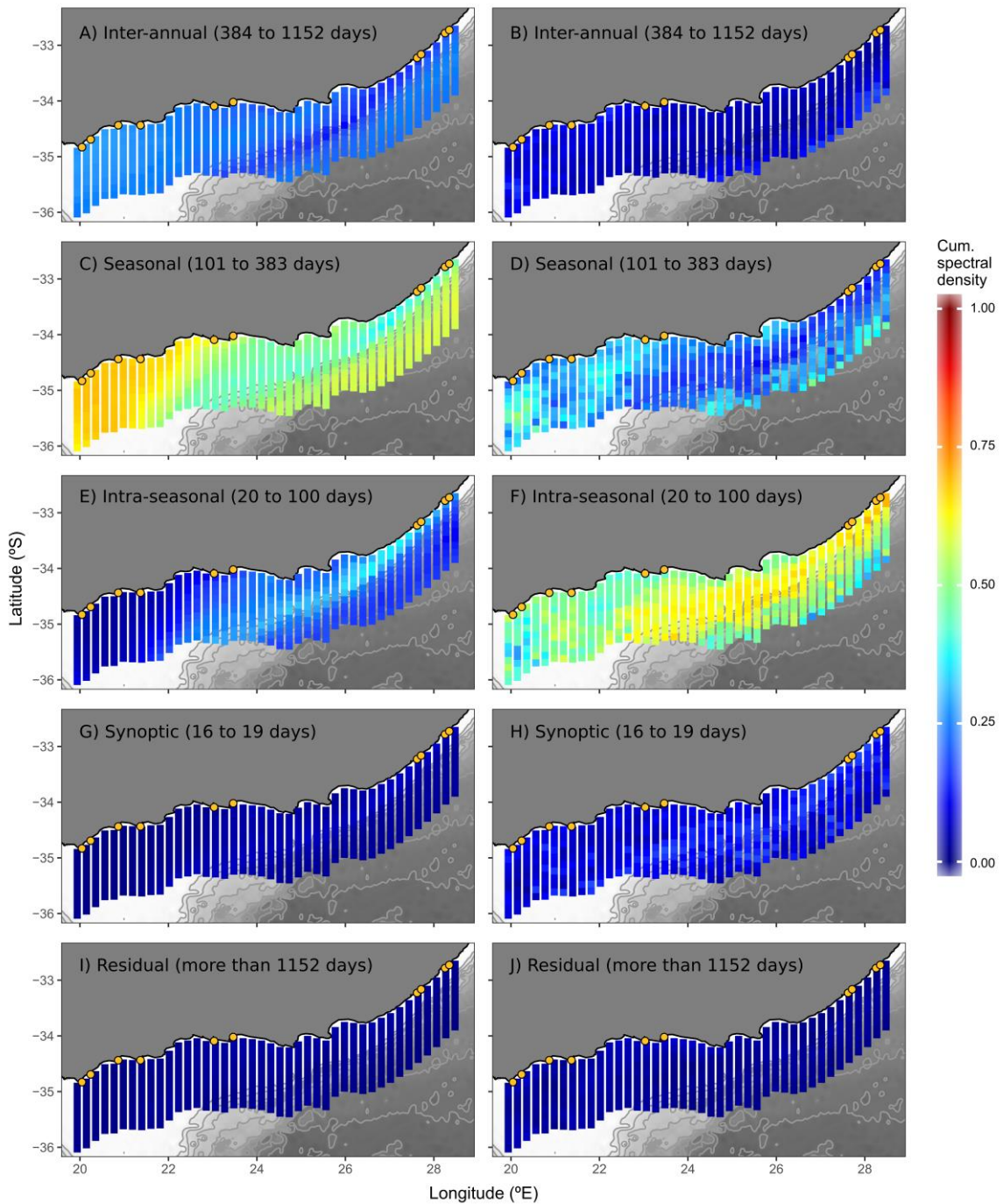
The procedure described here does not require any specialized equipment and can be adapted to any study that deals with sub-samples. Thus, the application of calibration and posterior model selection will help to decide if a minimum of 30 individuals found in the aliquot is enough (Peterson

et al. 1979), or if a minimum threshold of 700 to 1000 individuals (Brinton 1962) could be reduced to increase the efficiency of the sample processing. Although the advantages are many, it is important to consider that the model offers only a theoretical approach. A given number of organisms in the aliquot will produce percentages of error that differ among samples. Thus, it is important to understand that any model produced will provide guidance to justify future results, but there will always be variability between the aliquot and the sample counts (McEwen et al. 1954, Venrick 1978b). If the dispersion of the data in the model produced is high, confidence intervals can be used to determine whether the percentage of error is acceptable. Adopting a common criterion for an acceptable level of error would greatly facilitate comparisons among studies and increase the efficiency of such a time and effort consuming task.

Appendix II

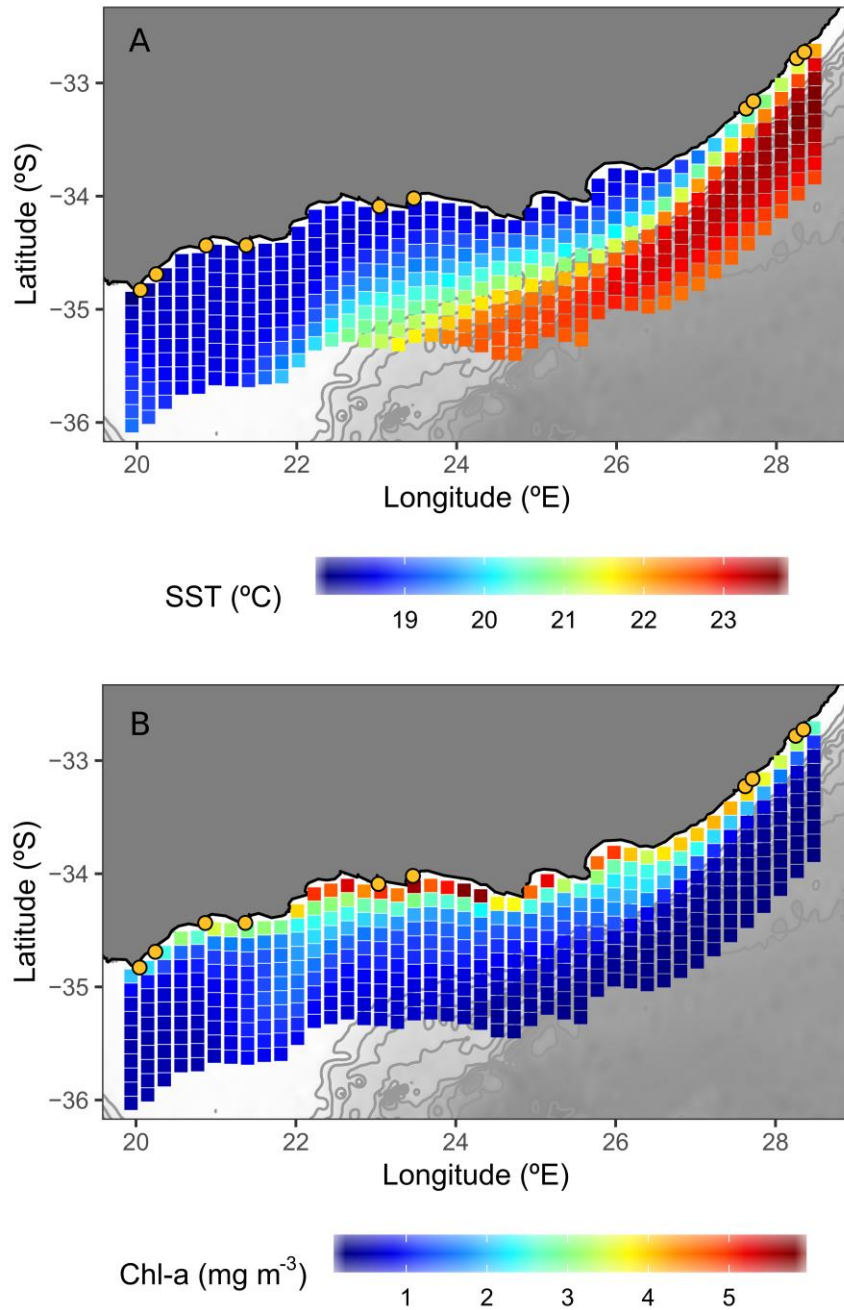
Appendix II.1

Frequencies of variability in SST (left column) and chl-a (right column) for each megapixel in the study area. Cumulative spectral densities were calculated for eight-day averages for each megapixel (see description in Chapter 5). Sampling sites along the coast are represented by yellow circles. Shaded areas and contour lines indicate the bottom profile, with the first contour line representing the 500m isobath.



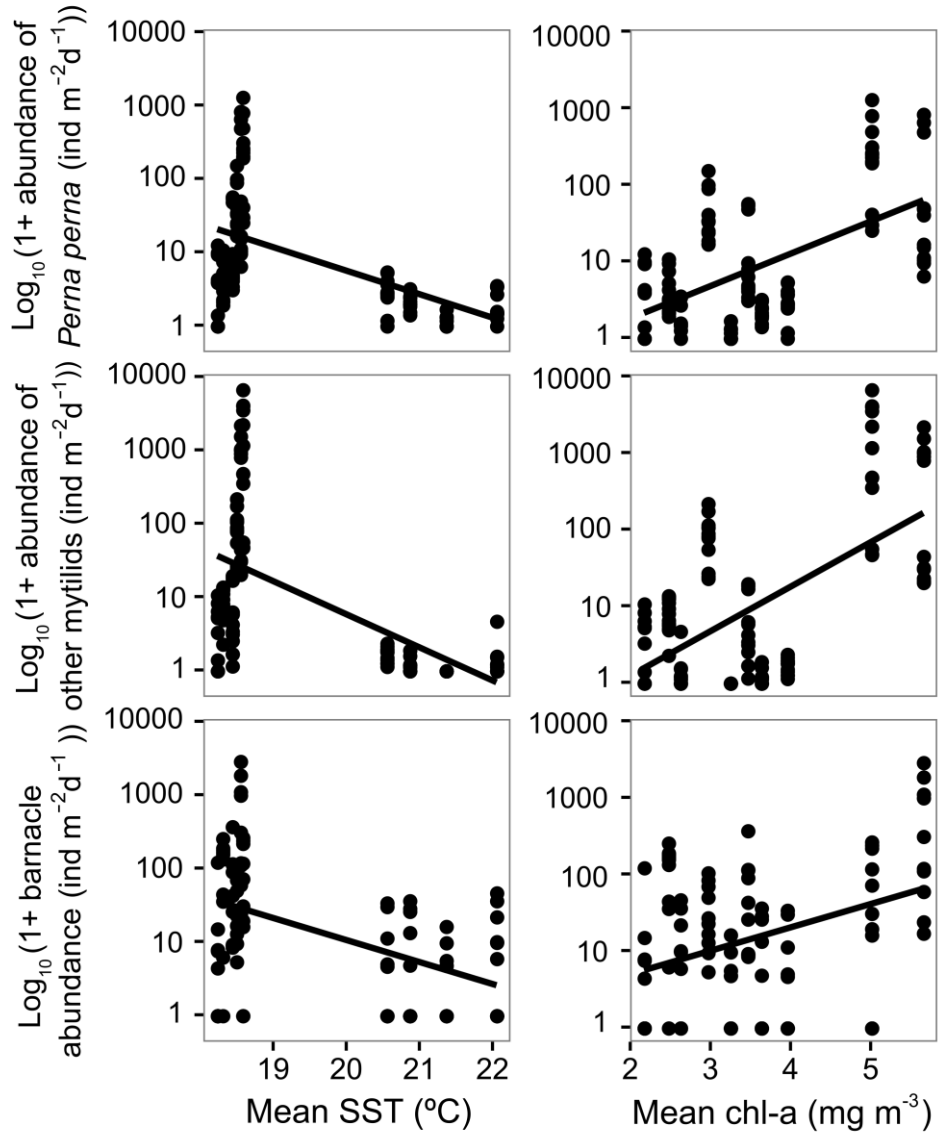
Appendix II.2

Average annual conditions of SST (A) and chl-a (B) for each megapixel in the study area. Averages were calculated for eight-day averages of each variable and megapixel. Sampling sites along the coast are represented by yellow circles. Shaded areas and contour lines delimit the bottom profile, with the first contour line representing the 500m isobath.



Appendix II.3

Linear regressions of the log-scaled recruitment rates ($\text{ind m}^{-2} \text{d}^{-1}$) for *Perna perna* (A and B), other mytilids (C and D), and barnacles (E and F), and the average annual conditions in SST and chl-a in the closest megapixel to each recruitment site (see Figs. 5.4 and 5.5 for megapixel positions).



References

“... Because the history of evolution is that life escapes all barriers. Life breaks free. Life expands to new territories. Painfully, perhaps even dangerously. But life finds a way.”

Michael Crichton (*Jurassic Park*)

- Aarab, L., A. Pérez-Camacho, M. del Pino Viera-Toledo, G. C. de Viçose, H. Fernández-Palacios, and L. Molina. 2013. Embryonic development and influence of egg density on early veliger larvae and effects of dietary microalgae on growth of brown mussel *Perna perna* (L. 1758) larvae under laboratory conditions. *Aquaculture international* **21**: 1065–1076.
- Alden, R. W., R. C. Dahiya, and R. J. Young. 1982. A method for the enumeration of zooplankton subsamples. *Journal of Experimental Marine Biology and Ecology* **59**: 185–206.
- Alexander, S. E., and J. Roughgarden. 1996. Larval transport and population dynamics of intertidal barnacles: a coupled benthic/oceanic model. *Ecological Monographs* **66**: 259–275.
- Allen, W. E. 1946. “Red Water” in La Jolla Bay in 1945. *Transactions of the American Microscopical Society* **65**: 149–153.
- Allison, G. 1994. Effects of temporary starvation on larvae of the sea star *Asterina miniata*. *Marine Biology* **118**: 255–261.
- Alvarez, D., and A. Nicieza. 2002. Effects of temperature and food quality on anuran larval growth and metamorphosis. *Functional Ecology* **16**: 640–648.
- Álvarez-Salgado, X., U. Labarta, M. Fernández-Reiriz, F. Figueiras, G. Rosón, S. Piedracoba, R. Filgueira, and J. Cabanas. 2008. Renewal time and the impact of harmful algal blooms on the extensive mussel raft culture of the Iberian coastal upwelling system (SW Europe). *Harmful Algae* **7**: 849–855.
- Anderson, D. M. 1989. Toxic algal blooms and red tides: a global perspective, p.p. 11–16. *In* Red tides: Biology, environmental science and toxicology. Elsevier, New York.
- Anderson, D. M., P. Andersen, V. M. Bricelj, J. J. Cullen, and J. J. Rensel. 2001. Monitoring and management strategies for harmful algal blooms in coastal waters. Unesco, Paris.
- Anderson, D. M., P. M. Glibert, and J. M. Burkholder. 2002. Harmful algal blooms and eutrophication: nutrient sources, composition, and consequences. *Estuaries* **25**: 704–726.
- Anderson, C. R., R. M. Kudela, C. Benitez-Nelson, and others. 2011. Detecting toxic diatom blooms from ocean color and a regional ocean model. *Geophysical Research Letters* **38**: L04603. doi:10.1029/2010GL045858.
- Anderson, D. M., A. D. Cembella, and G. M. Hallegraeff. 2012. Progress in Understanding Harmful Algal Blooms: Paradigm Shifts and New Technologies for Research, Monitoring, and Management. *Annual Review of Marine Science* **4**: 143–176. doi:10.1146/annurev-marine-120308-081121.
- Aranda-Burgos, J. A., F. da Costa, S. Nóvoa, J. Ojea, and D. Martínez-Patiño. 2014. Effects of microalgal diet on growth, survival, biochemical and fatty acid composition of *Ruditapes decussatus* larvae. *Aquaculture* **420**: 38–48.
- Arnone, V., M. González-Dávila, and J. M. Santana-Casiano. 2017. CO₂ fluxes in the South African coastal region. *Marine Chemistry* **195**: 41–49.
- Augustyn, C. 1990. Biological studies on the chokker squid *Loligo vulgaris reynaudii* (Cephalopoda; Myopsida) on spawning grounds off the south-east coast of South Africa. *South African Journal of Marine Science* **9**: 11–26.

- Awad, A. A., C. L. Griffiths, and J. K. Turpie. 2002. Distribution of South African marine benthic invertebrates applied to the selection of priority conservation areas. *Diversity and Distributions* **8**: 129–145.
- Backeberg, B. C., P. Penven, and M. Rouault. 2012. Impact of intensified Indian Ocean winds on mesoscale variability in the Agulhas system. *Nature Climate Change* **2**: 608–612.
- Bakun, A. 1973. Coastal upwelling indices, west coast of North America. US Department of Commerce. NOAA Technical Report, NMFS SSRF-671.
- Bakun, A. 1990. Global climate change and intensification of coastal ocean upwelling. *Science* **247**: 198–201.
- Balch, W., and F. Haxo. 1984. Spectral properties of *Noctiluca miliaris* Suriray, a heterotrophic dinoflagellate. *Journal of Plankton Research* **6**: 515–525.
- Baldwin, B. S., and R. I. Newell. 1991. Omnivorous feeding by planktotrophic larvae of the eastern oyster *Crassostrea virginica*. *Marine Ecology Progress Series* **78**: 285–301.
- Bally, R., C. McQuaid, and A. Brown. 1984. Shores of mixed sand and rock: An unexplored marine ecosystem. *South African Journal of Science*. **80**: 500–503.
- Bates, S., and V. Trainer. 2006. The ecology of harmful diatoms, pp. 81–93. *In Ecology of Harmful Algae*. Springer-Verlag, Berlin.
- Bayne, B. L. 1964. Primary and secondary settlement in *Mytilus edulis* L. (Mollusca). *The Journal of Animal Ecology* **33**: 513–523.
- Bayne, B. 1965. Growth and the delay of metamorphosis of the larvae of *Mytilus edulis* (L.). *Growth* **2**: 1–47.
- Bayoh, M. N., and S. W. Lindsay. 2003. Effect of temperature on the development of the aquatic stages of *Anopheles gambiae sensu stricto* (Diptera: Culicidae). *Bulletin of Entomological Research* **93**: 375–81.
- Beal, L. M., T. K. Chereskin, Y. D. Lenn, and S. Elipot. 2006. The sources and mixing characteristics of the Agulhas Current. *Journal of physical oceanography* **36**: 2060–2074.
- Beal, L. M., W. P. De Ruijter, A. Biastoch, and R. Zahn. 2011. On the role of the Agulhas system in ocean circulation and climate. *Nature* **472**: 429–436.
- Beaugrand, G., and P. C. Reid. 2003. Long-term changes in phytoplankton, zooplankton and salmon related to climate. *Global Change Biology* **9**: 801–817.
- Beaugrand, G., M. Edwards, K. Brander, C. Luczak, and F. Ibanez. 2008. Causes and projections of abrupt climate-driven ecosystem shifts in the North Atlantic. *Ecology Letters* **11**: 1157–68. doi:10.1111/j.1461-0248.2008.01218.x
- Beaugrand, G., and R. R. Kirby. 2010. Climate, plankton and cod. *Global Change Biology* **16**: 1268–1280.
- Beckley, L., and C. Van der Lingen. 1999. Biology, fishery and management of sardines (*Sardinops sagax*) in southern African waters. *Marine and Freshwater Research* **50**: 955–978.

- Behrenfeld, M. J., R. T. O'Malley, D. A. Siegel, and others. 2006. Climate-driven trends in contemporary ocean productivity. *Nature* **444**: 752–755.
- Belanger, C. L., D. Jablonski, K. Roy, S. K. Berke, A. Z. Krug, and J. W. Valentine. 2012. Global environmental predictors of benthic marine biogeographic structure. *Proceedings of the National Academy of Sciences* **109**: 14046–51. doi:10.1073/pnas.1212381109.
- Bell, J. L., and R. R. Hopcroft. 2008. Assessment of ZooImage as a tool for the classification of zooplankton. *Journal of Plankton Research* **30**: 1351–1367.
- Benfield, M. C., P. Grosjean, P. F. Culverhouse, and others. 2007. RAPID: research on automated plankton identification. *Oceanography* **20**: 172–187.
- Berdalet, E., M. McManus, O. Ross, and others. 2014. Understanding harmful algae in stratified systems: Review of progress and future directions. *Deep Sea Research Part II: Topical Studies in Oceanography* **101**: 4–20.
- Bertness, M. D., S. D. Gaines, and R. A. Wahle. 1996. Wind-driven settlement patterns in the acorn barnacle *Semibalanus balanoides*. *Marine Ecology Progress Series* **137**: 103–110.
- Bertness, M. D., S. D. Gaines, and S. M. Yeh. 1998. Making mountains out of barnacles: the dynamics of acorn barnacle hummocking. *Ecology* **79**: 1382–1394.
- Bi, H., Z. Guo, M. C. Benfield, C. Fan, M. Ford, S. Shahrestani, and J. M. Sieracki. 2015. A semi-automated image analysis procedure for *in situ* plankton imaging systems. *PLoS ONE* **10**: e0127121.
- Biastoch, A., C. W. Böning, and J. Lutjeharms. 2008. Agulhas leakage dynamics affects decadal variability in Atlantic overturning circulation. *Nature* **456**: 489–492.
- Biastoch, A., C. W. Böning, F. U. Schwarzkopf, and J. R. E. Lutjeharms. 2009. Increase in Agulhas leakage due to poleward shift of Southern Hemisphere westerlies. *Nature* **462**: 495–8. doi:10.1038/nature08519.
- Blanchette, C. A., C. Melissa Miner, P. T. Raimondi, D. Lohse, K. E. Heady, and B. R. Broitman. 2008. Biogeographical patterns of rocky intertidal communities along the Pacific coast of North America. *Journal of Biogeography* **35**: 1593–1607.
- Blasco, D. 1977. Red tide in the upwelling region of Baja California. *Limnology and Oceanography* **22**: 255–263.
- Blasco, D. 1978. Observations on the diel migration of marine dinoflagellates off the Baja California coast. *Marine Biology* **46**: 41–47.
- Bode, A., B. Casas, E. Fernández, E. Marañón, P. Serret, and M. Varela. 1996. Phytoplankton biomass and production in shelf waters off NW Spain: spatial and seasonal variability in relation to upwelling. *Hydrobiologia* **341**: 225–234.
- Boland, J. 1997. Is the geographic pattern in the abundance of South African barnacles due to pre-recruitment or post-recruitment factors? *African Journal of Marine Science* **18**: 63–73.
- Bolton, J., and H. Stegenga. 2002. Seaweed species diversity in South Africa. *African Journal of Marine Science* **24**: 9–18.

- Bond, N. A., M. F. Cronin, H. Freeland, and N. Mantua. 2015. Causes and impacts of the 2014 warm anomaly in the NE Pacific. *Geophysical Research Letters* **42**: 3414–3420.
- Bonicelli, J., J. Tyburczy, F. J. Tapia, G. R. Finke, M. Parragué, S. Dudas, B. A. Menge, and S. A. Navarrete. 2016. Diel vertical migration and cross-shore distribution of barnacle and bivalve larvae in the central Chile inner-shelf. *Journal of Experimental Marine Biology and Ecology* **485**: 35–46.
- Booth, J. D. 1977. Common bivalve larvae from New Zealand: Mytilacea. *New Zealand Journal of Marine and Freshwater Research* **11**: 407–440.
- Booth, A. J. 2000. Incorporating the spatial component of fisheries data into stock assessment models. *ICES Journal of Marine Science: Journal du Conseil* **57**: 858–865.
- Bornman, T.G., W.S. Goschen, S.H.P. Deyzel, E.E. Campbell, P.P. Steyn, M.J. Smale, P. Pistorius, and N. Hambaze, 2014. Environmental drivers, ecosystem response and socio-economic impact of the 2014 harmful algal bloom in Algoa Bay. Programme and Abstracts Book. In: Proceedings of the 15th Southern African Marine Science Symposium. 15–18 July 2014. Stellenbosch University, South Africa. pp. 196–197.
- Borthagaray, A., and A. Carranza. 2007. Mussels as ecosystem engineers: Their contribution to species richness in a rocky littoral community. *Acta Oecologica* **31**: 243–250. doi:10.1016/j.actao.2006.10.008
- Botsford, L. W. 2001. Physical influences on recruitment to California Current invertebrate populations on multiple scales. *ICES Journal of Marine Science* **58**: 1081–1091.
- Bownes, S. J., and C. D. McQuaid. 2006. Will the invasive mussel *Mytilus galloprovincialis* Lamarck replace the indigenous *Perna perna* L. on the south coast of South Africa? *Journal of Experimental Marine Biology and Ecology* **338**: 140–151.
- Bownes, S., N. Barker, and C. McQuaid. 2008. Morphological identification of primary settlers and post-larvae of three mussel species from the coast of South Africa. *African Journal of Marine Science* **30**: 233–240.
- Boyd, A. J., and F. A. Shillington. 1994. Physical forcing and circulation patterns on the Agulhas Bank. *South African Journal of Science* **90**: 143–154.
- Branch, G., C. L. Griffiths, M. L. Branch, and L. E. Beckley. 2008. Two oceans: a guide to the marine life of southern Africa. Struik Publishers.
- Brinton, E. 1962. Variable factors affecting the apparent range and estimated concentration of euphausiids in the North Pacific. *Pacific Science* **16**: 374–408.
- Broitman, B. R., S. A. Navarrete, F. Smith, and S. D. Gaines. 2001. Geographic variation of southeastern Pacific intertidal communities. *Marine Ecology Progress Series* **224**: 21–34.
- Broitman, B. R., C. A. Blanchette, and S. D. Gaines. 2005. Recruitment of intertidal invertebrates and oceanographic variability at Santa Cruz Island, California. *Limnology and Oceanography* **50**: 1473–1479.
- Broitman, B. R., and B. P. Kinlan. 2006. Spatial scales of benthic and pelagic producer biomass in a coastal upwelling ecosystem. *Marine Ecology Progress Series* **327**: 15–25.

- Broitman, B., C. Blanchette, B. Menge, and others. 2008. Spatial and temporal patterns of invertebrate recruitment along the west coast of the United States. *Ecological Monographs* **78**: 403–421.
- Bromirski, P. D., R. E. Flick, and D. R. Cayan. 2003. Storminess variability along the California coast: 1858–2000. *Journal of Climate* **16**: 982–993.
- Brown, P. 1992. Spatial and seasonal variation in chlorophyll distribution in the upper 30 m of the photic zone in the southern Benguela/Agulhas ecosystem. *South African Journal of Marine Science* **12**: 515–525.
- Brown, S. K., and J. Roughgarden. 1985. Growth, morphology, and laboratory culture of larvae of *Balanus glandula* (Cirripedia: Thoracica). *Journal of Crustacean Biology* **5**: 574–590.
- Bruno, J. F., J. J. Stachowicz, and M. D. Bertness. 2003. Inclusion of facilitation into ecological theory. *Trends in Ecology & Evolution* **18**: 119–125.
- Burkholder, J., R. Azanza, and Y. Sako. 2006. The ecology of harmful dinoflagellates, pp. 53–66. *In Ecology of Harmful Algae*. Springer-Verlag, Berlin.
- Burrows, M., S. Hawkins, and A. Southward. 1999. Larval development of the intertidal barnacles *Chthamalus stellatus* and *Chthamalus montagui*. *Journal of the Marine Biological Association of the United Kingdom* **79**: 93–101.
- Bustamante, R., G. Branch, S. Eekhout, B. Robertson, P. Zoutendyk, M. Schleyer, A. Dye, N. Hanekom, D. Keats, M. Jurd, and C. McQuaid. 1995. Gradients of intertidal primary productivity around the coast of South Africa and their relationships with consumer biomass. *Journal of Oecologia* **102**: 189–201.
- Bustamante, R., and G. Branch. 1996a. Large scale patterns and trophic structure of southern African rocky shores: the roles of geographic variation and wave exposure. *Journal of Biogeography* **23**: 339–351.
- Bustamante, R., and G. Branch. 1996b. The dependence of intertidal consumers on kelp-derived organic matter on the west coast of South Africa. *Journal of Experimental Marine Biology and Ecology* **196**: 1–28.
- Cairns, J. L. 1968. Thermocline strength fluctuations in coastal waters. *Journal of Geophysical Research* **73**: 2591–2595.
- Cairns, J. L., and K. W. Nelson. 1970. A description of the seasonal thermocline cycle in shallow coastal water. *Journal of Geophysical Research* **75**: 1127–1131.
- Carr, M.-E. 2001. Estimation of potential productivity in Eastern Boundary Currents using remote sensing. *Deep Sea Research Part II: Topical Studies in Oceanography* **49**: 59–80.
- Carr, M.-E., and E. J. Kearns. 2003. Production regimes in four Eastern Boundary Current systems. *Deep Sea Research Part II: Topical Studies in Oceanography* **50**: 3199–3221.
- Chan, B. K. K. 2003. Studies on *Tetraclita squamosa* and *Tetraclita japonica* (Cirripedia: Thoracica) II: larval morphology and development. *Journal of Crustacean Biology* **23**: 522–547.

- Chang, G., and T. Dickey. 2001. Optical and physical variability on timescales from minutes to the seasonal cycle on the New England shelf: July 1996 to June 1997. *Journal of Geophysical Research: Oceans* **106**: 9435–9453.
- Chapman, P., and J. Largier. 1989. On the origin of Agulhas Bank bottom water. *South African Journal of Science* **85**: 515–519.
- Chapman, P., and L. Shannon. 1987. Seasonality in the oxygen minimum layers at the extremities of the Benguela system. *South African Journal of Marine Science* **5**: 85–94.
- Chen, W. Y., and H. Van den Dool. 2003. Sensitivity of teleconnection patterns to the sign of their primary action center. *Monthly Weather Review* **131**: 2885–2899.
- Chia, F.-S., J. Buckland-Nicks, and C. M. Young. 1984. Locomotion of marine invertebrate larvae: a review. *Canadian Journal of Zoology* **62**: 1205–1222.
- Cloern, J. E. 1996. Phytoplankton bloom dynamics in coastal ecosystems: a review with some general lessons from sustained investigation of San Francisco Bay, California. *Reviews of Geophysics* **34**: 127–168.
- Cloern, J. E. 2001. Our evolving conceptual model of the coastal eutrophication problem. *Marine Ecology Progress Series* **210**: 223–253.
- Cole, V., C. McQuaid, and M. Nakin. 2011. Marine protected areas export larvae of infauna, but not of bioengineering mussels to adjacent areas. *Biological Conservation* **144**: 2088–2096.
- Connell, J. H. 1961a. Effects of competition, predation by *Thais lapillus*, and other factors on natural populations of the barnacle *Balanus balanoides*. *Ecological Monographs* **31**: 61–104.
- Connell, J. H. 1961b. The influence of interspecific competition and other factors on the distribution of the barnacle *Chthamalus stellatus*. *Ecology* **42**: 710–723.
- Connell, J. H. 1972. Community interactions on marine rocky intertidal shores. *Annual Review of Ecology and Systematics* **3**: 169–192.
- Connell, J. H. 1985. The consequences of variation in initial settlement vs. post-settlement mortality in rocky intertidal communities. *Journal of Experimental Marine Biology and Ecology* **93**: 11–45.
- Connolly, S. R., and J. Roughgarden. 1999. Theory of marine communities: competition, predation, and recruitment-dependent interaction strength. *Ecological Monographs* **69**: 277–296.
- Connolly, S. R., B. A. Menge, and J. Roughgarden. 2001. A latitudinal gradient in recruitment of intertidal invertebrates in the northeast Pacific Ocean. *Ecology* **82**: 1799–1813.
- Cowen, R. K., and S. Sponaugle. 2009. Larval Dispersal and Marine Population Connectivity. *Annual Review of Marine Science* **1**: 443–466. doi:10.1146/annurev.marine.010908.163757.
- Crawford, R. 1981. Distribution, availability and movements of pilchard *Sardinops ocellata* off South Africa, 1964–1976. Fisheries bulletin; contributions to oceanography and fisheries biology—South Africa, Dept. of Agriculture and Fisheries, Sea Fisheries Institute.
- Crisp, D. 1960. Factors influencing growth-rate in *Balanus balanoides*. *The Journal of Animal Ecology* **29**: 95–116.

- Crisp, D., and E. Bourget. 1985. Growth in barnacles. *Advances in Marine Biology* **22**:199–244.
- Cullen, J., and S. Horrigan. 1981. Effects of nitrate on the diurnal vertical migration, carbon to nitrogen ratio, and the photosynthetic capacity of the dinoflagellate *Gymnodinium splendens*. *Marine Biology* **62**: 81–89.
- Cushing, D. 1990. Plankton production and year-class strength in fish populations: an update of the match/mismatch hypothesis. *Advances in Marine Biology* **26**:249–293.
- Daan, R. 1987. Impact of egg predation by *Noctiluca miliaris* on the summer development of copepod populations in the southern North Sea. *Marine Ecology Progress Series* **37**: 9–17.
- Dam, H. G., and S. P. Colin. 2005. *Prorocentrum minimum* (clone Exuv) is nutritionally insufficient, but not toxic to the copepod *Acartia tonsa*. *Harmful Algae* **4**: 575–584.
- Dayton, P. K. 1971. Competition, disturbance, and community organization: the provision and subsequent utilization of space in a rocky intertidal community. *Ecological Monographs* **41**: 351–389.
- deYoung, B., M. Barange, G. Beaugrand, R. Harris, R. I. Perry, M. Scheffer, and F. Werner. 2008. Regime shifts in marine ecosystems: detection, prediction and management. *Trends in Ecology and Evolution (Amst.)* **23**: 402–9. doi:10.1016/j.tree.2008.03.008
- Di Lorenzo, E. 2015. Climate science: The future of coastal ocean upwelling. *Nature* **518**: 310–311.
- Di Lorenzo, E., V. Combes, J. E. Keister, and others. 2013. Synthesis of Pacific Ocean climate and ecosystem dynamics. *Oceanography* **26**: 68–81.
- Di Lorenzo, E., and N. Mantua. 2016. Multi-year persistence of the 2014/15 North Pacific marine heatwave. *Nature Climate Change* **6**: 1042–1047.
- Do Rosário Gomes, H., J. I. Goes, S. Matondkar, E. J. Buskey, S. Basu, S. Parab, and P. Thoppil. 2014. Massive outbreaks of *Noctiluca scintillans* blooms in the Arabian Sea due to spread of hypoxia. *Nature Communications* **5**: 4862. doi:10.1038/ncomms5862.
- Doney, S. C., V. J. Fabry, R. A. Feely, and J. A. Kleypas. 2009. Ocean acidification: the other CO₂ problem. *Annual Review of Marine Science* **1**: 169–192.
- Dudas, S. E., B. A. Grantham, A. R. Kirincich, B. A. Menge, J. Lubchenco, and J. A. Barth. 2009a. Current reversals as determinants of intertidal recruitment on the central Oregon coast. *ICES Journal of Marine Science* **66**: 396–407.
- Dudas, S. E., G. Rilov, J. Tyburczy, and B. A. Menge. 2009b. Linking larval abundance, onshore supply and settlement using instantaneous versus integrated methods. *Marine Ecology Progress Series* **387**: 81–95.
- Dye, A. 1992. Recruitment dynamics and growth of the barnacle *Tetraclita serrata* on the east coast of southern Africa. *Estuarine, Coastal and Shelf Science* **35**: 167–177.
- Eagle, G. A., and M. J. Orren. 1985. A seasonal investigation of the nutrients and dissolved oxygen in the water column along two lines of stations south and west of South Africa, Marine Chemistry Division, National Research Inst. for Oceanology, Council for Scientific and Industrial Research. Stellenbosch, South Africa. 52 pp.

- Edwards, M., and A. J. Richardson. 2004. Impact of climate change on marine pelagic phenology and trophic mismatch. *Nature* **430**: 881–884.
- Eilertsen, H. C., S. Sandberg, and H. Tøllefsen. 1995. Photoperiodic control of diatom spore growth: a theory to explain the onset of phytoplankton blooms. *Marine Ecology Progress Series* **116**: 303–307.
- Elbrächter, M., and Z. Qi. 1998. Aspects of *Noctiluca* (Dinophyceae) population dynamics, pp. 315–335. *In* *Physiological ecology of harmful algal blooms*. Springer, Berlin, Heidelberg.
- Emanuel, B., R. Bustamante, G. Branch, S. Eekhout, and F. Odendaal. 1992. A zoogeographic and functional approach to the selection of marine reserves on the west coast of South Africa. *South African Journal of Marine Science* **12**: 341–354.
- Emlet, R. B., and S. S. Sadro. 2006. Linking stages of life history: how larval quality translates into juvenile performance for an intertidal barnacle (*Balanus glandula*). *Integrative and Comparative Biology* **46**: 334–346.
- Engel, A., I. Zondervan, K. Aerts, and others. 2005. Testing the direct effect of CO₂ concentration on a bloom of the coccolithophorid *Emiliana huxleyi* in mesocosm experiments. *Limnology and Oceanography* **50**: 493–507.
- Eppley, R., F. Reid, J. Cullen, C. Winant, and E. Stewart. 1984. Subsurface patch of a dinoflagellate (*Ceratium tripos*) off Southern California: patch length, growth rate, associated vertically migrating species. *Marine Biology* **80**: 207–214.
- Erlandsson, J., P. Pal, and C. D. McQuaid. 2006. Re-colonisation rate differs between co-existing indigenous and invasive intertidal mussels following major disturbance. *Marine Ecology Progress Series* **320**: 169–176.
- Estrada, M., and E. Berdalet. 1997. Phytoplankton in a turbulent world. *Scientia Marina* **61**: 125–140.
- Fabry, V. J., B. A. Seibel, R. A. Feely, and J. C. Orr. 2008. Impacts of ocean acidification on marine fauna and ecosystem processes. *ICES Journal of Marine Science* **65**: 414–432.
- Falkowski, P. G., and M. J. Oliver. 2007. Mix and match: how climate selects phytoplankton. *Nature Reviews Microbiology* **5**: 813–819.
- Farrell, T. M., D. Bracher, and J. Roughgarden. 1991. Cross-shelf transport causes recruitment to intertidal populations in central California. *Limnology and Oceanography* **36**: 279–288.
- Fawcett, A., G. Pitcher, S. Bernard, A. Cembella, and R. Kudela. 2007. Contrasting wind patterns and toxigenic phytoplankton in the southern Benguela upwelling system. *Marine Ecology Progress Series* **348**: 19–31.
- Feely, R. A., C. L. Sabine, K. Lee, W. Berelson, J. Kleypas, V. J. Fabry, and F. J. Millero. 2004. Impact of anthropogenic CO₂ on the CaCO₃ system in the oceans. *Science* **305**: 362–366.
- Feely, R. A., S. C. Doney, and S. R. Cooley. 2009. Ocean acidification: Present conditions and future changes in a high-CO₂ world. *Oceanography* **22**: 36–47.

- Fenaux, L., M. F. Strathmann, and R. A. Strathmann. 1994. Five tests of food-limited growth of larvae in coastal waters by comparisons of rates of development and form of echinoplutei. *Limnology and Oceanography* **39**: 84–98.
- Fenberg, P. B., B. A. Menge, P. T. Raimondi, and M. M. Rivadeneira. 2015. Biogeographic structure of the northeastern Pacific rocky intertidal: the role of upwelling and dispersal to drive patterns. *Ecography* **38**: 83–95.
- Fernandez, F. 1979. Nutrition studies in the nauplius larva of *Calanus pacificus* (Copepoda: Calanoida). *Marine Biology* **53**: 131–147.
- Filgueira, R., M. S. Brown, L. A. Comeau, and J. Grant. 2015. Predicting the timing of the pediveliger stage of *Mytilus edulis* based on ocean temperature. *Journal of Molluscan Studies* **81**: 269–273.
- Folt, C. L., and C. W. Burns. 1999. Biological drivers of zooplankton patchiness. *Trends in Ecology & Evolution* **14**: 300–305.
- Foster, B. 1971. On the determinants of the upper limit of intertidal distribution of barnacles (Crustacea: Cirripedia). *The Journal of Animal Ecology* **40**: 33–48.
- Fraga, S., D. M. Anderson, I. Bravo, B. Reguera, K. A. Steidinger, and C. M. Yentsch. 1988. Influence of upwelling relaxation on dinoflagellates and shellfish toxicity in Ria de Vigo, Spain. *Estuarine, Coastal and Shelf Science* **27**: 349–361.
- Franks, P. J. 1992. Phytoplankton blooms at fronts: patterns, scales, and physical forcing mechanisms. *Reviews in Aquatic Sciences* **6**: 121–137.
- Frolander, H. F. 1968. Statistical variation in zooplankton numbers from subsampling with a Stempel pipette. *Journal (Water Pollution Control Federation)* **40**: 82–88.
- Fu, G. 1998. SeaDAS: The SeaWiFS data analysis system. *Proc. PORSEC'98, Qingdao, China* 73–79.
- Fuchs, H. L., L. S. Mullineaux, and A. R. Solow. 2004. Sinking behavior of gastropod larvae (*Ilyanassa obsoleta*) in turbulence. *Limnology and Oceanography* **49**: 1937–1948.
- Fuchs, H. L., and C. DiBacco. 2011. Mussel larval responses to turbulence are unaltered by larval age or light conditions. *Limnology and Oceanography: Fluids and Environments* **1**: 120–134.
- Gaines, S., and J. Roughgarden. 1985. Larval settlement rate: a leading determinant of structure in an ecological community of the marine intertidal zone. *Proceedings of the National Academy of Sciences* **82**: 3707–3711.
- Gallager, S. M. 1988. Visual observations of particle manipulation during feeding in larvae of a bivalve mollusc. *Bulletin of Marine Science* **43**: 344–365.
- Galley, T. H., F. M. Batista, R. Braithwaite, J. King, and A. R. Beaumont. 2010. Optimisation of larval culture of the mussel *Mytilus edulis* (L.). *Aquaculture International* **18**: 315–325.
- Garrabou, J., R. Coma, N. Bensoussan, and others. 2009. Mass mortality in Northwestern Mediterranean rocky benthic communities: effects of the 2003 heat wave. *Global Change Biology* **15**: 1090–1103.

- Gazeau, F., C. Quiblier, J. M. Jansen, J.-P. Gattuso, J. J. Middelburg, and C. H. Heip. 2007. Impact of elevated CO₂ on shellfish calcification. *Geophysical Research Letters* **34**: L07603. doi 10.1029/2006GL028554.
- Gazeau, F., J.-P. Gattuso, C. Dawber, A. Pronker, F. Peene, J. Peene, C. Heip, and J. Middelburg. 2010. Effect of ocean acidification on the early life stages of the blue mussel *Mytilus edulis*. *Biogeosciences* **7**: 2051–2060.
- Genin, A., J. S. Jaffe, R. Reef, C. Richter, and P. J. Franks. 2005. Swimming against the flow: a mechanism of zooplankton aggregation. *Science* **308**: 860–862.
- Gentemann, C. L., M. R. Fewings, and M. García-Reyes. 2017. Satellite sea surface temperatures along the West Coast of the United States during the 2014–2016 northeast Pacific marine heat wave. *Geophysical Research Letters* **44**: 312–319.
- Gibbons, M. J., E. Buecher, D. Thibault-Botha, and R. R. Helm. 2010. Patterns in marine hydrozoan richness and biogeography around southern Africa: implications of life cycle strategy. *Journal of Biogeography* **37**: 606–616.
- Gill, A., and E. Schumann. 1979. Topographically induced changes in the structure of an inertial coastal jet: application to the Agulhas Current. *Journal of Physical Oceanography* **9**: 975–991.
- Gillooly, J. F., J. H. Brown, G. B. West, V. M. Savage, and E. L. Charnov. 2001. Effects of size and temperature on metabolic rate. *Science* **293**: 2248–2251.
- Gillooly, J. F., E. L. Charnov, G. B. West, V. M. Savage, and J. H. Brown. 2002. Effects of size and temperature on developmental time. *Nature* **417**: 70–73.
- Glibert, P. M., D. M. Anderson, P. Gentien, E. Granéli, and K. G. Sellner. 2005. The global, complex phenomena of harmful algal blooms. *Oceanography* **18**: 136–147.
- Glibert, P. M., J. I. Allen, A. Bouwman, C. W. Brown, K. J. Flynn, A. J. Lewitus, and C. J. Madden. 2010. Modeling of HABs and eutrophication: status, advances, challenges. *Journal of Marine Systems* **83**: 262–275.
- Glibert, P. M., and J. M. Burkholder. 2011. Harmful algal blooms and eutrophication: “strategies” for nutrient uptake and growth outside the Redfield comfort zone. *Chinese Journal of Oceanology and Limnology* **29**: 724–738.
- Glibert, P. M., J. Icarus Allen, Y. Artioli, A. Beusen, L. Bouwman, J. Harle, R. Holmes, and J. Holt. 2014. Vulnerability of coastal ecosystems to changes in harmful algal bloom distribution in response to climate change: projections based on model analysis. *Global Change Biology* **20**: 3845–3858.
- Gobler, C. J., O. M. Doherty, T. K. Hattenrath-Lehmann, A. W. Griffith, Y. Kang, and R. W. Litaker. 2017. Ocean warming since 1982 has expanded the niche of toxic algal blooms in the North Atlantic and North Pacific oceans. *Proceedings of the National Academy of Sciences* **114**: 4975–4980.
- González-Gil, R., F. G. Taboada, J. Höfer, and R. Anadón. 2015. Winter mixing and coastal upwelling drive long-term changes in zooplankton in the Bay of Biscay (1993–2010). *Journal of Plankton Research* **37**: 337–351.

- Gorsky, G., M. D. Ohman, M. Picheral, and others. 2010. Digital zooplankton image analysis using the ZooScan integrated system. *Journal of Plankton Research* **32**: 285–303.
- Goschen, W. S., and E. H. Schumann. 2011. The physical oceanographic processes of Algoa Bay, with emphasis on the western coastal region. South African Environmental Observation Network (SAEON) and the Institute of Maritime Technology (IMT). IMT document number: PO106-10000-730002.
- Goschen, W., E. Schumann, K. Bernard, S. Bailey, and S. Deyzel. 2012. Upwelling and ocean structures off Algoa Bay and the south-east coast of South Africa. *African Journal of Marine Science* **34**: 525–536.
- Gosselin, L. A., and P.-Y. Qian. 1996. Early post-settlement mortality of an intertidal barnacle: a critical period for survival. *Marine Ecology Progress Series* **135**: 69–75.
- Grantham, B. A., F. Chan, K. J. Nielsen, D. S. Fox, J. A. Barth, A. Huyer, J. Lubchenco, and B. A. Menge. 2004. Upwelling-driven nearshore hypoxia signals ecosystem and oceanographic changes in the northeast Pacific. *Nature* **429**: 749–754.
- Grattan, L. M., S. Holobaugh, and J. G. Morris. 2016. Harmful algal blooms and public health. *Harmful algae* **57**: 2–8.
- Gray, C. A., and M. J. Kingsford. 2003. Variability in thermocline depth and strength, and relationships with vertical distributions of fish larvae and mesozooplankton in dynamic coastal waters. *Marine Ecology Progress Series* **247**: 211–224.
- De Greef, K., C. Griffiths, and Z. Zeeman. 2013. Deja vu? A second mytilid mussel, *Semimytilus algosus*, invades South Africa's west coast. *African Journal of Marine Science* **35**: 307–313.
- Griffiths, F., G. Brown, D. Reid, and R. Parker. 1984. Estimation of sample zooplankton abundance from Folsom splitter sub-samples. *Journal of Plankton Research* **6**: 721–731.
- Grindley, J., F. Taylor, and J. Day. 1964. Red water and marine fauna mortality near Cape Town. *Transactions of the Royal Society of South Africa* **37**: 111–130.
- Grindley, J., N. Sapeika, and others. 1969. The cause of mussel poisoning in South Africa. *South African Medical Journal* **43**: 275–279.
- Grosjean, P., M. Picheral, C. Warembourg, and G. Gorsky. 2004. Enumeration, measurement, and identification of net zooplankton samples using the ZOOSCAN digital imaging system. *ICES Journal of Marine Science* **61**: 518–525.
- Gyory, J., and J. Pineda. 2011. High-frequency observations of early-stage larval abundance: do storms trigger synchronous larval release in *Semibalanus balanoides*? *Marine Biology* **158**: 1581–1589.
- Hagerty, M. L., N. Reyns, and J. Pineda. 2018. Constrained nearshore larval distributions and thermal stratification. *Marine Ecology Progress Series* **595**: 105–122.
- Hallegraeff, G. M. 1993. A review of harmful algal blooms and their apparent global increase. *Phycologia* **32**: 79–99.
- Hallegraeff, G. 2003. Harmful algal blooms: a global overview. *Manual on Harmful Marine Microalgae* **33**: 1–22.

- Hallegraeff, G. M. 2010. Ocean climate change, phytoplankton community responses, and harmful algal blooms: a formidable predictive challenge. *Journal of Phycology* **46**: 220–235.
- Hallett, T., T. Coulson, J. Pilkington, T. Clutton-Brock, J. Pemberton, and B. Grenfell. 2004. Why large-scale climate indices seem to predict ecological processes better than local weather. *Nature* **430**: 71–75.
- Hampton, I. 1987. Acoustic study on the abundance and distribution of anchovy spawners and recruits in South African waters. *South African Journal of Marine Science* **5**: 901–917.
- Han, A., M. Dai, S.-J. Kao, J. Gan, Q. Li, L. Wang, W. Zhai, and L. Wang. 2012. Nutrient dynamics and biological consumption in a large continental shelf system under the influence of both a river plume and coastal upwelling. *Limnology and Oceanography* **57**: 486–502.
- Hansson, S., U. Larsson, and S. Johansson. 1990. Selective predation by herring and mysids, and zooplankton community structure in a Baltic Sea coastal area. *Journal of Plankton Research* **12**: 1099–1116.
- Harder, T., V. Thiyagarajan, and P.-Y. Qian. 2001. Combined effect of cyprid age and lipid content on larval attachment and metamorphosis of *Balanus amphitrite* Darwin. *Biofouling* **17**: 257–262.
- Harley, C. D. 2011. Climate change, keystone predation, and biodiversity loss. *Science* **334**: 1124–1127.
- Harley, C. D. G., A. Randall Hughes, K. M. Hultgren, and others. 2006. The impacts of climate change in coastal marine systems. *Ecology Letters* **9**: 228–41.
- Harris, J. M., G. M. Branch, B. L. Elliott, B. Currie, A. H. Dye, C. D. McQuaid, B. J. Tomalin, and C. Velasquez. 1998. Spatial and temporal variability in recruitment of intertidal mussels around the coast of southern Africa. *African Zoology* **33**: 1–11.
- Harrison, P. J., K. Furuya, P. M. Glibert, and others. 2011. Geographical distribution of red and green *Noctiluca scintillans*. *Chinese Journal of Oceanology and Limnology* **29**: 807–831.
- Hartnoll, R. G. 2001. Growth in Crustacea—twenty years on. *Hydrobiologia* **449**: 111–122.
- Hasle, G. R. 1950. Phototactic vertical migration in marine dinoflagellates. *Oikos* **2**: 162–175.
- Hastie, T., and R. Tibshirani. 1986. Generalized Additive Models. *Statistical Science* **1**: 297–310.
- Haury, L., J. McGowan, and P. Wiebe. 1978. Patterns and processes in the time-space scales of plankton distributions, pp. 277–327. *In* Spatial pattern in plankton communities. Springer, Boston.
- Hawkins, S., and R. Hartnoll. 1982. Settlement patterns of *Semibalanus balanoides* (L.) in the Isle of Man (1977–1981). *Journal of Experimental Marine Biology and Ecology* **62**: 271–283.
- Hawkins, S., A. Evans, L. Firth, and others. 2016. Impacts and effects of ocean warming on intertidal rocky habitats, pp. 147–176. *In* Explaining ocean warming: causes, scale, effects and consequences. IUCN, Gland, Switzerland.
- Heaney, S., and R. Eppley. 1981. Light, temperature and nitrogen as interacting factors affecting diel vertical migrations of dinoflagellates in culture. *Journal of Plankton Research* **3**: 331–344.

- Hecht, T., and R. Tilney. 1989. The Port Alfred fishery: a description and preliminary evaluation of a commercial linefishery on the South African east coast. *South African Journal of Marine Science* **8**: 103–117.
- Heisler, J., P. M. Glibert, J. M. Burkholder, and others. 2008. Eutrophication and harmful algal blooms: a scientific consensus. *Harmful Algae* **8**: 3–13.
- Helfrich, K. R., and J. Pineda. 2003. Accumulation of particles in propagating fronts. *Limnology and Oceanography* **48**: 1509–1520.
- Helson, J. G., and J. P. Gardner. 2004. Contrasting patterns of mussel abundance at neighbouring sites: does recruitment limitation explain the absence of mussels on Cook Strait (New Zealand) shores? *Journal of Experimental Marine Biology and Ecology* **312**: 285–298.
- Hentschel, B. T., and R. B. Emllet. 2000. Metamorphosis of barnacle nauplii: effects of food variability and a comparison with amphibian models. *Ecology* **81**: 3495–3508.
- Heyen, H., H. Fock, and W. Greve. 1998. Detecting relationships between the interannual variability in ecological time series and climate using a multivariate statistical approach—a case study on Helgoland Roads zooplankton. *Climate Research* **10**: 179–191.
- Hill, J., C. McQuaid, and S. Kaehler. 2006. Biogeographic and nearshore-offshore trends in isotope ratios of intertidal mussels and their food sources around the coast of southern Africa. *Marine Ecology Progress Series* **318**: 63–73.
- Hill, J. M., C. D. McQuaid, and S. Kaehler. 2008. Temporal and spatial variability in stable isotope ratios of SPM link to local hydrography and longer term SPM averages suggest heavy dependence of mussels on nearshore production. *Marine Biology* **154**: 899–909.
- Hoegh-Guldberg, O., and J. S. Pearse. 1995. Temperature, food availability, and the development of marine invertebrate larvae. *American Zoologist* **35**: 415–425.
- Hoegh-Guldberg, O., and J. F. Bruno. 2010. The impact of climate change on the world's marine ecosystems. *Science* **328**: 1523–1528.
- Höfer, J., C. Muñiz, N. Weidberg, L. García-Flórez, and J. L. Acuña. 2017. High densities of stalked barnacle larvae (*Pollicipes pollicipes*) inside a river plume. *Journal of Plankton Research* **39**: 316–329.
- Holligan, P. 1981. Biological implications of fronts on the northwest European continental shelf. *Philosophical Transactions of the Royal Society of London. Series A* **302**: 547–562.
- Hsu, S., E. A. Meindl, and D. B. Gilhousen. 1994. Determining the power-law wind-profile exponent under near-neutral stability conditions at sea. *Journal of Applied Meteorology* **33**: 757–765.
- Hu, C., J. Cannizzaro, K. Carder, Z. Lee, F. E. Muller-Karger, and I. Soto. 2011. Red tide detection in the eastern Gulf of Mexico using MODIS imagery, pp. 95–110. *In Handbook of Satellite Remote Sensing Image Interpretation: Applications for Marine Living Resources Conservation and Management*.
- Hu, C., F. E. Muller-Karger, C. J. Taylor, K. L. Carder, C. Kelble, E. Johns, and C. A. Heil. 2005. Red tide detection and tracing using MODIS fluorescence data: A regional example in SW Florida coastal waters. *Remote Sensing of Environment* **97**: 311–321.

- Huggett, J., and A. Richardson. 2000. A review of the biology and ecology of *Calanus agulhensis* off South Africa. *ICES Journal of Marine Science* **57**: 1834–1849.
- Huisman, J., P. van Oostveen, and F. J. Weissing. 1999. Critical depth and critical turbulence: two different mechanisms for the development of phytoplankton blooms. *Limnology and Oceanography* **44**: 1781–1787.
- Hunt, H. L., and R. E. Scheibling. 1997. Role of early post-settlement mortality in recruitment of benthic marine invertebrates. *Marine Ecology Progress Series* **155**: 269–301.
- Huntley, M., P. Sykes, S. Rohan, and V. Marin. 1986. Chemically-mediated rejection of dinoflagellate prey by the copepods *Calanus pacificus* and *Paracalanus parvus*: mechanism, occurrence and significance. *Marine Ecology Progress Series* **28**: 105–120.
- Hutchings, L. 1994. The Agulhas Bank: a synthesis of available information and a brief comparison with other east-coast shelf regions. *South African Journal of Science* **90**: 179–185.
- Inchausti, P. 1994. Reductionist approaches in community ecology. *The American Naturalist* **143**: 201–221.
- Irigoiien, X., J. A. Fernandes, P. Grosjean, K. Denis, A. Albaina, and M. Santos. 2008. Spring zooplankton distribution in the Bay of Biscay from 1998 to 2006 in relation with anchovy recruitment. *Journal of Plankton Research* **31**: 1–17.
- Jackson, J. M., L. Rainville, M. J. Roberts, C. D. McQuaid, and J. R. Lutjeharms. 2012. Mesoscale bio-physical interactions between the Agulhas Current and the Agulhas Bank, South Africa. *Continental Shelf Research* **49**: 10–24.
- Jarrett, J. N. 2000. Temporal variation in early mortality of an intertidal barnacle. *Marine Ecology Progress Series* **204**: 305–308.
- Jarrett, J. N. 2003. Seasonal variation in larval condition and postsettlement performance of the barnacle *Semibalanus balanoides*. *Ecology* **84**: 384–390.
- Jarrett, J. N., and J. A. Pechenik. 1997. Temporal variation in cyprid quality and juvenile growth capacity for an intertidal barnacle. *Ecology* **78**: 1262–1265.
- Jenkins, S. R., J. Murua, and M. T. Burrows. 2008. Temporal changes in the strength of density-dependent mortality and growth in intertidal barnacles. *Journal of Animal Ecology* **77**: 573–584.
- Jeong, H. J. 1994. Predation by the heterotrophic dinoflagellate *Protoperidinium cf. divergens* on copepod eggs and early naupliar stages. *Marine Ecology Progress Series* **114**: 203–208.
- Jeong, H. J., J. Y. Song, C. H. Lee, and S. T. Kim. 2004. Feeding by larvae of the mussel *Mytilus galloprovincialis* on red-tide dinoflagellates. *Journal of Shellfish Research* **23**: 185–196.
- Jeong, H. J., Y. Du Yoo, J. Y. Park, J. Y. Song, S. T. Kim, S. H. Lee, K. Y. Kim, and W. H. Yih. 2005a. Feeding by phototrophic red-tide dinoflagellates: five species newly revealed and six species previously known to be mixotrophic. *Aquatic Microbial Ecology* **40**: 133–150.

- Jeong, H. J., Y. Du Yoo, K. A. Seong, and others. 2005b. Feeding by the mixotrophic red-tide dinoflagellate *Gonyaulax polygramma*: mechanisms, prey species, effects of prey concentration, and grazing impact. *Aquatic Microbial Ecology* **38**: 249–257.
- Jones, C. G., J. H. Lawton, and M. Shachak. 1994. Organisms as ecosystem engineers, p. 130–147. *In* *Ecosystem management*. Springer, New York.
- Jury, M. R., H. R. Valentine, and J. R. Lutjeharms. 1993. Influence of the Agulhas Current on summer rainfall along the southeast coast of South Africa. *Journal of Applied Meteorology* **32**: 1282–1287.
- Kado, R., and M. H. Kim. 1996. Larval development of *Octomeris sulcata* Nilsson-Cantell (Cirripedia: Thoracica: Chthamalidae) from Japan and Korea. *Hydrobiologia* **325**: 65–76.
- Kahru, M., and B. G. Mitchell. 1998. Spectral reflectance and absorption of a massive red tide off southern California. *Journal of Geophysical Research: Oceans* **103**: 21601–21609.
- Kahru, M., Z. Lee, R. M. Kudela, M. Manzano-Sarabia, and B. G. Mitchell. 2015. Multi-satellite time series of inherent optical properties in the California Current. *Deep Sea Research Part II: Topical Studies in Oceanography* **112**: 91–106.
- Kandasamy, S., F. Baret, A. Verger, P. Neveux, and M. Weiss. 2013. A comparison of methods for smoothing and gap filling time series of remote sensing observations—application to MODIS LAI products. *Biogeosciences* **10**: 4055–4071.
- Kim, K. Y., Y. S. Kim, C. H. Hwang, C. K. Lee, W. A. Lim, and C. H. Kim. 2006. Phylogenetic analysis of dinoflagellate *Gonyaulax polygramma* Stein responsible for harmful algal blooms based on the partial LSU rDNA sequence data. *Algae* **21**: 283–286.
- Kimor, B. 1979. Predation by *Noctiluca miliaris* Souriray on *Acartia tonsa* Dana eggs in the inshore waters of southern California. *Limnology and Oceanography* **24**: 568–572.
- Kirby, R. R., G. Beaugrand, and J. A. Lindley. 2008. Climate-induced effects on the meroplankton and the benthic-pelagic ecology of the North Sea. *Limnology and Oceanography* **53**: 1805–1815.
- Kirby, R. R., and G. Beaugrand. 2009. Trophic amplification of climate warming. *Proceedings of the Royal Society of London B: Biological Sciences* **276**: 4095–4103.
- Kohler, K. E., and S. M. Gill. 2006. Coral Point Count with Excel extensions (CPCe): A Visual Basic program for the determination of coral and substrate coverage using random point count methodology. *Computers & Geosciences* **32**: 1259–1269.
- Kott, P. 1953. Modified whirling apparatus for the subsampling of plankton. *Marine and Freshwater Research* **4**: 387–393.
- Kudela, R., G. Pitcher, T. Probyn, F. Figueiras, T. Moita, and V. Trainer. 2005. Harmful algal blooms in coastal upwelling systems. *Oceanography* **18**: 184–197.
- Kurihara, H., and Y. Shirayama. 2004. Effects of increased atmospheric CO₂ on sea urchin early development. *Marine Ecology Progress Series* **274**: 161–169.
- Kydd, J., H. Rajakaruna, E. Briski, and S. Bailey. 2017. Examination of a high resolution laser optical plankton counter and FlowCAM for measuring plankton concentration and size. *Journal of Sea Research* **133**: 2–10.

- Largier, J., and V. Swart. 1987. East-west variation in thermocline breakdown on the Agulhas Bank. *South African Journal of Marine Science* **5**: 263–272.
- Largier, J., P. Chapman, W. Peterson, and V. Swart. 1992. The western Agulhas Bank: circulation, stratification and ecology. *South African Journal of Marine Science* **12**: 319–339.
- Lathlean, J. A., D. J. Ayre, and T. E. Minchinton. 2011. Rocky intertidal temperature variability along the southeast coast of Australia: comparing data from in situ loggers, satellite-derived SST and terrestrial weather stations. *Marine Ecology Progress Series* **439**: 83–95.
- Lathlean, J. A., L. Seuront, C. D. McQuaid, T. P. Ng, G. I. Zardi, and K. R. Nicastro. 2016. Cheating the locals: invasive mussels steal and benefit from the cooling effect of indigenous mussels. *PLoS ONE* **11**: e0152556.
- Lathlean, J. A., and C. D. McQuaid. 2017. Biogeographic variability in the value of mussel beds as ecosystem engineers on South African rocky shores. *Ecosystems* **20**: 568–582.
- Le Corre, N., A. L. Martel, F. Guichard, and L. E. Johnson. 2013. Variation in recruitment: differentiating the roles of primary and secondary settlement of blue mussels *Mytilus* spp. *Marine Ecology Progress Series* **481**: 133–146.
- Lee, W. Y., and B. J. McAlice. 1979. Sampling variability of marine zooplankton in a tidal estuary. *Estuarine and Coastal Marine Science* **8**: 565–582.
- Lennert-Cody, C. E., and P. J. Franks. 1999. Plankton patchiness in high-frequency internal waves. *Marine Ecology Progress Series* **186**: 59–66.
- León-Muñoz, J., M. A. Urbina, R. Garreaud, and J. L. Iriarte. 2018. Hydroclimatic conditions trigger record harmful algal bloom in western Patagonia (summer 2016). *Scientific Reports* **8**: 1330. doi:10.1038/s41598-018-19461-4.
- Leonardos, N., and I. A. Lucas. 2000a. The nutritional value of algae grown under different culture conditions for *Mytilus edulis* L. larvae. *Aquaculture* **182**: 301–315.
- Leonardos, N., and I. A. Lucas. 2000b. The use of larval fatty acids as an index of growth in *Mytilus edulis* L. larvae. *Aquaculture* **184**: 155–166.
- Lewis, J., and R. Hallett. 1997. *Lingulodinium polyedrum* (*Gonyaulux polyedra*) a blooming dinoflagellate. *Oceanography and Marine Biology* **35**: 97–162.
- Longhurst, A. R., and D. L. Seibert. 1967. Skill in the use of Folsom's plankton sample splitter. *Limnology and Oceanography* **12**: 334–335.
- López, S., X. Turon, E. Montero, C. Palacín, C. M. Duarte, and I. Tarjuelo. 1998. Larval abundance, recruitment and early mortality in *Paracentrotus lividus* (Echinoidea). Interannual variability and plankton-benthos coupling. *Marine Ecology Progress Series* **172**: 239–251.
- Lora-Vilchis, M., and A. Maeda-Martinez. 1997. Ingestion and digestion index of catarina scallop *Argopecten ventricosus-circularis*, Sowerby II, 1842, veliger larvae with ten microalgae species. *Aquaculture Research* **28**: 905–910.
- Lovenduski, N. 2012. Climate variability and Southern Ocean carbon uptake. *US, CLIVAR Variations, Summer* **10**: 6–8.

- Lutjeharms, J. 1981. Features of the southern Agulhas Current circulation from satellite remote sensing. *South African Journal of Science* **77**: 231–236.
- Lutjeharms, J. R. 2006. *The Agulhas Current*. Springer, Berlin.
- Lutjeharms, J., and R. Van Ballegooyen. 1988. The retroreflection of the Agulhas Current. *Journal of Physical Oceanography* **18**: 1570–1583.
- Lutjeharms, J., R. Catzel, and H. Valentine. 1989. Eddies and other boundary phenomena of the Agulhas Current. *Continental Shelf Research* **9**: 597–616.
- Lutjeharms, J., A. Meyer, I. Ansorge, G. Eagle, and M. Orren. 1996. The nutrient characteristics of the Agulhas Bank. *South African Journal of Marine Science* **17**: 253–274.
- Lutjeharms, J., J. Cooper, and M. Roberts. 2000. Upwelling at the inshore edge of the Agulhas Current. *Continental Shelf Research* **20**: 737–761.
- MacIntyre, J. G., J. J. Cullen, and A. D. Cembella. 1997. Vertical migration, nutrition and toxicity in the dinoflagellate *Alexandrium tamarense*. *Marine Ecology Progress Series* **148**: 201–216.
- Mangialajo, L., R. Bertolotto, R. Cattaneo-Vietti, and others. 2008. The toxic benthic dinoflagellate *Ostreopsis ovata*: quantification of proliferation along the coastline of Genoa, Italy. *Marine Pollution Bulletin* **56**: 1209–14. doi:10.1016/j.marpolbul.2008.02.028
- Mardones, J. I., J. J. Dorantes-Aranda, P. D. Nichols, and G. M. Hallegraeff. 2015. Fish gill damage by the dinoflagellate *Alexandrium catenella* from Chilean fjords: Synergistic action of ROS and PUFA. *Harmful Algae* **49**: 40–49.
- Margalef, R. 1956. Estructura y dinámica de la purga de mar en la Ría de Vigo. *Investigación Pesquera* **5**: 113–134.
- Margalef, R. 1978. Life-forms of phytoplankton as survival alternatives in an unstable environment. *Oceanologica Acta* **1**: 493–509.
- Marshall, R., S. McKinley, and C. M. Pearce. 2010. Effects of nutrition on larval growth and survival in bivalves. *Reviews in Aquaculture* **2**: 33–55.
- Martin, J. W., J. Olesen, and J. T. Høeg. 2014. *Atlas of crustacean larvae*, Johns Hopkins University Press, Baltimore.
- Mazzuco, A. C. D. A., R. A. Christofolletti, J. Pineda, V. R. Starczak, and A. M. Ciotti. 2015. Temporal variation in intertidal community recruitment and its relationships to physical forcings, chlorophyll-a concentration and sea surface temperature. *Marine Biology* **162**: 1705–1725.
- McCabe, R. M., B. M. Hickey, R. M. Kudela, and others. 2016. An unprecedented coastwide toxic algal bloom linked to anomalous ocean conditions. *Geophysical Research Letters* **43**: 10366–10376, doi:10.1002/2016GL070023.
- McCallum, I. 1979. A simple method of taking a subsample of zooplankton. *New Zealand Journal of Marine and Freshwater Research* **13**: 559–560.
- McEwen, G. F., M. W. Johnson, and T. R. Folsom. 1954. A statistical analysis of the performance of the Folsom plankton sample splitter, based upon test observations. *Archiv für Meteorologie, Geophysik und Bioklimatologie, Serie A* **7**: 502–527.

- McQuaid, C., and G. Branch. 1985. Trophic structure of rocky intertidal communities: Response to wave action and implications for energy flow. *Marine Ecology Progress Series* **22**: 153–161.
- McQuaid, C., and T. L. Lindsay. 2000. Effect of wave exposure on growth and mortality rates of the mussel *Perna perna*: bottom-up regulation of intertidal populations. *Marine Ecology Progress Series* **206**: 147–154.
- McQuaid, C., and S. Lawrie. 2005. Supply-side ecology of the brown mussel, *Perna perna*: an investigation of spatial and temporal variation in, and coupling between, gamete release and larval supply. *Marine Biology* **147**: 955–963.
- Menge, B. A. 1976. Organization of the New England rocky intertidal community: role of predation, competition, and environmental heterogeneity. *Ecological Monographs* **46**: 355–393.
- Menge, B. A. 1992. Community regulation: under what conditions are bottom-up factors important on rocky shores? *Ecology* **73**: 755–765.
- Menge, B. A. 2000. Top-down and bottom-up community regulation in marine rocky intertidal habitats. *Journal of Experimental Marine Biology and Ecology* **250**: 257–289.
- Menge, B. A., and J. P. Sutherland. 1987. Community regulation: variation in disturbance, competition, and predation in relation to environmental stress and recruitment. *The American Naturalist* **130**: 730–757.
- Menge, B. A., F. Chan, K. J. Nielsen, E. D. Lorenzo, and J. Lubchenco. 2009. Climatic variation alters supply-side ecology: impact of climate patterns on phytoplankton and mussel recruitment. *Ecological Monographs* **79**: 379–395.
- Monteiro, P., A. Van der Plas, V. Mohrholz, E. Mabile, A. Pascall, and W. Joubert. 2006. Variability of natural hypoxia and methane in a coastal upwelling system: Oceanic physics or shelf biology? *Geophysical Research Letters* **33**: L16614. doi:10.1029/2006GL026234.
- Moorthi, S. D., P. D. Countway, B. A. Stauffer, and D. A. Caron. 2006. Use of quantitative real-time PCR to investigate the dynamics of the red tide dinoflagellate *Lingulodinium polyedrum*. *Microbial ecology* **52**: 136–150.
- Morán, X. A. G., Á. López-Urrutia, A. Calvo-Díaz, and W. K. Li. 2010. Increasing importance of small phytoplankton in a warmer ocean. *Global Change Biology* **16**: 1137–1144.
- Morgan, S. G., J. L. Fisher, S. H. Miller, S. T. McAfee, and J. L. Largier. 2009. Nearshore larval retention in a region of strong upwelling and recruitment limitation. *Ecology* **90**: 3489–3502.
- Morgan, S. G., and J. L. Fisher. 2010. Larval behavior regulates nearshore retention and offshore migration in an upwelling shadow and along the open coast. *Marine Ecology Progress Series* **404**: 109–126.
- Motoda, S. 1959. Devices of simple plankton apparatus. *Memoirs of the Faculty of Fisheries Hokkaido University* **7**: 73–94.
- Moyse, J. 1963. A comparison of the value of various flagellates and diatoms as food for barnacle larvae. *ICES Journal of Marine Science* **28**: 175–187.

- Möllmann, C., G. Kornilovs, and L. Sidrevics. 2000. Long-term dynamics of main mesozooplankton species in the central Baltic Sea. *Journal of Plankton Research* **22**: 2015–2038. doi:10.1093/plankt/22.11.2015
- Möllmann, C., and F. W. Köster. 2002. Population dynamics of calanoid copepods and the implications of their predation by clupeid fish in the Central Baltic Sea. *Journal of Plankton Research* **24**: 959–978.
- Navarrete, S. A., E. A. Wieters, B. R. Broitman, and J. C. Castilla. 2005. Scales of benthic-pelagic coupling and the intensity of species interactions: from recruitment limitation to top-down control. *Proceedings of the National Academy of Sciences* **102**: 18046–18051.
- Navarrete, S., J. Largier, G. Vera, and others. 2015. Tumbling under the surf: wave-modulated settlement of intertidal mussels and the continuous settlement-relocation model. *Marine Ecology Progress Series* **520**: 101–121.
- Nelson, G. 1992. Equatorward wind and atmospheric pressure spectra as metrics for primary productivity in the Benguela system. *South African Journal of Marine Science* **12**: 19–28.
- Nicastro, K., G. Zardi, and C. McQuaid. 2010a. Differential reproductive investment, attachment strength and mortality of invasive and indigenous mussels across heterogeneous environments. *Biological Invasions* **12**: 2165–2177.
- Nicastro, K. R., G. I. Zardi, C. D. McQuaid, L. Stephens, S. Radloff, and G. L. Blatch. 2010b. The role of gaping behaviour in habitat partitioning between coexisting intertidal mussels. *BMC Ecology* **10**: 17 doi: 10.1186/1472-6785-10-17.
- O'Connor, M. I., J. F. Bruno, S. D. Gaines, B. S. Halpern, S. E. Lester, B. P. Kinlan, and J. M. Weiss. 2007. Temperature control of larval dispersal and the implications for marine ecology, evolution, and conservation. *Proceedings of the National Academy of Sciences* **104**: 1266–1271.
- O'Neil, J., T. Davis, M. Burford, and C. Gobler. 2011. The rise of harmful cyanobacteria blooms: The potential roles of eutrophication and climate change. *Harmful Algae* **14**: 313–334.
- Ohman, M. D., and B. E. Lavaniegos. 2002. Comparative zooplankton sampling efficiency of a ring net and bongo net with comments on pooling of subsamples. *California Cooperative Oceanic Fisheries Investigations Report* **43**: 162–173.
- Olson, R. R., and M. H. Olson. 1989. Food limitation of planktotrophic marine invertebrate larvae: does it control recruitment success? *Annual Review of Ecology and Systematics* **20**: 225–247.
- Omori, M., and W. Hamner. 1982. Patchy distribution of zooplankton: behavior, population assessment and sampling problems. *Marine Biology* **72**: 193–200.
- Orr, J. C., V. J. Fabry, O. Aumont, and others. 2005. Anthropogenic ocean acidification over the twenty-first century and its impact on calcifying organisms. *Nature* **437**: 681–686.
- Padmakumar, K., G. SreeRanjima, C. Fanimol, N. Menon, and V. Sanjeevan. 2010. Preponderance of heterotrophic *Noctiluca scintillans* during a multi-species diatom bloom along the southwest coast of India. *International Journal of Oceans and Oceanography* **4**: 55–63.
- Paerl, H., and R. Fulton. 2006. Ecology of harmful cyanobacteria, pp. 95–109. *In Ecology of Harmful Algae*. Springer-Verlag, Berlin.

- Paerl, H. W., and J. Huisman. 2008. Blooms like it hot. *Science* **320**: 57–58.
- Paerl, H. W., and J. Huisman. 2009. Climate change: a catalyst for global expansion of harmful cyanobacterial blooms. *Environmental Microbiology Reports* **1**: 27–37.
- Paine, R. T., J. C. Castillo, and J. Cancino. 1985. Perturbation and recovery patterns of starfish-dominated intertidal assemblages in Chile, New Zealand, and Washington State. *The American Naturalist* **125**: 679–691.
- Park, J. G., M. K. Jeong, J. A. Lee, K.-J. Cho, and O.-S. Kwon. 2001. Diurnal vertical migration of a harmful dinoflagellate, *Cochlodinium polykrikoides* (Dinophyceae), during a red tide in coastal waters of Namhae Island, Korea. *Phycologia* **40**: 292–297.
- Patel, B., and D. Crisp. 1960. Rates of development of the embryos of several species of barnacles. *Physiological Zoology* **33**: 104–119.
- Pearce, A. F., and M. Feng. 2013. The rise and fall of the “marine heat wave” off Western Australia during the summer of 2010/2011. *Journal of Marine Systems* **111**: 139–156.
- Pechenik, J. A. 2006. Larval experience and latent effects—metamorphosis is not a new beginning. *Integrative and Comparative Biology* **46**: 323–333.
- Pechenik, J. A., L. S. Eyster, J. Widdows, and B. L. Bayne. 1990. The influence of food concentration and temperature on growth and morphological differentiation of blue mussel *Mytilus edulis* L. larvae. *Journal of Experimental Marine Biology and Ecology* **136**: 47–64.
- Pechenik, J., D. Rittschof, and A. Schmidt. 1993. Influence of delayed metamorphosis on survival and growth of juvenile barnacles *Balanus amphitrite*. *Marine Biology* **115**: 287–294.
- Pechenik, J., M. Estrella, and K. Hammer. 1996. Food limitation stimulates metamorphosis of competent larvae and alters postmetamorphic growth rate in the marine prosobranch gastropod *Crepidula fornicata*. *Marine Biology* **127**: 267–275.
- Pechenik, J. A., D. E. Wendt, and J. N. Jarrett. 1998. Metamorphosis is not a new beginning. *Bioscience* **48**: 901–910.
- Peterson, W. T., C. B. Miller, and A. Hutchinson. 1979. Zonation and maintenance of copepod populations in the Oregon upwelling zone. *Deep Sea Research Part I: Oceanographic Research Papers* **26**: 467–494.
- Peterson, W., L. Hutchings, J. Huggett, and J. Largier. 1992. Anchovy spawning in relation to the biomass and the replenishment rate of their copepod prey on the western Agulhas Bank. *South African Journal of Marine Science* **12**: 487–500.
- Peterson, W. T., and L. Hutchings. 1995. Distribution, abundance and production of the copepod *Calanus agulhensis* on the Agulhas Bank in relation to spatial variations in hydrography and chlorophyll concentration. *Journal of Plankton Research* **17**: 2275–2294.
- Pfaff, M. C., G. M. Branch, E. A. Wieters, R. A. Branch, and B. R. Broitman. 2011. Upwelling intensity and wave exposure determine recruitment of intertidal mussels and barnacles in the southern Benguela upwelling region. *Marine Ecology Progress Series* **425**: 141–152.

- Pfaff, M. C., G. M. Branch, J. L. Fisher, V. Hoffmann, A. G. Ellis, and J. L. Largier. 2015. Delivery of marine larvae to shore requires multiple sequential transport mechanisms. *Ecology* **96**: 1399–1410.
- Philippart, C. J., H. M. van Aken, J. J. Beukema, O. G. Bos, G. C. Cadée, and R. Dekker. 2003. Climate-related changes in recruitment of the bivalve *Macoma balthica*. *Limnology and Oceanography* **48**: 2171–2185.
- Phillips, N. E. 2002. Effects of nutrition-mediated larval condition on juvenile performance in a marine mussel. *Ecology* **83**: 2562–2574.
- Phillips, N. E. 2004. Variable timing of larval food has consequences for early juvenile performance in a marine mussel. *Ecology* **85**: 2341–2346.
- Pierce, R., M. Henry, P. Blum, and others. 2005. Brevetoxin composition in water and marine aerosol along a Florida beach: Assessing potential human exposure to marine biotoxins. *Harmful Algae* **4**: 965–972.
- Pineda, J. 1991. Predictable upwelling and the shoreward transport of planktonic larvae by internal tidal bores. *Science* **253**: 548–549.
- Pineda, J. 1999. Circulation and larval distribution in internal tidal bore warm fronts. *Limnology and Oceanography* **44**: 1400–1414.
- Pineda, J. 2000. Linking larval settlement to larval transport: assumptions, potentials, and pitfalls. *Oceanography of the Eastern Pacific* **1**: 84–105.
- Pineda, J., J. A. Hare, and S. Sponaugle. 2007. Larval transport and dispersal in the coastal ocean and consequences for population connectivity. *Oceanography* **20**: 22–39.
- Pineda, J., F. Porri, V. Starczak, and J. Blythe. 2010. Causes of decoupling between larval supply and settlement and consequences for understanding recruitment and population connectivity. *Journal of Experimental Marine Biology and Ecology* **392**: 9–21.
- Pineda, J., N. Reynolds, and S. J. Lentz. 2018. Reduced barnacle larval abundance and settlement in response to large-scale oceanic disturbances: temporal patterns, nearshore thermal stratification, and potential mechanisms. *Limnology and Oceanography* **63**: 2618–2629.
- Pitcher, G., and D. Calder. 2000. Harmful algal blooms of the southern Benguela Current: a review and appraisal of monitoring from 1989 to 1997. *African Journal of Marine Science* **22**: 255–271.
- Pitcher, G. C., and G. Nelson. 2006. Characteristics of the surface boundary layer important to the development of red tide on the southern Namaqua shelf of the Benguela upwelling system. *Limnology and Oceanography* **51**: 2660–2674.
- Pitcher, G. C., and T. A. Probyn. 2011. Anoxia in southern Benguela during the autumn of 2009 and its linkage to a bloom of the dinoflagellate *Ceratium balechii*. *Harmful Algae* **11**: 23–32.
- Pitcher, G., J. Agenbag, D. Calder, D. Horstman, M. Jury, and J. Taunton-Clark. 1995. Red tides in relation to the meteorology of the southern Benguela upwelling system, pp. 657–662. *In* Harmful Marine Algal Blooms. Technique et Documentation, Lavoisier, Intercept Ltd. Paris.
- Pitcher, G., and A. Boyd. 1996. Across-shelf and alongshore dinoflagellate distributions and the mechanisms of red tide formation within the southern Benguela upwelling system, pp. 243–

246. In Harmful and Toxic Algal Blooms. Intergovernmental Oceanographic Commission of UNESCO 1996.
- Pitcher, G. C., A. J. Boyd, D. A. Horstman, and B. A. Mitchell-Innes. 1998. Subsurface dinoflagellate populations, frontal blooms and the formation of red tide in the southern Benguela upwelling system. *Marine Ecology Progress Series* **172**: 253–264. doi:10.3354/meps172253
- Pitcher, G. C., T. A. Probyn, A. du Randt, and others. 2014. Dynamics of oxygen depletion in the nearshore of a coastal embayment of the southern Benguela upwelling system. *Journal of Geophysical Research: Oceans* **119**: 2183–2200.
- Pitcher, G. C., A. B. Jiménez, R. M. Kudela, and B. Reguera. 2017. Harmful algal blooms in eastern boundary upwelling systems: A GEOHAB Core Research Project. *Oceanography* **30**: 22–35.
- Planque, B. 2015. Projecting the future state of marine ecosystems, “la grande illusion”? *ICES Journal of Marine Science* **73**: 204–208.
- Platt, T., C. Fuentes-Yaco, and K. T. Frank. 2003. Marine ecology: spring algal bloom and larval fish survival. *Nature* **423**: 398–399.
- Porri, F., C. D. McQuaid, and S. Radloff. 2006. Spatio-temporal variability of larval abundance and settlement of *Perna perna*: differential delivery of mussels. *Marine Ecology Progress Series* **315**: 141–150.
- Porri, F., C. McQuaid, S. Lawrie, and S. Antrobus. 2008. Fine-scale spatial and temporal variation in settlement of the intertidal mussel *Perna perna* indicates differential hydrodynamic delivery of larvae to the shore. *Journal of Experimental Marine Biology and Ecology* **367**: 213–218.
- Porri, F., J. M. Jackson, C. E. Von der Meden, N. Weidberg, and C. D. McQuaid. 2014. The effect of mesoscale oceanographic features on the distribution of mussel larvae along the south coast of South Africa. *Journal of Marine Systems* **132**: 162–173.
- Prince, E. K., L. Lettieri, K. J. McCurdy, and J. Kubanek. 2006. Fitness consequences for copepods feeding on a red tide dinoflagellate: deciphering the effects of nutritional value, toxicity, and feeding behavior. *Oecologia* **147**: 479–488.
- Pringle, J. M. 2007. Turbulence avoidance and the wind-driven transport of plankton in the surface Ekman layer. *Continental Shelf Research* **27**: 670–678.
- Probyn, T., B. Mitchell-Innes, P. Brown, L. Hutchings, and R. Carter. 1994. Review of primary production and related processes on the Agulhas-Bank. *South African Journal of Science* **90**: 166–173.
- Probyn, T., G. Pitcher, P. Monteiro, A. Boyd, and G. Nelson. 2000. Physical processes contributing to harmful algal blooms in Saldanha Bay, South Africa. *South African Journal of Marine Science* **22**: 285–297.
- Puccinelli, E., M. Noyon, and C. D. McQuaid. 2016. Hierarchical effects of biogeography and upwelling shape the dietary signatures of benthic filter feeders. *Marine Ecology Progress Series* **543**: 37–54.
- Pulfrich, A. 1997. Seasonal variation in the occurrence of planktic bivalve larvae in the Schleswig-Holstein Wadden Sea. *Helgoländer Meeresuntersuchungen* **51**: 23–39.

- Qiu, J.-W., and P.-Y. Qian. 1997. Effects of food availability, larval source and culture method on larval development of *Balanus amphitrite amphitrite* Darwin: implications for experimental design. *Journal of Experimental Marine Biology and Ecology* **217**: 47–61.
- R Core Team. 2015. R: A language and environment for statistical computing, v3.2.0. R Foundation for Statistical Computing, Vienna, Austria. Available from <http://www.R-project.org>
- Raby, D., M. Mingelbier, J. Dodson, B. Klein, Y. Lagadeuc, and L. Legendre. 1997. Food-particle size and selection by bivalve larvae in a temperate embayment. *Marine Biology* **127**: 665–672.
- Reason, C. 2001. Evidence for the influence of the Agulhas Current on regional atmospheric circulation patterns. *Journal of Climate* **14**: 2769–2778.
- Reaugh-Flower, K. E., G. M. Branch, J. M. Harris, C. D. McQuaid, B. Currie, A. Dye, and B. Robertson. 2010. Patterns of mussel recruitment in southern Africa: a caution about using artificial substrata to approximate natural recruitment. *Marine Biology* **157**: 2177–2185.
- Reaugh-Flower, K., G. M. Branch, J. M. Harris, C. D. McQuaid, B. Currie, A. Dye, and B. Robertson. 2011. Scale-dependent patterns and processes of intertidal mussel recruitment around southern Africa. *Marine Ecology Progress Series* **434**: 101–119.
- Rilov, G., S. E. Dudas, B. A. Menge, B. A. Grantham, J. Lubchenco, and D. R. Schiel. 2008. The surf zone: a semi-permeable barrier to onshore recruitment of invertebrate larvae? *Journal of Experimental Marine Biology and Ecology* **361**: 59–74.
- Rius, M., and C. D. McQuaid. 2006. Wave action and competitive interaction between the invasive mussel *Mytilus galloprovincialis* and the indigenous *Perna perna* in South Africa. *Marine Biology* **150**: 69–78.
- Rius, M., and C. D. McQuaid. 2009. Facilitation and competition between invasive and indigenous mussels over a gradient of physical stress. *Basic and Applied Ecology* **10**: 607–613.
- Rivas, A. L., A. I. Dogliotti, and D. A. Gagliardini. 2006. Seasonal variability in satellite-measured surface chlorophyll in the Patagonian Shelf. *Continental Shelf Research* **26**: 703–720.
- Roberts, M. J. 2005. Chokka squid (*Loligo vulgaris reynaudii*) abundance linked to changes in South Africa's Agulhas Bank ecosystem during spawning and the early life cycle. *ICES Journal of Marine Science* **62**: 33–55.
- Roemmich, D., and J. McGowan. 1995. Climatic warming and the decline of zooplankton in the California Current. *Science* **267**: 1324–1326.
- Roemmich, D., W. J. Gould, and J. Gilson. 2012. 135 years of global ocean warming between the Challenger expedition and the Argo Programme. *Nature Climate Change* **2**: 425–428.
- Rouault, M., A. Lee-Thorp, I. Ansorge, and J. Lutjeharms. 1995. Agulhas Current air-sea exchange experiment. *South African Journal of Science* **91**: 493–496.
- Rouault, M., P. Penven, and B. Pohl. 2009. Warming in the Agulhas Current system since the 1980s. *Geophysical Research Letters* **36**: L12602, doi:10.1029/2009GL037987.
- Rouault, M., B. Pohl, and P. Penven. 2010a. On the recent warming of the Agulhas Current, pp.268–270. *In* Observations on environmental change in South Africa. Sun Press, Stellenbosch.

- Rouault, M., B. Pohl, and P. Penven. 2010b. Coastal oceanic climate change and variability from 1982 to 2009 around South Africa. *African Journal of Marine Science* **32**: 237–246.
- Roughgarden, J., S. Gaines, and H. Possingham. 1988. Recruitment dynamics in complex life cycles. *Science* **241**: 1460–1466.
- Rowe, G. T., C. H. Clifford, K. Smith Jr, and P. L. Hamilton. 1975. Benthic nutrient regeneration and its coupling to primary productivity in coastal waters. *Nature* **255**: 215–217.
- Ryan, J., R. Kudela, J. Birch, and others. 2017. Causality of an extreme harmful algal bloom in Monterey Bay, California, during the 2014–2016 northeast Pacific warm anomaly. *Geophysical Research Letters* **44**: 5571–5579.
- Ryther, J. H. 1969. Photosynthesis and fish production in the sea. *Science* **166**: 72–76.
- Sabatés, A., M. Olivar, J. Salat, I. Palomera, and F. Alemany. 2007. Physical and biological processes controlling the distribution of fish larvae in the NW Mediterranean. *Progress in Oceanography* **74**: 355–376.
- Saji, N., B. Goswami, P. Vinayachandran, and T. Yamagata. 1999. A dipole mode in the tropical Indian Ocean. *Nature* **401**: 360–363.
- Saji, N., and T. Yamagata. 2003. Structure of SST and surface wind variability during Indian Ocean dipole mode events: COADS observations. *Journal of Climate* **16**: 2735–2751.
- Sameoto, D. 1975. Tidal and diurnal effects on zooplankton sample variability in a nearshore marine environment. *Journal of the Fisheries Board of Canada* **32**: 347–366.
- Sanford, E., and B. A. Menge. 2001. Spatial and temporal variation in barnacle growth in a coastal upwelling system. *Marine Ecology Progress Series* **209**: 143–157.
- Satuito, C. G., K. Natoyama, M. Yamazaki, and N. Fusetani. 1994. Larval development of the mussel *Mytilus edulis galloprovincialis* cultured under laboratory conditions. *Fisheries science* **60**: 65–68.
- Schlegel, R. W., E. C. Oliver, T. Wernberg, and A. J. Smit. 2017a. Nearshore and offshore co-occurrence of marine heatwaves and cold-spells. *Progress in Oceanography* **151**: 189–205.
- Schlegel, R. W., E. C. Oliver, S. Perkins-Kirkpatrick, A. Kruger, and A. J. Smit. 2017b. Predominant atmospheric and oceanic patterns during coastal marine heatwaves. *Frontiers in Marine Science* **4**: 323. doi:10.3389/fmars.2017.00323
- Schumann, E. 1982. Inshore circulation of the Agulhas Current off Natal. *Journal of Marine Research* **40**: 43–55.
- Schumann, E. 1987. The coastal ocean off the east coast of South Africa. *Transactions of the Royal Society of South Africa* **46**: 215–229.
- Schumann, E. 1989. The propagation of air pressure and wind systems along the South African coast. *South African Journal of Science* **85**: 382–385.
- Schumann, E., L. Perrins, and I. Hunter. 1982. Upwelling along the south coast of the Cape Province, South Africa. *South African Journal of Science* **78**: 238–242.

- Schumann, E., and I. L. van Heerden. 1988. Observations of Agulhas Current frontal features south of Africa, October 1983. *Deep Sea Research Part A. Oceanographic Research Papers* **35**: 1355–1362.
- Schumann, E., and J. Martin. 1991. Climatological aspects of the coastal wind field at Cape Town, Port Elizabeth and Durban. *South African Geographical Journal* **73**: 48–51.
- Sell, D. W., and M. S. Evans. 1982. A statistical analysis of subsampling and an evaluation of the Folsom plankton splitter. *Hydrobiologia* **94**: 223–230.
- Shanks, A. L., and L. Brink. 2005. Upwelling, downwelling, and cross-shelf transport of bivalve larvae: test of a hypothesis. *Marine Ecology Progress Series* **302**: 1–12.
- Shanks, A. L., and R. K. Shearman. 2009. Paradigm lost? Cross-shelf distributions of intertidal invertebrate larvae are unaffected by upwelling or downwelling. *Marine Ecology Progress Series* **385**: 189–204.
- Shanks, A. L., J. Largier, L. Brink, J. Brubaker, and R. Hooff. 2000. Demonstration of the onshore transport of larval invertebrates by the shoreward movement of an upwelling front. *Limnology and Oceanography* **45**: 230–236.
- Shanks, A. L., S. G. Morgan, J. MacMahan, and A. J. Reniers. 2017. Alongshore variation in barnacle populations is determined by surfzone hydrodynamics. *Ecological Monographs* **87**: 508–532.
- Shannon, L. V. 1985. The Benguela ecosystem Part 1. Evolution of the Benguela, physical features and processes. *Oceanography and Marine Biology, An Annual Review*. **23**: 105–182.
- Shears, N. T., and M. M. Bowen. 2017. Half a century of coastal temperature records reveal complex warming trends in western boundary currents. *Scientific Reports* **7**: 14527. doi:10.1038/s41598-017-14944-2
- Shkedy, Y., and J. Roughgarden. 1997. Barnacle recruitment and population dynamics predicted from coastal upwelling. *Oikos* **80**: 487–498.
- Siegel, D., S. Doney, and J. Yoder. 2002. The North Atlantic spring phytoplankton bloom and Sverdrup's critical depth hypothesis. *Science* **296**: 730–733.
- Skein, L., M. Alexander, and T. Robinson. 2018. Contrasting invasion patterns in intertidal and subtidal mussel communities. *African Zoology* **53**: 47–52.
- Smale, D. A., and T. Wernberg. 2009. Satellite-derived SST data as a proxy for water temperature in nearshore benthic ecology. *Marine Ecology Progress Series* **387**: 27–37.
- Smale, D. A., M. T. Burrows, P. Moore, N. O'Connor, and S. J. Hawkins. 2013. Threats and knowledge gaps for ecosystem services provided by kelp forests: a northeast Atlantic perspective. *Ecology and Evolution* **3**: 4016–4038. doi:10.1002/ece3.774
- Smayda, T. J. 1997. Harmful algal blooms: their ecophysiology and general relevance to phytoplankton blooms in the sea. *Limnology and Oceanography* **42**: 1137–1153.
- Smayda, T. 2000. Ecological features of harmful algal blooms in coastal upwelling ecosystems. *South African Journal of Marine Science* **22**: 219–253.

- Smayda, T. J. 2002. Turbulence, watermass stratification and harmful algal blooms: an alternative view and frontal zones as “pelagic seed banks.” *Harmful Algae* **1**: 95–112.
- Smayda, T. J., and C. S. Reynolds. 2003. Strategies of marine dinoflagellate survival and some rules of assembly. *Journal of Sea Research* **49**: 95–106.
- Smayda, T., and V. Trainer. 2010. Dinoflagellate blooms in upwelling systems: Seeding, variability, and contrasts with diatom bloom behaviour. *Progress in Oceanography* **85**: 92–107.
- Smit, A. J., M. Roberts, R. J. Anderson, F. Dufois, S. F. Dudley, T. G. Bornman, and others. 2013. A coastal seawater temperature dataset for biogeographical studies: large biases between in situ and remotely-sensed data sets around the coast of South Africa. *PLoS ONE* **8**: e81944.
- Smith, P. E. 1985. Year-class strength and survival of O-group clupeoids. *Canadian Journal of Fisheries and Aquatic Sciences* **42**: 69–82.
- Smith, J. R., and D. R. Strehlow. 1983. Algal-induced spawning in the marine mussel *Mytilus californianus* 4. *International Journal of Invertebrate Reproduction* **6**: 129–133.
- Sommer, U., and K. Lengfellner. 2008. Climate change and the timing, magnitude, and composition of the phytoplankton spring bloom. *Global Change Biology* **14**: 1199–1208.
- Starr, M., J. H. Himmelman, and J.-C. Therriault. 1990. Direct coupling of marine invertebrate spawning with phytoplankton blooms. *Science* **247**: 1071–1074.
- Starr, M., J. H. Himmelman, and J.-C. Therriault. 1991. Coupling of nauplii release in barnacles with phytoplankton blooms: a parallel strategy to that of spawning in urchins and mussels. *Journal of Plankton Research* **13**: 561–571.
- Stocker, T., D. Qin, G. Plattner, and others. 2013. IPCC, 2013: Climate Change 2013: The Physical Science Basis. Contribution of Working Group I to the Fifth Assessment Report of the Intergovernmental Panel on Climate Change, 1535 pp.
- Stoecker, D., U. Tillmann, and E. Granéli. 2006. Phagotrophy in harmful algae, pp. 177–187. *In Ecology of Harmful Algae*. Springer-Verlag, Berlin.
- Stone, C. J. 1989. A comparison of algal diets for cirripede nauplii. *Journal of Experimental Marine Biology and Ecology* **132**: 17–40.
- Stramma, L., and R. G. Peterson. 1990. The South Atlantic Current. *Journal of Physical Oceanography* **20**: 846–859.
- Strathmann, R. R. 1985. Feeding and nonfeeding larval development and life-history evolution in marine invertebrates. *Annual Review of Ecology and Systematics* **16**: 339–361.
- Sunda, W. G., E. Graneli, and C. J. Gobler. 2006. Positive feedback and the development and persistence of ecosystem disruptive algal blooms. *Journal of Phycology* **42**: 963–974.
- Sverdrup, H. 1953. On conditions for the vernal blooming of phytoplankton. *Journal du Conseil Permanent International pour l'Exploration de la Mer* **18**: 287–295.
- Swart, V., and J. Largier. 1987. Thermal structure of Agulhas Bank water. *South African Journal of Marine Science* **5**: 243–252.

- Tagliarolo, M., and C. D. McQuaid. 2015. Sub-lethal and sub-specific temperature effects are better predictors of mussel distribution than thermal tolerance. *Marine Ecology Progress Series* **535**: 145–159.
- Tagliarolo, M., V. Montalto, G. Sarà, J. A. Lathlean, and C. D. McQuaid. 2016. Low temperature trumps high food availability to determine the distribution of intertidal mussels *Perna perna* in South Africa. *Marine Ecology Progress Series* **558**: 51–63.
- Tallis, H. 2009. Kelp and rivers subsidize rocky intertidal communities in the Pacific Northwest (USA). *Marine Ecology Progress Series* **389**: 85–96.
- Tapia, F. J., and J. Pineda. 2007. Stage-specific distribution of barnacle larvae in nearshore waters: potential for limited dispersal and high mortality rates. *Marine Ecology Progress Series* **342**: 177–190.
- Tapia, F. J., and S. A. Navarrete. 2010. Spatial patterns of barnacle settlement in central Chile: Persistence at daily to inter-annual scales relative to the spatial signature of physical variability. *Journal of Experimental Marine Biology and Ecology* **392**: 151–159.
- Tapia, F. J., C. DiBacco, J. Jarrett, and J. Pineda. 2010. Vertical distribution of barnacle larvae at a fixed nearshore station in southern California: Stage-specific and diel patterns. *Estuarine, Coastal and Shelf Science* **86**: 265–270.
- Tapia, F. J., J. L. Largier, M. Castillo, E. A. Wieters, and S. A. Navarrete. 2014. Latitudinal discontinuity in thermal conditions along the nearshore of central-northern Chile. *PLoS ONE* **9**: e110841.
- Thiyagarajan, V., T. Harder, and P.-Y. Qian. 2002. Relationship between cyprid energy reserves and metamorphosis in the barnacle *Balanus amphitrite* Darwin (Cirripedia; Thoracica). *Journal of Experimental Marine Biology and Ecology* **280**: 79–93.
- Thiyagarajan, V., T. Harder, J.-W. Qiu, and P.-Y. Qian. 2003. Energy content at metamorphosis and growth rate of the early juvenile barnacle *Balanus amphitrite*. *Marine Biology* **143**: 543–554.
- Thiyagarajan, V., O. S. Hung, J. M. Y. Chiu, R. S. S. Wu, and P. Qian. 2005. Growth and survival of juvenile barnacle *Balanus amphitrite*: interactive effects of cyprid energy reserve and habitat. *Marine Ecology Progress Series* **299**: 229–237.
- Thomas, A., M.-E. Carr, and P. T. Strub. 2001. Chlorophyll variability in eastern boundary currents. *Geophysical Research Letters* **28**: 3421–3424.
- Thomas, W. H., and C. H. Gibson. 1990. Quantified small-scale turbulence inhibits a red tide dinoflagellate, *Gonyaulax polyedra* Stein. *Deep Sea Research Part A. Oceanographic Research Papers* **37**: 1583–1593.
- Thompson, P. A., and P. J. Harrison. 1992. Effects of monospecific algal diets of varying biochemical composition on the growth and survival of Pacific oyster (*Crassostrea gigas*) larvae. *Marine Biology* **113**: 645–654.
- Thompson, R., B. Wilson, M. Tobin, A. Hill, and S. Hawkins. 1996. Biologically generated habitat provision and diversity of rocky shore organisms at a hierarchy of spatial scales. *Journal of Experimental Marine Biology and Ecology* **202**: 73–84.
- Thomson, R. E., and W. J. Emery. 2014. *Data analysis methods in physical oceanography*. Elsevier, Amsterdam.

- Thorson, G. 1950. Reproductive and larval ecology of marine bottom invertebrates. *Biological Reviews* **25**: 1–45.
- TIBCO Software Inc. 2017. Statistica (data analysis software system), version 13. <http://statistica.io>.
- Toupoint, N., L. Gilmore-Solomon, F. Bourque, B. Myrand, F. Pernet, F. Olivier, and R. Tremblay. 2012. Match/mismatch between the *Mytilus edulis* larval supply and seston quality: effect on recruitment. *Ecology* **93**: 1922–1934.
- Townsend, D. W., L. M. Cammen, P. M. Holligan, D. E. Campbell, and N. R. Pettigrew. 1994. Causes and consequences of variability in the timing of spring phytoplankton blooms. *Deep Sea Research Part I: Oceanographic Research Papers* **41**: 747–765.
- Trainer, V. L., G. Pitcher, B. Reguera, and T. Smayda. 2010. The distribution and impacts of harmful algal bloom species in eastern boundary upwelling systems. *Progress in Oceanography* **85**: 33–52.
- Turner, J. T., and P. A. Tester. 1997. Toxic marine phytoplankton, zooplankton grazers, and pelagic food webs. *Limnology and Oceanography* **42**: 1203–1213.
- Turner, J. T., H. Levinsen, T. G. Nielsen, and B. W. Hansen. 2001. Zooplankton feeding ecology: grazing on phytoplankton and predation on protozoans by copepod and barnacle nauplii in Disko Bay, West Greenland. *Marine Ecology Progress Series* **221**: 209–219.
- Underwood, A., and P. Fairweather. 1989. Supply-side ecology and benthic marine assemblages. *Trends in Ecology & Evolution* **4**: 16–20.
- Underwood, A. J. 1997. *Experiments in ecology: their logical design and interpretation using analysis of variance*. Cambridge University Press, Cambridge.
- Underwood AJ, K. M. 2001. *Supply-side ecology: the nature and consequences of variations in recruitment of intertidal organisms*. Sinauer Associates Sunderland, Massachusetts.
- Urban, M. C. 2015. Accelerating extinction risk from climate change. *Science* **348**: 571–573.
- Urban, M. C., G. Bocedi, A. P. Hendry, and others. 2016. Improving the forecast for biodiversity under climate change. *Science* **353**: aad8466. doi:10.1126/science.aad8466
- Van Guelpen, L., D. F. Markle, and D. J. Duggan. 1982. An evaluation of accuracy, precision, and speed of several zooplankton subsampling techniques. *ICES Journal of Marine Science* **40**: 226–236.
- Van der Lingen, C., L. Hutchings, T. Lamont, and G. Pitcher. 2016. Climate change, dinoflagellate blooms and sardine in the southern Benguela Current Large Marine Ecosystem. *Environmental Development* **17**: 230–243.
- Van der Putten, W. H., M. Macel, and M. E. Visser. 2010. Predicting species distribution and abundance responses to climate change: why it is essential to include biotic interactions across trophic levels. *Philosophical Transactions of the Royal Society B: Biological Sciences* **365**: 2025–2034.
- Vargas, C. A., P. H. Manríquez, and S. A. Navarrete. 2006. Feeding by larvae of intertidal invertebrates: assessing their position in pelagic food webs. *Ecology* **87**: 444–57.

- Venrick, E. 1971. The statistics of subsampling. *Limnology and Oceanography* **16**: 811–818.
- Venrick, E. 1978a. The implications of subsampling, pp.75–78. *In* Phytoplankton manual. UNESCO, Paris.
- Venrick, E. 1978b. How many cells to count?, pp. 167–180. *In* Phytoplankton manual. UNESCO, Paris.
- Verheye, H., L. Hutchings, J. Huggett, R. Carter, W. Peterson, and S. Painting. 1994. Community structure, distribution and trophic ecology of zooplankton on the Agulhas Bank with special reference to copepods. *South African Journal of Science* **90**: 154–165.
- Vidal, J. 1980. Physioecology of zooplankton. I. Effects of phytoplankton concentration, temperature, and body size on the growth rate of *Calanus pacificus* and *Pseudocalanus* sp. *Marine Biology* **56**: 111–134.
- Viitasalo, M., I. Vuorinen, and S. Saesmaa. 1995. Mesozooplankton dynamics in the northern Baltic Sea: implications of variations in hydrography and climate. *Journal of Plankton Research* **17**: 1857–1878.
- Von Der Meden, C. E. O. 2009. Intertidal patterns and processes: tracking the effects of coastline topography and settlement choice across life stages of the mussels *Perna perna* and *Mytilus galloprovincialis*. Doctoral dissertation, Rhodes University, Grahamstown, South Africa.
- Von der Meden, C. E., F. Porri, J. Erlandsson, and C. D. McQuaid. 2008. Coastline topography affects the distribution of indigenous and invasive mussels. *Marine Ecology Progress Series* **372**: 135–145.
- Von der Meden, C. E., F. Porri, C. D. McQuaid, K. Faulkner, and J. Robey. 2010. Fine-scale ontogenetic shifts in settlement behaviour of mussels: changing responses to biofilm and conspecific settler presence in *Mytilus galloprovincialis* and *Perna perna*. *Marine Ecology Progress Series* **411**: 161–171.
- Von der Meden, C. E., F. Porri, and C. D. McQuaid. 2012. New estimates of early post-settlement mortality for intertidal mussels show no relationship with meso-scale coastline topographic features. *Marine Ecology Progress Series* **463**: 193–204.
- Walker, N. 1990. Links between South African summer rainfall and temperature variability of the Agulhas and Benguela Current systems. *Journal of Geophysical Research: Oceans* **95**: 3297–3319.
- Walsh, J. J., J. C. Kelley, T. E. Whitedge, J. J. MacIsaac, and S. A. Huntsman. 1974. Spin-up of the Baja California upwelling ecosystem. *Limnology and Oceanography* **19**: 553–572.
- Wang, D., T. C. Gouhier, B. A. Menge, and A. R. Ganguly. 2015. Intensification and spatial homogenization of coastal upwelling under climate change. *Nature* **518**: 390–394.
- Weidberg, N., C. Lobón, E. López, L. G. Flórez, M. del P. F. Rueda, J. L. Largier, and J. L. Acuña. 2014. Effect of nearshore surface slicks on meroplankton distribution: role of larval behaviour. *Marine Ecology Progress Series* **506**: 15–30.
- Weidberg, N., F. Porri, C. E. Von der Meden, J. M. Jackson, W. Goschen, and C. D. McQuaid. 2015. Mechanisms of nearshore retention and offshore export of mussel larvae over the Agulhas Bank. *Journal of Marine Systems* **144**: 70–80.

- Wells, M. L., V. L. Trainer, T. J. Smayda, and others. 2015. Harmful algal blooms and climate change: Learning from the past and present to forecast the future. *Harmful Algae* **49**: 68–93.
- West, T. L., and J. D. Costlow. 1988. Determinants of the larval molting pattern of the crustacean *Balanus eburneus* Gould (Cirripedia: Thoracica). *Journal of Experimental Zoology Part A: Ecological Genetics and Physiology* **248**: 33–44.
- Whitfield, A. K., N. C. James, S. J. Lamberth, J. B. Adams, R. Perissinotto, A. Rajkaran, and T. G. Bornman. 2016. The role of pioneers as indicators of biogeographic range expansion caused by global change in southern African coastal waters. *Estuarine, Coastal and Shelf Science* **172**: 138–153.
- Wiborg, K. F. 1951. The Whirling Vessel-An apparatus for the fractioning of plankton samples. *Fiskeridir Skr Ser Havunders* **9**:1–16.
- Wickham, H. 2009. *ggplot2: Elegant Graphics for Data Analysis*, Springer Science & Business Media.
- Widdows, J. 1991. Physiological ecology of mussel larvae. *Aquaculture* **94**: 147–163.
- Wiebe, P. H., G. D. Grice, and E. Hoagland. 1973. Acid-iron waste as a factor affecting the distribution and abundance of zooplankton in the New York Bight: II. Spatial variations in the field and implications for monitoring studies. *Estuarine and Coastal Marine Science* **1**: 51–64.
- Wieters, E. A., B. Broitman, and G. Brancha. 2009. Benthic community structure and spatiotemporal thermal regimes in two upwelling ecosystems: Comparisons between South Africa and Chile. *Limnology and Oceanography* **54**: 1060–1072.
- Winder, M., and D. E. Schindler. 2004. Climate change uncouples trophic interactions in an aquatic ecosystem. *Ecology* **85**: 2100–2106.
- Winder, M., and U. Sommer. 2012. Phytoplankton response to a changing climate. *Hydrobiologia* **698**: 5–16.
- Wing, S. R., L. W. Botsford, L. E. Morgan, J. M. Diehl, and C. J. Lundquist. 2003. Inter-annual variability in larval supply to populations of three invertebrate taxa in the northern California Current. *Estuarine, Coastal and Shelf Science* **57**: 859–872.
- Wood, S. N. 2006. *Generalized additive models: an introduction with R*, Chapman and Hall/CRC, Boca Raton.
- Woodson, C. B., M. A. McManus, J. A. Tyburczy, and others. 2012. Coastal fronts set recruitment and connectivity patterns across multiple taxa. *Limnology and Oceanography* **57**: 582–596.
- Wu, L., W. Cai, L. Zhang, and others. 2012. Enhanced warming over the global subtropical western boundary currents. *Nature Climate Change* **2**: 161–166.
- Xue, L., L. Gao, W.-J. Cai, W. Yu, and M. Wei. 2015. Response of sea surface fugacity of CO₂ to the SAM shift south of Tasmania: Regional differences. *Geophysical Research Letters* **42**: 3973–3979.
- Young, C. M. 1995. Behavior and locomotion during the dispersal phase of larval life, pp. 249–277. *In Ecology of Marine Invertebrate Larvae*. CRC Press, Boca Raton.
- Young, C. 2002. *Atlas of Marine Invertebrate Larvae*. Academic, San Francisco.

- Zardi, G., C. McQuaid, and K. Nicastro. 2007a. Balancing survival and reproduction: seasonality of wave action, attachment strength and reproductive output in indigenous *Perna perna* and invasive *Mytilus galloprovincialis* mussels. *Marine Ecology Progress Series* **334**: 155–163.
- Zardi, G., C. McQuaid, P. Teske, and N. Barker. 2007b. Unexpected genetic structure of mussel populations in South Africa: indigenous *Perna perna* and invasive *Mytilus galloprovincialis*. *Marine Ecology Progress Series* **337**: 135–144.
- Zardi, G., K. Nicastro, C. McQuaid, and J. Erlandsson. 2008. Sand and wave induced mortality in invasive (*Mytilus galloprovincialis*) and indigenous (*Perna perna*) mussels. *Marine Biology* **153**: 853–858.
- Zardi, G., K. Nicastro, C. McQuaid, M. Rius, and F. Porri. 2006a. Hydrodynamic stress and habitat partitioning between indigenous (*Perna perna*) and invasive (*Mytilus galloprovincialis*) mussels: constraints of an evolutionary strategy. *Marine Biology* **150**: 79–88.
- Zardi, G., K. Nicastro, F. Porri, and C. McQuaid. 2006b. Sand stress as a non-determinant of habitat segregation of indigenous (*Perna perna*) and invasive (*Mytilus galloprovincialis*) mussels in South Africa. *Marine Biology* **148**: 1031–1038.
- Zheng, Z., Z.-Z. Hu, and M. L'Heureux. 2016. Predictable Components of ENSO Evolution in Real-time Multi-Model Predictions. *Scientific Reports* **6**: 35909. doi:10.1038/srep35909.
- Zhu, Z., P. Qu, F. Fu, N. Tennenbaum, A. O. Tatters, and D. A. Hutchins. 2017. Understanding the blob bloom: Warming increases toxicity and abundance of the harmful bloom diatom *Pseudo-nitzschia* in California coastal waters. *Harmful Algae* **67**: 36–43.
- Zimmerman, R. C., and D. L. Robertson. 1985. Effects of El Niño on local hydrography and growth of the giant kelp, *Macrocystis pyrifera*, at Santa Catalina Island, California. *Limnology and Oceanography* **30**: 1298–1302.
- Zingone, A., and H. O. Enevoldsen. 2000. The diversity of harmful algal blooms: a challenge for science and management. *Ocean & Coastal Management* **43**: 725–748.